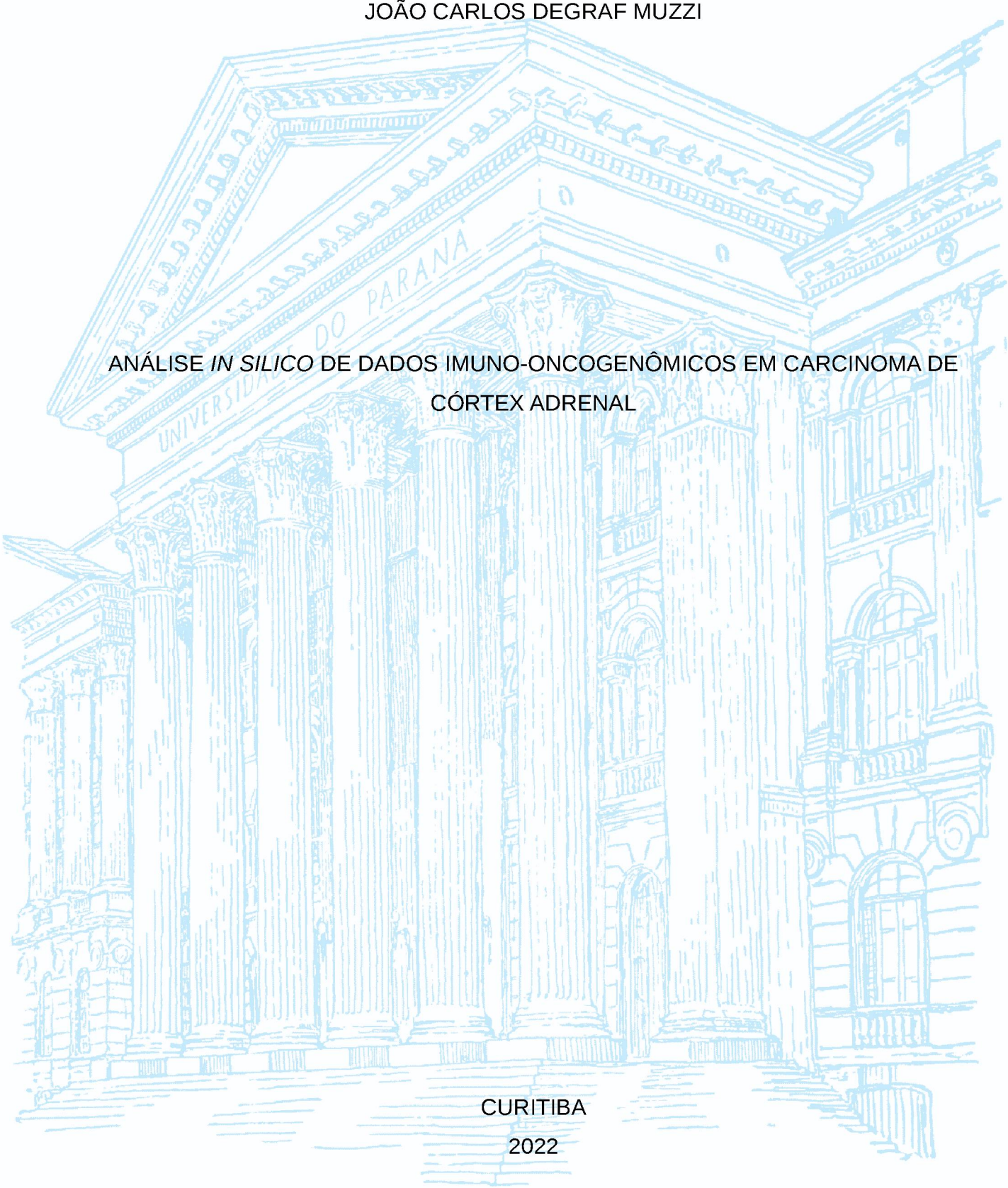
UNIVERSIDADE FEDERAL DO PARANÁ

JOÃO CARLOS DEGRAF MUZZI



ANÁLISE *IN SILICO* DE DADOS IMUNO-ONCOGENÔMICOS EM CARCINOMA DE CÓRTEX ADRENAL

CURITIBA

2022

JOÃO CARLOS DEGRAF MUZZI

ANÁLISE *IN SILICO* DE DADOS IMUNO-ONCOGENÔMICOS EM CARCINOMA DE CÓRTEX ADRENAL

Tese apresentada ao Curso de Pós-Graduação em Microbiologia, Parasitologia e Patologia, Setor de Ciências Biológicas da Universidade Federal do Paraná, como requisito parcial à obtenção do título de Doutor Microbiologia, Parasitologia e Patologia.

Orientadora: Profª. Drª. Juliana Ferreira de Moura

Coorientador: Prof. Dr. Mauro Antônio Alves Castro

Coorientador: Prof. Dr. Bonald Cavalcante Figueiredo

CURITIBA

2022

DADOS INTERNACIONAIS DE CATALOGAÇÃO NA PUBLICAÇÃO (CIP)
UNIVERSIDADE FEDERAL DO PARANÁ
SISTEMA DE BIBLIOTECAS – BIBLIOTECA DE CIÊNCIAS BIOLÓGICAS

Muzzi, João Carlos Degraf.
Análise in silico de dados imuno-oncogenômicos em carcinoma de córtex adrenal. / João Carlos Degraf Muzzi. – Curitiba, 2022.
1 recurso on-line : PDF.

Orientadora: Juliana Ferreira de Moura.
Coorientador: Mauro Antônio Alves Castro.
Coorientador: Bonald Cavalcante Figueiredo.

Tese (Doutorado) – Universidade Federal do Paraná, Setor de Ciências Biológicas. Programa de Pós-Graduação em Microbiologia, Parasitologia e Patologia.

1. Carcinoma. 2. Câncer – Aspectos imunológicos. 3. Câncer – Imunoterapia. 4. Oncologia – Efeito das drogas. 5. Bioinformática. I. Título. II. Moura, Juliana Ferreira de. III. Castro, Mauro Antônio Alves. IV. Figueiredo, Bonald Cavalcante. V. Universidade Federal do Paraná. Setor de Ciências Biológicas. Programa de Pós-Graduação em Microbiologia, Parasitologia e Patologia.

Bibliotecária: Rosilei Vilas Boas- CRB-9/939

ATA Nº55

ATA DE SESSÃO PÚBLICA DE DEFESA DE DOUTORADO PARA A OBTENÇÃO DO GRAU DE DOUTOR EM MICROBIOLOGIA, PARASITOLOGIA E PATOLOGIA

No dia trinta de novembro de dois mil e vinte e dois às 14 horas, na sala B08, SEPT, foram instaladas as atividades pertinentes ao rito de defesa de tese do doutorando **JOAO CARLOS DEGRAF MUZZI**, intitulada**: Análise *in silico* de dados imuno-oncogenômicos em carcinoma de córtex adrenal**. A Banca Examinadora, designada pelo Colegiado do Programa de Pós-Graduação MICROBIOLOGIA, PARASITOLOGIA E PATOLOGIA da Universidade Federal do Paraná, foi constituída pelos seguintes Membros: BONALD CAVALCANTE DE FIGUEIREDO (FACULDADE PEQUENO PRÍNCIPE E INSTITUTO PEQUENO PRÍNCIPE), DANIELA FIORI GRADIA (UNIVERSIDADE FEDERAL DO PARANÁ), FABIO PASSETTI (INSTITUTO CARLOS CHAGAS/FIOCRUZ), VLADMIR CLAUDIO CORDEIRO DE LIMA (FUNDAÇÃO ANTONIO PRUDENTE - HOSPITAL A. C. CAMARGO). A presidência iniciou os ritos definidos pelo Colegiado do Programa e, após exarados os pareceres dos membros do comitê examinador e da respectiva contra argumentação, ocorreu a leitura do parecer final da banca examinadora, que decidiu pela APROVAÇÃO. Este resultado deverá ser homologado pelo Colegiado do programa, mediante o atendimento de todas as indicações e correções solicitadas pela banca dentro dos prazos regimentais definidos pelo programa. A outorga de título de doutor está condicionada ao atendimento de todos os requisitos e prazos determinados no regimento do Programa de Pós-Graduação. Nada mais havendo a tratar a presidência deu por encerrada a sessão, da qual eu, BONALD CAVALCANTE DE FIGUEIREDO, lavrei a presente ata, que vai assinada por mim e pelos demais membros da Comissão Examinadora.

CURITIBA, 30 de Novembro de 2022.

Assinatura Eletrônica
06/12/2022 19:22:49.0
BONALD CAVALCANTE DE FIGUEIREDO
Presidente da Banca Examinadora

Assinatura Eletrônica
01/12/2022 11:19:10.0
DANIELA FIORI GRADIA
Avaliador Externo (UNIVERSIDADE FEDERAL DO PARANÁ)

Assinatura Eletrônica
09/12/2022 09:22:42.0
FABIO PASSETTI
Avaliador Externo (INSTITUTO CARLOS CHAGAS/FIOCRUZ)

Assinatura Eletrônica
05/12/2022 21:51:05.0
VLADMIR CLAUDIO CORDEIRO DE LIMA
Avaliador Externo (FUNDAÇÃO ANTONIO PRUDENTE - HOSPITAL A. C. CAMARGO)

Documento assinado eletronicamente de acordo com o disposto na legislação federal Decreto 8539 de 08 de outubro de 2015.
Gerado e autenticado pelo SIGA-UFPR, com a seguinte identificação única: 239483
Para autenticar este documento/assinatura, acesse https://www.prppg.ufpr.br/siga/visitante/autenticacaoassinaturas.jsp e insira o codigo 239483

TERMO DE APROVAÇÃO

Os membros da Banca Examinadora designada pelo Colegiado do Programa de Pós-Graduação MICROBIOLOGIA, PARASITOLOGIA E PATOLOGIA da Universidade Federal do Paraná foram convocados para realizar a arguição da tese de Doutorado de **JOAO CARLOS DEGRAF MUZZI** intitulada: **Análise *in silico* de dados imuno-oncogenômicos em carcinoma de córtex adrenal**, que após terem inquirido o aluno e realizada a avaliação do trabalho, são de parecer pela sua APROVAÇÃO no rito de defesa.

A outorga do título de doutor está sujeita à homologação pelo colegiado, ao atendimento de todas as indicações e correções solicitadas pela banca e ao pleno atendimento das demandas regimentais do Programa de Pós-Graduação.

CURITIBA, 30 de Novembro de 2022.

Assinatura Eletrônica
06/12/2022 19:22:49.0
BONALD CAVALCANTE DE FIGUEIREDO
Presidente da Banca Examinadora

Assinatura Eletrônica
01/12/2022 11:19:10.0
DANIELA FIORI GRADIA
Avaliador Externo (UNIVERSIDADE FEDERAL DO PARANÁ)

Assinatura Eletrônica
09/12/2022 09:22:42.0
FABIO PASSETTI
Avaliador Externo (INSTITUTO CARLOS CHAGAS/FIOCRUZ)

Assinatura Eletrônica
05/12/2022 21:51:05.0
VLADMIR CLAUDIO CORDEIRO DE LIMA
Avaliador Externo (FUNDAÇÃO ANTONIO PRUDENTE - HOSPITAL A. C. CAMARGO)

In memoriam de João Carlos Moraes Muzzi

A Deus, criador do Universo, da ciência e do conhecimento. A meus pais e avós por me trazerem até aqui e a minha esposa e filhos por me levarem adiante. Aos pacientes desenganados, dedico meu trabalho e esforço a vocês, para que um dia a esperança volte a florescer.

AGRADECIMENTOS

Acredito que por vezes Deus nos coloca em situações onde nossas próprias forças são incapazes de superar. Nesse momento, percebemos que não é e jamais foi por mérito próprio que conseguimos alcançar qualquer sucesso, por menor ou mais grandioso que seja. Apesar de esse trabalho carregar meu nome como autor e mesmo havendo algum grau de esforço de minha parte para que ele pudesse ser realizado, tenho a mais plena convicção de que ele jamais teria sido possível sem o amor que recebi ao longo desses anos, os quais me proporcionaram a ajuda, suporte e apoio indispensáveis para que algumas vezes eu simplesmente pudesse seguir em frente. Infelizmente, palavras não serão suficientes para expressar a dimensão de como pequenas (e grandes) atitudes foram muitas vezes o essencial para que eu pudesse continuar nesse caminho.

Antes de mais nada e acima de tudo, agradeço a Deus. Eu O agradeço por minha vida, por restaurar minha saúde e me dar a capacidade física e mental para realizar esse trabalho. Agradeço pelas orações atendidas nos momentos em que somente Ele poderia me responder. Agradeço por literalmente ter me tirado da escuridão e me trazido à luz de Sua Salvação e de Sua Palavra. A Ele seja dada a honra e a Glória para sempre.

Ao meu pai, João Carlos Moraes Muzzi, que me indicou o caminho, ensinou-me a honra, o amor a Deus, aos necessitados, à família e ao meu país. Ele que desde cedo me instruiu e conduziu no caminho do conhecimento, da ética e da moral. Espero que do Céu você possa receber meu amor e minha gratidão por tudo e espero que ao nos reencontrarmos, eu possa ter a certeza de ter honrado seus ensinamentos e seu exemplo.

À minha mãe, Jacqueline Degraf Muzzi, que me deu o exemplo da perseverança e do amor. A força de continuar quando não se tem mais forças, quando não se tem mais ânimo, quando necessário extrapolar as próprias capacidades físicas e emocionais, ainda assim, continuar por amor àqueles que dependem de nós. Só posso agradecer por confiar em mim mesmo quando eu não confiava mais e sempre me apoiar e me dar esperanças quando eu fraquejava.

Aos meus avós Silas e Leony Degraf pelas palavras tenras, boas histórias, pelos cafés, lições e por sempre abrirem um sorriso lindo no rosto quando eu

contava alguma nova conquista. Vocês são e foram minha inspiração e motivação para que eu sempre tenha boas notícias para lhes orgulhar.

À minha esposa Elaine e filhos Joaquim e Daniel, minhas maiores motivações. A vocês agradeço simplesmente por existirem, só suas presenças muitas vezes era o que eu precisava para me fortalecer, para tentar dar o melhor de mim e ser capaz de oferecer uma vida melhor a vocês. Vocês são o principal fruto de meu amor, e foi esse amor que me fez ir muito além do que eu jamais pensaria ser capaz de chegar. Só posso dizer muito obrigado por me apoiarem e estarem ao meu lado ao longo de toda essa trajetória preenchendo minha vida de amor e felicidade.

Ao meu irmão e melhor amigo, Julio C. D. Muzzi, meu companheiro de valores, conselheiro e confidente. Obrigado pelas palavras e incentivo e pelos conselhos sempre valiosos. Acima de tudo, obrigado por compartilhar dos mesmos valores essenciais e visões de mundo o que me ajuda a sempre me manter no caminho que nos propusemos. Obrigado à Elisa F. dos Santos por estar sempre presente quando eu precisei e ao João Gustavo e Leonardo por trazerem mais alegria à minha vida.

À minha orientadora, professora e amiga Dra. Juliana Ferreira de Moura, não sei se um dia serei capaz de agradecer à altura o que você fez por mim. Só desejo que Deus lhe retribua todo o bem que me fez nesse período. Agradeço seu carinho, sua orientação não somente acadêmica, mas muitas vezes pessoal e profissional, seu esforço e dedicação, sua preocupação e humanidade. Você me abriu portas quando eu estava sem caminhos a seguir e quando necessário me empurrou para que eu pudesse atravessá-las. Não tenho como descrever o significado e importância que você teve nesse momento de minha vida. Meu muito obrigado.

Ao prof. Dr. Bonald Figueiredo Cavalcanti, eu te agradeço por confiar em mim, agradeço por me dar tantas oportunidades, começando pela de trabalhar com o carcinoma de córtex adrenal quando meu projeto original de doutorado estava estagnado. Agradeço por me auxiliar a conseguir a bolsa pelo projeto Big Data em um dos momentos que mais precisei. Agradeço por ajudar na cirurgia de meu filho. Obrigado por além de me orientar e ensinar, ser um verdadeiro amigo.

Ao prof. Dr. Mauro Antônio de Castro, obrigado por me aceitar em seu laboratório, mesmo sem ter nenhuma experiência prévia em Bioinformática. Agradeço pela paciência em me ensinar e orientar, mesmo quando cometia erros crassos ou fazia comentários despropositados. Obrigado pelas excelentes

discussões, aprendizados e técnicas. Levarei para minha vida muitos dos seus conselhos e rigor científico. Agradeço muito por ter sua orientação nesse trabalho, o qual certamente não teria sido possível sem sua participação.

Aos professores doutores Larissa Magalhães Alvarenga, Giseli Klassen, Jaqueline Carvalho de Oliveira, Daniela F. Gradia, Liza Felicori Vilela, e demais professores e servidores do PPG em Patologia, Microbiologia e Parasitologia, do PPG em Bioinformática e das demais disciplinas e cursos que auxiliaram na minha formação ao longo desses anos, agradeço o amor ao ensino, as oportunidades, a paciência e a dedicação à tão nobre tarefa de formar novos profissionais.

Aos meus colegas Ms. Jéssica Maria Magno, Dra. Carolina Mathias, Ms. Bruna Borba Antunes, Jean da Silva Resende e Milena A. Cardoso, agradeço o companheirismo e horas de trabalho e aprendizado juntos. Vocês tornaram as atividades compartilhadas muito mais leves e prazerosas.

Aos meus sogros, José Roberto e Célia Seullner por me darem o apoio inicial na minha retomada profissional e me auxiliarem no sustento de minha casa enquanto eu ainda estava me reconstruindo financeiramente. Eu jamais teria aceitado esse desafio se não fosse pelo seu apoio. Muito obrigado! Ao William, Lívia e Lara Seullner, agradeço por torcerem por mim mesmo à distância.

Aos meus amigos Willian Keller, Sabrina Vega, Ronaldo e Mariana Nakato, Patrick e Renata Fonseca, Humberto e Vanessa Cavamura, Gustavo e Aline Katayama agradeço pelas risadas, pelos sempre bons momentos juntos, mas acima de tudo pelo apoio nos momentos difíceis. Não haverá palavras para agradecer o amor que vocês dedicaram a mim e a meus filhos quando precisamos. Eu só tenho a agradecer a vocês pela amizade e companheirismo de sempre, e a Deus por me dar bons amigos como vocês. Igor Vieira, meu amigo e ex-aluno, obrigado por sempre me apoiar e estar ao meu lado, obrigado por sempre torcer por mim. Seu respeito e consideração me impulsionam a ser melhor.

À família Degraf, vocês estiveram ao meu lado nos momentos tristes, vocês acompanharam minha trajetória e espero que possam acompanhar também meus momentos de sucesso. Obrigado por estarem presente nos bons e maus momentos e sempre torcerem pela minha felicidade!

À minha tia-avó Sirlei Degraf por desde cedo me incentivar a escrever e por vibrar com minhas conquistas acadêmicas. Saiba que sua luta contra o câncer foi

para mim exemplo de perseverar na esperança e serviu de motivação ao meu trabalho.

À 1ª Igreja Irmãos Menonitas do Boqueirão, obrigado por terem me acolhido quando mais precisei. Obrigado por me instruírem no Bom Caminho e compartilharem comigo a caminhada.

Ao meu sensei Douglas Carneiro e meus colegas de Karatê, obrigado por me ensinarem caráter, sinceridade, persistência, repeito e autocontrole. Atributos essenciais que me permitiram chegar aqui.

Agradeço à CAPES e à Associação Hospitalar de Proteção à Infância Raul Carneiro – AHPIRAC pela bolsa científica essencial para a execução desse trabalho e sustento de minha casa durante esse período. Agradeço pela oportunidade em ter tido uma renda fixa enquanto tantos a perderam durante a pandemia.

“Filho, não vou te deixar grandes bens como herança, mas te deixo conhecimento e através dele você deve ser capaz de alcançar seus próprios sonhos.” (João Carlos Moraes Muzzi, meu pai, em algum momento de 2004)

RESUMO

O carcinoma de córtex adrenal (CCA) é um tumor raro e agressivo com poucas alternativas de tratamento e mau prognóstico. Ensaios clínicos com imunoterápicos tiveram resultados modestos em parte devido ao microambiente tumoral imunologicamente "frio" desse tipo de tumor. Alguns autores afirmaram que pacientes de CCA dificilmente se beneficiariam de imunoterapia devido à baixa presença do infiltrado linfocitário nos estágios 3 e 4. Nesse trabalho, utilizamos dados públicos para investigar as características imunológicas do ambiente intratumoral de CCA de adultos correlacionando-as a fenótipos moleculares, dados clínicos e ao cenário regulatório. Nós mostramos que o fenótipo esteroidal distingue a resposta imunológica e pode ser usado para selecionar pacientes passíveis de se beneficiarem da imunoterapia. Mostramos que pacientes com o perfil esteroidal baixo apresentam uma presença significativa de infiltrado leucocitário e de marcadores de ativação imunológica, comparável a outros tumores considerados como imunologicamente "quentes". Apresentamos o cenário regulatório de CCA e como ele se correlaciona a essa classificação molecular, assim como a marcadores de proliferação. Finalmente, apontamos possíveis alvos e os principais reguladores associados a esse fenótipo e às variáveis imunológicas. Além da presença de hormônios imunossupressores, destacamos como possíveis causas para os resultados modestos de imunoterápicos a alta expressão de *CD276* (B7-H3), um inibidor de resposta às terapias de bloqueio anti-PD-1/PD-L1, e a maior expressividade de *PDCD1LG2* (PD-L2) comparada à de *CD274* (PD-L1) em pacientes com baixo perfil esteroidal. No cenário regulatório, destacamos o *CENPA* como um fator de transcrição a ser investigado, visto sua alta correlação com proliferação e prognóstico e *ZBTB-4* como um possível alvo anti-tumorigênico drogável. Nossos resultados apontam para um novo critério de seleção de pacientes à imunoterapia, além de indicar possíveis alvos a serem investigados em estudos *in vivo* e *in vitro*. Antecipamos que os dados aqui apresentados poderão servir como base para novas frentes de esforço clínico e científico no combate a esse câncer de difícil tratamento.

Palavras-chave: carcinoma de córtex adrenal, imunoterapia, imuno-oncologia, bioinformática

ABSTRACT

Adrenal cortex carcinoma (ACC) is a rare and aggressive tumor with few treatment alternatives and poor prognosis. Clinical trials with immunotherapeutics had modest results in part due to the immunologically “cold” tumor microenvironment of this type of tumor. Some authors stated that ACC patients would hardly benefit from immunotherapy due to the low presence of lymphocytic infiltrate. In this work, we used public data to investigate the immunological characteristics of the intratumoral environment of ACC by correlating them with molecular phenotypes, clinical data and the regulatory scenario. We show that the steroid phenotype distinguishes the immune response and can be used to select patients likely to benefit from immunotherapy. We showed that patients with a low steroid profile have a significant presence of leukocyte infiltrate and markers of immunological activation, comparable to other tumors considered to be immunologically “hot”. We present the regulatory landscape of CCA and how it correlates to this molecular classification, as well as to markers of proliferation. Finally, we point out possible targets and the main regulators associated with this phenotype and immunological variables. Beyond the presence of immunosuppressive hormones, we highlight as possible causes for the modest results of immunotherapies the high expression of *CD276 (*B7-H3), an inhibitor of response to anti-PD-1/PD-L1 blocking therapies, and the greater expressiveness of *PDCD1LG2* (PD-L2) compared to that of *CD274* (PD-L1) in patients with a low steroid profile. In the regulatory scenario, we highlight *CENPA* as a transcription factor to be investigated, given its high correlation with proliferation and prognosis, and *ZBTB-4* as a possible druggable anti-tumorigenic target. Our results point to a new criterion for selecting patients for immunotherapy, in addition to indicating possible targets to be investigated in *in vivo* and *in vitro* studies. We anticipate that the data presented here may serve as a basis for new fronts of clinical and scientific effort in the fight against this difficult-to-treat cancer.

Keywords: adrenal cortex carcinoma, immunotherapy, immuno-oncology, bioinformatics

SUMÁRIO

1 INTRODUÇÃO.....16
2 REVISÃO DE LITERATURA.....19
2.1 CARCINOMA DE CÓRTEX ADRENAL (CCA).....19
2.2 IMUNO-ONCOLOGIA E IMUNOTERAPIA.....22
2.3 CARCINOMA DE CÓRTEX ADRENAL E O SISTEMA IMUNOLÓGICO.....23
3 CAPÍTULO I: ADRENOCORTICAL CARCINOMA STEROID PROFILES: IN SILICO PAN-CANCER ANALYSIS OF TCGA DATA UNCOVERS IMMUNOTHERAPY TARGETS FOR POTENTIAL IMPROVED OUTCOMES (60). .25
3.1 ABSTRACT.....25
3.2 INTRODUCTION.....26
3.3 MATERIALS AND METHODS.....29
3.3.1 Data Sources.....29
3.3.2 Leukocyte Fraction and Immune Infiltrate Comparison.....30
3.3.3 RNA-seq Filtering, Processing, and Differential Expression (DE).....31
3.3.4 Enrichment Analysis.....31
3.3.5 Expression of Immune Modulators and Immune Checkpoints.....32
3.3.6 Leukocyte Fractions and Mutations in the ACC Cohort.....32
3.3.7 Extracellular Communication Networks in Immune Subtypes.....32
3.3.8 Survival Analysis.....33
3.3.9 Statistical Analysis.....33
3.4 RESULTS.....33
3.4.1 Pan-Cancer Comparison Showed Significant Immune Infiltrates in Patients With LSP ACC.....33
3.4.2 Immune Activation Was Enriched in Patients With LSP ACC.....37
3.4.3 Enrichment of T Cells, Monocytes, and Cytolytic Activity in LSP ACC.....40
3.4.4 LSP Was Associated With an Inflammatory Immune Response and HSP With a Lymphocyte Depleted Microenvironment.....40
3.4.5 Steroid Phenotype Generated a Confounding Effect on the Correlation Between Leukocyte Fraction and Driver Gene Mutations.....42
3.4.6 Extracellular Communication Networks and Possible Immunotherapy Targets Associated With Steroid Phenotypes.....43

3.4.7 Steroid Phenotype Was More Predictable of Outcome Than Immune Subtype Alone....48
3.5 DISCUSSION....48
3.6 CONCLUSIONS....54
3.7 CODE AVAILABILITY AND REPRODUCIBILITY....54
3.8 DATA AVAILABILITY STATEMENT....55
3.9 ETHICS STATEMENT....55
3.10 AUTHOR CONTRIBUTIONS....55
3.11 FUNDING....55
3.12 CONFLICT OF INTEREST....55
3.13 ACKNOWLEDGMENTS....55
3.14 SUPPLEMENTARY MATERIAL....56
3.15 REFERENCES....56
4 CAPÍTULO II: COMPREHENSIVE CHARACTERIZATION OF THE REGULATORY LANDSCAPE OF ADRENOCORTICAL CARCINOMA: NOVEL TRANSCRIPTION FACTORS AND TARGETS ASSOCIATED WITH PROGNOSIS (61)....63
4.1 GRAPHICAL ABSTRACT....64
4.2 INTRODUCTION....64
4.3 METHODS....66
4.3.1 The Cancer Genome Atlas-ACC data....66
4.3.2 Regulon inference....67
4.3.3 Regulon activity....67
4.3.4 Survival analysis....67
4.3.5 Clustering....67
4.3.6 Steroid and proliferation classification....68
4.3.7 Differential expression for Steroid and Proliferation phenotypes....68
4.3.8 Transcriptional Network Analysis (TNA)....68
4.3.9 Functional annotation with MSigDb Hallmarks....68
4.3.10 Immune correlation....68
4.3.11 Duals inference....69
4.3.12 ENSAT cohort data....69
4.3.13 Regulon activity and survival analysis in the ENSAT cohort....69
4.3.14 Statistics and visualization....69
4.4 3. RESULTS....70

4.4.1 The identification of 369 regulons with prognostic values related to molecular phenotypes and leukocyte fractions....70
4.4.2 Consensus clustering resulted in four regulon clusters with different functional and molecular characteristics....70
4.4.3 The ENSAT cohort confirmed the prognostic value of 89.5% of the regulons related to survival on TCGA-ACC....72
4.4.4 NR5A1 relates to worse outcomes in TCGA-ACC and ENSAT cohorts. CENPA has a strong association with proliferation and relates to a bad prognosis....76
4.5 DISCUSSION....80
4.6 CONCLUSIONS....83
4.7 SUPPLEMENTARY MATERIALS....83
4.8 AUTHOR CONTRIBUTIONS....84
4.9 FUNDING....84
4.10 DATA AVAILABILITY STATEMENT....85
4.11 ACKNOWLEDGMENTS....85
4.12 CONFLICTS OF INTEREST....85
4.13 REFERENCES....85
5 CONSIDERAÇÕES FINAIS....92
REFERÊNCIAS....96
APÊNDICE 1 - RESUMO DE ATIVIDADES REALIZADAS....122
APÊNDICE 2 – MATERIAL SUPLEMENTAR PARA A COMPREHENSIVE CHARACTERIZATION OF THE REGULATORY LANDSCAPE OF ADRENOCORTICAL CARCINOMA: NOVEL TRANSCRIPTION FACTORS AND TARGETS ASSOCIATED WITH PROGNOSIS....127
APÊNDICE 3 - UNRAVELING IMMUNE-RELATED LNCRNAS IN BREAST CANCER MOLECULAR SUBTYPES....138

1 INTRODUÇÃO

As neoplasias malignas representam uma das principais causas de morte em todo o mundo (1). Caracterizadas por grande instabilidade genética, as neoplasias são altamente heterogêneas, mesmo quando oriundas do mesmo tecido de origem, o que torna os tratamentos e prognósticos variáveis de paciente para paciente.

Os tumores mais comuns movimentam grandes somas de valores monetários e humanos no esforço de melhor compreender causas, fatores preditivos, prognósticos e tratamentos. Drogas antitumorais representam parcelas significativas do lucro de grandes farmacêuticas (2,3). Contudo, tumores raros não despertam o mesmo interesse. Segundo o *Orphan Drug Act* dos Estados Unidos da América, o custo de desenvolvimento de fármacos não seria recuperável em vendas para doenças que afetem menos do que 200.000 pessoas na população total estadunidense (4). Portanto, iniciativas públicas e filantrópicas são necessárias para o estudo de doenças raras. Nesse sentido, o Instituto de Pesquisas Pelé Pequeno Príncipe (IPPPP) e a Universidade Federal do Paraná (UFPR) se uniram em projetos de pesquisa referente ao carcinoma de córtex adrenal (CCA), sendo o presente estudo fruto dessa parceria.

O CCA é um tumor raro e agressivo, com uma incidência mundial entre 0,7 a 2 casos por milhão de habitantes, majoritariamente em adultos acima de 40 anos (5). Entretanto, no sul brasileiro essa taxa salta para 3,4 casos/milhão, afetando principalmente crianças, em função da maior prevalência da mutação de *TP53* R337H nessa região (6), a qual favorece o desenvolvimento desse carcinoma nos primeiros anos de vida (7–9). Nos últimos 30 anos, houve poucos avanços no tratamento do CCA. O tratamento primário envolve a ressecção cirúrgica, enquanto terapias adjuvantes como administração de mitotano, radioterapia ou agentes citotóxicos são indicados para estádios avançados (5). Entretanto, a sobrevida em 5 anos fica entre 0 a 28% em casos metastáticos (10).

A imunologia ganhou grande destaque na oncologia após o advento das imunoterapias. Essas técnicas têm como objetivo melhorar a resposta imunológica contra o tumor e apresentaram resultados muito promissores em tumores antes tidos como incuráveis, como em casos de melanoma metastático, carcinoma de células

renais e linfomas (11). Infelizmente, apesar das expectativas iniciais, os ensaios clínicos de imunoterápicos para CCA tiveram resultados modestos e heterogêneos (12). Alguns autores chegaram a afirmar que pacientes de CCA dificilmente se beneficiariam da imunoterapia (13).

Tumores raros como o CCA apresentam limitações extras na realização de ensaios clínicos ou estudos de acompanhamento devido à dificuldade em se encontrar pacientes e amostras em quantidade suficiente. Por esse motivo, análises *in silico* podem auxiliar a apontar frentes de pesquisa mais promissoras e assertivas para esses tumores.

Dentro desse contexto, o presente trabalho teve como objetivo utilizar da bioinformática e coortes públicas para investigar dados de expressão gênica de pacientes com CCA de adultos, com foco nas variáveis imunológicas e fenotípicas que possam auxiliar no entendimento da doença e sua correlação com o sistema imunológico. Os achados podem não refletir a mesma realidade no CCA pediátrico, considerando que há muitas diferenças clínicas, hormonais, moleculares e de prognóstico entre estas duas faixas etárias (14).

No Capítulo I, apresentamos o artigo "*Adrenocortical Carcinoma Steroid Profiles: In Silico Pan-Cancer Analysis of TCGA Data Uncovers Immunotherapy Targets for Potential Improved Outcomes*" publicado na revista *Frontiers in Endocrinology* (Fator de Impacto = 6.055) em 2021. Nesse artigo demonstramos como o fenótipo molecular Esteroidal Alto e Esteroidal Baixo é capaz de distinguir os pacientes com imunossupressão daqueles com sinais de ativação da resposta imunológica. Apresentamos como os pacientes com perfil Esteroidal Baixo comparados aos de perfil Esteroidal Alto apresentam mais marcadores de resposta citotóxica, maior presença de mecanismos de evasão, além de maior infiltrado linfocitário. Para esse último, mostramos que pacientes de CCA com perfil Esteroidal Baixo apresentam quantidades significativas de células imunológicas no ambiente intratumoral, mesmo quando comparados a outras malignidades. Esse resultado representou uma quebra de paradigma na área, visto que o CCA como um todo era tido como um tumor imunologicamente "frio" (13). Por fim, ainda apresentamos possíveis novos alvos e justificativas para os resultados modestos dos ensaios clínicos com imunoterápicos.

No Capítulo II, apresentamos o artigo intitulado "*Comprehensive characterization of the regulatory landscape of Adrenocortical Carcinoma: novel transcription factors and targets associated with prognosis*" publicado na revista *Cancers* (Fator de Impacto = 6.575) em 2022. Nesse trabalho, reconstruímos a rede regulatória de CCA utilizando a matriz de expressão de genes codificantes. Para isso inferimos unidades regulatórias denominadas regulons, os quais são caracterizados como um fator de transcrição e seus alvos diretos e indiretos. Selecionamos os regulons que apresentam associação à sobrevida geral e os caracterizamos com anotações funcionais e correlações com variáveis fenotípicas e imunológicas. Apontamos quatro grupos de regulons associados aos fenótipos moleculares relacionados ao perfil Esteroidal e à Proliferação, além de apresentar fatores de transcrição que se apresentam como promissores alvos terapêuticos em outros tumores e que também se destacaram em nossas análises associadas ao CCA.

Esse trabalho tem como objetivo compreender os mecanismos de interação entre o sistema imunológico e o CCA. Especificamente, buscamos possíveis causas para as falhas nos ensaios clínicos de imunoterapia até o momento, subgrupos de pacientes que possam diferenciar a ativação ou supressão da resposta imunológica e apontar possíveis alvos terapêuticos ou prognósticos.

2 REVISÃO DE LITERATURA

2.1 CARCINOMA DE CÓRTEX ADRENAL (CCA)

Apesar de raro, o CCA é um tumor agressivo, cujo estádio de apresentação é um fator prognóstico crucial. Para tumores limitados à adrenal, a expectativa de sobrevivência em cinco anos é de 60 a 80%, a qual cai para 0 a 28% nos casos metastáticos (10). Apesar de poder se desenvolver em qualquer faixa etária, o CCA apresenta uma incidência etária bimodal, sendo mais comum em adultos na quarta e quinta décadas de vida e em crianças até 5 anos (12). Além disso, aparece em maior frequência em mulheres tanto nos casos pediátricos quanto adultos (55-60%) (5).

Os sintomas típicos tendem a se manifestar devido à produção excessiva de hormônios (50 a 60% dos pacientes) ou dores abdominais causadas pelo crescimento tumoral nos estádios 3 e 4 (30 a 40% dos pacientes) (15,16). Aproximadamente 60% dos pacientes adultos apresentam atividade endócrina aumentada, comumente com aumento na produção de esteroides (associados à Síndrome de Cushing, a qual atinge de 50 a 60% dos pacientes de CCA) e com menor frequência de hormônios sexuais (12,16). Nos casos pediátricos, a produção de hormônios sexuais são mais frequentes e em menor proporção a presença de excesso de corticoides (17). Alguns dos sintomas associados ao excesso de corticoides são o aumento na gordura abdominal, hipertensão arterial, resistência à insulina, além de redução da atividade imunológica (18)

A avaliação histopatológica é a recomendação primária para confirmação da malignidade e é baseada no escore de Weiss (16,19,20). Na Classificação de Tumores de Córtex Adrenal da Organização Mundial da Saúde de 2022, além do escore de Weiss, há indicação do uso de outros esquemas multiparamétricos de diagnóstico como o sistema Lin-Weiss-Bisceglia, algoritmo de reticulina e o sistema de escore de Helsinki para tumores adultos e o sistema Wieneke para tumores pediátricos (19). Além disso, a avaliação da taxa de proliferação tumoral pela contagem mitótica e índice de marcação de Ki67 são indicadas, visto sua importância prognóstica (19). O Fator Esteroidogênico 1 (SF1) é o biomarcador mais confiável na confirmação da origem adrenocortical e se associa ao aumento do metabolismo de esteroides, de proliferação e pior prognóstico (19,21). Além do SF1,

a superexpressão do fator de crescimento semelhante à insulina (IGF2) pode ser utilizada na distinção de malignidade (19).

As alterações genéticas mais comuns em CCA se associam aos genes *TP53*, *CTNNB1*, *SF1* e alterações no locus 11p15. Mutações germinativas em *TP53* são encontradas em cerca de 4% dos pacientes adultos de CCA e em 60 a 80% dos casos pediátricos (5). No sul e sudeste brasileiros, a mutação de *TP53* R337H pode ser encontrada em até 90% dos pacientes pediátricos de CCA (8), o que justifica a maior taxa mundial de incidência desse tumor raro nessa região. As mutações somáticas mais comuns em CCA são encontradas nos genes *TP53*, encontrada em até 50% dos pacientes adultos (5), e *CTNNB1.* Nesse último, levando à ativação da via WNT/β-catenina conferindo vantagens proliferativas à neoplasia (5,16), enquanto o aumento na expressão de SF1 se associa a pior prognóstico e ao hipercortisolismo (22,23). Por fim, alterações no locus 11p15 levam ao aumento da expressão de *IGF2*, a qual foi identificada como associada à maior proliferação *in vitro.* Entretanto, correlações prognósticas não foram possíveis de serem verificadas, pelo fato de a superexpressão de *IGF2* ser encontrada em quase 90% dos casos de CCA (5).

Vários estudos moleculares demonstraram que o CCA poderia ser classificado em subtipos com distinções biológicas e prognósticas (16). O *European Network for the Study of Adrenal Tumors* (ENSAT), a partir do agrupamento de dados de expressão gênica de 44 participantes, classificou as amostras de CCA em dois subgrupos: a forma mais agressiva C1A e uma forma mais indolente e de melhor prognóstico, C1B (24). A maior coorte pública de CCA se encontra dentro do programa do *The Cancer Genomic Atlas* (TCGA) com 91 amostras de CCA. A caracterização pan-molecular dessas amostras, permitiu a classificação em três grupos com diferenças prognósticas: CoC I, CoC II e CoC III (25). Os mesmos autores apresentaram outras possíveis classificações baseadas no perfil de metilação (*CIMP high, intermediate e low*), proteoma (1, 2 e 3), miRNA (miRNA 1 a 6) e transcriptoma. Para essa última, os autores separam em dois subgrupos inicialmente: Perfil Esteroidal Alto e Perfil Esteroidal Baixo. Esses grupos se associavam à maior e menor ativação das vias de biossíntese de esteroides respectivamente. O refinamento dessa classificação gerou quatro subgrupos adicionando ao perfil esteroidal o escore molecular de proliferação: Perfil Esteroidal

Alto, Perfil Estoidal Alto + Proliferação, Perfil Esteroidal Baixo e Perfil Esteroidal Baixo + Proliferação (25).

Além das classificações moleculares, outros estudos foram feitos em busca de assinaturas prognósticas a partir de redes de interação proteína-proteína ou de co-expressão. O estudo de Xu e colaboradores (26) identificou cinco genes como fatores prognósticos independentes usando regressão de Lasso Cox: *ZWINT, PRC1, CDKN3, CDK1* e *CCNA2.* Xing e colaboradores *(27)* apontaram 11 genes relacionados a pior prognóstico a partir da análise de Kaplan-Meier: A*URKA, TYMS, GINS1, RACGAP1, RRM2, EZH2, ZWINT, CDK1, CCNB1, NCAPG* e *TPX2.* Por fim, um estudo de Yuan e colaboradores (28) apresentou 12 genes associados à sobrevida: *ANLN, ASPM, CDCA5, CENPF, FOXM1, PCLAF, MELK, NDC80, PRC1, RACGAP1, SPAG5* e *TPX2.*

Apesar de as classificações e marcadores moleculares apresentarem importância prognóstica, ainda não foi possível convertê-las em estratégias de tratamento. A única intervenção com potencial curativo é a ressecção cirúrgica. Contudo, essa opção só é aplicável em pacientes em estádios I e II e raramente, para estádios III. Ainda assim, de 30 a 70% dos pacientes que passam pela ressecção radical apresentam recorrência do tumor (13). O mitotano é a única droga aprovada para tratamento de CCA, apesar de apresentar eficácia limitada e efeitos adversos significativos (12,13,29). Esse medicamento pode ser administrado sozinho ou em conjunto com etoposida, doxorubicina e cisplatina. Para pacientes com progressão mesmo após o tratamento primário, podem ser administrados estreptozotocina, gemcitabina ou capecitabina como tratamentos de segunda linha, apesar da baixa eficácia (12,29,30).

Após o advento das imunoterapias, ensaios clínicos foram feitos em pacientes de CCA, mas infelizmente apresentaram resultados modestos. No ensaio clínico 1B internacional JAVELIN, 50 pacientes metastáticos de CCA foram tratados com avelumabe (anti-PDL1), dos quais somente 3 (6%) apresentaram uma resposta parcial. A sobrevida média observada foi de 10,6 meses, um resultado próximo aos obtidos com os tratamentos de segunda linha para CCA como gemcitabina e capecitabina (13,31). Com esses resultados, a imunoterapia, apesar de promissora para outros tumores, não representou um avanço no tratamento de CCA. Além desse primeiro ensaio clínico, outros quatro estudos foram realizados testando

outros imunoterápicos como nivolumabe, pembrolizumabe e ipilimumabe em pacientes de CCA, mas todos com resultados modestos (31–35).

2.2 IMUNO-ONCOLOGIA E IMUNOTERAPIA

Hanahan e Weinberg em 2000 (36) apresentaram os seis *hallmarks* do câncer, tornando-se um marco na oncologia. Onze anos após sua primeira publicação, os mesmos autores adicionaram à sua lista anterior quatro novos *hallmarks,* à época considerados emergentes (37). Em sua última listagem de 2022, esses quatro novos *hallmarks* foram considerados integrantes do grupo principal, em função de sua “suficiente validação” (38). Dos quatro *hallmarks* acrescentados, dois se referem à associação entre o tumor e o sistema imunológico: evasão de destruição imunológica e inflamação promotora do tumor.

Estudos visando compreender a complexa interação entre o sistema imunológico e a progressão levaram à identificação de mecanismos pelos quais os tumores são capazes de evadir da resposta imunológica. Esse conhecimento conduziu às terapias de bloqueio dessas vias, representando um dos maiores avanços nos tratamentos oncológicos das últimas décadas (39). Em 2011, foi aprovado o primeiro inibidor de *checkpoint* imunológico pelo *Food and Drug Administration* (FDA) estadunidense, um bloqueador do atenuador imunológico proteína 4 associada a linfócitos de células T citotóxicas (CTLA-4) (ipilumabe). Até 2022, duas classes de imunoterápicos foram aprovadas pelo FDA: inibidores de CTLA-4 e inibidores do receptor de morte celular (PD-1) (nivolumabe, pembrolizumabe, pidilizumabe) e seu ligante (PD-L1) (avelumabe, atezolizumabe e durvalumabe). Esses imunoterápicos vêm sendo utilizados com sucesso no tratamento de melanoma metastático, câncer de pulmão de células não pequenas (NSCLC), carcinoma de células renais, câncer de bexiga e urotelial, carcinoma epidermoide cutâneo, linfoma de Hodgkin, câncer de fígado, câncer gástrico e carcinoma colorretal, além de estarem sendo testados em outros tumores (39–41).

Apesar dos bons resultados da imunoterapia em alguns tipos tumorais, análises transversais apontaram que somente 13% dos pacientes nos Estados Unidades foram responsivos a esse tratamento (42,43). As causas para esse percentual baixo ainda estão sendo estudadas, assim como a busca por biomarcadores que possam indicar uma melhor resposta a essa estratégia.

Algumas características foram associadas à melhor resposta a imunoterápicos, como por exemplo, a presença de infiltrado linfocitário, alta carga mutacional e alta expressão de *checkpoints* imunológicos, como por exemplo o PD-L1 (44,45). Ainda assim, os resultados podem ser heterogêneos nos diversos tipos tumorais e pacientes (46–53).

Em busca de compreender os possíveis mecanismos associados e uma melhor ou pior resposta imunológica ao tumor, Thorsson e colaboradores (53) realizaram uma análise compreensiva e abrangente das 10.000 amostras de tumores sólidos do TCGA, utilizando o estado da arte para caracterizá-las quanto às variáveis imunológicas e agrupando-as em seis grupos com características particulares de prognóstico e resposta antitumoral. Os autores inferiram o percentual de infiltrado leucocitário, caracterizaram a presença de diferentes células do sistema imunológico no ambiente intratumoral, avaliaram o repertório de resposta imunológica adaptativa, elucidaram a presença de mutações, infecções virais e a expressão de imunorreguladores-chave, além de avaliar as redes de interações curadas entre imunorreguladores e células imunológicas. Seus resultados foram disponibilizados para todas as 10.000 amostras, incluindo 78 amostras de CCA.

2.3 CARCINOMA DE CÓRTEX ADRENAL E O SISTEMA IMUNOLÓGICO

No estudo de Thorsson *et al.* (53), o CCA apresentou uma das menores taxas de infiltrado leucocitário entre os 30 tipos de tumores sólidos analisados, corroborando achados anteriores que apontavam o CCA como um dos tumores com menor presença de infiltrado imunológico (25,54). Relativo aos seis subtipos imunológicos, as 78 amostras de CCA foram majoritariamente classificadas nos subtipos C3 (n=23) e C4 (n=49). C3 é caracterizado como um ambiente intratumoral inflamado, com presença de infiltrado linfocitário, maior resposta Th1 e Th17 e uma presença equilibrada entre macrófagos e linfócitos, apresentando o melhor prognóstico dos seis subtipos imunológicos apresentados pelos autores. O subtipo C4 é o grupo mais representativo em CCA e apresenta um ambiente imunossuprimido, com o menor infiltrado linfocitário entre os seis subtipos, maior presença de macrófagos M2, supressão da resposta Th1 e também um dos piores prognósticos dentre os seis subtipos.

A imunossupressão encontrada nas amostras de CCA se justifica por algumas particularidades do microambiente tumoral. O aumento na produção de glucocorticoides, os quais tem papel imunossupressor, está presente em cerca de 60% dos tumores e confere a depleção linfocitária, diminuição da resposta ao Interferon-γ e atenuação da atividade citotóxica de células T e Natural Killers (NK) (13,55,56). Ademais, mutações comuns em CCA como em *TP53* e ativação da via WNT/β-catenina podem se associar à diminuição na produção de citocinas impactando negativamente o recrutamento linfocitário (29,57–59).

Fiorentini e colaboradores (13) afirmaram que devido a todas essas características e aos resultados modestos dos ensaios clínicos, os pacientes de CCA dificilmente se beneficiariam da imunoterapia. Os autores discutem que novas estratégias de seleção de pacientes deveriam ser empregadas para obter melhores resultados aliado a esforços na identificação de novos alvos ou possíveis formas de superar o ambiente imunossuprimido de CCA.

3 CAPÍTULO I: ADRENOCORTICAL CARCINOMA STEROID PROFILES: IN SILICO PAN-CANCER ANALYSIS OF TCGA DATA UNCOVERS IMMUNOTHERAPY TARGETS FOR POTENTIAL IMPROVED OUTCOMES (60)

frontiers in Endocrinology

ORIGINAL RESEARCH
published: 14 June 2021
doi: 10.3389/fendo.2021.672319



Adrenocortical Carcinoma Steroid Profiles: *In Silico* Pan-Cancer Analysis of TCGA Data Uncovers Immunotherapy Targets for Potential Improved Outcomes

*João C. D. Muzzi[1,2,3], Jessica M. Magno[2,3], Milena A. Cardoso[2,3], Juliana de Moura[1], Mauro A. A. Castro[2] and Bonald C. Figueiredo[3,4]**

[1] Laboratório de Imunoquímica (LIMQ), Pós-Graduação em Microbiologia, Parasitologia e Patologia, Departamento de Patologia Básica, Universidade Federal do Paraná (UFPR), Curitiba, Brazil, [2] Laboratório de Bioinformática e Biologia de Sistemas, Pós-Graduação em Bioinformática, Universidade Federal do Paraná (UFPR), Curitiba, Brazil, [3] Instituto de Pesquisa Pelé Pequeno Príncipe, Oncology Division, Curitiba, Brazil, [4] Centro de Genética Molecular e Pesquisa do Câncer em Crianças (CEGEMPAC), Molecular Oncology Laboratory, Curitiba, Brazil

OPEN ACCESS

3.1 ABSTRACT

Despite progress in understanding the biology of adrenocortical carcinoma (ACC), treatment options have not dramatically changed in the last three decades, nor have we learned how to avoid some of its long-term side effects. Our goal was to improve the understanding of immune pathways that may include druggable targets to enhance immune responses of patients with ACC, focusing on immune evasion and the activation of immune cells against ACC. Our strategy was aimed at improving insight regarding gene expression without steroid interference. Using approaches based on high and low steroid phenotypes (HSP and LSP, respectively), we characterized immune pathways using The Cancer Genome Atlas (TCGA) ACC cohort data. Although previous studies have suggested that patients with ACC receive minimal benefit from immunotherapy, high expression of immune modulators was noted in patients with LSP, suggesting the activation of these biomarkers may be an important adjuvant therapy target after clearance of excess glucocorticoids. In

addition, patients with LSP ACC had higher immune cell infiltration than patients with HSP ACC and other cancer subtypes. Our findings can be summarized as follows (1): we confirmed and improved the definition of two immune response pathways to ACC (HSP and LSP) based on *in silico* transcriptome analysis (2), we demonstrated the steroid profile should be considered, otherwise analyses of ACC immune characteristics can generate confounding results (3), among the overexpressed immunotherapy targets, we demonstrated that LSP was rich in *PDCD1LG2* (*PD-L2)* and both HSP and LSP overexpressed *CD276* (*B7-H3)*, which was associated with resistance to anti-PD1 therapy and may have accounted for the modest results of previous clinical trials, and (4) identification of patients with LSP or HSP ACC can be used to help determine whether immunotherapy should be used. In conclusion, we highlighted the differences between LSP and HSP, drawing attention to potential therapeutic targets (*CD276*, *PDCD1*, and *PDCD1LG2*). Treatments to reduce immune evasion, as well as the use of other natural and pharmacological immune activators, should include prior pharmacological inhibition of steroidogenesis. Attempts to combine these with tumor cell proliferation inhibitors, if they do not affect cells of the immune system, may produce interesting results.

3.2 INTRODUCTION

Adrenocortical carcinoma (ACC) is a rare highly aggressive malignancy of which >80% are steroidogenic (1–4). Overt hypercortisolism is observed in 37.6% (197/524) of adults with ACC, excluding cases with elevated cortisol levels without clinical manifestations, which may also have some molecular impact (4). The phenotypes seen with molecular changes in ACC may be largely derived from the dominant co-secretion of cortisol and androgens. These differences in combinations of steroid underlie the importance of defining steroid phenotypes and identifying the relevant genetic alterations that characterize the various immune system profiles observed.

Pan-genomic and molecular characterizations of ACC have been the focus of diverse studies in an attempt to establish useful classifications for prognosis or therapy. Zheng et al. (5) suggested the differentiation of patients with ACC based on three CpG island hypermethylated phenotype (CIMP) statuses: high, intermediate, and low. To date, CIMP is the most robust biomarker for ACC pan-molecular subgroups (6). Despite providing meaningful prognosis, this classification cannot be translated into determining optimal target treatment options (6, 7). Besides DNA methylation status, other molecular strategies have been used to characterize ACC subtypes (5, 8, 9). Based on transcriptome profiling, de Reyniès et al. (8) and

Giordano et al. (9) defined two ACC subgroups, C1A and C1B, while Zheng et al. (5) clustered ACC mRNA-seq data in two subgroups with a high steroid phenotype (HSP) and low steroid phenotype (LSP), separating the expression pattern of genes in the steroid synthesis pathway. This was further refined into four subgroups: HSP (n = 25), HSP + proliferation (n = 22), LSP (n = 27), and LSP + proliferation (n = 4). The proliferation profile was mainly associated with HSP, whereas the LSP + proliferation was restricted to only four cases in The Cancer Genome Atlas (TCGA) cohort (n = 78). These four subgroups demonstrated a high overlap of C1A and C1B subtypes, with most HSP patients classified as C1A and LSP patients classified as C1B (5). Zheng and colleagues found an immune signature associated with the LSP profile upon comparison of immune-suppressed ACC with strong steroidogenesis (5).

Landmark studies have extensively focused on profiling biomarkers and cells associated with cancer immunity with extensive immunogenomic analysis of tumors (10, 11). Thorsson et al. (11) provided new insights into the immune landscape of cancers using TCGA data. Assembling all ACC cases without consideration of more specific clinical or steroidal phenotypes, ACC was found to exhibit the second lowest leukocyte fraction among the cancer types studied (11). These investigators analyzed over 10,000 TCGA tumors and using cluster analysis of a robust list of immune expression signatures reported by other studies proposed six immune subtypes with specific features and prognoses: C1, wound healing; C2, IFN-γ dominant; C3, inflammatory; C4, lymphocyte depleted; C5, immunologically quiet; and C6, TGF-ß dominant (11). Based on the dominant sample characteristics, they proposed the ACCs in the TCGA database (patient ages ranging from 14 to 77 years) fit better within the C4 immune subtype, with a more prominent macrophage signature, suppression of T helper type 1 (Th1) cells, and a high M2 response (11). These cancers are among those with the least favorable outcome. This immunosuppressed profile is associated with hypercortisolism and low survival in the majority of adult patients with ACC (12), while younger children with a dominant androgen steroid phenotype have a better prognosis (13, 14).

As tumors grow, they acquire mutations. These mutations may impair the function of the immune system in ACC subtypes (with both low and high steroidogenesis). These genetic changes include mutations in driver genes, DNA damage, copy number variation, aneuploidy, loss of heterozygosity, intratumor heterogeneity, and decreased telomere length (5, 15). Consequently, overall survival (OS) analyses are frequently less accurate in ACC cases because of the complex interactions between these changes in the tumor and the immune system (16). The worse prognosis for adults with ACC is explained by molecular differences and the higher frequency of elevated glucocorticoids (17–19). After C4 (49 of the 78 ACC cases), the second most common immune subtype was C3, found in 23 of the 78 ACC cases, predominantly in LSP (16/31). The C3 immune subtype is represented by an inflammatory response with higher presence of Th1 and Th17 responses and a

balanced presence of macrophages and lymphocytes. In a pan-cancer analysis, the C3 immune subtype presented the best prognosis. The other six ACC cases were C5 (n = 3) and one each of subtypes C1, C2, and C6.

Lymphocyte expression signature, high number of unique T-cell receptor clonotypes, cytokines produced by activated CD4+ Th1 and Th17 lymphocytes, and M1 macrophages, which secrete pro-inflammatory cytokines and chemokines, are associated with improved OS in some cancer subtypes (11). The ability to kill transformed cells is essential for an effective anti-tumor response by the immune system. This ability relies on the cytotoxic activity of natural killer (NK) cells and CD8+ T lymphocytes (CD8+TL) (20). Activated NK cells are able to recruit dendritic cells and elicit an antitumor T-cell response (21). The presence of activated tumor-infiltrating CD8+TL in human cancers is associated with improved prognosis, expression of specific antigens, and increased immune-cancer interactions (10). For example, there is a positive correlation between melanoma-associated antigen 3 (*MAGEA3*) expression and CD8+TL infiltration in melanoma, explaining the success of the *MAGEA3*-based vaccine (22). Another successful example of immunomodulation is the stimulation of blood cells with bacille Calmette-Guérin (BCG) or recombinant BCG to enhance the expression of CD25 and CD69 on human CD4+ T cells, a highly effective immunotherapeutic agent against bladder cancer (23, 24). Interestingly, most patients with bladder cancer are diagnosed in their seventies when the immune system may be impaired (25). Similarly, more than 50% of adults with ACC are diagnosed in patients 50 years or older (26). As CD8+TL are crucial for protective immunity, it is vital to identify candidate activators of the host immune response to cancer. Specific driver mutations (e.g., *TP53*) are correlated with higher leukocyte levels across all cancers (11). This is not the case in pediatric ACC with the germline *TP53* R337H variant, where higher CD8+TL infiltration is associated with other factors, such as stage 1 and diagnosis at a younger age (14). This is in line with the observed changes in the immune infiltrate composition at each tumor stage, where there is a decrease in T-cell density and an increase in T-follicular helper cells and innate immune cells with tumor progression (27).

T-cell activation requires two distinct signaling pathways, one mediated by the binding of T-cell receptor (TCR) with an antigen bound major histocompatibility complex (MHC) and the second by the binding of CD28 to T cells with B7-1 (*CD80*) or B7-2 (*CD86*) of antigen-presenting cells (28). In addition to B7-1 and B7-2, other B7 family proteins interact with other T-cell membrane molecules and may act as co-inhibitors, such as B7-H1, which is well known as programmed cell death ligand 1 (PD-L1), B7-DC, which is known as programmed cell death ligand 2 (PD-L2), and B7-H3 (*CD276)*, among others (29). Blockade of immune checkpoint evasion was expected to provide a more effective treatment for patients with ACC. However, the use of antibodies targeting programmed cell death 1 (PD-1) expressed by T cells (30–32) or PD-L1 (33) is associated with poor efficacy. In the latter study (33), 50% of

patients were under concomitant treatment with mitotane to block immunosuppressive glucocorticoids. However, this study did not consider the possibility of evasion through PD-1/PD-L2. Despite these setbacks, other approaches have been suggested to overcome the reported modest responses (7, 34).

The impact of excess steroids on the immune system interaction with ACC tumors, including a complete understanding of the related molecular profiles, has not been fully evaluated. Our aim was to perform a comprehensive and translational analysis of ACC immune biomarkers to identify those that could predict a favorable outcome with and without steroid interference. We evaluated possible modifiers of immune evasion (*CD274* that encodes PD-L1 and *PDCD1LG2* that encodes PD-L2), and investigated how these ligands correlate with *CD8B* expression in ACC, revisiting TCGA cohort data and the molecular steroidogenic classification established by Zheng et al. (5). Considering the hypothesis that HSP has a worse prognosis because of its effect on the immune system, we discuss strategies, supported by prior studies, for downregulating steroid biosynthesis before using possible immune activators.

3.3 MATERIALS AND METHODS

3.3.1 Data Sources

Data sources used in this study were obtained from the ACC cohort in TCGA (5). Inclusion criteria, quality control, and characterization of these participants were previously described (5). The data are available on the National Cancer Institute (NCI) Genomic Data Commons (GDC) Data Portal (https://gdc.cancer.gov/about-data/publications/acc_2016). The transcriptome profiles of 78 patients with ACC for whom the steroid phenotype was available were used for the subsequent analysis. This group included 31 men and 47 women with a mean age of 46.7 years (range, 14–77 years). Based on mRNA data, the patients were classified as HSP (n = 25), HSP + Proliferation (n = 22), LSP (n = 27), and LSP + Proliferation (n = 4) (5). For the current study, we used only the steroid phenotype classification, HSP (n = 47) and LSP (n = 31). Clinical data were obtained using the R/Bioconductor package TCGABiolinks v 2.18.0 (35–37) from the GDC Data Portal. History of excessive hormone expression was downloaded from the GDC Data Portal and classified as (i) Cortisol Excess (n = 32) for patients with a history of excess Cortisol (n = 15), Mineralocorticoids|Cortisol (n = 1), and Androgen|Cortisol (n = 16); (ii) Mineralocorticoids Excess (n = 4) for patients with a history of Mineralocorticoids (n = 3) and Mineralocorticoids|Cortisol (n = 1); and (iii) Sexual Hormone Excess (n = 28) for patients with a history of excess Androgen (n = 8), Androgen|Cortisol (n = 16),

Androgen|Estrogen (n = 2), and Estrogen (n = 2). There were no notations on hormone levels for 5 patients.

The data on immune characteristics were obtained from Thorsson et al. (11) (https://www.cell.com/cms/10.1016/j.immuni.2018.03.023/attachment/1b63d4bc-af31-4a23-99bb-7ca23c7b4e0a/mmc2) and xCell immune infiltrate cell scores were downloaded from TIMER2.0 (http://timer.cistrome.org/infiltration_estimation_for_tcga.csv.gz) (10, 38, 39). For comparison between two steroid groups, data were filtered using the patients' barcodes.

The study was approved by the Ethics Committee of Pequeno Príncipe Hospital and National Research Ethics Committee (CAAE number 50622315.0.0000.0097), without use of a consent form as it involved only anonymous public data from the original cohorts deposited at TCGA.

3.3.2 Leukocyte Fraction and Immune Infiltrate Comparison

Leukocyte fractions data for pan-cancer analysis were extracted from Thorsson et al. (11). The study included 11,080 patients from TCGA of which 10,448 were annotated with a leukocyte fraction. TCGA studies were used and were arranged by median leukocyte fraction values. For grouping based on the ACC steroid phenotype, patients from this cohort were selected according to their barcode identifiers.

Previous studies used two methods to estimate immune cell infiltration in the ACC cohort: xCell (38) scores using a marker-gene-based approach, inferred by Sturm et al. (39), and Cibersort using a deconvolution-based approach (40), calculated by Thorsson et al. (11). A more detailed evaluation on the limitations and characteristics of these approaches has been reviewed by Sturm et al. (39).

The immune cell proportions based on Cibersort estimations were multiplied by the leukocyte fraction, resulting in a final score that could be used for intra- and inter-sample comparisons, as previously described (11). For the ACC cohort analysis, scores of CD8+TL and activated NK cells were used for pan-cancer comparisons, while the scores for all 22 cell types were used for intra-cohort analysis. For pan-cancer comparisons, the barcodes were merged with the Thorsson dataset, and xCell results for CD8+TL and NK cells of the TCGA study and were grouped and ordered by median values. For comparisons within the ACC cohort, samples were filtered for all xCell infiltrate estimates by patient barcodes. Beyond cell estimations, xCell offers microenvironment, immune, and stroma scores. However, the enrichment scores do not allow for a comparison between different cell types of the same sample, but does allow for comparison of the same cell type between different

samples. Accordingly, the two groups of patients could be compared using this method, but the relative abundance of each cell type within a patient could not be compared.

The Wilcoxon test was used to compare the xCell and Cibersort immune infiltrate scores between the HSP and LSP groups. The R package ComplexHeatmap v 2.6.2 (41) was used for heatmap construction. Column-wise z-scores were calculated for the immune cell scores, and maximum and minimum values were limited to +2 and −2, respectively. Samples were clustered for immune characteristics and cell scores scaled data in a semi-supervised manner using the McQuitty and Euclidean distance methods.

3.3.3 RNA-seq Filtering, Processing, and Differential Expression (DE)

High-throughput sequencing (HTSeq) mRNA data were obtained for the 78 ACC patients with steroid phenotype characterization using the R package TCGAbiolinks v 2.18.0 (35–37) and SummarizedExperiment v 1.20.0 (42). The 56,457 transcripts were filtered for protein-coding genes using EnsembleDb version 101 and notated using AnnotationHub R package v 2.22.0 (43). The genes with a sum of zero counts were excluded, resulting in the inclusion of 19,169 genes. The two steroid phenotype groups underwent DE analysis using the R package DESeq2 v 1.30.0 as previously described (44). P-values were calculated using Wald's test and adjusted with Benjamini–Hochberg estimation. The gene count expression matrix was normalized by variance-stabilizing transformation using the DESeq2 package. Three genes had duplicated symbol names (*PINX1, TMSB15B*, and *MATR3*). To differentiate these three genes, we added an underscore after the first entry in the DE results.

3.3.4 Enrichment Analysis

After ordering based on adjusted p-values, the ranked genes list underwent gene set enrichment analysis (GSEA) with the Coincident Extreme Ranks in Numerical Observations (CERNO) test (45, 46) using the R package tmod v 0.46.2, as previously described (46, 47). The CERNO test is an application of modified Fisher p-value integration for creating a GSEA ranked list, which avoids the arbitrary choice of a p-value or log-fold change threshold (46). Two gene sets were used for the enrichment analysis. Hallmark gene sets were obtained from MSigDb v7.1 (https://data.broadinstitute.org/gsea-msigdb/msigdb/release/7.1/msigdb_v7.1.xml) (48, 49) and blood transcriptional modules (BTM) (50) were obtained from the tmod R package. The hallmark gene set is comprised of 50 modules summarizing the

molecular signature database gene sets and reducing redundancy (49). These modules are divided into eight categories: cellular component, development, DNA damage, immune, metabolic, pathway, proliferation, and signaling. The other gene set consists of 334 BTMs combining information about adaptive and innate immune responses.

3.3.5 Expression of Immune Modulators and Immune Checkpoints

Expression profiles of the immunomodulatory genes listed by Thorsson et al. (11) (https://www.cell.com/cms/10.1016/j.immuni.2018.03.023/attachment/8d3ffc74-4db4-4531-a4ad-389dfc8bb7ec/mmc7.xlsx) were obtained from a variance stabilizing transformation gene expression matrix. Of the 75 immune modulators, only one (*C10orf54*) was not found in the expression matrix. *CSF2* expression was added based on the study by Wang et al. (51), which showed its importance for dendritic cell recruitment in poorly immunogenic tumors. Adjusted p-values for the findings from the DE analysis were used for comparison between groups. The R package ComplexHeatmap v 2.6.2 (41) was used for heatmap construction, column-wise z-scores were calculated for immune modulator gene expressions, and maximum and minimum values were limited to +2 and −2, respectively. Columns were arranged following the order of the semi-supervised clusters of immune characteristics and cell scores determined previously. For expression of immune checkpoint genes *CD8B*, *CD274* (*PD-L1)*, and *PDCD1LG2* (*PD-L2)*, Pearson's correlation coefficients and p-values were calculated and the confidence interval was inferred based on Fisher's Z transformation.

3.3.6 Leukocyte Fractions and Mutations in the ACC Cohort

Pan-Cancer Atlas data from TCGA regarding ACC patients with mutations in *TP53* (n = 16), *CTNNB1* (n = 13), and *MEN1* (n = 7) were obtained from the cBioPortal (https://www.cbioportal.org/) and merged with the leukocyte fraction information. Comparison between patients with and without mutations in these driver genes was performed using the Wilcoxon test.

3.3.7 Extracellular Communication Networks in Immune Subtypes

Extracellular communication networks were inferred based on the study by Thorsson et al. (11) and the data for the TCGA ACC cohort were obtained from iAtlas (https://isb-cgc.shinyapps.io/shiny-iatlas/). The networks involved ligand-receptor, cell-receptor, and cell-ligand pairs described by Ramilowski et al. (52) and enhanced

by Thorsson et al. (11). Nodes with more than 50% abundance and concordance interaction greater than 2.5 were chosen as the C3 and C4 immune subtypes. The networks were reconstructed using R packages igraph v 1.2.6 and RedeR v 1.38.0 (53). The node line width varies proportionally to the abundance score and the edge width varies proportionally to the concordance.

A batch corrected and normalized gene expression matrix for the 11,060 TCGA samples was downloaded from the Supplemental Data of Hoadley et al. (54) (https://api.gdc.cancer.gov/data/9a4679c3-855d-4055-8be9-3577ce10f66e). The matrix was filtered for the 25 ligands and receptors present in the C3 and C4 networks. Samples were selected from primary tumors only and duplicate entries were removed. The matrix was merged with the Thorsson dataset according to the participant barcode. Gene expression data were ranked from lowest to highest counts for each gene, and patients were divided into terciles (low, intermediate, and high) and filtered for the ACC patients' barcodes.

3.3.8 Survival Analysis

The prognostic impact of LSP (n = 31) versus HSP (n = 47), immune subtype C3 (n = 23) versus C4 (n = 49), and LSP + Immune Subtype C3 (n = 16) versus other configurations (n = 62) were evaluated using Kaplan-Meier analysis for OS and progression-free interval (PFI) using R packages survival v3.2-7 (55, 56) and survminer v0.4.8. P-values were calculated using the log-rank test.

3.3.9 Statistical Analysis

Q values and false discovery rate (FDR) quantities were calculated using R package qvalue v2.20.0 (57). For DE results, q-values were calculated based on π estimation. Due to the small number of p-values available for π estimation, the q-value was determined using Benjamini-Hochberg estimation for enrichment analysis.

3.4 RESULTS

3.4.1 Pan-Cancer Comparison Showed Significant Immune Infiltrates in Patients With LSP ACC

ACC had one of the lowest immune infiltrate profiles in the TCGA pan-cancer comparison (Figure 1A). However, when distinguishing by steroid profiles, patients with LSP ACC had considerable leukocyte infiltration, placing them in the top 40% of

tumor types (Figure 1B). This was also seen with CD8+TL and NK cells infiltrates, as measured by the Cibersort and xCell scores (Figures 2A–D).

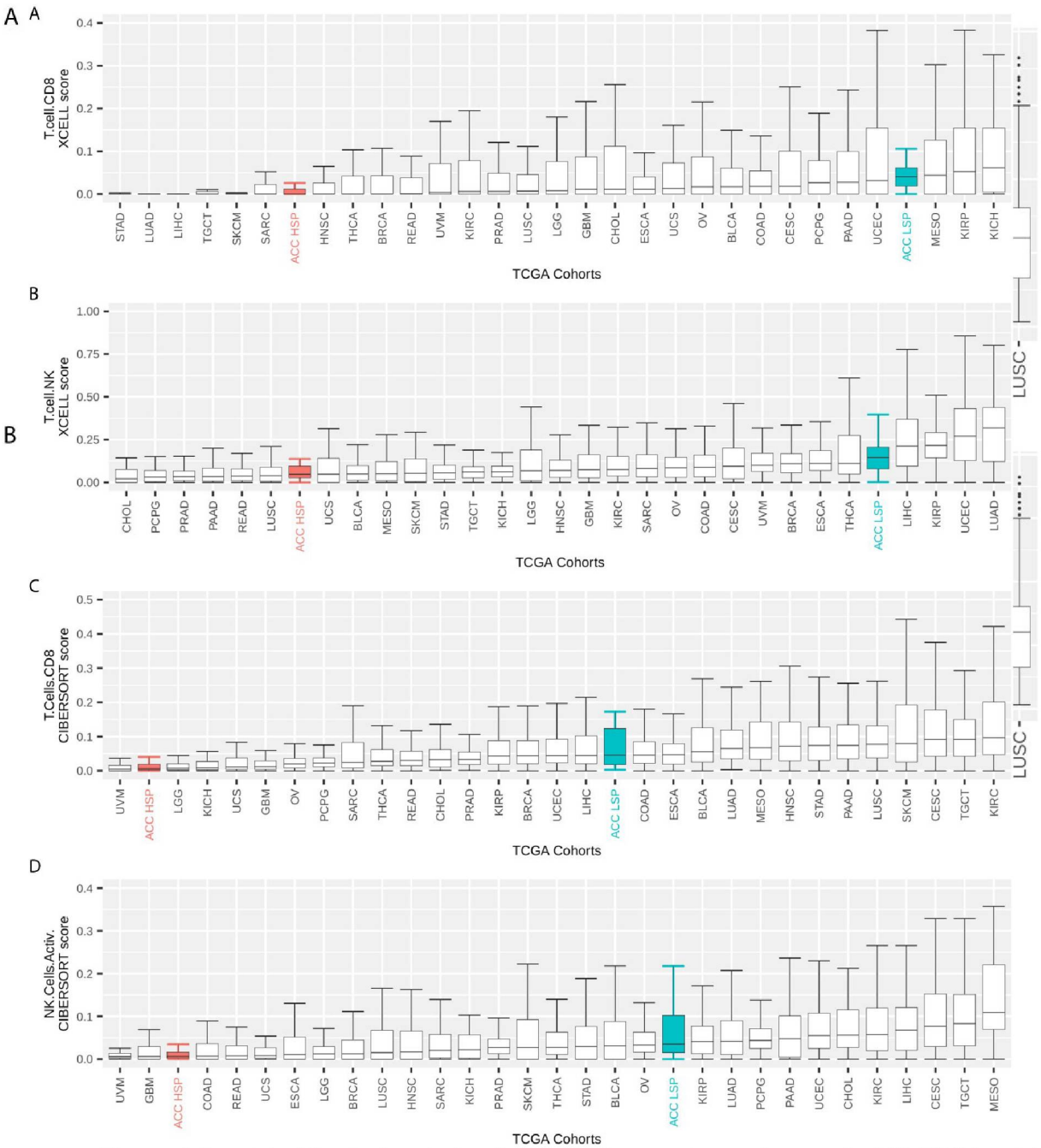


Figure 1 Boxplot of the leukocyte fraction in the tumor microenvironment of 30 TCGA solid tumors. The leukocyte fraction was inferred by Thorsson et al. (11) for 10,448 participants included in The Cancer Genome Atlas (TCGA) database using molecular methods and compared with hematoxylin and eosin stained images, which demonstrated good correlation. Participants were grouped by TCGA cohort. The boxplot shows the median and interquartile range (IQR) for the leukocyte fraction of each cohort. Whiskers are set at 1.5 IQR and outliers (above and below the 1.5 IQR) are presented as points. TCGA cohorts were ordered by median values. **(A)** Patients with adrenocortical carcinoma (ACC) are represented as one group. **(B)** Patients with ACC are divided according to steroid phenotypes.**Figure 2** TCGA pan-cancer comparison of immune infiltrates.

Immune infiltrate scores (y-axis) were rescaled to range from 0 to 1. The maximum on the y-axis is independently set for each plot for better visualization. Participants were grouped by TCGA cohort and the boxplot shows median and IQR for immune cell infiltrate scores of each cohort. Whiskers are set at 1.5 IQR and outliers (above and below the 1.5 IQR) are not shown. TCGA cohorts were ordered by median values. Patients with ACC were divided according to steroid phenotypes **(A, B)** xCell scores for CD8+ T cells and T natural killer (NK) cells inferred by Sturm et al. (39). **(C, D)** Cibersort scores for activated CD8+ T cells and NK cells as inferred by Thorsson et al. (11) and multiplied by the leukocyte fraction as described by these authors.

The main clinical characteristics of HSP and LSP are shown in Table 1. Cortisol was the most frequently elevated hormone (57.4% in HSP and 16.1% in LSP) compared to less frequently observed sex steroids, mineralocorticoids, and others, as described by Zheng et al. (5). The prognostic differences were remarkable, with only 3 death events (9.7%) in patients with LSP versus 24 (51.1%) in patients with HSP. This was in addition to a higher proportion of advanced cancer stages observed in the HSP group, which may have been associated with a higher proliferation rate.

Table 1 Clinical data.

	HSP	LSP
Total (Dead)	47 (24)	31 (3)
Mean Age ± SD	46.5 ± 17	48.5 ± 14.3
Males	16 (9)	15 (2)
Mean age ± SD	46 ± 14.6	52.9 ± 11
Females	31 (15)	16 (1)
Mean age ± SD	46.8 ± 18.3	44.3 ± 16.1
High Proliferation	22 (15)	4 (2)
Tumor Stage		
Stage I	3 (1)	6 (0)
Stage II	18 (6)	19 (1)
Stage III	12 (6)	4 (1)
Stage IV	12 (10)	2 (1)
Hormone Excess		
Cortisol	27 (14)	5 (1)
Mineralocorticoids	3 (1)	1 (0)
Sexual	20 (14)	8 (1)
Immune Subtype		
C1	1 (1)	0 (0)
C2	0 (0)	1 (1)
C3	7 (3)	16 (0)
C4	37 (19)	12 (1)
C5	2 (1)	1 (0)
C6	0 (0)	1 (1)

The total number of patients for each clinical category for the Low Steroid Phenotype (LSP) and High Steroid Phenotype (HSP) is shown with the number of dead patients in parenthesis. The mean age of participants with the standard deviation (SD) is shown for both groups and subdivided into males and females. All clinical data were retrieved from Zheng et al. (5) and the immune subtype classification from Thorsson et al. (11). Proliferation is bipartite as presented by Zheng et al. (5) based on transcriptomic classification and associated with markers such KI67 and BUB1.

3.4.2 Immune Activation Was Enriched in Patients With LSP ACC

The results from the DE analysis of LSP versus HSP are presented in Figure 3. The order is based on LSP versus HSP and is used in all analyses presented in this study. Opposite values for the log-fold change would have been determined if HSP versus LSP was used. The full DE results are available in Supplementary Table 1.

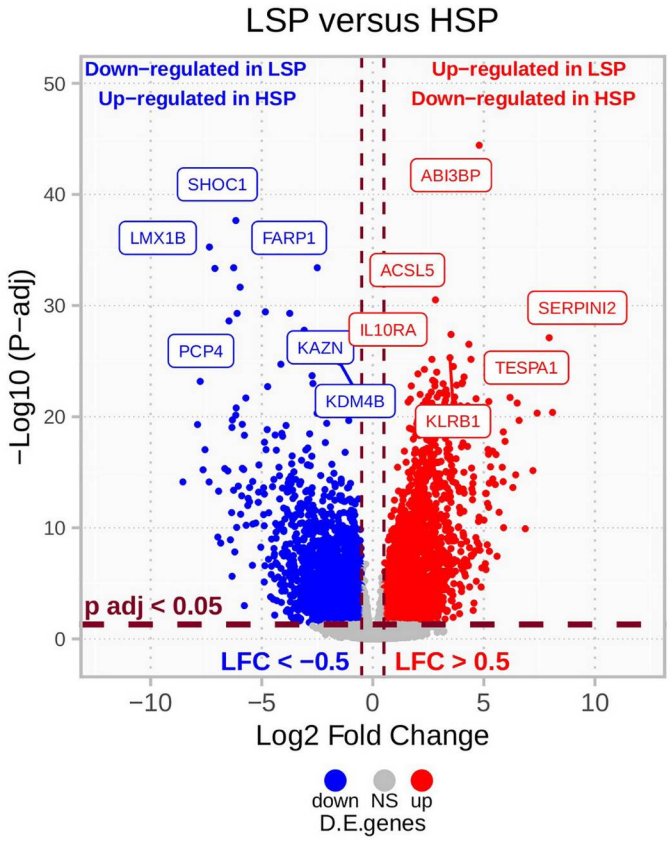


Figure 3 LSP *versus* HSP DE in TCGA ACC cohort (n = 78). After filtering for protein-coding genes and excluding those with sums of zero counts, a total of 19,169 genes were used for a LSP *versus* HSP differential expression (DE) analysis. P-values were calculated using the Wald's test and adjusted using Benjamini-Hochberg estimation. Genes with absolute log2 fold change lower than 0.5 and adjusted p-value greater than 0.05 are colored in gray. Above these cut-offs, genes upregulated in LSP and downregulated in HSP are indicated in red and genes downregulated in LSP and upregulated in HSP are indicated in blue.

Enrichment analysis using the hallmark gene sets is presented in Figure 4A and Supplementary Table 2. Most gene sets were enriched for genes related mainly to the immune response and were upregulated in LSP and downregulated in HSP. The gene sets significantly enriched with genes downregulated in LSP and upregulated in HSP were associated with estrogen response, cholesterol homeostasis, and hedgehog signaling (Figure 4A), which was consistent with the steroidogenic profile used for the DE analysis.

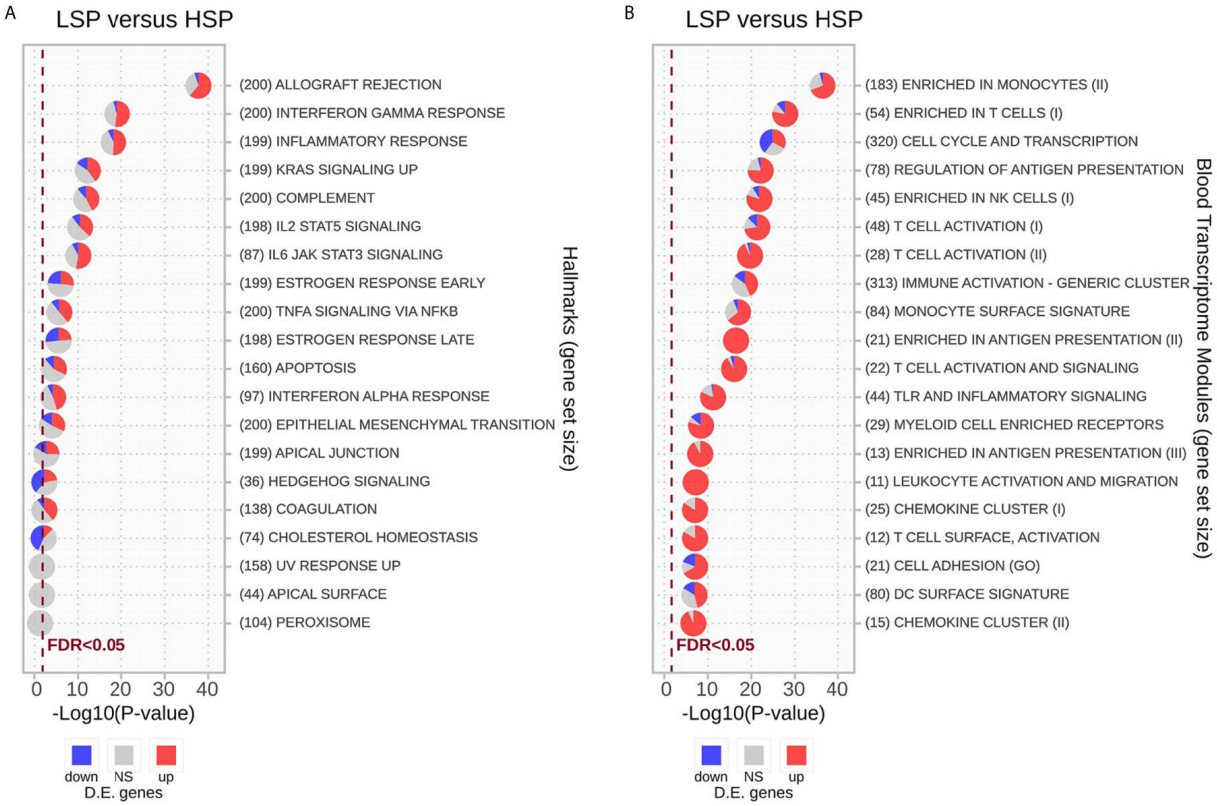


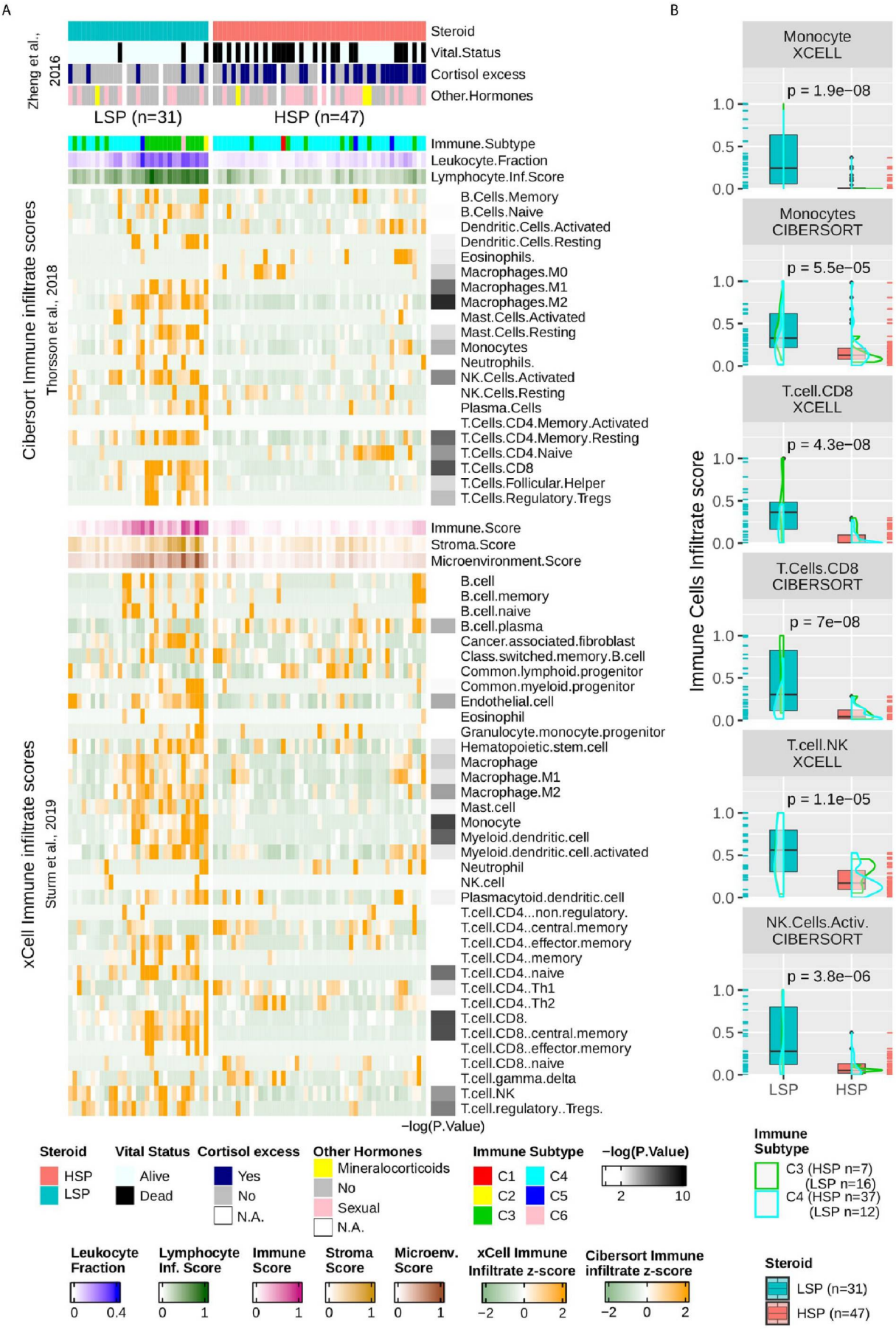
Figure 4 Enrichment analysis for differentially expressed genes using the CERNO test. The CERNO test was applied to the differentially expressed genes using the hallmark gene sets **(A)** and blood transcriptome modules (BTMs) **(B)**. The modules are ordered according to the adjusted p-values and are considered non-significant based on a false discovery rate (FDR) of 0.05. The number of genes in each module is presented before the module names in brackets. The charts are colored based on the DE results: red for module genes upregulated in low steroid phenotype (LSP) and downregulated in high steroid phenotype (HSP), gray for module genes with no significant p-value, and blue for module genes down-regulated in LSP and upregulated in HSP.

As the immune response was strongly associated with the different steroid phenotypes, we conducted GSEA with the BTMs described by Li et al. (50). In general, modules associated with T lymphocytes and NK cells, monocytes, and antigen presentation displayed the strongest association with ranked genes, especially those upregulated in LSP. With exception of the “Cell Cycle and Transcription” module, most immune modules were markedly enriched with genes up-regulated in LSP and down-regulated in HSP, with some modules such as “Enriched in Antigen Presentation (II)” and “Leukocyte Activation and Migration” fully represented by DE genes up-regulated in LSP (Figure 4B).

3.4.3 Enrichment of T Cells, Monocytes, and Cytolytic Activity in LSP ACC

The column-wise z-scores for the xCell and Cibersort results for TCGA ACC patients are presented in Figure 5A. Both methods found a higher immune cell presence in patients with LSP compared to those in patients with HSP, which appeared immunosuppressed. Not all cell types identified using one method were present in the results obtained using the other method, indicating differences in some specificities. Consistent with the BTM enrichment analysis (Figure 4B), the presence of monocytes and T cells differed significantly between the two steroid phenotypes (Figures 5A, B). As xCell detected NK cells in only a few samples and Cibersort differentiated resting NK cells from activated NK cells but did not distinguish between subtypes of CD8+ T cells, the last two panels of Figure 5B show a boxplot comparison of the xCell T NK cells and the Cibersort activated NK cells. Because xCell generates arbitrary scores, y values were rescaled to a range of 0 to 1. Most discrepancies between the xCell and Cibersort scores were observed for B cells, plasma cells, naive CD4+ T cells, and eosinophils, which may have been a result of the spillover effect from the methods (39).

3.4.4 LSP Was Associated With an Inflammatory Immune Response and HSP With a Lymphocyte Depleted Microenvironment


A
B
Zheng et al., 2016
Steroid
Vital.Status
Cortisol excess
Other.Hormones
LSP (n=31)
HSP (n=47)
Cibersort Immune infiltrate scores
Thorsson et al., 2018
Immune.Subtype
Leukocyte.Fraction
Lymphocyte.Inf.Score
B.Cells.Memory
B.Cells.Naive
Dendritic.Cells.Activated
Dendritic.Cells.Resting
Eosinophils.
Macrophages.M0
Macrophages.M1
Macrophages.M2
Mast.Cells.Activated
Mast.Cells.Resting
Monocytes
Neutrophils.
NK.Cells.Activated
NK.Cells.Resting
Plasma.Cells
T.Cells.CD4.Memory.Activated
T.Cells.CD4.Memory.Resting
T.Cells.CD4.Naive
T.Cells.CD8
T.Cells.Follicular.Helper
T.Cells.Regulatory.Tregs
xCell Immune infiltrate scores
Sturm et al., 2019
Immune.Score
Stroma.Score
Microenvironment.Score
B.cell
B.cell.memory
B.cell.naive
B.cell.plasma
Cancer.associated.fibroblast
Class.switched.memory.B.cell
Common.lymphoid.progenitor
Common.myeloid.progenitor
Endothelial.cell
Eosinophil
Granulocyte.monocyte.progenitor
Hematopoietic.stem.cell
Macrophage
Macrophage.M1
Macrophage.M2
Mast.cell
Monocyte
Myeloid.dendritic.cell
Myeloid.dendritic.cell.activated
Neutrophil
NK.cell
Plasmacytoid.dendritic.cell
T.cell.CD4...non.regulatory.
T.cell.CD4..central.memory
T.cell.CD4..effector.memory
T.cell.CD4..memory
T.cell.CD4..naive
T.cell.CD4..Th1
T.cell.CD4..Th2
T.cell.CD8.
T.cell.CD8..central.memory
T.cell.CD8..effector.memory
T.cell.CD8..naive
T.cell.gamma.delta
T.cell.NK
T.cell.regulatory..Tregs.
−log(P.Value)
Steroid
HSP
LSP
Vital Status
Alive
Dead
Cortisol excess
Yes
No
N.A.
Other Hormones
Mineralocorticoids
No
Sexual
N.A.
Immune Subtype
C1
C2
C3
C4
C5
C6
−log(P.Value)
2
10
Leukocyte Fraction
0
0.4
Lymphocyte Inf. Score
0
1
Immune Score
0
1
Stroma Score
0
1
Microenv. Score
0
1
xCell Immune Infiltrate z-score
−2
0
2
Cibersort Immune infiltrate z-score
−2
0
2
Monocyte XCELL
p = 1.9e−08
Monocytes CIBERSORT
p = 5.5e−05
T.cell.CD8 XCELL
p = 4.3e−08
T.Cells.CD8 CIBERSORT
p = 7e−08
T.cell.NK XCELL
p = 1.1e−05
NK.Cells.Activ. CIBERSORT
p = 3.8e−06
Immune Cells Infiltrate score
1.0
0.5
0.0
LSP
HSP
Immune Subtype
C3 (HSP n=7) (LSP n=16)
C4 (HSP n=37) (LSP n=12)
Steroid
LSP (n=31)
HSP (n=47)

According to the classification by Thorsson et al. (11), ACC patients fit mainly into the C4 subtype (n = 46), with a subset of patients in C3 subtype (n = 23), where C3 seemed to be associated with LSP (n = 16) and C4 with HSP (n = 37) (Table 1 and Figure 5A). Only one participant each fit into the C1, C2, and C6 subtypes, and three patients presented with a C5 subtype profile. Density plots show the distribution of C3 and C4 ACC patients separated into the steroid phenotypes based on monocyte, CD8+TL, and NK cell scores (Figure 5B).The higher immune activation of patients with LSP ACC was also seen in the expression of immunomodulator genes (Figure 6A). Patients with LSP had a higher expression pattern of immune activators and inhibitors compared to patients with HSP. From the immune characteristics analyzed by Thorsson et al. (11), the differences between LSP and HSP were significant for leukocyte fraction, lymphocyte infiltration score, and macrophage regulation (Figure 6B), which demonstrates immune activation and recruitment in patients with LSP, in contrast with the immunosuppressed tumor microenvironment (TME) seen in patients with HSP.**Figure 5** Immune infiltrate comparison. **(A)** Heatmap with column-wise z-scores for TCGA ACC immune infiltrates as inferred by Sturm et al. (39) using xCell and by Thorsson et al. (11) using Cibersort. Maximum and minimum z-scores for the color gradient were set at +2 and −2 standard deviations from the mean. Each column represents a patient and columns were subjected to semi-supervised clustering. In addition to the immune infiltrate, Thorsson et al. (11) presented a classification of six immune subtypes (C1–C6) and inferred the leukocyte fraction and a molecular signature associated with the lymphocyte infiltrate score. xCell provides a stroma, immune, and microenvironment score in addition to the immune cell infiltrate. Lymphocyte infiltrate, immune, stroma, and microenvironment scores were rescaled to a range of 0 to 1. The clinical information was provided by Zheng et al. (5) and appears in the top annotation rows. The p-value calculated using the Wilcoxon test comparing LSP and HSP for each cell type is represented in the right as a color gradient ranging from 2 to 10 for −log10 (p-value), values lesser than 2 are set as white. **(B)** Boxplot comparing LSP and HSP in terms of monocytes, CD8+ T cells (xCell and Cibersort), T natural killer (NK) cells (xCell), and activated NK cells (Cibersort). All scores (y-axis) are rescaled from 0 to 1. The density plot shows the distribution according to the immune subtypes: C3 (green) and C4 (cyan). Each sample is shown in a rug plot and colored according to the HSP and LSP classification. The p-value calculated using the Wilcoxon test comparing both phenotypes is shown above each pair of boxplots.

Thorsson et al. (11) also evaluated the T-cell receptor (TCR) and B-cell receptor (BCR) repertoire. However, this information for most patients with ACC unfortunately could not be retrieved from bulk mRNA sequencing, probably due to the small numbers of these cell fractions in the TME. For instance, only 5 of 78 patients had information regarding BCR (3 LSP and 2 HSP) and 37 regarding TCR (21 LSP and 16 HSP) of which 16 had a 0 score on TCR Shannon entropy (3 LSP and 13 HSP).

3.4.5 Steroid Phenotype Generated a Confounding Effect on the Correlation Between Leukocyte Fraction and Driver Gene Mutations

Thorsson et al. (11) reported that mutations in driver genes are significantly correlated with the leukocyte fraction. Among driver genes, the most common mutations found in the ACC cohort were in *TP53* (n = 16), *CTNNB1* (n = 13), and *MEN1* (n = 7); however, these mutations were mainly present in patients with HSP (n = 13 of 16, n = 13 of 13, and n = 6 of 7, respectively). It was not possible to determine whether differences in the leukocyte fraction were caused by the mutations or due to the steroid phenotype. Using the Wilcoxon test to evaluate the differences in the leukocyte fraction based on the presence or absence of these mutations resulted in p-values of 1.8×10^{-1}, 3.8×10^{-2}, and 4.8×10^{-1} for *TP53*, *CTNNB1*, and *MEN1*, respectively.

3.4.6 Extracellular Communication Networks and Possible Immunotherapy Targets Associated With Steroid Phenotypes

Based on the study by Thorsson et al. (11), two extracellular communication networks were reconstructed for ACC subtypes C3 and C4 with 50% abundance and 2.5 concordance thresholds (Figure 7A). A small network was also obtained for the C5 subtype with these parameters centered on macrophages; however, as it contained only 3 patients and was not further considered in the current study. The abundance was representative of the prevalence of the node in the samples (%), while concordance was relative to the concordance to discordance ratio (a pair with concordant high or low expression versus a pair with distinct expression patterns in each sample).

The nodes in the C3 and C4 networks were used to compare all TCGA participants. The ACC patient classification is shown in Figure 7B. Most ACC patients, despite phenotype distinction, were in the top third group for expression of *CD276 (B7-H3)*, *GPC1*, vascular endothelial growth factor A (*VEGFA)*, vascular endothelial growth factor B (*VEGFB)*, and vascular endothelial growth factor receptor 1 *(VEGFR1) FLT1* (Figure 7B).

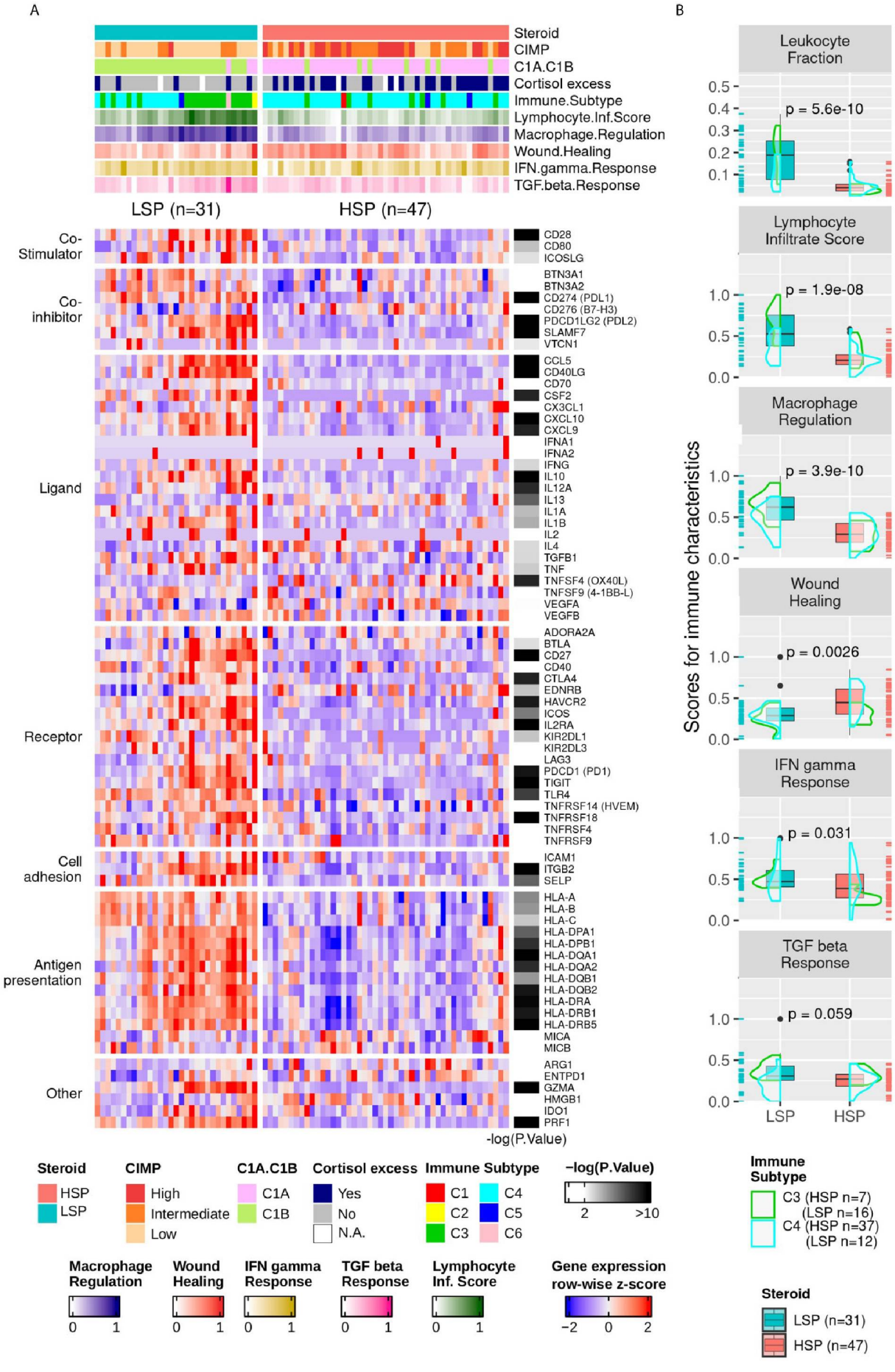

A
Steroid
CIMP
C1A.C1B
Cortisol excess
Immune.Subtype
Lymphocyte.Inf.Score
Macrophage.Regulation
Wound.Healing
IFN.gamma.Response
TGF.beta.Response
LSP (n=31)
HSP (n=47)
Co-Stimulator
CD28
CD80
ICOSLG
Co-inhibitor
BTN3A1
BTN3A2
CD274 (PDL1)
CD276 (B7-H3)
PDCD1LG2 (PDL2)
SLAMF7
VTCN1
Ligand
CCL5
CD40LG
CD70
CSF2
CX3CL1
CXCL10
CXCL9
IFNA1
IFNA2
IFNG
IL10
IL12A
IL13
IL1A
IL1B
IL2
IL4
TGFB1
TNF
TNFSF4 (OX40L)
TNFSF9 (4-1BB-L)
VEGFA
VEGFB
Receptor
ADORA2A
BTLA
CD27
CD40
CTLA4
EDNRB
HAVCR2
ICOS
IL2RA
KIR2DL1
KIR2DL3
LAG3
PDCD1 (PD1)
TIGIT
TLR4
TNFRSF14 (HVEM)
TNFRSF18
TNFRSF4
TNFRSF9
Cell adhesion
ICAM1
ITGB2
SELP
Antigen presentation
HLA-A
HLA-B
HLA-C
HLA-DPA1
HLA-DPB1
HLA-DQA1
HLA-DQA2
HLA-DQB1
HLA-DQB2
HLA-DRA
HLA-DRB1
HLA-DRB5
MICA
MICB
Other
ARG1
ENTPD1
GZMA
HMGB1
IDO1
PRF1
-log(P.Value)
Steroid
HSP
LSP
CIMP
High
Intermediate
Low
C1A.C1B
C1A
C1B
Cortisol excess
Yes
No
N.A.
Immune Subtype
C1
C2
C3
C4
C5
C6
−log(P.Value)
2
>10
Macrophage Regulation
Wound Healing
IFN gamma Response
TGF beta Response
Lymphocyte Inf. Score
Gene expression row-wise z-score
0
1
−2
0
2
B
Leukocyte Fraction
p = 5.6e-10
Lymphocyte Infiltrate Score
p = 1.9e-08
Macrophage Regulation
p = 3.9e-10
Wound Healing
p = 0.0026
IFN gamma Response
p = 0.031
TGF beta Response
p = 0.059
Scores for immune characteristics
LSP
HSP
Immune Subtype
C3 (HSP n=7)
(LSP n=16)
C4 (HSP n=37)
(LSP n=12)
Steroid
LSP (n=31)
HSP (n=47)

Figure 6 Gene expression of immune modulators and Thorsson and colleagues' immune signatures. **(A)** Heatmap with column-wise z-scores for expression of immune modulator genes. The maximum and minimum z-scores for the color gradient is set at +2 and −2 standard deviations from the mean. Each column represents a patient. The order from Figure 5A was maintained. The p-value for the DE analysis for each gene determined using the Wald's test is represented in the right. The −log10 (p-value) color gradient is set as white up to the minimum value of 2 and the maximum is set to 10; however, its range exceeds 20 for *GZMA, CCL5*, and *CD40LG*. The absolute p-values for all differentially expressed genes can be found in Supplementary Table 1. *Clinical cortisol excess and the molecular classification were described by Zheng et al. (5) and presented in the top annotation. **Immune subtype classification and the five molecular immune signatures rescaled to a range of 0 to 1 were according to Thorsson et al. (11) and are shown in the top annotation. **(B)** Boxplot comparing LSP and HSP for leukocyte fractions and the five immune signatures associated with lymphocyte infiltrate scores, macrophage regulation, wound healing, IFN-γ response, and TGF-ß response according to Thorsson et al. (11). The scores for each of the five signatures are rescaled to a range of 0 to 1 (y-axis). The density plot shows the distribution according to the immune subtypes C3 (green) and C4 (cyan). Each sample is shown in a rug plot and colored according to HSP and LSP classification. The p-value calculated using Wilcoxon test comparing both phenotypes is shown above each pair of boxplots.

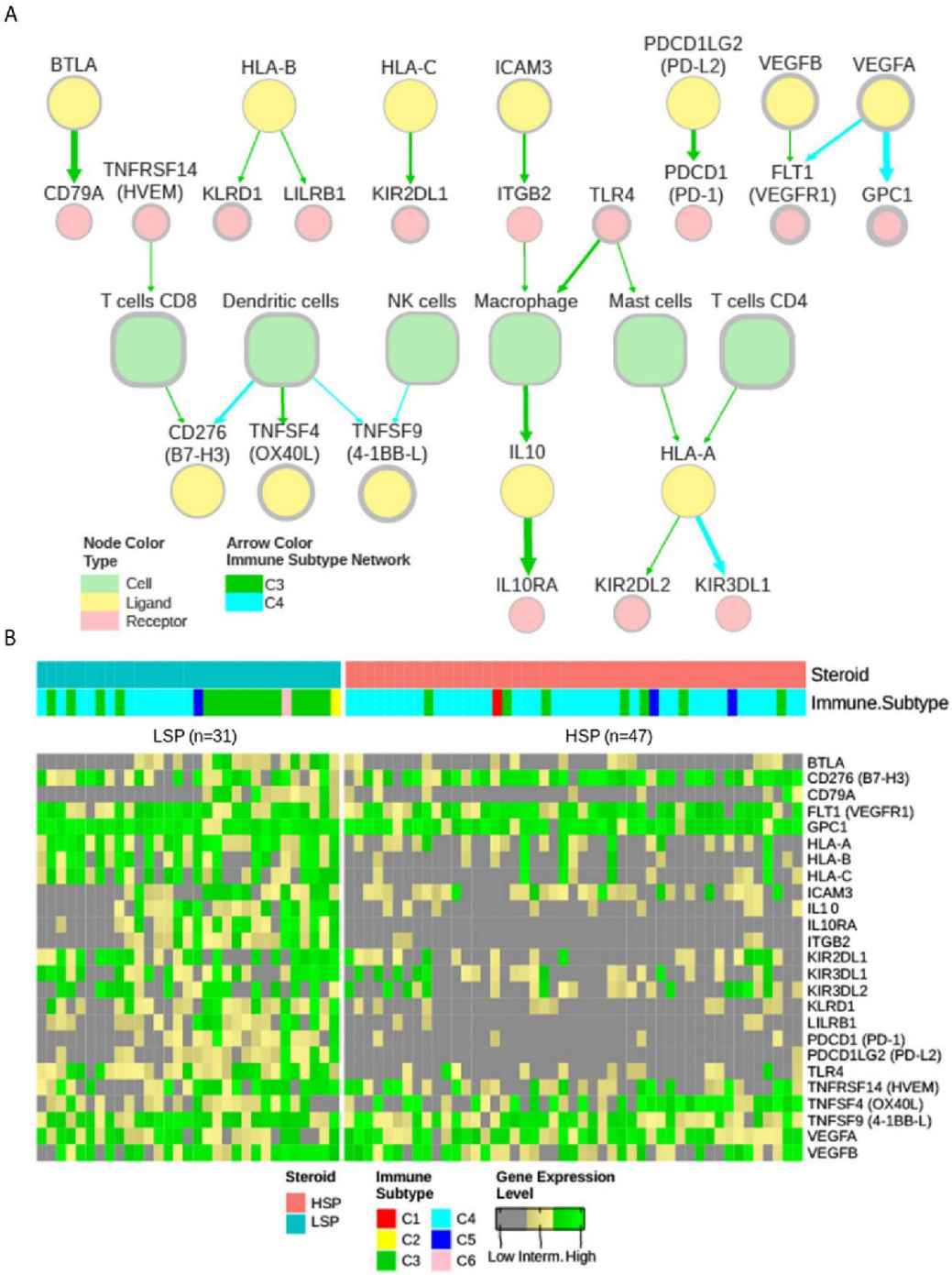


Figure 7 iAtlas explorer-extracellular communication network. **(A)** The extracellular communication network according to Thorsson et al. (11) and available on CRI Atlas (https://isb-cgc.shinyapps.io/shiny-iatlas/) was reconstructed for the C3 and C4 patients of TCGA ACC cohort. Nodes with greater than 50% abundance and a concordance interaction larger than 2.5 were selected. The node line width varies proportionally to abundance and the edge width varies proportionally to concordance. Green arrows represent interactions of C3 patients and cyan arrows represent interactions of C4 patients. Node colors represent immune cells (light green), receptors (pink), and ligands (yellow). **(B)** The receptors and ligands present in the network were evaluated based on gene expression levels in a pan-cancer comparison. Gene expression of the 25 nodes in the network were ranked among 9,361 primary tumor samples available in the TCGA database and classified as low

(grey), intermediate (yellow), or high (green) expression level based on ranking terciles. Each column represents a patient with ACC. Column order is maintained from Figures 5A and 6A heatmaps. Steroid phenotype and immune subtype classifications are indicated in the top annotation.

Despite its greater representativity in the ACC cohort (49 of 78 patients), C4 formed a smaller network (Figure 7A) with generally lower abundance and weaker connections. Curiously, a high abundance of *TNFSF9 (4-1BB-L)*, commonly expressed by antigen-presenting cells, was found to be related to the C4 network, but not its receptor *TNFRSF9 (4-1BB)*, which is normally expressed in CD8+ T cells.

In the C3 network, which was mainly associated with patients with LSP (Figure 7A), antigen presentation molecules and some of their receptors were prominently present. It is noteworthy that *PDCD1LG2 (PD-L2)*, but not *CD274 (PD-L1)*, appeared in good concordance with its receptor *PDCD1 (PD-1)*. Interestingly, a relative positive correlation was observed between *CD8B* and *CD274* expression, but it was more evident between *CD8B* and *PDCD1LG2* expression (Figure 8).

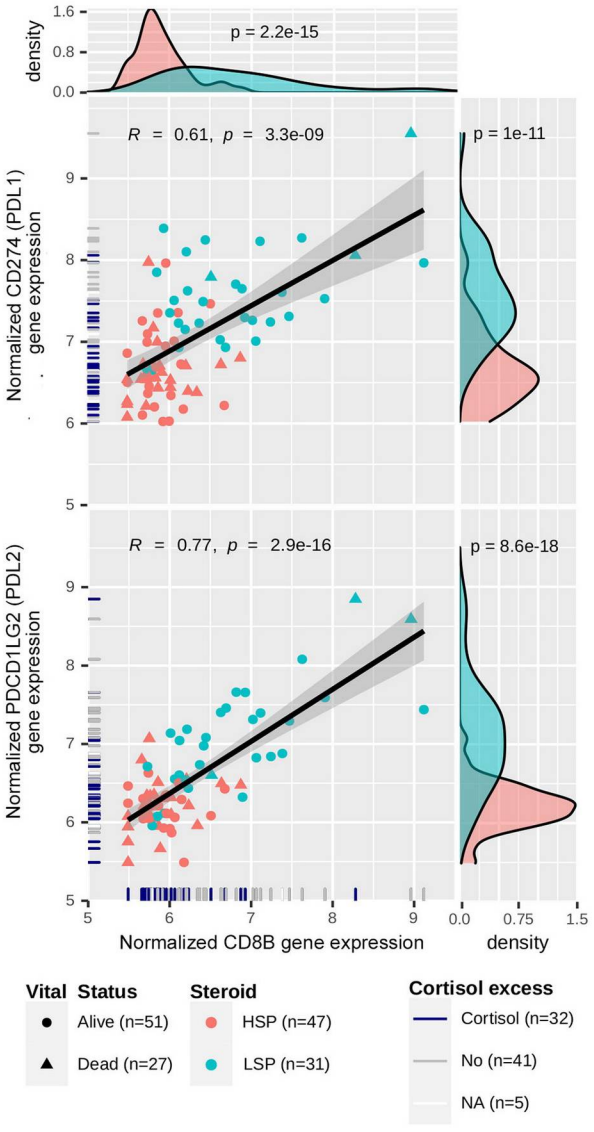


Figure 8 Correlation between *CD274/PDCD1LG2* and *CD8B* expression. Gene expression levels for *CD274, PDCD1LG2* and *CD8B* were normalized using a variance-stabilizing transformation from DESeq2 R package. Pearson's correlation coefficients and p-values are shown in the scatter plots, as well as the regression line. The confidence interval was inferred using Fisher's Z transform. Point colors are set according to the steroid phenotype: salmon for HSP and blue for LSP. Point shapes are set according to the patient's vital status: triangles for dead and circles for alive. In the rug plot, navy blue indicates the presence of cortisol excess, gray indicates absence, and white indicates non-annotated patients regarding cortisol levels. In the density plot, p-values determined using Wald's test for DE analysis between LSP and HSP is shown.

Finally, *CD276 (B7-H3)* and *FLT1* (*VEGFR1)* were present in abundance in both networks. *CD276* was in concordance with CD8+ T cells in C3 and in concordance with dendritic cells in C4, while *FLT1* was in concordance with *VEGFA* in C4 and in concordance with *VEGFB* in C3.

3.4.7 Steroid Phenotype Was More Predictable of Outcome Than Immune Subtype Alone

Based on Kaplan-Meier analysis, LSP presented better outcomes, both in OS ($p = 2 \times 10^{-4}$) and PFI (p-value $< 1 \times 10^{-4}$) (Figure 9A). When comparing the C3 and C4 immune subtypes, a slightly better prognosis was seen for C3 ($p = 3.2 \times 10^{-2}$ for OS and $p = 4.7 \times 10^{-2}$ for PFI) (Figure 9B). The separation between C3 and patients with LSP from the other configurations showed a significant difference in survival analysis ($p = 4.5 \times 10^{-3}$ for OS and $p = 7.1 \times 10^{-3}$ for PFI) (Figure 9C).

3.5 DISCUSSION

We present a complementary approach to the analyses of the pioneering studies by Zheng et al. (5) and Thorsson et al. (11) and revisit the potential biomarkers underlying the immunological processes in ACC, considering important contributions from previous studies (7–9, 12). The interplay between steroid production and the immune response in ACC has been a topic of recent studies (5, 12, 14, 18, 19). We have uncovered further interesting findings from the ACC datasets, deepened the investigation of immune pathways, and revealed possible druggable targets that may guide the selection criteria for ACC-targeted immunotherapy.

We demonstrated the immune system capabilities were dramatically better in patients with LSP (Figures 1 and 2), which is in agreement with studies describing

the immune suppression caused by excess glucocorticoids (12). This higher immune activation seen in a subset of patients with ACC was in contrast with worst outcomes previously demonstrated for ACC in a pan-cancer analysis of solid tumors, which considered all patients with ACC without distinction of subtypes (5, 11). Our analyses, which considered steroid phenotype, improved our understanding of how the immune system reacts to ACC.

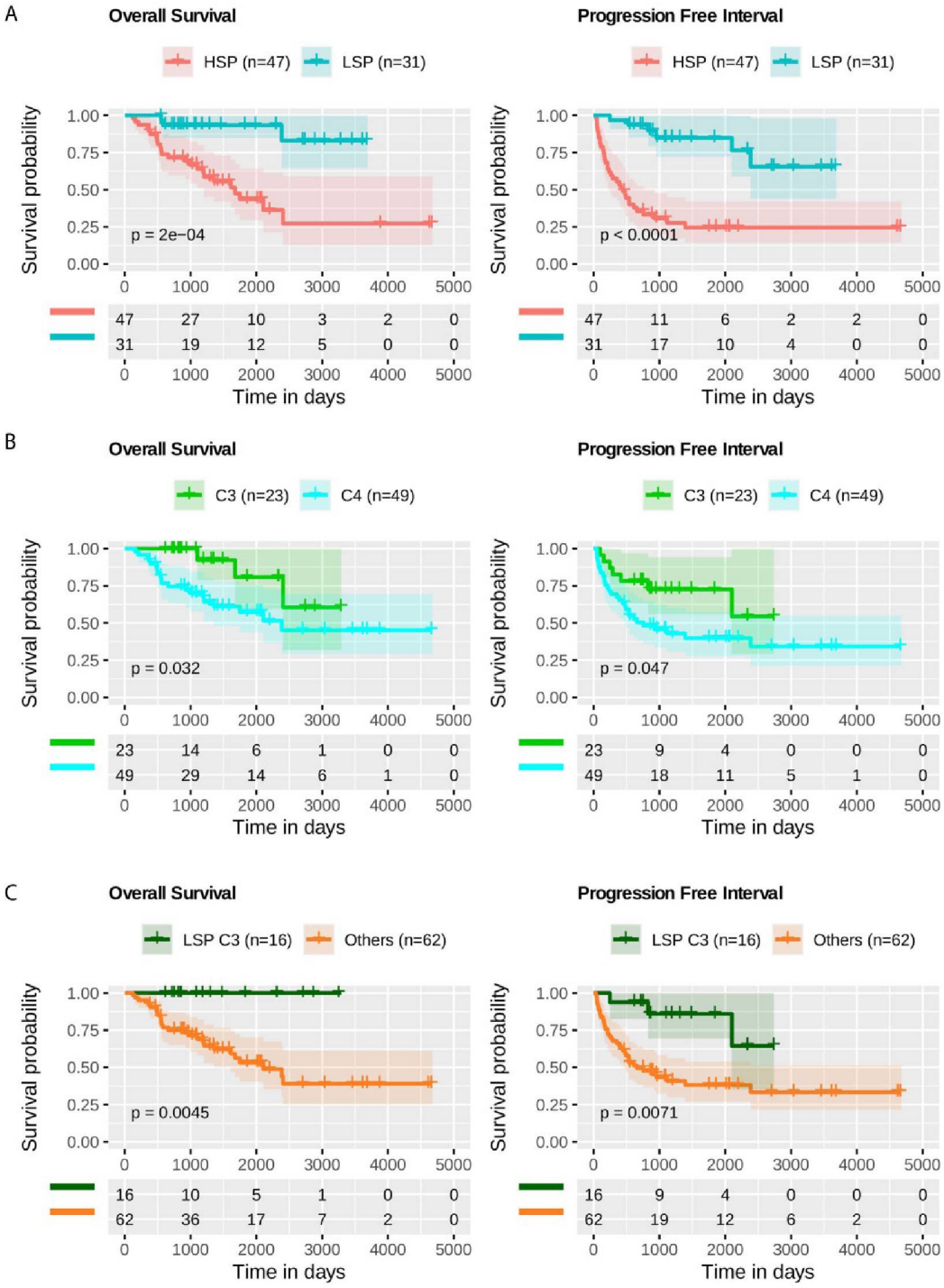


Figure 9 Survival analysis. Kaplan-Meier analysis for overall survival (OS) and progression free interval (PFI) of ACC profiles. The p-value was calculated using a log-rank test and the confidence interval is shown. Below each plot a survival table with the absolute number of participants over time.

(A) OS and PFI for LSP (n = 31) versus HSP (n = 47). **(B)** OS and PFI for immune subtype C3 (n = 23) versus immune subtype C4 (n = 49). **(C)** OS and PFI for LSP and C3 patients (n = 16) versus other combinations (LSP C2, C4, C5, and C6, or HSP C1, C3, C4, and C5; total n = 62).

The immune cell composition in the TME is associated with important prognostic and therapeutic characteristics (14, 39). Our analysis of TME was based on scores inferred by previous studies (11, 39) and used two different methods, xCell and Cibersort, to detect immune cells according to bulk RNA-seq data. Some observed divergences (e.g., native CD4+ T cells) may be explained by limitation of the methods, such as background prediction or the spillover effect, as discussed by Sturm et al. (39). However, a higher immune cell infiltrate was observed in general for patients with LSP compared with that for patients with HSP (Figures 5A, B). Furthermore, both methods showed a significantly higher presence of cells associated with cytotoxic activity (Figure 5B), such as CD8+ T cells ($p = 4.3 \times 10^{-8}$ for xCell and $p = 7 \times 10^{-8}$ for Cibersort scores), T NK cells ($p = 1.1 \times 10^{-5}$ for xCell scores), and activated NK cells ($p = 3.8 \times 10^{-6}$ for Cibersort scores).

Notably, we observed an activation of immune system-related genes (Figure 6A), as well as expression of immune evasion-related genes in patients with LSP (Figures 6A and 8). We also demonstrated a positive correlation between *CD8B* and *CD274 (PD-L1)* expression ($R = 0.61$, $p = 1 \times 10^{-11}$) and *CD8B* and *PDCD1LG2* (*PD-L2)* ($R = 0.77$, $p = 8.6 \times 10^{-18}$) (Figure 8). This may indicate that selective pressure induced enhanced immune evasion by tumor cells, which is in agreement with recent studies (51). PD-1/PD-L1-related and PD-1/PD-L2-related immune escape mechanisms are known to downregulate the CD8+ T-cell activation process. *CD274* is expressed by other immune cells in greater a proportion than that of *PDCD1LG2* expression (58), which may help explain why the dispersion seen in scatter plots was more evident for *CD274*. In addition, patients with HSP ACC overall presented lower levels of *CD8B* and *CD274/PDCD1LG2* expression compared to those of patients with LSP ACC. However, the positive correlation observed between *CD8B* and *CD274/PDCD1LG2* expression may imply that following glucocorticoid suppression, mechanisms of immune evasion may be induced in patients with HSP ACC. The correlation between CD8+TL and PD-L1 expression levels cannot be determined using immunohistochemistry (14, 59). However, findings from a previous study (59) and our current study suggest that PD-L2 plays a greater role than that of PD-L1 in ACC cells (Figure 6A). Nevertheless, this hypothesis has not been assessed in a clinical trial. Anti-PD-1 clinical trials conducted without inhibiting steroidogenesis (30–32) may have had modest results due to the immune suppression caused by hormone production in the TME. On the other hand, Le Tourneau et al. (33) evaluated the concomitant suppression of steroidogenesis with and without mitotane administration. However, only anti-PD-L1 was used in their

study and they did not consider the possibility of PD-L2 being an important immune checkpoint in ACC.

In agreement with recent findings showing that 90% of ACC samples (n = 48) were positive for B7-H3 (*CD276*) in immunohistochemical assays (60), our analysis demonstrated that *CD276* overexpression was detected in both LSP and HSP. Remarkably, its expression was considered high in a pan-cancer comparison of most ACC patients (Figure 7B). Moreover, *CD276* overexpression has been implicated in resistance to anti-PD1 therapies (61–63). B7-H3 is a member of the B7 ligand family and is a recent and attractive target for antibody-based immunotherapy. B7-H3 is differentially overexpressed in malignant cells at high frequency (60% of 25,000 tumor samples), is detected at low levels in normal tissues, and probably has an inhibitory role in adaptive immunity, suppressing T-cell activation and proliferation (60–62). B7-H3 modulates T-cell responses, but unlike PD-1 and CTLA-4, may inhibit T-cell activation, possibly by interacting with tumor necrosis family receptors (64). However, other investigators believe the B7-H3 receptor remains unknown (61). Recent studies have shown that blocking B7-H3 results in a response of tumor resistance to treatments with anti-PD1/PD-L1 antibodies (61). Yonesaka et al. (63) demonstrated the dual blockade of B7-H3 and PD-L1 enhances the antitumor reaction compared to that of PD-L1 blockade alone, which may indicate a role of B7-H3 overexpression in immune evasion. These findings suggest that anti-B7-H3 combined with anti-PD-1/PD-L1 antibody therapy is a promising approach for B7-H3-expressing cancers, such as ACC. In addition to *CD276* (B7-H3), *FLT1* (VEGFR1) appeared in both C3 and C4 networks (Figure 7A) and was highly expressed in ACC compared with that in other cancers (Figure 7B). This may imply a role in angiogenesis, which has been described as an important pathway in ACC (65, 66). However, clinical trials to date using VEGFR inhibitors for ACC have demonstrated limited results (67, 68).

In contrast to *CD276* (B7-H3) and *FLT1* (VEGFR1), *BTLA*, interleukin 10 (*IL10*), IL10 receptor subunit alpha *(IL10RA)*, integrin beta chain-2 (*ITGB2*), *CD274* (*PD-L1*), and *PDCD1LG2* (*PD-L2*) are significantly downregulated in HSP (Supplementary Table 1, Figures 6A and 7B). Similar to PD-1 and CTLA-4, BTLA is an immune checkpoint associated with suppression of the immune response and its blockade has been related to a reduction of ovarian carcinoma *via* the regulation of IL6 and IL10 (69). IL10 mediates immunosuppressive signals through its interaction with IL10 receptors, leading to inhibition of synthesis of proinflammatory cytokines (70). Integrins, such as ITGB2, play significant roles in cellular adhesion and cell surface signaling, and also participate in leukocyte adhesion and extravasation to inflame tissues, and mediate the formation of immunological synapses (71).

Curiously, *TNFSF9 (4-1BB-L)* was present at a surprisingly high abundance in ACC when compared to that of other TCGA tumor types, but not its receptor

TNFRSF9 (*4-1BB)*, which was present mainly on CD8+ T cells, (Figure 7B). In the C4 network, *TNFSF9* appeared in concordance with dendritic and NK cells (Figure 7A). TNFSF9 is commonly expressed by antigen-presenting cells and its interaction with its receptor TNFRSF9 tends to stimulate T cells and cytotoxic activity, demonstrating strong anti-tumor activity (72). Although the use of TNFSF9 analogues as an immunotherapy strategy has been considered (73), the relatively low level expression of its receptor TNFRSF9 on T cells may limit the efficacy of this type of treatment. Understanding the role of *TNFSF9* overexpression in ACC may be a subject of future studies.

Classification of ACC into subgroups based on methylation profiles, which was also proposed by Zheng et al. (5), appears to be robust as reviewed by Crona and Beuschlein (6). However, despite providing good clinical prognostic indications, this classification has not resulted in novel treatment possibilities for each of the groups (6, 7, 74). One strong point of our current study using the molecular classification of steroidal profiles was the possibility of separating the immune activation profile of tumor subtypes. This is in agreement with the suggestion by Fiorentini et al. (7) that patients who may benefit from immunotherapies should be selected based on some type of molecular classification. We believe that separation based on steroid profiles may provide useful information regarding this criterion. Furthermore, the LSP classification successfully grouped all patients with higher expression of immune modulator genes, in addition to higher leukocyte fractions. Remarkably, the immune activation distinction was not clear when using the classification of cases based solely on clinical parameters, that is, hypercortisolism versus non-hypercortisolism (data not shown). This was despite its good correlation with HSP (Fisher's exact test, $p = 2.55 \times 10^{-4}$). In addition, the available HSP data are associated with downregulation of the immune system, higher tumor proliferation, and worst prognosis (75).

Genomic and epigenetic changes frequently occur in ACC, in both childhood (15, 76) and adulthood (5, 75, 77) cases. However, the TCGA ACC cohort is mainly limited to adults (median age, 46 years). The accumulation of these alterations may alter lymphocyte recruitment (11) and drive a higher proliferation profile, which would consequently result in a worse prognosis. It is currently not clear if the anti-tumor immune response is not strong enough to surpass tumor proliferation or if there is a surge in proliferation due to the immunosuppressed TME.

Interestingly, it was not possible to determine a clear correlation between leukocyte fraction and mutations in driver gene known to impact the immune response. This could have been due to the small number of patients with these mutations, as well as the fact that most of these patients were from the immunosuppressed HSP group. In analysis of the whole cohort (LSP + HSP patients) *CTNNB1* mutations were noted only in patients of the HSP group and they

demonstrated a weak negative correlation with leukocyte fraction ($p = 3.8 \times 10^{-2}$ on Wilcoxon test). However, when analyzing only the HSP group, the presence of *CTNNB1* mutations did not demonstrate any significant impact on leukocyte fraction ($p = 9.9 \times 10^{-1}$ on Wilcoxon test), indicating the weak correlation observed was mainly due to the steroid phenotype. This indicates the steroid phenotype should be taken into account during immune response analysis of ACC. Failing to do so may generate confounding effects.

When comparing the inflammatory C3 and lymphocyte-depleted C4 immune signatures, we found a slightly better survival for C3 ($p = 3.2 \times 10^{-2}$ for OS and $p = 4.7 \times 10^{-2}$ for PFI; log-rank test) (Figure 9B). In the pan-cancer analysis performed by Thorsson and colleagues, C3 had a significantly better outcome than that of C4; however, the steroid phenotype provides more characteristics regarding tumor aggressiveness and outcome prognosis in ACC than that of the C3-C4 signatures. For example, there were no death events among the 16 patients with C3 LSP, whereas there were 3 deaths among the 7 patients with C3 HSP (42.9%). Furthermore, among the 12 patients with C4 LSP, only 1 died (8.33%) compared with 19 deaths in the group of 37 patients with C4 HSP (51,35%). When distinguishing C3 and C4 patients within the steroid phenotypes (density plots in Figures 5B, 6B), differences were observed in LSP C3 versus C4, especially in the leukocyte fraction and lymphocyte infiltration scores; however, HSP C3 versus C4 does not in general present great distinction. Considering there were only seven patients with HSP C3, the steroid phenotype distinguished some immune features better than that of the C1–C6 subtype classification alone.

In addition to differences in the targeted immune checkpoints, a crucial difference affecting the success of immunotherapies for other tumors (22–24, 78) and the modest results of immunotherapy in ACC, such as less than 15% of patients with ACC benefiting from PD-1 or PD-L1 inhibition (30–33), seems to be the immunosuppressive and anti-inflammatory effects of intratumoral glucocorticoids (12). Among potential prognostic factors, CD3+ and CD8+ cytotoxic T lymphocytes were found in 84% of 146 patients with ACC and were associated with overall and recurrence-free survival (12). This parameter could be further improved by blocking steroidogenesis in combination with different immune checkpoint inhibitors. Patients with tumor progression and mitotane-resistance may still benefit from a reduction in the dose aiming for steroidogenesis blockade. One important feature of mitotane treatment is the ability to block steroid biosynthesis at lower daily doses and with less toxic side effects (approximately <10 µg/mL of plasma) (79). Future studies may investigate if this blockade is adequate to induce an efficient immune response.

Despite the reduced number of cases, we found evidence of considerable immune cell infiltrates within LSP and sought to characterize the interactions and networks in order to identify transcriptomic biomarkers associated with significant

immune activation. Our analysis also exploited target immune modulators that may regulate potential pathways associated with the anti-tumor response. Our analysis framework had limitations as it relied on a small number of accessible profiles and a simple binary change (LSP and HSP) where HSP combined different steroid subtypes that could not be identified using only the clinical manifestations of hypercortisolism. It is important to note that the activation of steroid biosynthesis pathways seen in HSP was based on a transcriptome profile, which may imply a possible hormone excess in the TME had not been related to clinical manifestations. Our experimental design using a probabilistic approach to identify potential targets for immunotherapy was restricted to *in silico* findings. Despite the rationale, this may not be translatable to *in vivo* assays. Further work is needed to fully understand the possibility of changing the outcome of ACC immunotherapy, which may start with the selection of patients with LSP ACC and the inhibition of steroidogenesis in patients with HSP ACC. Despite significant progress in identifying immunogenic biomarkers in ACC through evaluation of the TCGA cohort (5), there are still many limitations and puzzles to be solved. Additional efforts beyond RNAseq analyses are needed to validate functional studies to define the key pathways in a larger number of patients with LSP ACC. Considering we are still in the early stage of understanding the B7-H3 network, it is important to define the actual B7-H3 receptor in order to fully understand this pathway in ACC.

3.6 CONCLUSIONS

An important frontier of ACC therapeutics to improve the anti-tumor activity of the immune system starts explicitly by modeling steroidogenic differences. The analytical approach we describe herein requires further studies to ascertain the possible druggable role of B7-H3 in relation to PD1-PDL1/PDL2 in ACC. Our present approach was unable to predict improved outcomes of immunotherapy; however, it points to possible selection criteria and potential targets. Future work should confirm these findings using a larger cohort, in addition to including pre-clinical or clinical trials.

3.7 CODE AVAILABILITY AND REPRODUCIBILITY

All scripts, datasets, software and algorithms used to generate results, figures, and tables for this study are available on the GitHub repository (https://github.com/sysbiolab/Sup_Material_Muzzi2021) and Supplementary Tables 3 and 4.

3.8 DATA AVAILABILITY STATEMENT

The original contributions presented in the study are included in the article/Supplementary Material. Further inquiries can be directed to the corresponding author.

3.9 ETHICS STATEMENT

The studies involving human participants were reviewed and approved by Pequeno Príncipe Ethics Committee. Written informed consent from the participants' legal guardian/next of kin was not required to participate in this study in accordance with the national legislation and the institutional requirements.

3.10 AUTHOR CONTRIBUTIONS

All authors made substantial contributions to the conception of the work. JCDM was responsible for data acquisition and analysis. MAAC contributed to the acquisition of data and method analyses. All authors contributed to data interpretation. JCDM and BF wrote the first draft of the manuscript. JMM and MAC helped in code review and creating the public repository. All authors contributed to the article and approved the submitted version.

3.11 FUNDING

JCDM, JMM, and MAC receive scholarships from the BIG DATA innovation program from the Associação Hospitalar de Proteção à Infância Raul Carneiro-AHPIRAC (2020). MAAC and JM are funded by the Conselho Nacional de Desenvolvimento Científico e Tecnológico (CNPq).

3.12 CONFLICT OF INTEREST

The authors declare the current research was conducted in the absence of any commercial or financial relationships that could be construed as a potential conflict of interest.

3.13 ACKNOWLEDGMENTS

Data used in this manuscript were obtained from The Cancer Genome Atlas (TCGA) ACC database. We are grateful to AHPIRAC for the scientific editing support.

3.14 SUPPLEMENTARY MATERIAL

The Supplementary Material for this article can be found online at: https://www.frontiersin.org/articles/10.3389/fendo.2021.672319/full#supplementary-material

3.15 REFERENCES

1. Allolio B, Fassnacht M. Adrenocortical Carcinoma: Clinical Update. *J Clin Endocrinol Metab* (2006) 91:2027–37. doi: 10.1210/jc.2005-2639
PubMed Abstract | CrossRef Full Text | Google Scholar
2. Libè R, Fratticci A, Bertherat J. Adrenocortical Cancer: Pathophysiology and Clinical Management. *Endocr Relat Cancer* (2007) 14:13–28. doi: 10.1677/erc.1.01130
PubMed Abstract | CrossRef Full Text | Google Scholar
3. Fassnacht M, Kroiss M, Allolio B. Update in Adrenocortical Carcinoma. *J Clin Endocrinol Metab* (2013) 98:4551–64. doi: 10.1210/jc.2013-3020
PubMed Abstract | CrossRef Full Text | Google Scholar
4. Berruti A, Fassnacht M, Haak H, Else T, Baudin E, Sperone P, et al. Prognostic Role of Overt Hypercortisolism in Completely Operated Patients With Adrenocortical Cancer. *Eur Urol* (2014) 65:832–38. doi: 10.1016/j.eururo.2013.11.006
PubMed Abstract | CrossRef Full Text | Google Scholar
5. Zheng S, Cherniack AD, Dewal N, Moffitt RA, Danilova L, Murray BA, et al. Comprehensive Pan-Genomic Characterization of Adrenocortical Carcinoma. *Cancer Cell* (2016) 29:723–36. doi: 10.1016/j.ccell.2016.04.002
PubMed Abstract | CrossRef Full Text | Google Scholar
6. Crona J, Beuschlein F. Adrenocortical Carcinoma — Towards Genomics Guided Clinical Care. *Nat Rev Endocrinol* (2019) 15:548–60. doi: 10.1038/s41574-019-0221-7
PubMed Abstract | CrossRef Full Text | Google Scholar
7. Fiorentini C, Grisanti S, Cosentini D, Abate A, Rossini E, Berruti A, et al. Molecular Drivers of Potential Immunotherapy Failure in Adrenocortical Carcinoma. *J Oncol* (2019) 2019:6072863. doi: 10.1155/2019/6072863
PubMed Abstract | CrossRef Full Text | Google Scholar
8. de Reyniès A, Assié G, Rickman DS, Tissier F, Groussin L, René-Corail F, et al. Gene Expression Profiling Reveals a New Classification of Adrenocortical Tumors and Identifies Molecular Predictors of Malignancy and Survival. *J Clin Oncol* (2009) 27:1108–15. doi: 10.1200/JCO.2008.18.5678
PubMed Abstract | CrossRef Full Text | Google Scholar
9. Giordano TJ, Kuick R, Else T, Gauger PG, Vinco M, Bauersfeld J, et al. Molecular Classification and Prognostication of Adrenocortical Tumors by Transcriptome Profiling. *Clin Cancer Res* (2009) 15:668–76. doi: 10.1158/1078-0432.CCR-08-1067
PubMed Abstract | CrossRef Full Text | Google Scholar
10. Li B, Severson E, Pignon J-CC, Zhao H, Li T, Novak J, et al. Comprehensive Analyses of Tumor Immunity: Implications for Cancer Immunotherapy. *Genome Biol* (2016) 17:174. doi: 10.1186/s13059-016-1028-7
PubMed Abstract | CrossRef Full Text | Google Scholar

11. Thorsson V, Gibbs DL, Brown SD, Wolf D, Bortone DS, Ou Yang TH, et al. The Immune Landscape of Cancer. *Immunity* (2018) 48:812–30.e14. doi: 10.1016/j.immuni.2018.03.023
PubMed Abstract | CrossRef Full Text | Google Scholar
12. Landwehr L-S, Altieri B, Schreiner J, Sbiera I, Weigand I, Kroiss M, et al. Interplay Between Glucocorticoids and Tumor-Infiltrating Lymphocytes on the Prognosis of Adrenocortical Carcinoma. *J Immunother Cancer* (2020) 8:e000469. doi: 10.1136/jitc-2019-000469
PubMed Abstract | CrossRef Full Text | Google Scholar
13. Michalkiewicz E, Sandrini R, Figueiredo B, Miranda ECMM, Caran E, Oliveira-Filho AG, et al. Clinical and Outcome Characteristics of Children With Adrenocortical Tumors: A Report From the International Pediatric Adrenocortical Tumor Registry. *J Clin Oncol* (2004) 22:838–45. doi: 10.1200/JCO.2004.08.085
PubMed Abstract | CrossRef Full Text | Google Scholar
14. Parise IZS, Parise GA, Noronha L, Surakhy M, Woiski TD, Silva DB, et al. The Prognostic Role of CD8+ T Lymphocytes in Childhood Adrenocortical Carcinomas Compared to Ki-67, Pd-1, PD-L1, and the Weiss Score. *Cancers (Basel)* (2019) 11:1730. doi: 10.3390/cancers11111730
CrossRef Full Text | Google Scholar
15. Pinto EM, Chen X, Easton J, Finkelstein D, Liu Z, Pounds S, et al. Genomic Landscape of Paediatric Adrenocortical Tumours. *Nat Commun* (2015) 6:6302. doi: 10.1038/ncomms7302
PubMed Abstract | CrossRef Full Text | Google Scholar
16. Finn OJ. Cancer Immunology. *N Engl J Med* (2008) 358:2704–15. doi: 10.1056/NEJMra072739
PubMed Abstract | CrossRef Full Text | Google Scholar
17. Custódio G, Komechen H, Figueiredo FRO, Fachin ND, Pianovski MAD, Figueiredo BC. Molecular Epidemiology of Adrenocortical Tumors in Southern Brazil. *Mol Cell Endocrinol* (2012) 351:44–51. doi: 10.1016/j.mce.2011.10.019
PubMed Abstract | CrossRef Full Text | Google Scholar
18. Vanbrabant T, Fassnacht M, Assie G, Dekkers OM. Influence of Hormonal Functional Status on Survival in Adrenocortical Carcinoma: Systematic Review and Meta-Analysis. *Eur J Endocrinol* (2018) 179:429–36. doi: 10.1530/EJE-18-0450
PubMed Abstract | CrossRef Full Text | Google Scholar
19. Lalli E, Figueiredo BC. Pediatric Adrenocortical Tumors: What They Can Tell Us on Adrenal Development and Comparison With Adult Adrenal Tumors. *Front Endocrinol (Lausanne)* (2015) 6:23. doi: 10.3389/fendo.2015.00023
PubMed Abstract | CrossRef Full Text | Google Scholar
20. Prager I, Liesche C, van Ooijen H, Urlaub D, Verron Q, Sandström N, et al. NK Cells Switch From Granzyme B to Death Receptor–Mediated Cytotoxicity During Serial Killing. *J Exp Med* (2019) 216:2113–27. doi: 10.1084/jem.20181454
PubMed Abstract | CrossRef Full Text | Google Scholar
21. Cursons J, Souza-Fonseca-Guimaraes F, Foroutan M, Anderson A, Hollande F, Hediyeh-Zadeh S, et al. A Gene Signature Predicting Natural Killer Cell Infiltration and Improved Survival in Melanoma Patients. *Cancer Immunol Res* (2019) 7:1162–74. doi: 10.1158/2326-6066.CIR-18-0500
PubMed Abstract | CrossRef Full Text | Google Scholar
22. Drake CG, Lipson EJ, Brahmer JR. Breathing New Life Into Immunotherapy: Review of Melanoma, Lung and Kidney Cancer. *Nat Rev Clin Oncol* (2014) 11:24–37. doi: 10.1038/nrclinonc.2013.208

PubMed Abstract | CrossRef Full Text | Google Scholar
23. Rodriguez D, Goulart C, Pagliarone AC, Silva EP, Cunegundes PS, Nascimento IP, et al. *In Vitro* Evidence of Human Immune Responsiveness Shows the Improved Potential of a Recombinant Bcg Strain for Bladder Cancer Treatment. *Front Immunol* (2019) 10:1460. doi: 10.3389/fimmu.2019.01460
PubMed Abstract | CrossRef Full Text | Google Scholar
24. Pettenati C, Ingersoll MA. Mechanisms of BCG Immunotherapy and its Outlook for Bladder Cancer. *Nat Rev Urol* (2018) 15:615–25. doi: 10.1038/s41585-018-0055-4
PubMed Abstract | CrossRef Full Text | Google Scholar
25. Hong H, Wang Q, Li J, Liu H, Meng X, Zhang H. Aging, Cancer and Immunity. *J Cancer* (2019) 10:3021–7. doi: 10.7150/jca.30723
PubMed Abstract | CrossRef Full Text | Google Scholar
26. Wasserman JD, Zambetti GP, Malkin D. Towards an Understanding of the Role of p53 in Adrenocortical Carcinogenesis. *Mol Cell Endocrinol* (2012) 351:101–10. doi: 10.1016/j.mce.2011.09.010
PubMed Abstract | CrossRef Full Text | Google Scholar
27. Bindea G, Mlecnik B, Tosolini M, Kirilovsky A, Waldner M, Obenauf AC, et al. Spatiotemporal Dynamics of Intratumoral Immune Cells Reveal the Immune Landscape in Human Cancer. *Immunity* (2013) 39:782–95. doi: 10.1016/j.immuni.2013.10.003
PubMed Abstract | CrossRef Full Text | Google Scholar
28. Rieder SA, Wang J, White N, Qadri A, Menard C, Stephens G, et al. B7-H7 (HHLA2) Inhibits T-cell Activation and Proliferation in the Presence of TCR and CD28 Signaling. *Cell Mol Immunol* (2020). doi: 10.1038/s41423-020-0361-7
PubMed Abstract | CrossRef Full Text | Google Scholar
29. Greenwald RJ, Freeman GJ, Sharpe AH. The B7 Family Revisited. *Annu Rev Immunol* (2005) 23:515–48. doi: 10.1146/annurev.immunol.23.021704.115611
PubMed Abstract | CrossRef Full Text | Google Scholar
30. Carneiro BA, Konda B, Costa RB, Costa RLB, Sagar V, Gursel DB, et al. Nivolumab in Metastatic Adrenocortical Carcinoma: Results of a Phase 2 Trial. *J Clin Endocrinol Metab* (2019) 104:6193–200. doi: 10.1210/jc.2019-00600
PubMed Abstract | CrossRef Full Text | Google Scholar
31. Raj N, Zheng Y, Kelly V, Katz SS, Chou J, Do RKG, et al. Pd-1 Blockade in Advanced Adrenocortical Carcinoma. *J Clin Oncol* (2020) 38:71–80. doi: 10.1200/JCO.19.01586
PubMed Abstract | CrossRef Full Text | Google Scholar
32. Habra MA, Stephen B, Campbell M, Hess K, Tapia C, Xu M, et al. Phase II Clinical Trial of Pembrolizumab Efficacy and Safety in Advanced Adrenocortical Carcinoma. *J Immunother Cancer* (2019) 7:253. doi: 10.1186/s40425-019-0722-x
PubMed Abstract | CrossRef Full Text | Google Scholar
33. Le Tourneau C, Hoimes C, Zarwan C, Wong DJ, Bauer S, Claus R, et al. Avelumab in Patients With Previously Treated Metastatic Adrenocortical Carcinoma: Phase 1b Results From the JAVELIN Solid Tumor Trial. *J Immunother Cancer* (2018) 6:111. doi: 10.1186/s40425-018-0424-9
PubMed Abstract | CrossRef Full Text | Google Scholar
34. Cosentini D, Grisanti S, Volta AD, Laganà M, Fiorentini C, Perotti P, et al. Immunotherapy Failure in Adrenocortical Cancer: Where Next? *Endocr Connect* (2018) 7:E5–8. doi: 10.1530/EC-18-0398
PubMed Abstract | CrossRef Full Text | Google Scholar

35. Colaprico A, Silva TC, Olsen C, Garofano L, Cava C, Garolini D, et al. Tcgabiolinks: An R/Bioconductor Package for Integrative Analysis of TCGA Data. *Nucleic Acids Res* (2016) 44:e71. doi: 10.1093/nar/gkv1507
PubMed Abstract | CrossRef Full Text | Google Scholar
36. Silva TC, Colaprico A, Olsen C, D'Angelo F, Bontempi G, Ceccarelli M, et al. Tcga Workflow: Analyze Cancer Genomics and Epigenomics Data Using Bioconductor Packages. *F1000Research* (2016) 5:1542. doi: 10.12688/f1000research.8923.2
PubMed Abstract | CrossRef Full Text | Google Scholar
37. Mounir M, Lucchetta M, Silva TC, Olsen C, Bontempi G, Chen X, et al. New Functionalities in the TCGAbiolinks Package for the Study and Integration of Cancer Data From GDC and Gtex. *PloS Comput Biol* (2019) 15:e1006701. doi: 10.1371/journal.pcbi.1006701
PubMed Abstract | CrossRef Full Text | Google Scholar
38. Aran D, Hu Z, Butte AJ. xCell: Digitally Portraying the Tissue Cellular Heterogeneity Landscape. *Genome Biol* (2017) 18:220. doi: 10.1186/s13059-017-1349-1
PubMed Abstract | CrossRef Full Text | Google Scholar
39. Sturm G, Finotello F, Petitprez F, Zhang JD, Baumbach J, Fridman WH, et al. Comprehensive Evaluation of Transcriptome-Based Cell-Type Quantification Methods for Immuno-Oncology. *Bioinformatics* (2019) 35:i436–45. doi: 10.1093/bioinformatics/btz363
PubMed Abstract | CrossRef Full Text | Google Scholar
40. Newman AM, Liu CL, Green MR, Gentles AJ, Feng W, Xu Y, et al. Robust Enumeration of Cell Subsets From Tissue Expression Profiles. *Nat Methods* (2015) 12:453–7. doi: 10.1038/nmeth.3337
PubMed Abstract | CrossRef Full Text | Google Scholar
41. Gu Z, Eils R, Schlesner M. Complex Heatmaps Reveal Patterns and Correlations in Multidimensional Genomic Data. *Bioinformatics* (2016) 32:2847–9. doi: 10.1093/bioinformatics/btw313
PubMed Abstract | CrossRef Full Text | Google Scholar
42. Morgan M, Obenchain V, Hester J, Pagès H. Summarizedexperiment: SummarizedExperiment Container. In: *R package version 1.20.0* (2020). doi: 10.18129/B9.bioc.SummarizedExperiment
CrossRef Full Text | Google Scholar
43. Morgan M, Shepherd L. Annotationhub: Client to Access AnnotationHub Resources. In: *R package, version 2.22.0* (2020). doi: 10.18129/B9.bioc.AnnotationHub
CrossRef Full Text | Google Scholar
44. Love MI, Huber W, Anders S. Moderated Estimation of Fold Change and Dispersion for RNA-seq Data With Deseq2. *Genome Biol* (2014) 15:550. doi: 10.1186/s13059-014-0550-8
PubMed Abstract | CrossRef Full Text | Google Scholar
45. Yamaguchi KD, Ruderman DL, Croze E, Wagner TC, Velichko S, Reder AT, et al. Ifn-β-Regulated Genes Show Abnormal Expression in Therapy-Naïve Relapsing–Remitting MS Mononuclear Cells: Gene Expression Analysis Employing All Reported Protein–Protein Interactions. *J Neuroimmunol* (2008) 195:116–20. doi: 10.1016/j.jneuroim.2007.12.007
PubMed Abstract | CrossRef Full Text | Google Scholar
46. Weiner J 3rd, Domaszewska T. Tmod: An R Package for General and Multivariate Enrichment Analysis. *PeerJ* (2016) 4:1–9. doi: 10.7287/peerj.preprints.2420

CrossRef Full Text | Google Scholar
47. Zyla J, Marczyk M, Domaszewska T, Kaufmann SHE, Polanska J, Weiner J. Gene Set Enrichment for Reproducible Science: Comparison of CERNO and Eight Other Algorithms. *Bioinformatics* (2019) 35:5146–54. doi: 10.1093/bioinformatics/btz447
PubMed Abstract | CrossRef Full Text | Google Scholar
48. Subramanian A, Tamayo P, Mootha VK, Mukherjee S, Ebert BL, Gillette MA, et al. Gene Set Enrichment Analysis: A Knowledge-Based Approach for Interpreting Genome-Wide Expression Profiles. *Proc Natl Acad Sci* (2005) 102:15545–50. doi: 10.1073/pnas.0506580102
PubMed Abstract | CrossRef Full Text | Google Scholar
49. Liberzon A, Birger C, Thorvaldsdóttir H, Ghandi M, Mesirov JP, Tamayo P. The Molecular Signatures Database Hallmark Gene Set Collection. *Cell Syst* (2015) 1:417–25. doi: 10.1016/j.cels.2015.12.004
PubMed Abstract | CrossRef Full Text | Google Scholar
50. Li S, Rouphael N, Duraisingham S, Romero-Steiner S, Presnell S, Davis C, et al. Molecular Signatures of Antibody Responses Derived From a Systems Biology Study of Five Human Vaccines. *Nat Immunol* (2014) 15:195–204. doi: 10.1038/ni.2789
PubMed Abstract | CrossRef Full Text | Google Scholar
51. Wang H, Najibi AJ, Sobral MC, Seo BR, Lee JY, Wu D, et al. Biomaterial-Based Scaffold for in Situ Chemo-Immunotherapy to Treat Poorly Immunogenic Tumors. *Nat Commun* (2020) 11:5696. doi: 10.1038/s41467-020-19540-z
PubMed Abstract | CrossRef Full Text | Google Scholar
52. Ramilowski JA, Goldberg T, Harshbarger J, Kloppmann E, Lizio M, Satagopam VP, et al. A Draft Network of Ligand–Receptor-Mediated Multicellular Signalling in Human. *Nat Commun* (2015) 6:7866. doi: 10.1038/ncomms8866
PubMed Abstract | CrossRef Full Text | Google Scholar
53. Castro MA, Wang X, Fletcher MN, Meyer KB, Markowetz F. Reder: R/Bioconductor Package for Representing Modular Structures, Nested Networks and Multiple Levels of Hierarchical Associations. *Genome Biol* (2012) 13:R29. doi: 10.1186/gb-2012-13-4-r29
PubMed Abstract | CrossRef Full Text | Google Scholar
54. Hoadley KA, Yau C, Hinoue T, Wolf DM, Lazar AJ, Drill E, et al. Cell-of-Origin Patterns Dominate the Molecular Classification of 10,000 Tumors From 33 Types of Cancer. *Cell* (2018) 173:291–304. doi: 10.1016/j.cell.2018.03.022
PubMed Abstract | CrossRef Full Text | Google Scholar
55. Therneau T. A Package for Survival Analysis in R. In: *R package version 3.2-7* (2020). Available at: https://cran.r-project.org/package=survival.
Google Scholar
56. Therneau TM, Grambsch PM. *Modeling Survival Data: Extending the Cox Model*. New York, NY: Springer New York (2000). doi: 10.1007/978-1-4757-3294-8
CrossRef Full Text | Google Scholar
57. Storey J, Bass A, Dabney A, Robinson D. *Qvalue: Q-value Estimation for False Discovery Rate Control R Package Version 2.22.0*. (2020). doi: 10.18129/B9.bioc.qvalue.
CrossRef Full Text | Google Scholar
58. Monaco G, Lee B, Xu W, Mustafah S, Hwang YY, Carré C, et al. Rna-Seq Signatures Normalized by Mrna Abundance Allow Absolute Deconvolution of Human Immune Cell Types. *Cell Rep* (2019) 26:1627–40.e7. doi: 10.1016/j.celrep.2019.01.041

PubMed Abstract | CrossRef Full Text | Google Scholar
59. Tierney JF, Vogle A, Poirier J, Min IM, Finnerty B, Zarnegar R, et al. Expression of Programmed Death Ligand 1 and 2 in Adrenocortical Cancer Tissues: An Exploratory Study. *Surgery* (2019) 165:196–201. doi: 10.1016/j.surg.2018.04.086
PubMed Abstract | CrossRef Full Text | Google Scholar
60. Liang J, Liu Z, Pei T, Xiao Y, Zhou L, Tang Y, et al. Clinicopathological and Prognostic Characteristics of CD276 (B7-H3) Expression in Adrenocortical Carcinoma. *Dis Markers* (2020) 2020:1–10. doi: 10.1155/2020/5354825
CrossRef Full Text | Google Scholar
61. Kontos F, Michelakos T, Kurokawa T, Sadagopan A, Schwab JH, Ferrone CR, et al. B7-H3: An Attractive Target for Antibody-based Immunotherapy. *Clin Cancer Res* (2021) 27:1227–35. doi: 10.1158/1078-0432.CCR-20-2584
PubMed Abstract | CrossRef Full Text | Google Scholar
62. Flem-Karlsen K, Fodstad Ø, Tan M, Nunes-Xavier CE. B7-H3 in Cancer – Beyond Immune Regulation. *Trends Cancer* (2018) 4:401–4.
doi: 10.1016/j.trecan.2018.03.010
PubMed Abstract | CrossRef Full Text | Google Scholar
63. Yonesaka K, Haratani K, Takamura S, Sakai H, Kato R, Takegawa N, et al. B7-H3 Negatively Modulates CTL-Mediated Cancer Immunity. *Clin Cancer Res* (2018) 24:2653–64. doi: 10.1158/1078-0432.CCR-17-2852
PubMed Abstract | CrossRef Full Text | Google Scholar
64. Loos M, Hedderich DM, Friess H, Kleeff J. B7-H3 and Its Role in Antitumor Immunity. *Clin Dev Immunol* (2010) 2010:1–7. doi: 10.1155/2010/683875
CrossRef Full Text | Google Scholar
65. Xu Y, Zhu Y, Shen Z, Sheng J, He H, Ma G, et al. Significance of Heparanase-1 and Vascular Endothelial Growth Factor in Adrenocortical Carcinoma Angiogenesis: Potential for Therapy. *Endocrine* (2011) 40:445–51. doi: 10.1007/s12020-011-9502-1
PubMed Abstract | CrossRef Full Text | Google Scholar
66. Pereira SS, Costa MM, Guerreiro SG, Monteiro MP, Pignatelli D. Angiogenesis and Lymphangiogenesis in the Adrenocortical Tumors. *Pathol Oncol Res* (2018) 24:689–93. doi: 10.1007/s12253-017-0259-6
PubMed Abstract | CrossRef Full Text | Google Scholar
67. O'Sullivan C, Edgerly M, Velarde M, Wilkerson J, Venkatesan AM, Pittaluga S, et al. The VEGF Inhibitor Axitinib has Limited Effectiveness as a Therapy for Adrenocortical Cancer. *J Clin Endocrinol Metab* (2014) 99:1291–7.
doi: 10.1210/jc.2013-2298
PubMed Abstract | CrossRef Full Text | Google Scholar
68. Berruti A, Sperone P, Ferrero A, Germano A, Ardito A, Priola AM, et al. Phase II Study of Weekly Paclitaxel and Sorafenib as Second/Third-Line Therapy in Patients With Adrenocortical Carcinoma. *Eur J Endocrinol* (2012) 166:451–8.
doi: 10.1530/EJE-11-0918
PubMed Abstract | CrossRef Full Text | Google Scholar
69. Chen Y-L, Lin H-W, Chien C-L, Lai Y-L, Sun W-Z, Chen C-A, et al. BTLA Blockade Enhances Cancer Therapy by Inhibiting IL-6/IL-10-induced Cd19high B Lymphocytes. *J Immunother Cancer* (2019) 7:313. doi: 10.1186/s40425-019-0744-4
PubMed Abstract | CrossRef Full Text | Google Scholar
70. Pestka S, Krause CD, Sarkar D, Walter MR, Shi Y, Fisher PB. Interleukin-10 and Related Cytokines and Receptors. *Annu Rev Immunol* (2004) 22:929–79.
doi: 10.1146/annurev.immunol.22.012703.104622
PubMed Abstract | CrossRef Full Text | Google Scholar

71. Rojas K, Baliu-Piqué M, Manzano A, Saiz-Ladera C, García-Barberán V, Cimas FJ, et al. In Silico Transcriptomic Mapping of Integrins and Immune Activation in Basal-like and HER2+ Breast Cancer. *Cell Oncol* (2021). doi: 10.1007/s13402-020-00583-9
CrossRef Full Text | Google Scholar
72. Vinay DS, Kwon BS. 4-1BB Signaling Beyond T Cells. *Cell Mol Immunol* (2011) 8:281–4. doi: 10.1038/cmi.2010.82
PubMed Abstract | CrossRef Full Text | Google Scholar
73. Chester C, Sanmamed MF, Wang J, Melero I. Immunotherapy Targeting 4-1BB: Mechanistic Rationale, Clinical Results, and Future Strategies. *Blood* (2018) 131:49–57. doi: 10.1182/blood-2017-06-741041
PubMed Abstract | CrossRef Full Text | Google Scholar
74. Jasim S, Habra MA. Management of Adrenocortical Carcinoma. *Curr Oncol Rep* (2019) 21:20. doi: 10.1007/s11912-019-0773-7
PubMed Abstract | CrossRef Full Text | Google Scholar
75. Assié G, Letouzé E, Fassnacht M, Jouinot A, Luscap W, Barreau O, et al. Integrated Genomic Characterization of Adrenocortical Carcinoma. *Nat Genet* (2014) 46:607–12. doi: 10.1038/ng.2953
PubMed Abstract | CrossRef Full Text | Google Scholar
76. Figueiredo BC, Stratakis CA, Sandrini R, DeLacerda L, Pianovsky MAD, Giatzakis C, et al. Comparative Genomic Hybridization Analysis of Adrenocortical Tumors of Childhood 1. *J Clin Endocrinol Metab* (1999) 84:1116–21. doi: 10.1210/jcem.84.3.5526
PubMed Abstract | CrossRef Full Text | Google Scholar
77. Kjellman M, Kallioniemi OP, Karhu R, Höög A, Farnebo LO, Auer G, et al. Genetic Aberrations in Adrenocortical Tumors Detected Using Comparative Genomic Hybridization Correlate With Tumor Size and Malignancy. *Cancer Res* (1996) 56:4219–23.
PubMed Abstract | Google Scholar
78. Hodi FS, O'Day SJ, McDermott DF, Weber RW, Sosman JA, Haanen JB, et al. Improved Survival With Ipilimumab in Patients With Metastatic Melanoma. *N Engl J Med* (2010) 363:711723. doi: 10.1056/NEJMoa1003466
CrossRef Full Text | Google Scholar
79. Zancanella P, Pianovski MAD, Oliveira BH, Ferman S, Piovezan GC, Lichtvan LL, et al. Mitotane Associated With Cisplatin, Etoposide, and Doxorubicin in Advanced Childhood Adrenocortical Carcinoma. *J Pediatr Hematol Oncol* (2006) 28:513–24. doi: 10.1097/01.mph.0000212965.52759.1c
PubMed Abstract | CrossRef Full Text | Google Scholar

4 CAPÍTULO II: COMPREHENSIVE CHARACTERIZATION OF THE REGULATORY LANDSCAPE OF ADRENOCORTICAL CARCINOMA: NOVEL TRANSCRIPTION FACTORS AND TARGETS ASSOCIATED WITH PROGNOSIS (61)

João C. D. Muzzi1,2,3, Jéssica M. Magno2,3, Jean S. Souza,3, Larissa M. Alvarenga1, Juliana F. de Moura1, Bonald C. Figueiredo3,4,, and Mauro A. A. Castro2,*

1 Laboratório de Imunoquímica (LIMQ), Pós-Graduação em Microbiologia, Parasitologia e Patologia, Departamento de Patologia Básica, Universidade Federal do Paraná (UFPR), Curitiba, Brazil; joao.muzzi@gmail.com (J.C.D.M.); lmalvarenga@gmail.com (L.M.A.); julianademoura@ufpr.br (J.F.M.)

2 Laboratório de Bioinformática e Biologia de Sistemas, Pós-Graduação em Bioinformática, Universidade Federal do Paraná (UFPR), Curitiba, Brazil; joao.muzzi@gmail.com (J.C.D.M.); jessicamagno@outlook.com (J.M.M.); jean.souza@edu.unipar.br (J.S.S.); mauro.castro@ufpr.br (M.A.A.C.)

3 Instituto de Pesquisa Pelé Pequeno Príncipe, Oncology Division, Curitiba, Brazil; joao.muzzi@gmail.com (J.C.D.M.); jessicamagno@outlook.com (J.M.M.); jean.souza@edu.unipar.br (J.S.S.); bonaldf@yahoo.com.br (B.C.F.)

4 Centro de Genética Molecular e Pesquisa do Câncer em Crianças (CEGEMPAC), Molecular Oncology Laboratory, Curitiba, Brazil; bonaldf@yahoo.com.br (B.C.F.)

* Correspondence: bonaldf@yahoo.com.br (B.C.F.); mauro.castro@ufpr.br (M.A.A.C.)

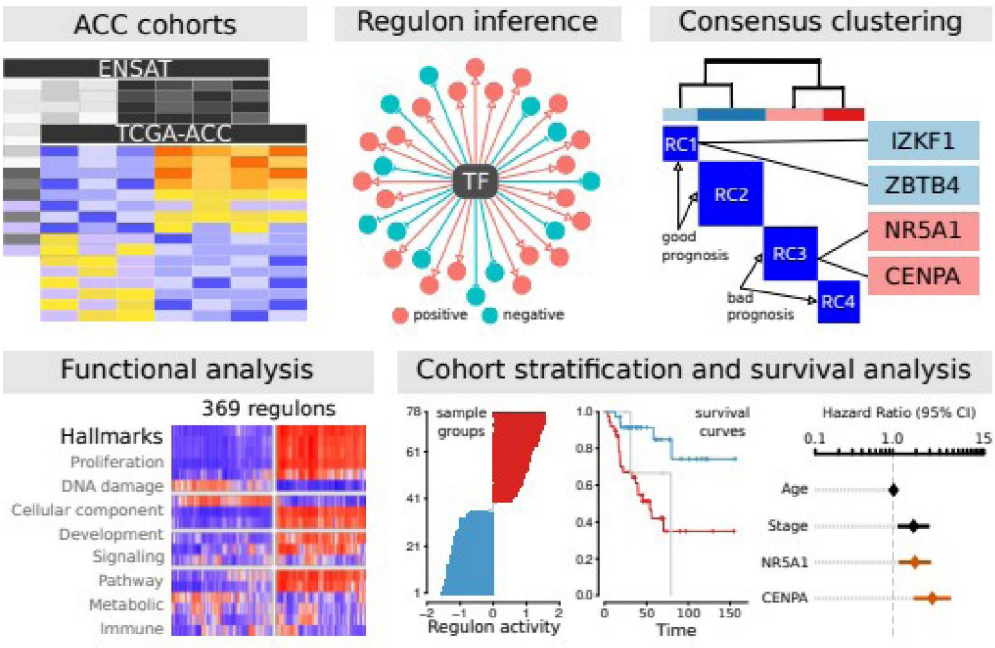
Simple Summary: Adult adrenocortical carcinoma (ACC) is a rare and aggressive tumor in adults, usually associated with excessive steroid secretion. It is highly metastatic and has few therapeutic options and a poor prognosis. Here, we explore the hallmarks of ACC influenced by transcription factors and their target genes (regulons) to provide a prognostic overview of ACC biology. Using an *in silico* clinical data analysis approach we assessed human transcriptomic data from publicly available datasets. We found four distinct clusters of regulons associated with good and worse prognoses that were associated with cell proliferation and/or with immunologic activity. Some of the findings require further bench analyses, especially focusing on worse prognostic regulons and their targets.

Abstract: We reconstructed a transcriptional regulatory network for adrenocortical carcinoma (ACC) using transcriptomic and clinical data from The Cancer Genome Atlas (TCGA)-ACC cohort. We investigated the association of transcriptional regulatory units (regulons) with overall survival, molecular phenotypes, and immune signatures. We annotated the ACC regulons with cancer hallmarks and assessed single sample regulon activities in the European Network for the Study of

Adrenal Tumors (ENSAT) cohort. We found 369 regulons associated with overall survival and subdivided them into four clusters: RC1 and RC2 associated with good prognosis and RC3 and RC4 associated with worse outcomes. The RC1 and RC3 regulons were highly correlated with the ‘Steroid Phenotype’, while the RC2 and RC4 regulons were highly correlated with a molecular proliferation signature. We selected two regulons, NR5A1 (steroidogenic factor 1, SF-1) and CENPA, (Centromeric Protein A) that were consistently associated with overall survival for further downstream analyses. The CENPA regulon was the main regulator of MKI-67 (marker of proliferation kI-67) while the NR5A1 regulon is a well-described transcription factor (TF) in ACC tumorigenesis. We also found that the ZBTB4 (Zinc finger and BTB domain-containing protein 4) regulon, which is negatively associated with CENPA in our transcriptional regulatory network, is also a druggable anti-tumorigenic TF. We anticipate that the ACC regulons may be used as a reference for further investigations concerning the complex molecular interactions in ACC tumors.

Keywords: adrenocortical carcinoma; transcriptomics; regulatory network; transcription factor; immuno-oncology; KI-67; NR5A1; CENPA; ZBTB4; IZKF1.

4.1 GRAPHICAL ABSTRACT



4.2 INTRODUCTION

Adrenocortical carcinoma (ACC) is a rare and aggressive endocrine malignancy with a bimodal age distribution and distinct characteristics between

pediatric and adult tumors [1,2]. ACC is characterized by a highly proliferative and immune-suppressed tumor microenvironment, high production of corticoids, *TP53* mutation, and an upregulation of the WNT/β-Catenin pathway [3–6].

Zheng et al. (2016) classified The Cancer Genome Atlas (TCGA)-ACC patients into four groups based on mRNA K4 clustering: Steroid Phenotype High (HSP), HSP + Proliferation, Steroid Phenotype Low (LSP), and LSP + Proliferation [7]. The Steroid Phenotype is related to the activation of steroid biosynthesis pathways, while Proliferation was assessed by a proliferation score proposed by Wirapati et al. (2008) [8]. This classification presented a high overlap with the C1A/C1B molecular classification presented by Reynies et al. (2009) [9], being HSP and HSP + Proliferation related to C1A and worse outcomes, and LSP associated with C1B. In our previous study [6], we have shown that LSP and LSP + Proliferation presented a significant presence of immune infiltration compared to the immune suppressed microenvironment of HSP and HSP + Proliferation. Landwehr et al. (2020) showed that excessive glucocorticoid levels, present in nearly 60 % of ACC patients, is related to T cell depletion in the tumor microenvironment [5].

The functional interplay between the tumor and infiltrating immune cells within the tumor microenvironment provides insights into genes associated with the anti-tumor immune response [10–12]. The levels and distribution of CD3+ and CD8+ T cell infiltration distinguish four solid tumor phenotypes: hot (or inflamed), altered excluded, altered immunosuppressed, and cold (or non-inflamed) [11–13]. ACC is described as an immunologically cold tumor, presenting one of the lowest immune infiltrates among 30 solid cancer types from TCGA [7,14]. However, the amount and efficacy of the immune infiltrate depend on pre-existing low levels of intratumoral steroids [5,6]. This suggests that to boost the anti-tumor immune response, it is necessary to eliminate excessive glucocorticoid levels, and that may be the main reason for heterogeneous results in five clinical trials using four different immune checkpoint inhibitors (avelumab, nivolumab, pembrolizumab, and ipilimumab) [15–19].

2022 WHO Classification of Adrenal Cortical Tumors recommends diagnosticians specify the mitotic count and the nuclear protein Ki-67 (pKi-67) labeling index in all ACCs [20]. A Ki-67 (or *MKi-67*) labeling index relates to proliferation and malignancy, besides being used in the risk stratification and the

rationale of adjuvant mitotane therapy [20–22]. Steroidogenic Factor 1 (SF1) immunohistochemistry is the most reliable and specific biomarker to confirm the adrenal cortical origin [23]. This transcription factor (TF) is encoded by the Nuclear Receptor Subfamily 5 Group 1 (*NR5A1*) gene, whose overexpression is associated with increased steroid metabolism, proliferation, and a worse outcome [24,25].

Different combinations of regulators and molecular factors may be associated with cancer development. The inference of regulatory networks helps to understand how these factors may be related, converging on cellular mechanisms, which can add to the understanding of the biology of the disease or intervention strategies [26–29]. To reconstruct a regulatory network, gene expression data can be used to evaluate mutual information between a TF and potential target genes, generating regulatory hubs called regulons [26]. This reverse-engineering method has been successfully applied in other cancer types (e.g., [26,27,29]).

In the present study, we inferred a transcriptional regulatory network for ACC using publicly available transcriptomic and clinical data from the TCGA-ACC cohort [7]. Through multivariate Cox analysis, we found 369 regulons, composed of a TF and its direct and indirect targets, relating to overall survival. We investigated how these regulons correlate with molecular phenotypes and immune signatures [14]. In addition, we annotated these regulons with Molecular Signatures Database (MSigDb) Hallmarks, representing well-defined biological states or processes [30]. Finally, we tested the prognostic value of the regulon activity in the European Network for the Study of Adrenal Tumors (ENSAT) cohort [31].

4.3 METHODS

4.3.1 The Cancer Genome Atlas-ACC data

The TCGA-ACC RNA-seq and clinical data [7] available from the GDC repository were downloaded using the TCGABiolinks package v.2.20.1 in R [32–34]. We assessed the curated survival data of TCGA-ACC participants using the Xena Browser [35]. The gene expression matrix was filtered using the AnnotationHub package v.3.0.2 in R [36] for protein-coding genes. We normalized the raw counts with the variance stabilizing transformation (VST) method from the DESeq2 package v.1.32.0 in R [37], using the Steroid Phenotype classification in the experimental design (see Section 2.6).

4.3.2 Regulon inference

The normalized gene expression matrix was used to call regulons with the RTN package v.2.16.0 in R [26]. We reconstructed regulons for 1,605 TFs [38,39] using the ARACNe algorithm [40]. We used the *tni.alpha.adjust*() function [41] to define a statistical threshold that controls the trade-offs between Type I and Type II errors at a similar level described by Castro et al. (2016) [26], using a Benjamini-Hochberg [42] adjusted p-value cutoff of 0.05.

4.3.3 Regulon activity

The regulon activity was estimated using a two-tailed gene set enrichment analysis (GSEA2) [26] which produces a differential enrichment score (dES) for each sample. A positive dES represents activated regulons, while a negative dES represents suppressed regulon activity. Values near zero indicate inconclusive activity. We selected regulons with a minimum of 15 positive and 15 negative targets [30] to assess regulon activity, which is regarded as the minimum gene set size for downstream enrichment analyses [30].

4.3.4 Survival analysis

We used the regulon activity for multivariate Cox analysis [43] relating to overall survival (OS) and Progression-Free Interval (PFI) (the period from the date of diagnosis until loco-regional or systemic recurrence, second malignancy, or death from any cause) [35]. For this analysis, we considered the tumor stage and age as covariates using the RTNSurvival package v.1.20.0 pipeline [44], generating the hazard ratio (HR) and 95% confidence interval (CI) for each regulon. Since the Cox analysis assessed the time-to-event association between steroid-related regulons and OS, steroid-secreting status was not included in the Cox model due to potential co-linearity with steroid-related regulons. Therefore, the regulons with an adjusted p-value below 0.05 for OS were selected for the subsequent analysis. For Kaplan-Meier survival curves [45], samples were divided into high, inconclusive, or low regulon activity, and the p-values were calculated using log-rank statistics [46,47].

4.3.5 Clustering

The regulons' activity dES was used for the unsupervised consensus clustering using the ConsensusClusterPlus package v.1.56.0 in R [48]. We chose k equal to four.

4.3.6 Steroid and proliferation classification

Of the 92 samples available in the TCGA-ACC cohort, 79 had RNA-seq data, and 78 were listed in the mRNA K4 molecular classification [7], which assigns a Steroid Phenotype to the samples.

The mRNA K4 classified the participants in “steroid-phenotype-high” (n = 25), “steroid-phenotype-high+proliferation” (n = 22), “steroid-phenotype-low” (n = 27), and “steroid-phenotype-low+proliferation” (n = 4).

We separated the Steroid Phenotype and the Proliferation profiles, resulting in two groups for the Steroid Phenotype, HSP (n = 47) and LSP (n = 31), and two groups for the higher and lower proliferation scores (n = 26 and 52, respectively). The proliferation score used by Zheng et al. (2016) [7] was based on a proliferation gene set signature described by Wirapati et al. (2008) [8].

4.3.7 Differential expression for Steroid and Proliferation phenotypes

We called differentially expressed genes (DEGs) for the Steroid and Proliferation phenotypes using the DESeq2 package v.1.32.0 in R [37]. To avoid confounding effects, the two profiles were independently analyzed, generating DEGs relating to the Steroid independent of Proliferation (IP) classification and the Proliferation independent of Steroid (IS) classification. We considered significant DEGs with adjusted p-values below 0.05 in the Wald test [37].

4.3.8 Transcriptional Network Analysis (TNA)

The association between the activity of a regulon and the Steroid and Proliferation phenotypes was assessed using GSEA2 implemented in the TNA pipeline [38]. Here, we used the list of DEGs described in section 2.7. Associations with adjusted p-values below 0.01 were considered significant.

4.3.9 Functional annotation with MSigDb Hallmarks

The prognostic regulons were annotated with MSigDb Hallmarks [30] using the *tni.annotate.regulons()* function from the RTN package in R [26]. We used the Hallmark gene sets from the msigdbr package v.7.4.1 [49].

4.3.10 Immune correlation

Values for leukocyte fraction, immune signatures, T-cell receptor (TCR), and B-Cell Receptor (BCR) metrics were retrieved from the master table for TCGA-ACC participants from Thorsson et al. (2018) [14]. We calculated the Spearman correlation between these values and the regulon activity.

4.3.11 Duals inference

To search for co-regulatory associations between pairs of the prognostic regulons, we used the RTNduals pipeline as described in Chagas et al. (2019) [50].

4.3.12 ENSAT cohort data

The clinical data and the normalized gene expression matrix were assessed from the ENSAT cohort using the GEOquery package v.2.60.0 [51]. This cohort comprises 44 ACC samples and is available in the Gene Expression Omnibus (GEO) portal under the accession number GSE49278 [31]. When more than one entry from the gene expression data referred to the same gene symbol, we selected the one with the higher coefficient of variation between the samples. The additional clinical data was obtained from the supplementary tables of Assié et al. (2014) [31].

4.3.13 Regulon activity and survival analysis in the ENSAT cohort

The regulatory network inferred in the TCGA-ACC cohort was used to calculate the regulon activity in the ENSAT cohort using GSEA2 [26]. We selected the regulons related to OS in the TCGA-ACC for multivariate Cox analysis in the ENSAT cohort. The HR and 95 % CI for OS was inferred using tumor stage and age as covariates. For the Kaplan-Meier survival analysis, we followed the same protocol described in section 2.4.

4.3.14 Statistics and visualization

For the statistical analyses, we used the R packages available in CRAN [52] and Bioconductor [53] repositories. All p-values were corrected for multiple hypotheses using the Benjamini-Hochberg correction [42], and, if not specified otherwise, we considered the result significant when below 0.05.

For the boxplot comparison, the two-sided Mann-Whitney-Wilcoxon test [54,55] was used when only two pairs were available. For general comparison between more than two groups, we used the Kruskal-Wallis rank-sum test [56] followed by Dunn's test [57] for multiple pairwise comparisons.

For the construction of heatmaps, we used the ComplexHeatmap package v.2.8.0 [58] in R. To visualize the regulon network, we used the RedeR package v.2.0.0 [59] in R.

4.4 3. RESULTS

4.4.1 The identification of 369 regulons with prognostic values related to molecular phenotypes and leukocyte fractions.

The TCGA-ACC RNA-seq data was used to call regulons using the RTN R package [26] (Supplementary Table S1). Of the 1,605 TFs annotated in the Lambert et al. (2018) collection [39], 611 had at least 15 positive and 15 negative targets in our transcriptional regulatory network (Supplementary Table S2, Supplementary Figure S1), which is regarded as the minimum gene set size for downstream enrichment analyses [30]. In Figure 1A, we present the general workflow used in this study. In Figure 1B, an example of a regulon and its targets' distribution along the karyogram is illustrated.

We used the OS data to assess the association with the regulons' activity using multivariate Cox analysis. Of the 611 regulons, we found 369 related to OS, of which 330 (89.4 %) were also related to PFI (Supplementary Table S3, Supplementary Table S4). Figure 2A shows the activity profile of the 369 prognostic regulons in the TCGA-ACC cohort (Supplementary Table S5). In the unsupervised clustering, the 188 good prognostic regulons showed higher activity in the LSP and C1B participants, as well as in participants with a higher leukocyte fraction. Conversely, the 181 poor prognosis regulons showed higher activity in the HSP and C1A participants, along with participants with a lower leukocyte fraction. Consistently, the activity of high- and low-risk regulons presented opposite correlations with the leukocyte fraction (Figure 2B, Supplementary Table S4), and with the Steroid IP and Proliferation IS scores (Figures 2C and 2D, respectively, Supplementary Table S4, Supplementary Table S6).

4.4.2 Consensus clustering resulted in four regulon clusters with different functional and molecular characteristics

We used consensus clustering to look for subgroups within the low- and high-risk regulons (Supplementary Figure S2). The 188 regulons with good prognosis were divided into two clusters: regulon cluster (RC) 1 and RC2, with 62 and 126 regulons, respectively. The 181 regulons related to a worse prognosis were divided into RC3 and RC4, with 113 and 68 regulons, respectively (Figure 3A). RC1 activity showed the highest positive correlation with the presence of immune infiltrate and with the Steroid IP score, as opposed to RC3 (Figure 3B and 3C). RC2 had the

lowest scores for the Proliferation IS classification, in contrast to RC4 (Figure 3D). The regulons' correlation with leukocyte fraction was negatively associated with the Steroid IP ($\rho = -0.94$, p-value $< 2.2 \times 10^{-16}$) (Figure 3E) and the Proliferation IS scores ($\rho = -0.52$, p-value $< 2.2 \times 10^{-16}$) (Figure 3F).

Figure 4A shows the regulon enrichment in the MSigDb Hallmarks (Supplementary Figure S3, Supplementary Table S7). RC3 and RC4, in contrast to RC1 and RC2, were positively enriched in proliferation Hallmarks such as MYC targets v1 and v2, E2F targets, Mitotic Spindle, G2M checkpoint, and WNT/β-Catenin Signaling (Figure 4B). RC1 was activated, while RC3 was repressed, in the immune Hallmarks (i.e., IL6 JAK STAT3 Signaling, Interferon (IFN) γ and α, and Inflammatory responses - Figure 4C, Complement, Allograft rejection, and Coagulation), in addition to Apoptosis, P53 pathway, and some immune-related signaling pathways (i.e., IL2 STAT5 signaling and TNF-α signaling via NFK-β). RC2 had the lowest, while RC4 had the highest scores for PI3K Akt mTOR (Figure 4D) and Hedgehog signaling.

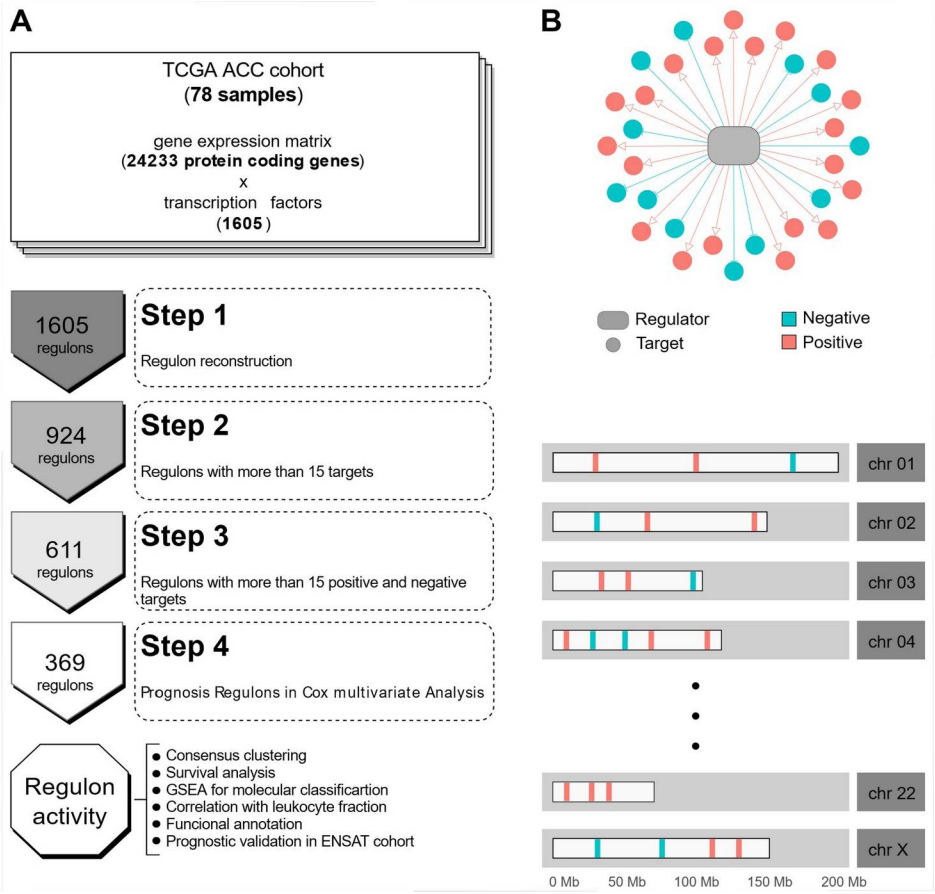


Figure 1. Workflow and regulon representation. (**A**) Schematic workflow of the study. (**B**) Example of a regulon and the distribution of possible target genes in chromosomes.

We also evaluated the RCs concerning the six immune signatures and the TCR metrics inferred by Thorsson et al. (2018) [14] for the TCGA-ACC participants (Supplementary Figure S4A, Supplementary Table S4). RC1 had the highest and RC3 the lowest correlations for Macrophage Regulation and Lymphocyte Infiltrate Signature Scores. Moreover, RC1 and RC2 had a negative correlation with Proliferation and Wound Healing signatures, as opposed to the positive values found in RC3 and RC4. The four clusters showed a weak correlation with the IFN-γ Response and TGF-β Response signatures. Regarding the adaptive immune response (Supplementary Figure S4B, Supplementary Table S4), RC1 related positively to TCR Shannon and TCR Richness, while RC3 related negatively to these features. The RC activities did not present a significant correlation with TCR Evenness. Concerning the B cell response, the BCR metrics inferred by Thorsson et al. (2018) [14] were available for only five samples, making comparisons with sufficient statistical power unfeasible.

4.4.3 The ENSAT cohort confirmed the prognostic value of 89.5% of the regulons related to survival on TCGA-ACC

We investigated the regulon activity in the ENSAT cohort (44 ACC samples) (Supplementary Figure S5, Supplementary Table S5) and confirmed the association with survival for the 369 regulons. Of the 369 regulons, 361 were present in the ENSAT gene expression matrix, of which 323 (89.5 % of the 361) had significant HRs in multivariate Cox analysis for OS (Supplementary Table S3). High-risk regulons (RC3 and RC4) showed greater activity in the C1A phenotype and were suppressed in the C1B phenotype, contrary to what was observed for the low-risk regulons (RC1 and RC2), which is in agreement with the pattern observed in the TCGA-ACC cohort (Figure 5A and B).

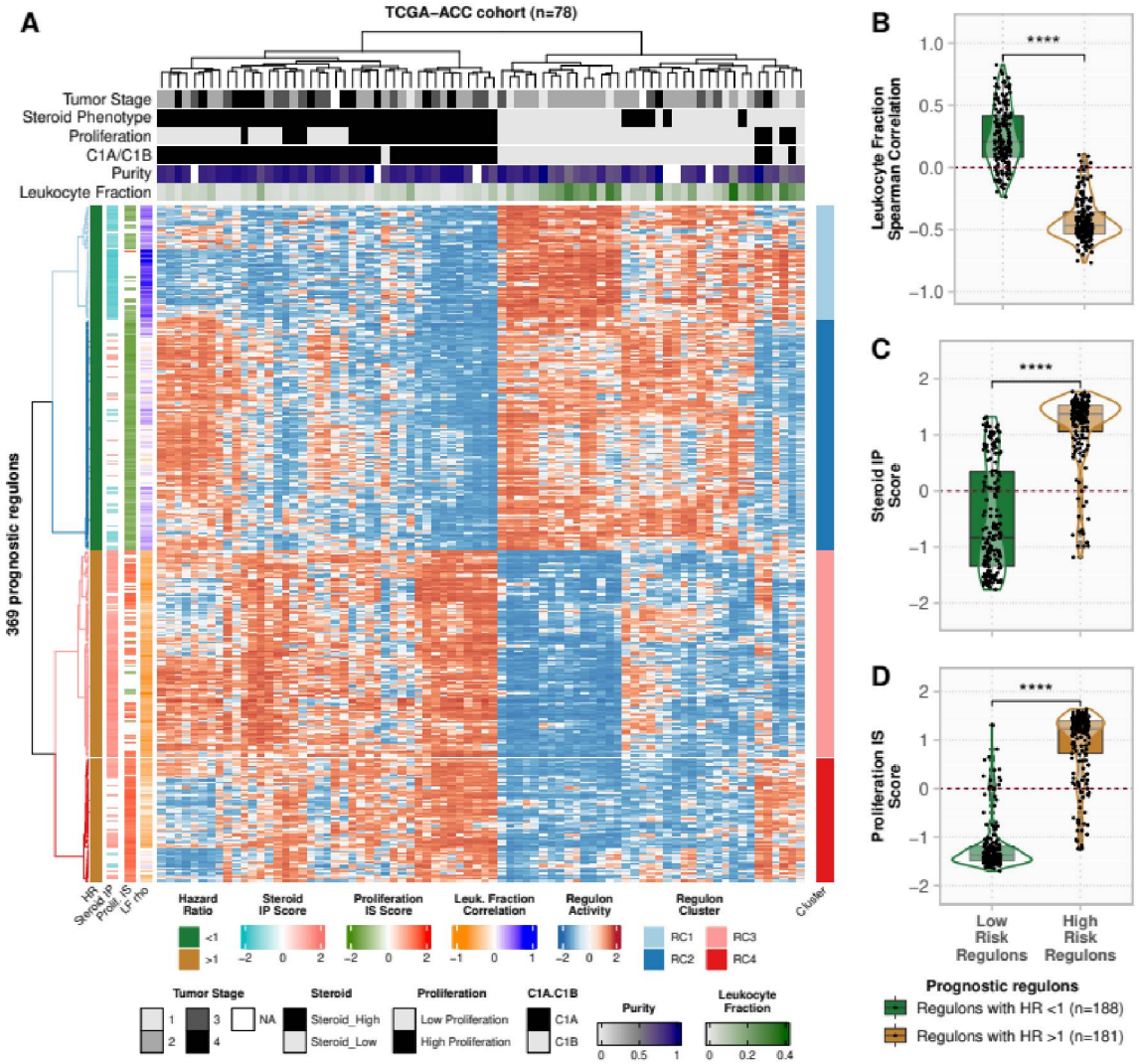


Figure 2. Activity profile of prognostic regulons (n = 369) in TCGA-ACC cohort (n = 78). (A) Heatmap with the activity of the 369 prognostic regulons. Each row represents a regulon, and each column is a sample from the TCGA-ACC cohort. Both were subjected to unsupervised clustering. The upper tracks present the clinical and molecular classification for the samples defined by Zheng et al. (2016) [7] and Thorsson et al. (2018) [14]. The left tracks show the regulon association with the hazard ratio (HR) for overall survival (OS), the Steroid independent of Proliferation (IP) and Proliferation independent of Steroid (IS), and the correlation with the Leukocyte Fraction. The right track presents the regulon clusters defined by Consensus Clustering (Supplementary Figure S3). (B–D) Regulons are grouped into High- and Low-risk categories according to the HR in Multivariate Cox Analysis. Each point represents a regulon, and the contour presents the distribution density of the regulons for each group. The boxplots show the distinction between the groups for (B) the Spearman's correlation between the leukocyte fraction and the regulon activity, (C) the Steroid IP score, and (D) the Proliferation IS score. **** $p \leq 0.0001$ in the two-sided Mann-Whitney-Wilcoxon test.

Concerning the tumor stages in the TCGA-ACC and ENSAT cohorts, RC1 and RC2 had stronger activity at low tumor stages, while RC3 and RC4 had stronger

activity at higher stages (Figure 5C and D). We summarized the results for the 369 regulons in Supplementary Table S4.

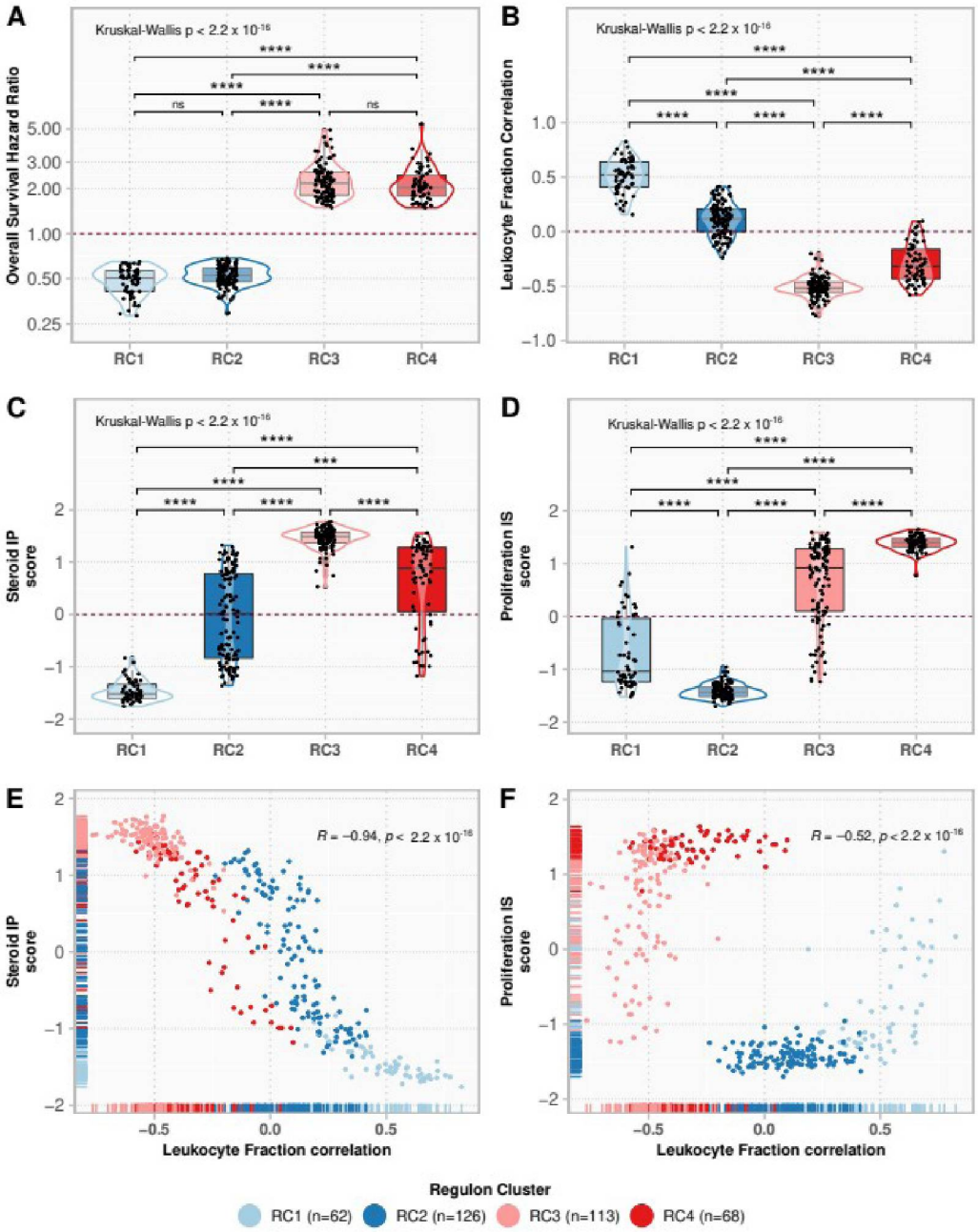


Figure 3. Comparison of regulon clusters (RC). The boxplots show the regulon distributions in each cluster for the overall survival (OS) hazard ratio (HR) (A), leukocyte fraction correlation (B), Steroid independent of Proliferation (IP) score (C), and Proliferation independent of Steroid (IS) score (D). Each point represents a regulon, and the box's horizontal lines show the median and the 25–75% percentiles, while the whiskers (vertical lines) cover the 0–25% and 75–100% percentiles. The contour presents the distribution density of the regulons. The results of Kruskal-Wallis and Dunn's tests for

multiple pairwise comparisons of the ranked data are presented on top. Asterisks indicate the significance level as follows: *** p ≤ 0.001, and **** p ≤ 0.0001. Non-significant p-values (p > 0.05) are represented by “ns”. (E,F) show the scatter plot for the leukocyte fraction correlation with the Steroid IP score and Proliferation IS score, respectively. Each point represents a regulon, colored by its respective cluster. The rugs show the distribution of the points along the x and y-axes. The Spearman correlation rho and the associated p-value are shown in the top-right corner.

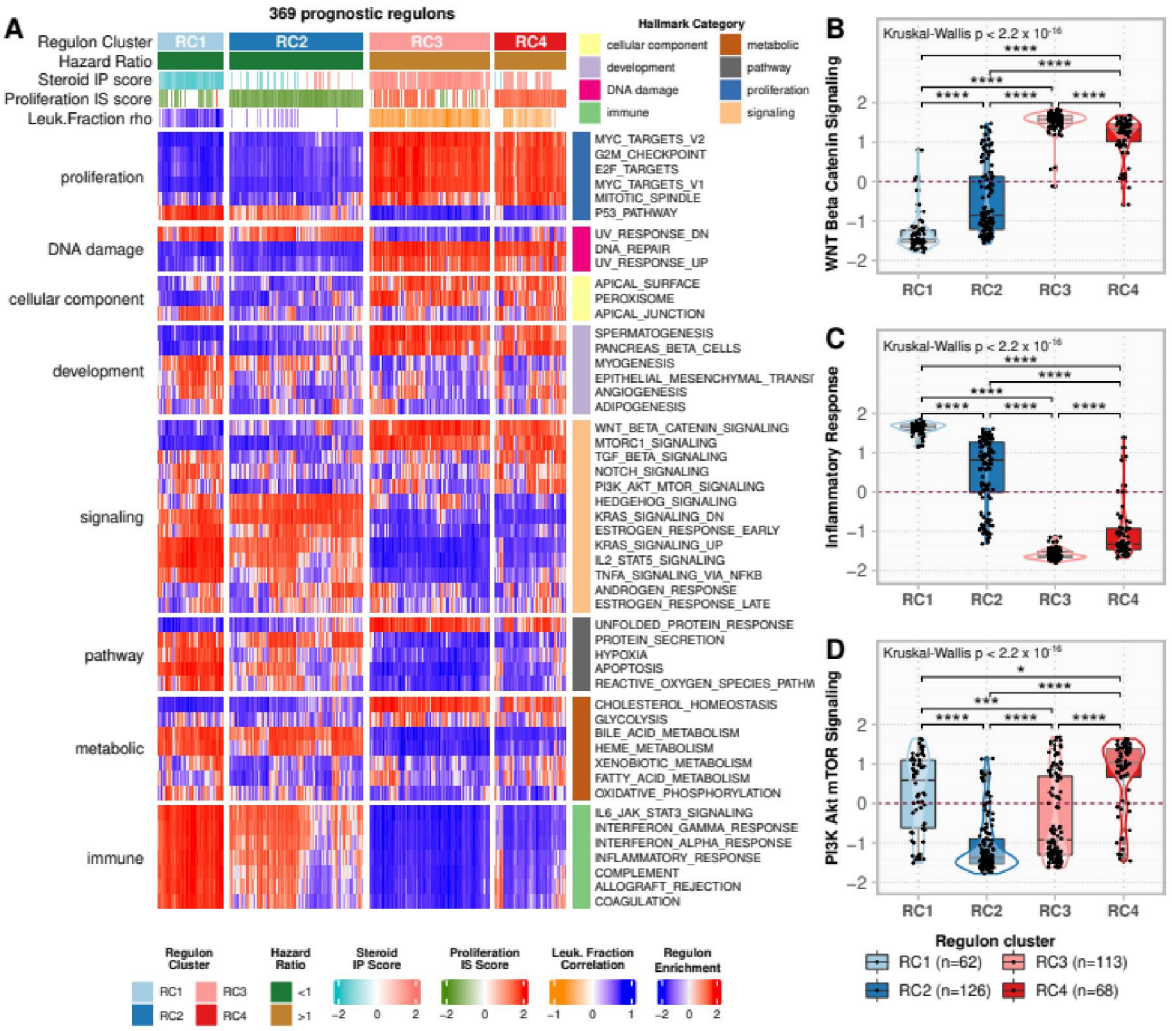


Figure 4. HHallmarks enrichment analysis. (A) A heatmap representing the regulon activity enrichment analysis for the MSigDb Hallmarks. Each column represents a prognostic regulon grouped by the regulon cluster, and the rows represent the 50 Hallmarks divided by category. Both rows and columns were subjected to semi-supervised clustering within the groups. In the main heatmap, red indicates a positive enrichment score, while blue indicates the opposite. The top annotation depicts the regulons classification in the clusters, besides the overall survival (OS) hazard ratio (HR), the Steroid independent of Proliferation (IP) and Proliferation independent of Steroid (IS) scores, and the leukocyte fraction correlation for the regulons as presented in Figure 3A. (B–D) Boxplots comparing the enrichment scores in the regulon clusters for (B) Inflammatory Response, (C) WNT/β-Catenin Signaling, and (D) Mitotic Spindle Hallmarks. Each point represents a regulon separated by the

regulon cluster in the x-axis and vertically spread according to its enrichment score for each Hallmark described. The contour presents the distribution density of the regulons for each cluster. The results of Kruskal-Wallis and Dunn's tests for multiple pairwise comparisons of the ranked data are presented on top. Asterisks indicate the significance level as follows: * p ≤ 0.05, *** p ≤ 0.001, and **** p ≤ 0.0001.

4.4.4 NR5A1 relates to worse outcomes in TCGA-ACC and ENSAT cohorts. CENPA has a strong association with proliferation and relates to a bad prognosis

NR5A1 is a well-described TF related to a worse prognosis, adrenal differentiation, and steroidogenesis in ACC. In the regulatory network, *NR5A1* presented 248 targets, with 176 negatives and 72 positives (Supplementary Figure S6, Supplementary Table S1, and Supplementary Table S2). In the Cox multivariate analysis, the *NR5A1* regulon related to worse outcomes in PFI (HR = 2.15 [95 % CI, 1.49–3.11], p-value = 7.12 x 10^{-5}) and OS (HR = 1.94 [95 % CI, 1.21–3.11], p-value = 7.13 x 10^{-3}) in the TCGA-ACC cohort, and to OS in the ENSAT cohort (HR = 3.86 [95 % CI, 1.61–9.25], p-value = 7.45 x 10^{-3}) (Supplementary Table S3). The Kaplan-Meier analysis also presented a significant value relating to worse outcomes in OS both in the TCGA-ACC and the ENSAT cohorts (Figure 6A and B respectively).

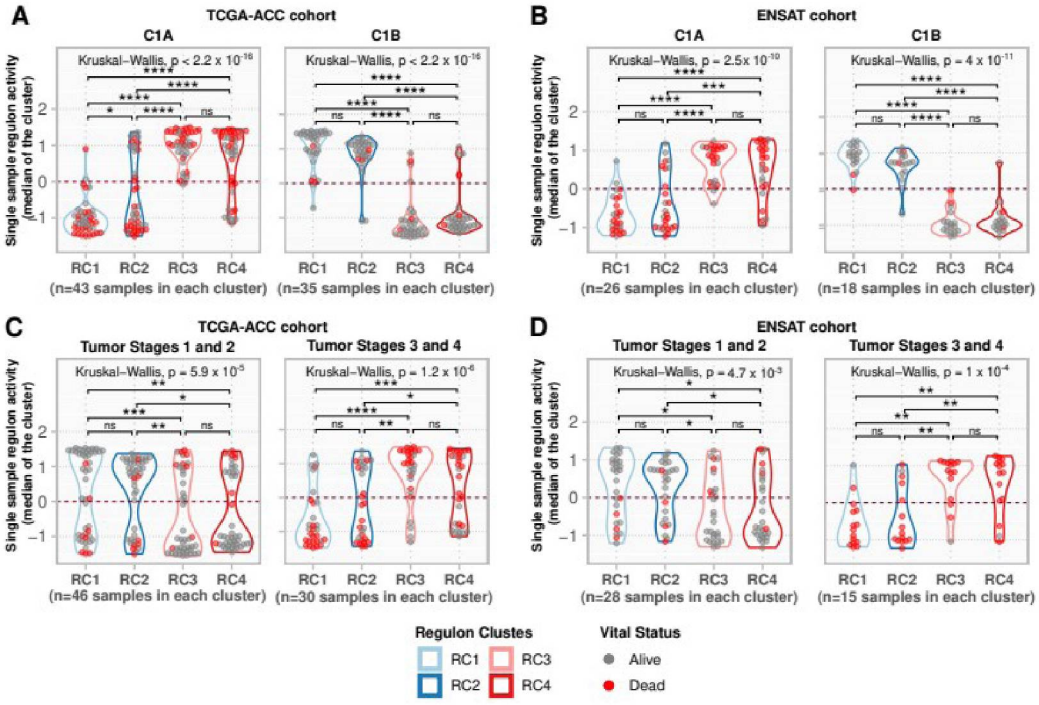


Figure 5. Single-sample regulon activities in regulon clusters. (A,B) Samples were divided into C1A and C1B as assigned by Zheng et al. (2016) [7] for (A) the TCGA-ACC cohort and by Assié et al. (2014) [31] for (B) the ENSAT cohort. (C,D) Samples were divided into a group with tumor stages 1 and 2 and a group with tumor stages 3 and 4 for the (C) TCGA-ACC and (D) ENSAT cohorts. For each

sample, the median regulon activity for each regulon cluster was calculated and represented by the values on the y-axis. Grey points indicate participants alive during the follow-up period, while red indicates participants who died during this time. The contour presents the distribution density of the sample. The results of Kruskal-Wallis and Dunn's tests for multiple pairwise comparisons of the ranked data are presented on top. Asterisks indicate the significance level as follows: * $p \leq 0.05$, ** $p \leq 0.01$, *** $p \leq 0.001$, and **** $p \leq 0.0001$. Non-significant p-values ($p > 0.05$) are represented by "ns".

This regulon presented a significant relation both with HSP (dES = 1.49, p-value = 1.65×10^{-3}) and Proliferation IS phenotypes (dES = 1.33, p-value = 1.36×10^{-3}) and clustered in the RC3. Concerning the immune features analyzed, its activity showed a significant negative correlation with leukocyte fraction ($\rho = -0.52$, p-value = 4.84×10^{-6}), TGF-β response ($\rho = -0.41$, p-value = 1.71×10^{-2}, the lowest correlation among the 369 regulons), Macrophage Regulation ($\rho = -0.52$, p-value = 6.84×10^{-6}), Lymphocyte Infiltration Signature Score ($\rho = -0.56$, p-value = 4.90×10^{-7}), TCR Shannon ($\rho = -0.61$, p-value = 2.14×10^{-3}), and TCR Richness ($\rho = -0.47$, p-value = 2.87×10^{-4}). Moreover, this regulons' activity showed a significant positive correlation with the Proliferation and Wound Healing signatures ($\rho = 0.32$, p-value = 5.84×10^{-3}, and $\rho = 0.35$, p-value = 2.07×10^{-3}, respectively) (Supplementary Table S4).

Within the 369 regulons, we found 150 pairs of regulons that significantly shared targets (Supplementary Table S8), and were therefore called "Duals" [50]. Despite being the second regulon with most targets (n = 248, Supplementary Figure S6), the *NR5A1* regulon did not show significant targets' sharing with other prognostic regulons.

Of the inferred Duals, Centromeric Protein A (*CENPA*), Small Nuclear RNA Activating Complex Polypeptide 4 (*SNAPC4*), and *LIN54* [a component of the LINC (Linker of Nucleoskeleton and Cytoskeleton) complex, an essential regulator of cell cycle genes], were the regulons with the most associations (9, 8, and 7, respectively) (Supplementary Table S8). Interestingly, *CENPA* had the highest score in the correlation with Proliferation ($\rho = 0.90$, p-value = 4.01×10^{-27}) and Wound Healing signatures ($\rho = 0.79$, p-value = 2.55×10^{-15}), and a significant negative correlation with leukocyte fraction ($\rho = -0.55$, p-value = 1.44×10^{-6}), Macrophage Regulation ($\rho = -0.42$, p-value = 4.29×10^{-4}), and Lymphocyte Infiltration Signature Score ($\rho = -0.48$, p-value = 2.67×10^{-5}) (Supplementary Table S4).

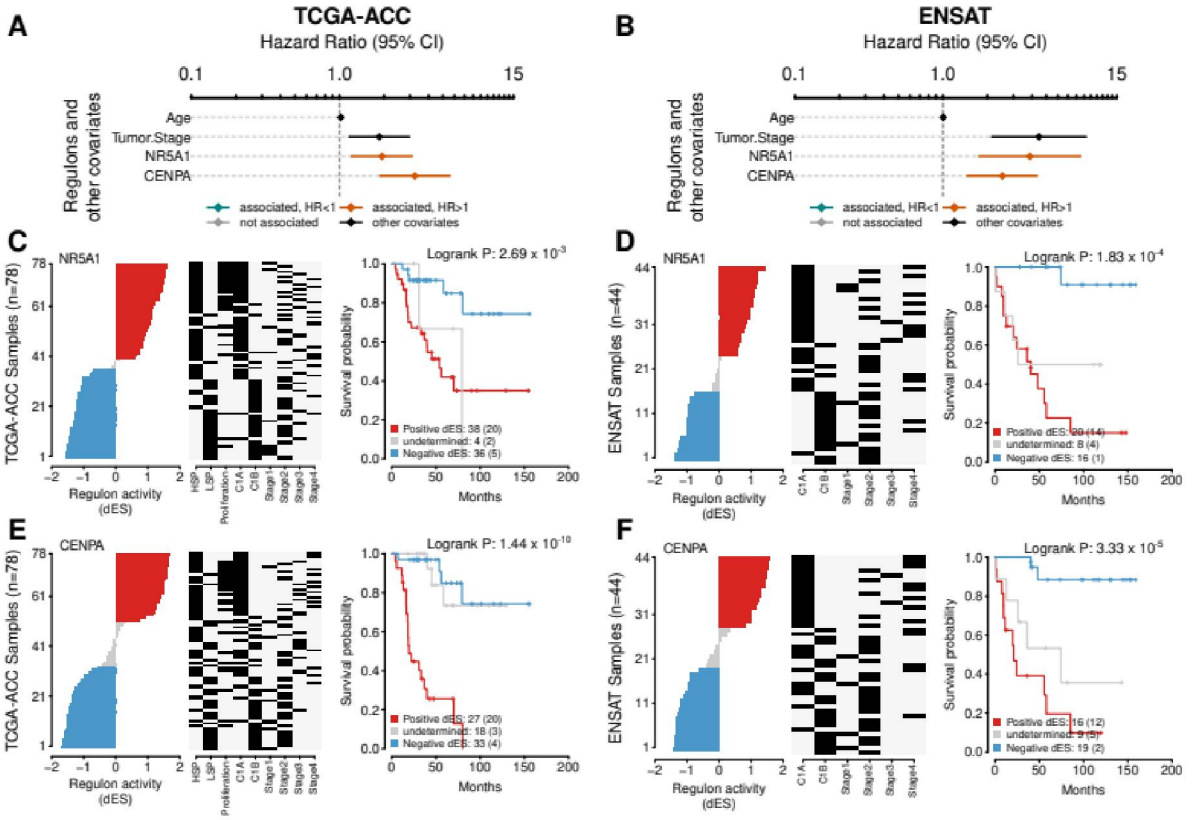


Figure 6. Survival analysis for the *NR5A1* and *CENPA* regulons. (**A**, **B**) A Forest plot with the Hazard Ratios (HRs) and Confidence Interval (CI) for the Cox multivariate analysis. Age and Tumor Stage were used as covariates. The activities of the *NR5A1* and *CENPA* regulons were evaluated for overall survival (OS). (**A**) presents the results for the TCGA-ACC cohort and (**B**) for the ENSAT cohort. (**C**, **D**, **E**, **F**) The Kaplan-Meier analysis for the *NR5A1* regulon in the (**C**) TCGA and (**D**) ENSAT cohorts, and for *CENPA* regulon in the (**E**) TCGA-ACC and (**F**) ENSAT cohorts. In the first and second panels, the rows represent the samples, which were ordered according to the differential enrichment score (dES) for the regulon activity and divided by the median into three groups: positive dES (red), negative dES (blue), and undetermined (grey) as depicted in the first panel. The middle panel shows the molecular classification or tumor stage for each sample, as provided by the publicly available data from the cohorts. The last panel shows the Kaplan-Meier survival analysis between the high and the low regulon activity groups. The adjusted p-value for the Log-Rank test is provided. The number of participants in each group is shown, followed by the number of events between parentheses.

We found that *CENPA* was the main regulator of the *MKI-67* gene (MI = 0.77), the most common histopathologic marker of proliferation, followed by *FOXM1* (MI = 0.59), *MXD3* (MI = 0.48), and *DNMT1* (MI = 0.34) (Supplementary Table S1). *MXD3* and *DNMT1* are *CENPA* Duals (Supplementary Table S8), and *FOXM1*, *MXD3*, and *DNMT1* are *CENPA* positive targets.

CENPA was significantly associated with both the Steroid IP and the Proliferation IS (ρ = 1.45, p-value = 1.65 x 10^{-3}, and ρ = 1.32, p-value = 1.36 x 10^{-3}, respectively) and clustered together with RC3 (Supplementary Table S4). In the Cox's analysis, *CENPA* related to worse outcomes in the TCGA-ACC cohort in PFI (HR = 2.23 [95 % CI, 1.54–3.21], p-value = 4.55 x 10^{-5}) and in OS (HR = 3.24 [95 % CI, 1.88–5.57], p-value = 1.82 x 10^{-4}), in addition to the ENSAT cohort for OS (HR = 2.52 [95 % CI, 1.39–4.59], p-value = 7.45 x 10^{-3}) (Supplementary Table S3). In the Kaplan-Meier analysis, *CENPA* presented a significant relation in both the TCGA-ACC and ENSAT cohorts (Figure 6A and B respectively). Figure 7A presents *CENPA*'s targets and Figure 7B shows their distribution in a karyogram.

In the TCGA-ACC cohort, the three regulons with higher negative Spearman correlation with *CENPA*'s activity were *THRB* (Thyroid Hormone Receptor Beta), *STAT5B (Signal Transducer and Activator of Transcription 5B),* and *ZBTB4* (Zinc Finger And BTB Domain Containing 4) (ρ = -0.87, -0.86, and -0.85, respectively, all p-values < 2.2 x 10^{-16}). All of them from RC1 related to good prognosis in the TCGA-ACC and ENSAT cohorts (Supplementary Table S3 and S4) and presented a negative correlation with the Proliferation signature (ρ = -0.72, -0.75, and -0.68, respectively, all p-values < 10^{-9}).

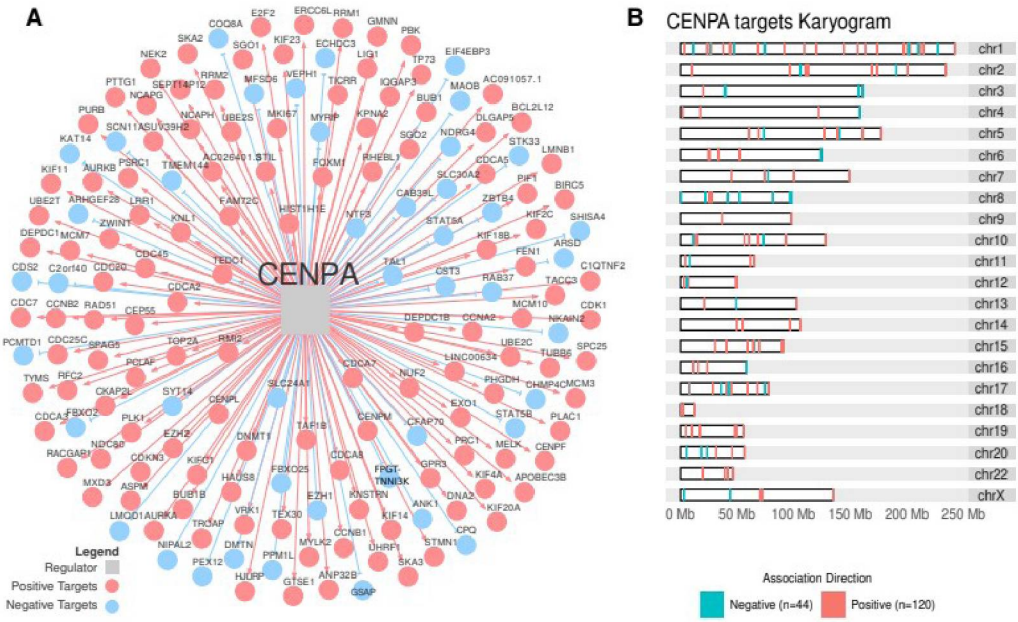


Figure 7. The *CENPA* regulon. (**A**) The transcription factor *CENPA* (grey square at the center) and its targets inferred by the regulatory network analysis. Blue circles indicate targets with a negative association, while the red circles indicate targets with a positive association. (**B**) The karyogram presents the distribution of *CENPA* targets in the chromosomes.

4.5 DISCUSSION

The TCGA-ACC cohort is the largest ACC cohort, thus being the most suitable for regulatory network inference. The inferred network had a good balance between positive and negative targets (Supplementary Figure S2) with 611 regulons comprising more than 15 positive and 15 negative targets. We described regulons of prognostic value and provide an overview of the main regulons that control the expression of target genes and, consequently, the observed phenotypes associated with OS. To achieve this, we made functional annotations associating the regulon activity with molecular phenotypes and immunological characteristics.

Here we present 369 regulons associated with OS, where 188 are related to a good prognosis and 181 to a worse ACC prognosis. Within these regulons, we were able to identify subgroups with specific relationships for each set of molecular characteristics and functional annotations, resulting in four RCs. Regulon cluster 1 and RC3 are more related to the Steroid Phenotype, while RC2 and RC4 are more related to the molecular Proliferation Score as defined by Zheng et al. (2016) [7]. As the high Score Proliferation classification was present in 22 of the 47 HSP cases, and in only 4 of the 31 LSP cases, we distinguished these two features, the Steroid and Proliferation classifications, by analyzing them independently, removing the interference from each other.

RC1 and RC3 are related to Steroid IP, with RC1 associated with LSP and RC3 with HSP. These two clusters presented opposite profiles, both in activity and in functional annotations. These clusters were at high activity in the immune and proliferation pathways, respectively, as previously shown for the Steroid Phenotype [6]. The strong correlation between RC1 activity and the pro-immune features (Figure 4, Supplementary Figure S3, Supplementary Figure S4), in addition to increased activity in early tumor stages (Figure 5B), suggests that regulons in the RC1 may play a role in activating the immune system against different targets at early phases of ACC, which is progressively lost by opposing forces of the RC3 regulons in more advanced stages.

We also observed that RC2 and RC4 follow opposite patterns in terms of activity and characteristics. RC2, with a good prognosis, is related to low scores in the Proliferation IS, while RC4, with a poor prognosis, is related to high scores in this phenotype. We identified from the Hallmarks enrichment (Figure 4, Supplementary Figure S3, Supplementary Table S7), that these prognostic clusters are particularly associated with the PI3K Akt mTOR and Hedgehog signaling pathways, which may help uncover risk factors other than immune response and Steroid Phenotype [5,6,60].

Our functional analysis using the MSigDb Hallmarks presented an overall panorama, providing insights into the biology and function of each group of inferred regulons. However, the MSigDb Hallmarks represent themes of gene sets rather than pathways [30], which may result in supposed contradictory findings. For example, the classical P53 pathway is known to activate DNA repair in response to DNA damage [61,62]. However, in our analysis, the P53 pathway and the DNA repair Hallmarks presented opposite activities (i.e., low for P53 and high for DNA repair in both RC3 and RC4). Increased activity of DNA repair is observed after increased proliferation [62,63], which may explain the observed profiles in RC3 and RC4. In addition, some mutations like in the *TP53* gene may alter the P53 pathway and its DNA repair activity [61,64]. The overall pattern relating to immune response and proliferation pathways was coherent with the good and poor prognosis clusters. Specific functional correlations need further clarification using *in vitro* and *in vivo* studies.

The TCGA pan-cancer analysis, including the ACC cohort by Thorsson et al. (2018) [14], shows that TFs regulating immune-modulators tend to be shared between different tissue-of-origin malignancies, in contrast to somatic mutations. They also highlight some immune-related TFs shared among the tumors of which three appeared in our analysis with association to good prognosis in ACC: *FLI1* (Friend Leukemia Virus Integration 1), *STAT5A* (Signal Transducer and Activator of Transcription 5A), and *IKZF1* (Ikaros Family Zinc Finger Protein 1). For example, in our results, *IKZF1* appeared related to good prognosis (HR = 0.61 [95 % CI, 0.40–0.94], p-value = 2.65×10^{-2}), and with the strongest association with the LSP (Steroid IP score of -1.76, p-value = 1.65×10^{-3}) and the highest positive correlation with leukocyte fraction ($\rho = 0.83$, p-value = 5.47×10^{-18}), Macrophage Regulation ($\rho = 0.86$, p-value = 1.12×10^{-21}), and Lymphocyte Infiltration Signature Score ($\rho = 0.83$,

p-value = 1.56 x 10^{-18}) among the 369 regulons (Supplementary Table S4). Finding TFs shared between other tumors and ACC with importance to the immune activation may help to optimize clinical and research efforts in this rare carcinoma.

In ACC, the *NR5A1* TF, an important player in adrenal development and ACC tumorigenesis [65,66], generated one of the largest regulons in our analysis with 248 targets. Consistent with studies on the overexpression of this TF relating to a worse outcome and increased steroid metabolism [23,24,67], the *NR5A1* regulon correlated with low OS in the multivariate Cox and Kaplan-Meier analyses in the TCGA-ACC cohort, which was also confirmed in the ENSAT cohort (Figure 6). Interestingly, of the 369 prognostic regulons, the *NR5A1* regulon showed the lowest correlation with the TGF-β response. Although the steroid hormones are well-known immunosuppressors [68,69], the pathways by which they dampen the immune response in the ACC microenvironment are not completely understood. Further studies are needed to examine the immune variables directly altered by *NR5A1* overexpression in the context of ACC.

Remarkably, we identified *CENPA* with interesting correlations with many proliferative markers. *CENPA* is a histone H3-like protein involved in centromeric nucleosome formation [70]. In this study, the *CENPA* regulon showed the highest association with the Proliferation signature. In addition, *CENPA* also appears as the main regulator of *MKI67 (*Ki-67), a common prognostic and proliferation marker widely used in cancer histopathology [22].

CENPA was described as relating to proliferation and prognosis in ovarian cancer [71], being crucial in prostate cancer growth [72], regulating metabolic reprogramming in colon cancer cells leading to its growth [73], and being associated with immune infiltration and prognosis in lung cancer [74]. Notably, *CENPA* overexpression was also associated with proliferation and metastasis in kidney carcinoma by activating the WNT/β-Catenin signaling pathway [75], an important pathway described in the progression of ACC [3]. In our analysis, *CENPA* appeared positively enriched in this pathway (Supplementary Table S7). Further studies may elucidate whether the relationship in renal carcinoma between *CENPA* activity and the WNT/β-Catenin signaling pathway may also apply to ACC.

The three regulons with the highest negative correlation with CENPA's activity were *THRB, STAT5B,* and *ZBTB4*, all from RC1 and of good prognosis.

Interestingly, *ZBTB4* is known to act as a tumor suppressor in various types of cancers (prostate cancer [76]; glioma [77]; colorectal cancer [78]; breast cancer [79]; Ewing sarcoma [80]), but more importantly, it is being investigated as a promissory anti-cancer druggable target. For example, Kim et al. (2012) [76] showed that Methyl 2-cyano-3,11-dioxo-18β-olean-1,12-dien-30-oate (CDODA-Me) can increase *ZBTB4* expression *in vivo* and *in vitro*, having an antitumorigenic activity in prostate cancer. Whether the increased expression of *ZBTB4* could inhibit *CENPA* and its proliferative activity may be an interesting area for future studies.

It should be noted that our study had some limitations. Our selection strategy may have removed some interesting regulons, which are therefore not listed in the 369 prognostic regulons, thereby excluding their possible role in the ACC regulatory scenario. For example, *FOXM1* is assigned as a prognostic marker in ACC by Yuan et al. (2018) [81]. This TF presented 111 targets, of which only 11 were downregulated, thus not passing through our filter of at least 15 positive and 15 negative targets. We also used protein-coding genes only, which excludes possible important regulators, such as miRNAs or lncRNAs. Despite these limitations, our results may offer a reference for future studies aiming to understand transcriptional alterations in ACC, prognostic markers, or even therapeutic targets.

4.6 CONCLUSIONS

In conclusion, we have generated a regulatory network for ACC, evaluated the regulons inferred in concern to OS, clustered them in four RCs, and investigated how they relate to characteristics associated with worse outcomes like the steroid phenotype and the immune and proliferation pathways. The list of prognostic regulons, together with their characterization, may open new research avenues and relevant questions to be answered in this hard-to-treat and aggressive malignancy.

4.7 SUPPLEMENTARY MATERIALS

The following supporting information can be downloaded at: https://www.mdpi.com/article/10.3390/cancers14215279/s1. Figure S1: Distribution of the positive and negative targets of the regulons; Figure S2: Consensus matrix and silhouettes of regulon clusters; Figure S3: Boxplots comparing the Hallmark enrichment scores in the regulon clusters; Figure S4: Boxplots comparing the Spearman's correlation between the immune features described by Thorsson et al. (2018) [14] and the regulon activity in the clusters; Figure S5: A heatmap showing

regulon activity in the ENSAT cohort (n = 44 ACC samples); Figure S6: Targets of the *NR5A1* regulon and the related karyogram; Table S1: ACC regulatory network presenting the mutual information between the 1,605 transcription factors and their targets; Table S2: Number of positive and negative targets for each regulon; Table S3: Results for the multivariate Cox analysis for overall survival in the TCGA-ACC and ENSAT cohorts, and PFI in the TCGA-ACC cohort; Table S4: A master table resuming the data generated for the 369 prognostic regulons; Table S5: Activity of the 369 prognostic regulons in each sample for the TCGA-ACC and ENSAT cohorts; Table S6: Master Regulator Analysis (MRA) and two-tails gene set enrichment analysis (GSEA2) for the enrichment between the 369 regulons and the Steroid and Proliferation Phenotypes; Table S7: Regulon activity in MsigDb Hallmarks; Table S8: Duals correlation.

4.8 AUTHOR CONTRIBUTIONS

Conceptualization, J.C.D.M. and M.A.A.C.; methodology, J.C.D.M. and M.A.A.C.; software, M.A.A.C.; formal analysis, J.C.D.M., M.A.A.C., J.F.M., and B.C.F.; data curation, J.C.D.M.; writing—original draft preparation, J.C.D.M. and B.C.F.; writing—review and editing, J.C.D.M., J.M.M., J.S.S., L.M.A., J.F.M., B.C.F., and M.A.A.C.; visualization, J.C.D.M., J.M.M., J.S.S., and M.A.A.C.; supervision, L.M.A., J.F.M., B.C.F., and M.A.A.C.; project administration, M.A.A.C., L.M.A., J.F.M., and B.C.F.; funding acquisition, B.C.F. All authors have read and agreed to the published version of this manuscript.

4.9 FUNDING

J.C.D.M., J.M.M. and J.S.S.R. received scholarships from the BIG DATA innovation program from the Associação Hospitalar de Proteção à Infância Raul Carneiro—AHPIRAC (2020). M.A.A.C., L.M.A. and J.F.d.M. are funded by the Conselho Nacional de Desenvolvimento Cientıífico e Tecnológico (CNPq). M.A.A.C. is also funded by NAPI Bioinformática—Fundação Araucária (FA). J.C.D.M., J.M.M. and J.S.S. were funded by Associação Hospitalar de Proteção à Infância Dr. Raul Carneiro (AHPIRAC).

4.10 DATA AVAILABILITY STATEMENT

All data and software used in this study are publicly available in the sources described in the Methods section. All scripts and R data (rtni object) to generate results, figures, and tables for this study are available on the GitHub repository (https://github.com/sysbiolab/Sup_Material_Muzzi2022) (accessed on 30 August 2022).

4.11 ACKNOWLEDGMENTS

Data used in this manuscript were obtained from The Cancer Genome Atlas (TCGA) ACC database and of the European Network for the Study of Adrenal Tumors (ENSAT).

4.12 CONFLICTS OF INTEREST

The authors declare no conflict of interest. The funders had no role in the design of the study; in the collection, analyses, or interpretation of data; in the writing of the manuscript, or in the decision to publish the results.

4.13 REFERENCES

1. Wasserman, J.D.; Zambetti, G.P.; Malkin, D. Towards an understanding of the role of P53 in adrenocortical carcinogenesis. *Mol. Cell. Endocrinol.* **2012**, *351*, 101–110. DOI:10.1016/j.mce.2011.09.010.
2. Else, T.; Kim, A.C.; Sabolch, A.; Raymond, V.M.; Kandathil, A.; Caoili, E.M.; Jolly, S.; Miller, B.S.; Giordano, T.J.; Hammer, G.D. Adrenocortical carcinoma. *Endocr. Rev.* **2014**, *35*, 282–326. DOI:10.1210/er.2013-1029.
3. Cosentini, D.; Grisanti, S.; Dalla Volta, A.; Laganà, M.; Fiorentini, C.; Perotti, P.; Sigala, S.; Berruti, A. Immunotherapy failure in adrenocortical cancer: Where next? *Endocr. Connect.* **2018**, *7*, E5–E8. DOI:10.1530/EC-18-0398.
4. Baechle, J.J.; Hanna, D.N.; Sekhar, K.R.; Rathmell, J.C.; Rathmell, W.K.; Baregamian, N. Integrative computational immunogenomic profiling of cortisol-secreting adrenocortical carcinoma. *J. Cell. Mol. Med.* **2021**, *25*, 10061–10072. DOI:10.1111/jcmm.16936.
5. Landwehr, L.S.; Altieri, B.; Schreiner, J.; Sbiera, I.; Weigand, I.; Kroiss, M.; Fassnacht, M.; Sbiera, S. Interplay between glucocorticoids and tumor-infiltrating lymphocytes on the prognosis of adrenocortical carcinoma. *J. Immunother. Cancer*. **2020**, *8*, e000469. DOI:10.1136/jitc-2019-000469.
6. Muzzi, J.C.D.; Magno, J.M.; Cardoso, M.A.; de Moura, J.; Castro, M.A.A.; Figueiredo, B.C. Adrenocortical carcinoma steroid profiles: *In silico* pan-cancer analysis of TCGA data uncovers immunotherapy targets for potential improved outcomes. *Front. Endocrinol. (Lausanne).* **2021**, *12*, 672319. DOI:10.3389/fendo.2021.672319.

7. Zheng, S.; Cherniack, A.D.; Dewal, N.; Moffitt, R.A.; Danilova, L.; Murray, B.A.; Lerario, A.M.; Else, T.; Knijnenburg, T.A.; Ciriello, G.; et al. Comprehensive pan-genomic characterization of adrenocortical carcinoma. *Cancer Cell*. **2016**, *29*; ISBN 0000052442, 723–736. DOI:10.1016/j.ccell.2016.04.002.
8. Wirapati, P.; Sotiriou, C.; Kunkel, S.; Farmer, P.; Pradervand, S.; Haibe-Kains, B.; Desmedt, C.; Ignatiadis, M.; Sengstag, T.; Schütz, F.; et al. Meta-analysis of gene expression profiles in breast cancer: Toward a unified understanding of breast cancer subtyping and prognosis signatures. *Breast Cancer Res.* **2008**, *10*, R65. DOI:10.1186/bcr2124.
9. De Reyniès, A.; Assié, G.; Rickman, D.S.; Tissier, F.; Groussin, L.; René-Corail, F.; Dousset, B.; Bertagna, X.; Clauser, E.; Bertherat, J. Gene expression profiling reveals a new classification of adrenocortical tumors and identifies molecular predictors of malignancy and survival. *J. Clin. Oncol.* **2009**, *27*, 1108–1115. DOI:10.1200/JCO.2008.18.5678.
10. Galon, J.; Costes, A.; Sanchez-Cabo, F.; Kirilovsky, A.; Mlecnik, B.; Lagorce-Pagès, C.; Tosolini, M.; Camus, M.; Berger, A.; Wind, P.; et al. Type, density, and location of immune cells within human colorectal tumors predict clinical outcome. *Science*. **2006**, *313*, 1960–1964. DOI:10.1126/science.1129139.
11. Gajewski, T.F.; Corrales, L.; Williams, J.; Horton, B.; Sivan, A.; Spranger, S. Cancer immunotherapy targets based on understanding the T cell-inflamed versus non-T cell-inflamed tumor microenvironment. In. *Adv. Exp. Med. Biol.* **2017**, *1036*, pp. 19–31. DOI:10.1007/978-3-319-67577-0_2.
12. Galon, J.; Bruni, D. Approaches to treat immune hot, altered, and cold tumours with combination immunotherapies. *Nat. Rev. Drug Discov.* **2019**, *18*, 197–218. DOI:10.1038/s41573-018-0007-y.
13. Hegde, P.S.; Karanikas, V.; Evers, S. The where, the when, and the how of immune monitoring for cancer immunotherapies in the era of checkpoint inhibition. *Clin. Cancer Res.* **2016**, *22*, 1865–1874. DOI:10.1158/1078-0432.CCR-15-1507.
14. Thorsson, V.; Gibbs, D.L.; Brown, S.D.; Wolf, D.; Bortone, D.S.; Ou Yang, T.-H.; Porta-Pardo, E.; Gao, G.F.; Plaisier, C.L.; Eddy, J.A.; et al. The immune landscape of cancer. *Immunity*. **2018**, *48*, 812–830.e14. DOI:10.1016/j.immuni.2018.03.023.
15. Le Tourneau, C.; Hoimes, C.; Zarwan, C.; Wong, D.J.; Bauer, S.; Claus, R.; Wermke, M.; Hariharan, S.; von Heydebreck, A.; Kasturi, V.; et al. Avelumab in patients with previously treated metastatic adrenocortical carcinoma: Phase 1b results from the JAVELIN solid tumor trial. *J. Immunother. Cancer*. **2018**, *6*, 111. DOI:10.1186/s40425-018-0424-9.
16. Carneiro, B.A.; Konda, B.; Costa, R.B.; Costa, R.L.B.; Sagar, V.; Gursel, D.B.; Kirschner, L.S.; Chae, Y.K.; Abdulkadir, S.A.; Rademaker, A.; et al. Nivolumab in metastatic adrenocortical carcinoma: Results of a phase 2 trial. *J. Clin. Endocrinol. Metab.* **2019**, *104*, 6193–6200. DOI:10.1210/jc.2019-00600.
17. Habra, M.A.; Stephen, B.; Campbell, M.; Hess, K.; Tapia, C.; Xu, M.; Rodon Ahnert, J.; Jimenez, C.; Lee, J.E.; Perrier, N.D.; et al. Phase II clinical trial of pembrolizumab efficacy and safety in advanced adrenocortical carcinoma. *J. Immunother. Cancer*. **2019**, *7*, 253. DOI:10.1186/s40425-019-0722-x.
18. Raj, N.; Zheng, Y.; Kelly, V.; Katz, S.S.; Chou, J.; Do, R.K.G.; Capanu, M.; Zamarin, D.; Saltz, L.B.; Ariyan, C.E.; et al. PD-1 blockade in advanced adrenocortical carcinoma. *J. Clin. Oncol.* **2020**, *38*, 71–80. DOI:10.1200/JCO.19.01586.

19. McGregor, B.A.; Sonpavde, G.P. Rare genitourinary malignancies: Current status and future directions of immunotherapy. *Eur. Urol. Focus*. **2020**, *6*, 14–16. DOI:10.1016/j.euf.2019.03.011.
20. Mete, O.; Erickson, L.A.; Juhlin, C.C.; de Krijger, R.R.; Sasano, H.; Volante, M.; Papotti, M.G. Overview of the 2022 WHO classification of adrenal cortical tumors. *Endocr. Pathol.* **2022**, *33*, 155–196. DOI:10.1007/s12022-022-09710-8.
21. Hodgson, A.; Pakbaz, S.; Mete, O. A diagnostic approach to adrenocortical tumors. *Surg. Pathol. Clin.* **2019**, *12*, 967–995. DOI:10.1016/j.path.2019.08.005.
22. Fassnacht, M.; Dekkers, O.M.; Else, T.; Baudin, E.; Berruti, A.; de Krijger, R.; Haak, H.R.; Mihai, R.; Assie, G.; Terzolo, M. European society of endocrinology clinical practice guidelines on the management of adrenocortical carcinoma in adults, in collaboration with the European network for the study of adrenal tumors. *Eur. J. Endocrinol.* **2018**, *179*, G1–G46. DOI:10.1530/EJE-18-0608.
23. Mete, O.; Asa, S.L.; Giordano, T.J.; Papotti, M.; Sasano, H.; Volante, M. Immunohistochemical biomarkers of adrenal cortical neoplasms. *Endocr. Pathol.* **2018**, *29*, 137–149. DOI:10.1007/s12022-018-9525-8.
24. Lalli, E. Adrenocortical development and cancer: Focus on SF-1. *J. Mol. Endocrinol.* **2010**, *44*, 301–307. DOI:10.1677/JME-09-0143.
25. Crona, J.; Beuschlein, F. Adrenocortical carcinoma — Towards genomics guided clinical care. *Nat. Rev. Endocrinol.* **2019**, *15*, 548–560. DOI:10.1038/s41574-019-0221-7.
26. Castro, M.A.A.A.; de Santiago, I.; Campbell, T.M.; Vaughn, C.; Hickey, T.E.; Ross, E.; Tilley, W.D.; Markowetz, F.; Ponder, B.A.J.J.; Meyer, K.B. Regulators of genetic risk of breast cancer identified by integrative network analysis. *Nat. Genet.* **2016**, *48*, 12–21. DOI:10.1038/ng.3458.
27. Robertson, A.G.; Kim, J.; Al-Ahmadie, H.; Bellmunt, J.; Guo, G.; Cherniack, A.D.; Hinoue, T.; Laird, P.W.; Hoadley, K.A.; Akbani, R.; et al. Comprehensive molecular characterization of muscle-invasive bladder Cancer. *Cell*. **2017**, *171*, 540–556.e25. DOI:10.1016/j.cell.2017.09.007.
28. Kamoun, A.; de Reyniès, A.; Allory, Y.; Sjödahl, G.; Robertson, A.G.; Seiler, R.; Hoadley, K.A.; Groeneveld, C.S.; Al-Ahmadie, H.; Choi, W.; et al. A consensus molecular classification of muscle-invasive bladder cancer. *Eur. Urol.* **2020**, *77*, 420–433. DOI:10.1016/j.eururo.2019.09.006.
29. Cangiano, M.; Grudniewska, M.; Salji, M.J.; Nykter, M.; Jenster, G.; Urbanucci, A.; Granchi, Z.; Janssen, B.; Hamilton, G.; Leung, H.Y.; et al. Gene regulation network analysis on human prostate orthografts highlights a potential role for the JMJD6 regulon in clinical prostate cancer. *Cancers (Basel).* **2021**, *13*, 2094. DOI:10.3390/cancers13092094.
30. Liberzon, A.; Birger, C.; Thorvaldsdóttir, H.; Ghandi, M.; Mesirov, J.P.; Tamayo, P. The molecular signatures database Hallmark gene set collection. *Cell Syst.* **2015**, *1*, 417–425. DOI:10.1016/j.cels.2015.12.004.
31. Assié, G.; Letouzé, E.; Fassnacht, M.; Jouinot, A.; Luscap, W.; Barreau, O.; Omeiri, H.; Rodriguez, S.; Perlemoine, K.; René-Corail, F.; et al. Integrated genomic characterization of adrenocortical carcinoma. *Nat. Genet.* **2014**, *46*, 607–612. DOI:10.1038/ng.2953.
32. Colaprico, A.; Silva, T.C.; Olsen, C.; Garofano, L.; Cava, C.; Garolini, D.; Sabedot, T.S.; Malta, T.M.; Pagnotta, S.M.; Castiglioni, I.; et al. TCGAbiolinks: An R/bioconductor package for integrative analysis of TCGA data. *Nucleic Acids Res.* **2016**, *44*, e71. DOI:10.1093/nar/gkv1507.

33. Silva, T.C.; Colaprico, A.; Olsen, C.; D'Angelo, F.; Bontempi, G.; Ceccarelli, M.; Noushmehr, H. TCGA workflow: Analyze cancer genomics and epigenomics data using bioconductor packages. *F1000Research*. **2016**, *5*, 1542. DOI:10.12688/f1000research.8923.2.
34. Mounir, M.; Lucchetta, M.; Silva, T.C.; Olsen, C.; Bontempi, G.; Chen, X.; Noushmehr, H.; Colaprico, A.; Papaleo, E. New functionalities in the TCGAbiolinks package for the study and integration of cancer data from GDC and GTEx. *PLOS Comput. Biol.* **2019**, *15*, e1006701. DOI:10.1371/journal.pcbi.1006701.
35. Liu, J.; Lichtenberg, T.; Hoadley, K.A.; Poisson, L.M.; Lazar, A.J.; Cherniack, A.D.; Kovatich, A.J.; Benz, C.C.; Levine, D.A.; Lee, A.V.; et al. An integrated TCGA pan-cancer clinical data resource to drive high-quality survival outcome analytics. *Cell*. **2018**, *173*, 400–416.e11. DOI:10.1016/j.cell.2018.02.052.
36. Morgan, M.; Shepherd, L. *Annotation*Hub: Client to Access AnnotationHub Resources. R Package, version 2.22.0, 2020.
37. Love, M.I.; Huber, W.; Anders, S. Moderated estimation of fold change and dispersion for RNA-seq data with DESeq2. *Genome Biol.* **2014**, *15*, 550. DOI:10.1186/s13059-014-0550-8.
38. Fletcher, M.N.C.C.; Castro, M.A.A.A.; Wang, X.; De Santiago, I.; O'Reilly, M.; Chin, S.F.; Rueda, O.M.; Caldas, C.; Ponder, B.A.J.J.; Markowetz, F.; et al. Master regulators of FGFR2 signalling and breast cancer risk. *Nat. Commun.* **2013**, *4*, 2464. DOI:10.1038/ncomms3464.
39. Lambert, S.A.; Jolma, A.; Campitelli, L.F.; Das, P.K.; Yin, Y.; Albu, M.; Chen, X.; Taipale, J.; Hughes, T.R.; Weirauch, M.T. The human transcription factors. *Cell*. **2018**, *172*, 650–665. DOI:10.1016/j.cell.2018.01.029.
40. Margolin, A.A.; Wang, K.; Lim, W.K.; Kustagi, M.; Nemenman, I.; Califano, A. Reverse engineering cellular networks. *Nat. Protoc.* **2006**, *1*, 662–671. DOI:10.1038/nprot.2006.106.
41. Cohen, J. *Statistical Power Analysis for the Behavioral Science*; Routledge; ISBN 9781134742707, 2013.
42. Benjamini, Y.; Hochberg, Y. Controlling the false discovery rate: A practical and powerful approach to multiple testing. *J. R. Stat. Soc. B*. **1995**, *57*, 289–300. DOI:10.1111/j.2517-6161.1995.tb02031.x.
43. Cox, D.R. Regression models and Life-Tables. *J. R. Stat. Soc. B*. **1972**, *34*, 187–202. DOI:10.1111/j.2517-6161.1972.tb00899.x.
44. Groeneveld, C.S.; Chagas, V.S.; Jones, S.J.M.; Robertson, A.G.; Ponder, B.A.J.; Meyer, K.B.; Castro, M.A.A. RTNsurvival: An R/bioconductor package for regulatory network survival analysis. *Bioinformatics*. **2019**, *35*, 4488–4489. DOI:10.1093/bioinformatics/btz229.
45. Kaplan, E.L.; Meier, P. Nonparametric estimation from incomplete observations. *J. Am. Stat. Assoc.* **1958**, *53*, 457–481. DOI:10.1080/01621459.1958.10501452.
46. Mantel, N. Evaluation of survival data and two new rank order statistics arising in its consideration. *Cancer Chemother. Rep.* **1966**, *50*, 163–170.
47. Peto, R.; Peto, J. Asymptotically efficient rank invariant test procedures. *J. R. Stat. Soc. A*. **1972**, *135*, 185. DOI:10.2307/2344317.
48. Wilkerson, M.D.; Hayes, D.N. ConsensusClusterPlus: A class discovery tool with confidence assessments and item tracking. *Bioinformatics*. **2010**, *26*, 1572–1573. DOI:10.1093/bioinformatics/btq170.
49. Dolgalev, I. Msigdbr: MSigDB gene sets for multiple organisms in a tidy data format. Available online: https://igordot.github.io/msigdbr/.

50. Chagas, V.S.; Groeneveld, C.S.; Oliveira, K.G.; Trefflich, S.; de Almeida, R.C.; Ponder, B.A.J.; Meyer, K.B.; Jones, S.J.M.; Robertson, A.G.; Castro, M.A.A. RTNduals: An R/bioconductor package for analysis of co-regulation and inference of dual regulons. *Bioinformatics*. **2019**, *35*, 5357–5358. DOI:10.1093/bioinformatics/btz534.
51. Davis, S.; Meltzer, P.S. GEOquery: A bridge between the gene expression omnibus (GEO) and BioConductor. *Bioinformatics*. **2007**, *23*, 1846–1847. DOI:10.1093/bioinformatics/btm254.
52. R Core Team. *R: A Language and Environment for Statistical Computing*.
53. Huber, W.; Carey, V.J.; Gentleman, R.; Anders, S.; Carlson, M.; Carvalho, B.S.; Bravo, H.C.; Davis, S.; Gatto, L.; Girke, T.; et al. Orchestrating high-throughput genomic analysis with bioconductor. *Nat. Methods*. **2015**, *12*, 115–121. DOI:10.1038/nmeth.3252.
54. Wilcoxon, F. Individual comparisons by ranking methods. *Biom. Bull.* **1945**, *1*, 80. DOI:10.2307/3001968.
55. Mann, H.B.; Whitney, D.R. On a test of whether one of two random variables is stochastically larger than the other. *Ann. Math. Statist.* **1947**, *18*, 50–60. DOI:10.1214/aoms/1177730491.
56. Kruskal, W.H.; Wallis, W.A. Use of ranks in one-criterion variance analysis. *J. Am. Stat. Assoc.* **1952**, *47*, 583–621. DOI:10.1080/01621459.1952.10483441.
57. Dunn, O.J. Multiple comparisons using rank sums. *Technometrics*. **1964**, *6*, 241–252. DOI:10.1080/00401706.1964.10490181.
58. Gu, Z.; Eils, R.; Schlesner, M. Complex heatmaps reveal patterns and correlations in multidimensional genomic data. *Bioinformatics*. **2016**, *32*, 2847–2849. DOI:10.1093/bioinformatics/btw313.
59. Castro, M.A.; Wang, X.; Fletcher, M.N.; Meyer, K.B.; Markowetz, F. RedeR: R/bioconductor package for representing modular structures, nested networks and multiple levels of hierarchical associations. *Genome Biol.* **2012**, *13*, R29. DOI:10.1186/gb-2012-13-4-r29.
60. Fiorentini, C.; Grisanti, S.; Cosentini, D.; Abate, A.; Rossini, E.; Berruti, A.; Sigala, S. Molecular drivers of potential immunotherapy failure in adrenocortical carcinoma. *J. Oncol.* **2019**, *2019*, 6072863. DOI:10.1155/2019/6072863.
61. SenGupta, S.; Harris, C.C. P53: Traffic cop at the crossroads of DNA repair and recombination. *Nat. Rev. Mol. Cell Biol.* **2005**, *6*, 44–55. DOI:10.1038/nrm1546.
62. Jaber, S.; Toufektchan, E.; Lejour, V.; Bardot, B.; Toledo, F. P53 downregulates the Fanconi anaemia DNA repair pathway. *Nat. Commun.* **2016**, *7*, 11091. DOI:10.1038/ncomms11091.
63. Kotoula, V.; Krikelis, D.; Karavasilis, V.; Koletsa, T.; Eleftheraki, A.G.; Televantou, D.; Christodoulou, C.; Dimoudis, S.; Korantzis, I.; Pectasides, D.; et al. Expression of DNA repair and replication genes in non-small cell lung cancer (NSCLC): A role for thymidylate synthetase (TYMS). *BMC Cancer*. **2012**, *12*, 342. DOI:10.1186/1471-2407-12-342.
64. Ge, Z.; Leighton, J.S.; Wang, Y.; Peng, X.; Chen, Z.; Chen, H.; Sun, Y.Y.; Yao, F.; Li, J.; Zhang, H.; et al. Integrated genomic analysis of the ubiquitin pathway across cancer types. *Cell Rep.* **2018**, *23*, 213–226.e3. DOI:10.1016/j.celrep.2018.03.047.
65. Pianovski, M.A.D.; Cavalli, L.R.; Figueiredo, B.C.; Santos, S.C.L.; Doghman, M.; Ribeiro, R.C.; Oliveira, A.G.; Michalkiewicz, E.; Rodrigues, G.A.; Zambetti, G.; et al. SF-1 overexpression in childhood adrenocortical tumours. *Eur. J. Cancer*. **2006**, *42*, 1040–1043. DOI:10.1016/j.ejca.2006.01.022.

66. Doghman, M.; Karpova, T.; Rodrigues, G.A.; Arhatte, M.; De Moura, J.; Cavalli, L.R.; Virolle, V.; Barbry, P.; Zambetti, G.P.; Figueiredo, B.C.; et al. Increased steroidogenic Factor-1 dosage triggers adrenocortical cell proliferation and cancer. *Mol. Endocrinol.* **2007**, *21*, 2968–2987. DOI:10.1210/me.2007-0120.
67. Sbiera, S.; Schmull, S.; Assie, G.; Voelker, H.U.; Kraus, L.; Beyer, M.; Ragazzon, B.; Beuschlein, F.; Willenberg, H.S.; Hahner, S.; et al. High diagnostic and prognostic value of steroidogenic Factor-1 expression in adrenal tumors. *J. Clin. Endocrinol. Metab.* **2010**, *95*, E161–E171. DOI:10.1210/jc.2010-0653.
68. Kronfol, Z.; Starkman, M.; Schteingart, D.E.; Singh, V.; Zhang, Q.; Hill, E. Immune regulation in Cushing's syndrome: Relationship to hypothalamic-pituitary-adrenal axis hormones. *Psychoneuroendocrinology*. **1996**, *21*, 599–608. DOI:10.1016/S0306-4530(96)00021-2.
69. Jefferies, W.M. Cortisol and immunity. *Med. Hypo.* **1991**, *34*, 198–208. DOI:10.1016/0306-9877(91)90212-H.
70. Howman, E.V.; Fowler, K.J.; Newson, A.J.; Redward, S.; MacDonald, A.C.; Kalitsis, P.; Choo, K.H.A. Early disruption of centromeric chromatin organization in centromere protein A (Cenpa) null mice. *Proc. Natl Acad. Sci. U. S. A.* **2000**, *97*, 1148–1153. DOI:10.1073/pnas.97.3.1148.
71. Han, J.; Xie, R.; Yang, Y.; Chen, D.; Liu, L.; Wu, J.; Li, S. CENPA is one of the potential key genes associated with the proliferation and prognosis of ovarian cancer based on integrated bioinformatics analysis and regulated by MYBL2. *Transl. Cancer Res.* **2021**, *10*, 4076–4086. DOI:10.21037/tcr-21-175.
72. Saha, A.K.; Contreras-Galindo, R.; Niknafs, Y.S.; Iyer, M.; Qin, T.; Padmanabhan, K.; Siddiqui, J.; Palande, M.; Wang, C.; Qian, B.; et al. The role of the histone H3 variant CENPA in prostate cancer. *J. Biol. Chem.* **2020**, *295*, 8537–8549. DOI:10.1074/jbc.RA119.010080.
73. Liang, Y.C.; Su, Q.; Liu, Y.J.; Xiao, H.; Yin, H.Z. Centromere protein A (CENPA) regulates metabolic reprogramming in the colon cancer cells by transcriptionally activating karyopherin subunit alpha 2 (KPNA2). *Am. J. Pathol.* **2021**, *191*, 2117–2132. DOI:10.1016/j.ajpath.2021.08.010.
74. Zhou, H.; Bian, T.; Qian, L.; Zhao, C.; Zhang, W.; Zheng, M.; Zhou, H.; Liu, L.; Sun, H.; Li, X.; et al. Prognostic model of lung adenocarcinoma constructed by the CENPA complex genes is closely related to immune infiltration. *Pathol. Res. Pract.* **2021**, *228*, 153680. DOI:10.1016/j.prp.2021.153680.
75. Wang, Q.; Xu, J.; Xiong, Z.; Xu, T.; Liu, J.; Liu, Y.; Chen, J.; Shi, J.; Shou, Y.; Yue, C.; et al. CENPA promotes clear cell renal cell carcinoma progression and metastasis via Wnt/β-catenin signaling pathway. *J. Transl. Med.* **2021**, *19*, 417. DOI:10.1186/s12967-021-03087-8.
76. Kim, K.; Chadalapaka, G.; Pathi, S.S.; Jin, U.H.; Lee, J.S.; Park, Y.Y.; Cho, S.G.; Chintharlapalli, S.; Safe, S. Induction of the transcriptional repressor ZBTB4 in prostate cancer cells by drug-induced targeting of MicroRNA-17-92/106b-25 clusters. *Mol. Cancer Ther.* **2012**, *11*, 1852–1862. DOI:10.1158/1535-7163.MCT-12-0181.
77. Dong, W.; Liu, X.; Yang, C.; Wang, D.; Xue, Y.; Ruan, X.; Zhang, M.; Song, J.; Cai, H.; Zheng, J.; et al. Glioma glycolipid metabolism: MSI2–SNORD12B–FIP1L1–ZBTB4 feedback loop as a potential treatment target. *Clin. Transl. Med.* **2021**, *11*, e411. DOI:10.1002/ctm2.411.
78. Xiang, T.; He, K.; Wang, S.; Chen, W.; Li, H. Expression of zinc Finger and Btb domain-containing 4 in colorectal cancer and its clinical significance. *Cancer Manag. Res.* **2020**, *12*, 9621–9626. DOI:10.2147/CMAR.S266529.

79. Kim, K.; Chadalapaka, G.; Lee, S.O.; Yamada, D.; Sastre-Garau, X.; Defossez, P.A.; Park, Y.Y.; Lee, J.S.; Safe, S. Identification of oncogenic MicroRNA-17-92/ZBTB4/Specificity protein axis in breast cancer. *Oncogene*. **2012**, *31*, 1034–1044. DOI:10.1038/onc.2011.296.
80. Yu, Y.; Shang, R.; Chen, Y.; Li, J.; Liang, Z.; Hu, J.; Liu, K.; Chen, C. Tumor suppressive ZBTB4 inhibits cell growth by regulating cell cycle progression and apoptosis in Ewing sarcoma. *Biomed. Pharmacother.* **2018**, *100*, 108–115. DOI:10.1016/j.biopha.2018.01.132.
81. Yuan, L.; Qian, G.; Chen, L.; Wu, C.L.; Dan, H.C.; Xiao, Y.; Wang, X. Co-expression network analysis of biomarkers for adrenocortical carcinoma. *Front. Genet.* **2018**, *9*, 328. DOI:10.3389/fgene.2018.00328.

5 CONSIDERAÇÕES FINAIS

Dentro dos objetivos iniciais desse projeto em aprofundar a compreensão dos mecanismos de malignidade em CCA, pudemos alcançar resultados importantes no entendimento da interação desse tumor com o sistema imunológico e apontar possíveis frentes de pesquisa. Primeiramente, pudemos quebrar o paradigma de que o CCA como um todo seria um tumor imunologicamente "frio". Nós demonstramos que um subgrupo de pacientes, classificados como de Fenótipo Esteroidal Baixo, apresentam sinais de ativação imunológica significativa, mesmo quando comparados a tumores considerados "quentes". Essa classificação molecular pode ser investigada para a seleção de pacientes a imunoterapias, os quais esperamos que tenham resultados mais promissores a esse tratamento do que os obtidos sem prévia seleção. Além disso, apontamos possíveis causas para a imunossupressão dos pacientes com Fenótipo Esteroidal Alto, a qual se associa à produção de glucocorticoides no ambiente intratumoral e mais importante, mostramos que essa produção não necessariamente será identificada a nível de cortisol no sangue periférico. De encontro a outros estudos, reforçamos a importância em se investigar se o bloqueio das vias esteroidais é capaz de mitigar a imunossupressão. Ainda, defendemos que o Fenótipo Esteroidal deve ser levado em consideração ao tratar das variáveis imunológicas por acrescentar um fator de confundimento importante nesse tipo de análise.

Em seguida, apontamos 369 regulons associados à sobrevida e demonstramos que dos quatro subgrupos apresentados, dois tinham correlação significativa com o Fenótipo Esteroidal. Entretanto, além desse fenótipo, apresentamos outros dois grupos associados a prognóstico, mas com fatores de risco diferentes daqueles já demonstrados pelo Fenótipo Esteroidal, possibilitando novas frentes de pesquisa.

Finalmente, ao longo desse trabalho, apresentamos uma série de possíveis novos alvos que se destacaram em expressão no contexto do CCA, muitos dos quais não haviam sido enfatizados anteriormente. Por exemplo, demonstramos que a expressão de B7-H3 *(CD276)* se encontra elevada em CCA mesmo quando comparada a outros tumores, a qual pode justificar a resistência a terapias anti-PD-1. Apresentamos o *CENPA* como um fator prognóstico importante e fortemente

associado à proliferação e finalmente apontamos o *ZBTB4*, um alvo drogável, como uma via antitumoral promissora a ser testada em CCA.

Importante ressaltar que nesse estudo utilizamos amostras dos quatro estádios tumorais. Pacientes metastáticos, classificados como em estádio IV, podem apresentar particularidades intrínsecas, as quais poderiam gerar efeitos de confundimento, principalmente quando levamos em consideração que a maioria dessas amostras eram classificadas no perfil Esteroidal Alto. Apesar disso, em nosso segundo trabalho apresentado no Capítulo II, utilizamos o estádio tumoral como covariável na análise de sobrevida, ajustando nossa avaliação às influências desse fator.

Durante a realização das análises aqui apresentadas, pudemos observar outros dados que eventualmente seriam passíveis de maiores investigações. Por exemplo, notoriamente apesar de os alvos associados a um fator de transcrição na análise regulatória não serem o fruto principal de análise, mas sim a atividade da unidade regulatória como um todo, destacou-se uma particularidade observada nos alvos regulados pelo *CENPA*. 20 dos 23 genes elencados em três assinaturas prognósticas apontadas por autores diferentes (26–28) eram regulados positivamente pelo regulon *CENPA*. Certamente, o papel desse fator de transcrição na proliferação e quais seriam os seus alvos biológicos são questionamentos interessantes a serem confirmados em bancada.

Além disso, pudemos observar alguns genes com forte associação ao perfil esteroidal alto, como por exemplo o *Neural Pantraxin 1* (*NPTX1*). Apesar de existirem outros estudos investigando o significado desse gene no contexto tumoral (179), para nós se destaca o fato de essa ser uma proteína secretada e normalmente não identificada a nível sanguíneo. Portanto, um aumento de sua expressão no perfil Esteroidal Alto poderia conferir uma detecção dessa proteína no sangue periférico, servindo de biomarcador para esse fenótipo molecular no CCA. Esperamos observar se esse resultado se confirma na prática clínica.

Outro aspecto interessante a esse tumor raro é o fato de que as amostras do perfil Esteroidal Alto, associadas à imunossupressão, apresentavam maior carga mutacional quando comparadas ao perfil Esteroidal Baixo. Dessa forma, caso a imunossupressão hormonal nesse fenótipo seja superada, acreditamos que uma resposta imunológica robusta possa vir a surgir em função da maior apresentação

de neoantígenos nesse grupo. Esperamos que esses questionamentos possam ser sanados com futuros ensaios clínicos nessas frentes de pesquisa.

No capítulo I, observamos uma alta expressão de *VEGFA, VEGFB* e *FLT1* (VEGFR1) nas amostras de CCA quando comparadas a outras tumores. Além disso, no capítulo II, observamos que regulons do grupo três e quatro (RC3 e RC4) se correlacionaram positivamente à assinatura de reparo celular (*wound healing*). Esses resultados apontariam para uma possível correlação com aumento nas vias de angiogênese. Portanto, nós investigamos se essa alta expressão de marcadores de angiogênese em CCA aconteciam no processo de malignidade ou eram uma característica intrínseca ao tecido de origem. Para isso, fizemos uma investigação *in silico* comparando as vias de angiogênese em amostras de CCA com amostras de adenoma de córtex adrenal e amostras normais desse tecido. Interessantemente, percebemos que não havia aumento significativo dessas vias nas amostras de carcinoma, mesmo quando separadas nos perfis esteroidais. Portanto, entendemos que para esse tumor a angiogênese não representa uma via de alteração significativa, apesar da alta expressão de alguns de seus marcadores. Esse resultado vem de encontro aos diversos estudos que demonstraram que inibidores de angiogênese não apresentaram resultados significativos no controle de progressão de CCA (111,180,181).

Como principal limitação a esse trabalho foi o seu desenvolvimento exclusivamente *in silico*. Esperamos ver ensaios *in vitro* e *in vivo* que venham a corroborar e aprofundar esses achados. Além disso, focamos em genes codificantes, o que certamente não exclui outros importantes atores e possibilidades no complexo cenário genético do CCA. Por fim, as amostras analisadas foram somente de pacientes adultos. Almejamos verificar se as amostras pediátricas correspondem aos padrões aqui observados.

Buscamos seguir as melhores condutas de pesquisa reproduzível, utilizando somente softwares livres e gratuitos e disponibilizando todos os códigos produzidos, assim como várias tabelas suplementares sumarizando todos os dados obtidos.

Esperamos com esse trabalho termos contribuído para o desenvolvimento científico de nosso país, especialmente associado a problemas regionais eventualmente negligenciados por falta de interesse econômico. Acima de tudo,

esperamos que os achados aqui apresentados possam originar novas linhas de tratamento para pacientes desenganados nesse tumor tão raro e difícil de tratar.

REFERÊNCIAS

1. Vinay DS, Ryan EP, Pawelec G, Talib WH, Stagg J, Elkord E, et al. Immune evasion in cancer: Mechanistic basis and therapeutic strategies. Semin Cancer Biol [Internet]. 2015;35:S185–98. Disponível em: http://dx.doi.org/10.1016/j.semcancer.2015.03.004

2. Kantarjian HM, Fojo T, Mathisen M, Zwelling LA. Cancer Drugs in the United States: Justum Pretium —The Just Price. J Clin Oncol [Internet]. 2013 Oct 1;31(28):3600–4. Disponível em: https://ascopubs.org/doi/10.1200/JCO.2013.49.1845

3. Prasad V, De Jesús K, Mailankody S. The high price of anticancer drugs: origins, implications, barriers, solutions. Nat Rev Clin Oncol [Internet]. 2017 Jun 14;14(6):381–90. Disponível em: http://www.nature.com/articles/nrclinonc.2017.31

4. United States of America Public Law 107-280, Nov 6, 2002 [Internet]. Disponível em: https://history.nih.gov/display/history/Legislative+Chronology?preview=%2F1016866%2F30736799%2FPL107-280.pdf

5. Fassnacht M, Kroiss M, Allolio B. Update in Adrenocortical Carcinoma. J Clin Endocrinol Metab [Internet]. 2013 Dec 1;98(12):4551–64. Disponível em: https://academic.oup.com/jcem/article/98/12/4551/2833638

6. Ribeiro RC, Sandrini F, Figueiredo B, Zambetti GP, Michalkiewicz E, Lafferty AR, et al. An inherited p53 mutation that contributes in a tissue-specific manner to pediatric adrenal cortical carcinoma. Proc Natl Acad Sci U S A. 2001;98(16):9330–5.

7. Ribeiro RC, Pinto EM, Zambetti GP, Rodriguez-Galindo C. The International Pediatric Adrenocortical Tumor Registry initiative: Contributions to clinical, biological, and treatment advances in pediatric adrenocortical tumors. Mol Cell Endocrinol [Internet]. 2012 Mar;351(1):37–43. Disponível em: http://dx.doi.org/10.1016/j.mce.2011.10.015

8. Custódio G, Parise GA, Filho NK, Komechen H, Sabbaga CC, Rosati R, et al. Impact of Neonatal Screening and Surveillance for the TP53 R337H Mutation on Early Detection of Childhood Adrenocortical Tumors. J Clin Oncol [Internet]. 2013 Jul 10;31(20):2619–26. Disponível em: http://ascopubs.org/doi/10.1200/JCO.2012.46.3711

9. Pianovski MADD, Maluf EMCPCP, de Carvalho DS, Ribeiro RC, Rodriguez-Galindo C, Boffetta P, et al. Mortality rate of adrenocortical tumors in children under 15 years of age in Curitiba, Brazil. Pediatr Blood Cancer [Internet]. 2006 Jul;47(1):56–60. Disponível em: http://doi.wiley.com/10.1002/pbc.20624

10. Araújo AN, Bugalho MJ. Advanced Adrenocortical Carcinoma: Current Perspectives on Medical Treatment. Horm Metab Res [Internet]. 2021 May 7;53(5):285–92. Disponível em: http://www.thieme-connect.de/DOI/DOI?10.1055/a-1453-0806

11. Wang RF, Wang HY. Immune targets and neoantigens for cancer immunotherapy and precision medicine. Cell Res. 2017;27(1):11–37.

12. Kiesewetter B, Riss P, Scheuba C, Mazal P, Kretschmer-Chott E, Haug A, et al. Management of adrenocortical carcinoma: are we making progress? Ther Adv Med Oncol [Internet]. 2021 Jan 31;13:1–14. Disponível em: http://journals.sagepub.com/doi/10.1177/17588359211038409

13. Fiorentini C, Grisanti S, Cosentini D, Abate A, Rossini E, Berruti A, et al. Molecular Drivers of Potential Immunotherapy Failure in Adrenocortical Carcinoma. J Oncol. 2019;2019.

14. Lalli E, Figueiredo BC. Pediatric Adrenocortical Tumors: What They Can Tell Us on Adrenal Development and Comparison with Adult Adrenal Tumors. Front Endocrinol (Lausanne) [Internet]. 2015 Feb 18;6(FEB):1–9. Disponível em: http://journal.frontiersin.org/Article/10.3389/fendo.2015.00023/abstract

15. Libè R, Fratticci A, Bertherat J. Adrenocortical cancer: pathophysiology and clinical management. Endocr Relat Cancer [Internet]. 2007 Mar;14(1):13–28. Disponível em: https://erc.bioscientifica.com/view/journals/erc/14/1/0140013.xml

16. Crona J, Beuschlein F. Adrenocortical carcinoma — towards genomics guided clinical care. Nat Rev Endocrinol [Internet]. 2019;15(9):548–60. Disponível em: http://dx.doi.org/10.1038/s41574-019-0221-7

17. Michalkiewicz E, Sandrini R, Figueiredo B, Miranda ECMCMM, Caran E, Oliveira-Filho AGG, et al. Clinical and Outcome Characteristics of Children With Adrenocortical Tumors: A Report From the International Pediatric Adrenocortical Tumor Registry. J Clin Oncol [Internet]. 2004 Mar 1;22(5):838–45. Disponível em: https://ascopubs.org/doi/10.1200/JCO.2004.08.085

18. Aranda G, Lopez C, Fernandez-Ruiz R, Esteban Y, Garcia-Eguren G, Mora M, et al. Circulatory Immune Cells in Cushing Syndrome: Bystanders or Active Contributors to Atherometabolic Injury? A Study of Adhesion and Activation of Cell Surface Markers. Int J Endocrinol. 2017;2017.

19. Mete O, Erickson LA, Juhlin CC, de Krijger RR, Sasano H, Volante M, et al. Overview of the 2022 WHO Classification of Adrenal Cortical Tumors. Endocr Pathol [Internet]. 2022 Mar 14;33(1):155–96. Disponível em: https://link.springer.com/10.1007/s12022-022-09710-8

20. Weiss LM. Comparative histologic study of 43 metastasizing and nonmetastasizing adrenocortical tumors. Am J Surg Pathol [Internet]. 1984 Mar;8(3):163–70. Disponível em: http://journals.lww.com/00000478-198403000-00001

21. Lalli E. Adrenocortical development and cancer: focus on SF-1. J Mol Endocrinol [Internet]. 2010 Jun;44(6):301–7. Disponível em: https://jme.bioscientifica.com/view/journals/jme/44/6/301.xml

22. Lalli E, Doghman M, Latre de Late P, Wakil A El, Mus-Veteau I. Beyond steroidogenesis: Novel target genes for SF-1 discovered by genomics. Mol Cell Endocrinol [Internet]. 2013 May;371(1–2):154–9. Disponível em: http://dx.doi.org/10.1016/j.mce.2012.11.005

23. Doghman M, Figueiredo BC, Volante M, Papotti M, Lalli E. Integrative analysis of SF-1 transcription factor dosage impact on genome-wide binding and gene expression regulation. Nucleic Acids Res [Internet]. 2013 Oct;41(19):8896–907. Disponível em: https://academic.oup.com/nar/article-lookup/doi/10.1093/nar/gkt658

24. de Reyniès A, Assié G, Rickman DS, Tissier F, Groussin L, René-Corail F, et al. Gene Expression Profiling Reveals a New Classification of Adrenocortical Tumors and Identifies Molecular Predictors of Malignancy and Survival. J Clin Oncol [Internet]. 2009 Mar 1;27(7):1108–15. Disponível em: http://ascopubs.org/doi/10.1200/JCO.2008.18.5678

25. Zheng S, Cherniack AD, Dewal N, Moffitt RA, Danilova L, Murray BA, et al. Comprehensive pan-genomic characterization of adrenocortical carcinoma. Cancer Cell [Internet]. 2016 May;29(5):723–36. Disponível em: https://linkinghub.elsevier.com/retrieve/pii/S153561081630160X

26. Xu W-H, Wu J, Wang J, Wan F-N, Wang H-K, Cao D-L, et al. Screening and Identification of Potential Prognostic Biomarkers in Adrenocortical Carcinoma. Front Genet [Internet]. 2019 Sep 11;10(September):1–13. Disponível em: https://www.frontiersin.org/article/10.3389/fgene.2019.00821/full

27. Xing Z, Luo Z, Yang H, Huang Z, Liang X. Screening and identification of key biomarkers in adrenocortical carcinoma based on bioinformatics analysis. Oncol Lett [Internet]. 2019 Sep 6;18(5):4667–76. Disponível em: http://www.spandidos-publications.com/10.3892/ol.2019.10817

28. Yuan L, Qian G, Chen L, Wu C-L, Dan HC, Xiao Y, et al. Co-expression Network Analysis of Biomarkers for Adrenocortical Carcinoma. Front Genet [Internet]. 2018 Aug 15;9(3):3267–72. Disponível em: https://www.frontiersin.org/article/10.3389/fgene.2018.00328/full

29. Cosentini D, Grisanti S, Dalla Volta A, Laganà M, Fiorentini C, Perotti P, et al. Immunotherapy failure in adrenocortical cancer: where next? Endocr Connect [Internet]. 2018 Dec;7(12):E5–8. Disponível em: https://ec.bioscientifica.com/view/journals/ec/7/12/EC-18-0398.xml

30. De Filpo G, Mannelli M, Canu L. Adrenocortical carcinoma: current treatment options. Curr Opin Oncol [Internet]. 2021 Jan;33(1):16–22. Disponível em: https://journals.lww.com/10.1097/CCO.0000000000000695

31. Le Tourneau C, Hoimes C, Zarwan C, Wong DJ, Bauer S, Claus R, et al. Avelumab in patients with previously treated metastatic adrenocortical carcinoma: phase 1b results from the JAVELIN solid tumor trial. J Immunother Cancer [Internet]. 2018 Dec 22;6(1):111. Disponível em: https://jitc.bmj.com/lookup/doi/10.1186/s40425-018-0424-9

32. Carneiro BA, Konda B, Costa RB, Costa RLB, Sagar V, Gursel DB, et al. Nivolumab in Metastatic Adrenocortical Carcinoma: Results of a Phase 2 Trial. J Clin Endocrinol Metab [Internet]. 2019 Dec 1;104(12):6193–200. Disponível em: https://academic.oup.com/jcem/article/104/12/6193/5528226

33. Habra MA, Stephen B, Campbell M, Hess K, Tapia C, Xu M, et al. Phase II clinical trial of pembrolizumab efficacy and safety in advanced adrenocortical carcinoma. J Immunother Cancer [Internet]. 2019 Dec 18;7(1):253. Disponível em: https://jitc.bmj.com/lookup/doi/10.1186/s40425-019-0722-x

34. Raj N, Zheng Y, Kelly V, Katz SS, Chou J, Do RKG, et al. PD-1 Blockade in Advanced Adrenocortical Carcinoma. J Clin Oncol [Internet]. 2020 Jan 1;38(1):71–80. Disponível em: https://ascopubs.org/doi/10.1200/JCO.19.01586

35. McGregor BA, Sonpavde GP. Rare Genitourinary Malignancies: Current Status and Future Directions of Immunotherapy. Eur Urol Focus [Internet]. 2020 Jan;6(1):14–6. Disponível em: https://linkinghub.elsevier.com/retrieve/pii/S2405456919300860

36. Hanahan D, Weinberg RA. The Hallmarks of Cancer. Cell [Internet]. 2000 Jan;100(1):57–70. Disponível em: https://linkinghub.elsevier.com/retrieve/pii/S0092867400816839

37. Hanahan D, Weinberg RA. Hallmarks of Cancer: The Next Generation. Cell [Internet]. 2011 Mar;144(5):646–74. Disponível em: https://linkinghub.elsevier.com/retrieve/pii/S0092867411001279

38. Hanahan D. Hallmarks of Cancer: New Dimensions. Cancer Discov [Internet]. 2022 Jan 1;12(1):31–46. Disponível em: https://aacrjournals.org/cancerdiscovery/article/12/1/31/675608/Hallmarks-of-Cancer-New-DimensionsHallmarks-of

39. Alsaab HO, Sau S, Alzhrani R, Tatiparti K, Bhise K, Kashaw SK, et al. PD-1 and PD-L1 Checkpoint Signaling Inhibition for Cancer Immunotherapy: Mechanism, Combinations, and Clinical Outcome. Front Pharmacol [Internet]. 2017 Aug 23;8. Disponível em: http://journal.frontiersin.org/article/10.3389/fphar.2017.00561/full

40. Liebl MC, Hofmann TG. Identification of responders to immune checkpoint therapy: which biomarkers have the highest value? J Eur Acad Dermatology Venereol [Internet]. 2019 Dec 13;33(S8):52–6. Disponível em: https://onlinelibrary.wiley.com/doi/10.1111/jdv.15992

41. Tang T, Huang X, Zhang G, Hong Z, Bai X, Liang T. Advantages of targeting the tumor immune microenvironment over blocking immune checkpoint in cancer immunotherapy. Signal Transduct Target Ther [Internet]. 2021 Feb 20;6(1):72. Disponível em: https://www.nature.com/articles/s41392-020-00449-4

42. Haslam A, Prasad V. Estimation of the Percentage of US Patients With Cancer Who Are Eligible for and Respond to Checkpoint Inhibitor Immunotherapy Drugs. JAMA Netw Open [Internet]. 2019 May 3;2(5):e192535. Disponível em: http://jamanetworkopen.jamanetwork.com/article.aspx?doi=10.1001/jamanetworkopen.2019.2535

43. Raskov H, Orhan A, Christensen JP, Gögenur I. Cytotoxic CD8+ T cells in cancer and cancer immunotherapy. Br J Cancer [Internet]. 2021 Jan 19;124(2):359–67. Disponível em: http://dx.doi.org/10.1038/s41416-020-01048-4

44. Farkona S, Diamandis EP, Blasutig IM. Cancer immunotherapy: the beginning of the end of cancer? BMC Med [Internet]. 2016 Dec 5;14(1):73. Disponível em: http://dx.doi.org/10.1186/s12916-016-0623-5

45. Melero I, Berman DM, Aznar MA, Korman AJ, Gracia JLP, Haanen J. Evolving synergistic combinations of targeted immunotherapies to combat cancer. Nat Rev Cancer [Internet]. 2015 Aug 24;15(8):457–72. Disponível em: https://www.nature.com/articles/nrc3973

46. Van Allen EM, Miao D, Schilling B, Shukla SA, Blank C, Zimmer L, et al. Genomic correlates of response to CTLA-4 blockade in metastatic melanoma. Science (80-) [Internet]. 2015 Oct 9;350(6257):207–11. Disponível em: https://www.science.org/doi/10.1126/science.aad0095

47. Llosa NJ, Cruise M, Tam A, Wicks EC, Hechenbleikner EM, Taube JM, et al. The Vigorous Immune Microenvironment of Microsatellite Instable Colon Cancer Is Balanced by Multiple Counter-Inhibitory Checkpoints. Cancer Discov [Internet]. 2015 Jan 1;5(1):43–51. Disponível em:

https://aacrjournals.org/cancerdiscovery/article/5/1/43/4777/The-Vigorous-Immune-Microenvironment-of

48. Rizvi NA, Hellmann MD, Snyder A, Kvistborg P, Makarov V, Havel JJ, et al. Mutational landscape determines sensitivity to PD-1 blockade in non–small cell lung cancer. Science (80-) [Internet]. 2015 Apr 3;348(6230):124–8. Disponível em: https://www.science.org/doi/10.1126/science.aaa1348

49. Kazama A, Bilim V, Tasaki M, Anraku T, Kuroki H, Shirono Y, et al. Tumor-infiltrating immune cell status predicts successful response to immune checkpoint inhibitors in renal cell carcinoma. Sci Rep [Internet]. 2022 Nov 27;12(1):20386. Disponível em: https://www.nature.com/articles/s41598-022-24437-6

50. Thompson RH, Gillett MD, Cheville JC, Lohse CM, Dong H, Webster WS, et al. Costimulatory B7-H1 in renal cell carcinoma patients: Indicator of tumor aggressiveness and potential therapeutic target. Proc Natl Acad Sci [Internet]. 2004 Dec 7;101(49):17174–9. Disponível em: https://pnas.org/doi/full/10.1073/pnas.0406351101

51. Sharma P, Allison JP. The future of immune checkpoint therapy. Science (80-) [Internet]. 2015 Apr 3;348(6230):56–61. Disponível em: https://www.science.org/doi/10.1126/science.aaa8172

52. Wolchok JD, Kluger H, Callahan MK, Postow MA, Rizvi NA, Lesokhin AM, et al. Nivolumab plus Ipilimumab in Advanced Melanoma. N Engl J Med [Internet]. 2013 Jul 11;369(2):122–33. Disponível em: http://www.nejm.org/doi/10.1056/NEJMoa1302369

53. Thorsson V, Gibbs DL, Brown SD, Wolf D, Bortone DS, Ou Yang T-H, et al. The Immune Landscape of Cancer. Immunity [Internet]. 2018 Apr;48(4):812-830.e14. Disponível em: https://linkinghub.elsevier.com/retrieve/pii/S1074761318301213

54. Paré L, Pascual T, Seguí E, Teixidó C, Gonzalez-Cao M, Galván P, et al. Association between PD1 mRNA and response to anti-PD1 monotherapy across multiple cancer types. Ann Oncol [Internet]. 2018 Oct;29(10):2121–8. Disponível em: https://linkinghub.elsevier.com/retrieve/pii/S0923753419342085

55. Hasenmajer V, Sbardella E, Sciarra F, Minnetti M, Isidori AM, Venneri MA. The Immune System in Cushing's Syndrome. Trends Endocrinol Metab [Internet]. 2020 Sep;31(9):655–69. Disponível em: https://doi.org/10.1016/j.tem.2020.04.004

56. Landwehr L-SS, Altieri B, Schreiner J, Sbiera I, Weigand I, Kroiss M, et al. Interplay between glucocorticoids and tumor-infiltrating lymphocytes on the prognosis of adrenocortical carcinoma. J Immunother Cancer [Internet]. 2020

May;8(1):e000469. Disponível em: https://jitc.bmj.com/lookup/doi/10.1136/jitc-2019-000469

57. Liu S, Ding G, Zhou Z, Feng C. $β$-Catenin-driven adrenocortical carcinoma is characterized with immune exclusion. Onco Targets Ther. 2018;11:2029–36.

58. Wasserman JD, Zambetti GP, Malkin D. Towards an understanding of the role of p53 in adrenocortical carcinogenesis. Mol Cell Endocrinol [Internet]. 2012 Mar;351(1):101–10. Disponível em: https://linkinghub.elsevier.com/retrieve/pii/S0303720711005442

59. Spranger S, Gajewski TF. Impact of oncogenic pathways on evasion of antitumour immune responses. Nat Rev Cancer [Internet]. 2018 Mar 12;18(3):139–47. Disponível em: http://dx.doi.org/10.1038/nrc.2017.117

60. Muzzi JCD, Magno JM, Cardoso MA, de Moura J, Castro MAA, Figueiredo BC. Adrenocortical Carcinoma Steroid Profiles: In Silico Pan-Cancer Analysis of TCGA Data Uncovers Immunotherapy Targets for Potential Improved Outcomes. Front Endocrinol (Lausanne) [Internet]. 2021 Jun 14;12(June):1–19. Disponível em: https://www.frontiersin.org/articles/10.3389/fendo.2021.672319/full

61. Allolio B, Fassnacht M. Adrenocortical Carcinoma: Clinical Update. J Clin Endocrinol Metab [Internet]. 2006 Jun 1;91(6):2027–37. Disponível em: https://academic.oup.com/jcem/article/91/6/2027/2843324

62. Berruti A, Fassnacht M, Haak H, Else T, Baudin E, Sperone P, et al. Prognostic Role of Overt Hypercortisolism in Completely Operated Patients with Adrenocortical Cancer. Eur Urol [Internet]. 2014 Apr;65(4):832–8. Disponível em: https://linkinghub.elsevier.com/retrieve/pii/S0302283813012037

63. Giordano TJ, Kuick R, Else T, Gauger PG, Vinco M, Bauersfeld J, et al. Molecular Classification and Prognostication of Adrenocortical Tumors by Transcriptome Profiling. Clin Cancer Res [Internet]. 2009 Jan 15;15(2):668–76. Disponível em: http://clincancerres.aacrjournals.org/cgi/doi/10.1158/1078-0432.CCR-08-1067

64. Li B, Severson E, Pignon J-CC, Zhao H, Li T, Novak J, et al. Comprehensive analyses of tumor immunity: implications for cancer immunotherapy. Genome Biol [Internet]. 2016 Dec 22;17(1):174. Disponível em: http://genomebiology.biomedcentral.com/articles/10.1186/s13059-016-1028-7

65. Parise IZS, Parise GA, Noronha L, Surakhy M, Woiski TD, Silva DB, et al. The Prognostic Role of CD8+ T Lymphocytes in Childhood Adrenocortical Carcinomas Compared to Ki-67, PD-1, PD-L1, and the Weiss Score. Cancers (Basel) [Internet]. 2019 Nov 5;11(11):1730. Disponível em: https://www.mdpi.com/2072-6694/11/11/1730

66. Pinto EM, Chen X, Easton J, Finkelstein D, Liu Z, Pounds S, et al. Genomic landscape of paediatric adrenocortical tumours. Nat Commun [Internet]. 2015 May 6;6(1):6302. Disponível em: http://www.nature.com/articles/ncomms7302

67. Finn OJ. Cancer Immunology. N Engl J Med [Internet]. 2008 Jun 19;358(25):2704–15. Disponível em: http://www.nejm.org/doi/abs/10.1056/NEJMra072739

68. Custódio G, Komechen H, Figueiredo FRO, Fachin ND, Pianovski MAD, Figueiredo BC. Molecular epidemiology of adrenocortical tumors in southern Brazil. Mol Cell Endocrinol [Internet]. 2012 Mar;351(1):44–51. Disponível em: https://linkinghub.elsevier.com/retrieve/pii/S0303720711006332

69. Vanbrabant T, Fassnacht M, Assie G, Dekkers OM. Influence of hormonal functional status on survival in adrenocortical carcinoma: systematic review and meta-analysis. Eur J Endocrinol [Internet]. 2018 Dec;179(6):429–36. Disponível em: https://eje.bioscientifica.com/view/journals/eje/179/6/EJE-18-0450.xml

70. Prager I, Liesche C, van Ooijen H, Urlaub D, Verron Q, Sandström N, et al. NK cells switch from granzyme B to death receptor–mediated cytotoxicity during serial killing. J Exp Med [Internet]. 2019 Sep 2;216(9):2113–27. Disponível em: https://rupress.org/jem/article/216/9/2113/120710/NK-cells-switch-from-granzyme-B-to-death

71. Cursons J, Souza-Fonseca-Guimaraes F, Foroutan M, Anderson A, Hollande FF, Hediyeh-Zadeh S, et al. A Gene Signature Predicting Natural Killer Cell Infiltration and Improved Survival in Melanoma Patients. Cancer Immunol Res [Internet]. 2019 Jul;7(7):1162–74. Disponível em: http://cancerimmunolres.aacrjournals.org/lookup/doi/10.1158/2326-6066.CIR-18-0500

72. Drake CG, Lipson EJ, Brahmer JR. Breathing new life into immunotherapy: review of melanoma, lung and kidney cancer. Nat Rev Clin Oncol [Internet]. 2014 Jan 19;11(1):24–37. Disponível em: http://www.nature.com/articles/nrclinonc.2013.208

73. Rodriguez D, Goulart C, Pagliarone AC, Silva EP, Cunegundes PS, Nascimento IP, et al. In vitro Evidence of Human Immune Responsiveness Shows the Improved Potential of a Recombinant BCG Strain for Bladder Cancer Treatment. Front Immunol [Internet]. 2019 Jun 26;10. Disponível em: https://www.frontiersin.org/article/10.3389/fimmu.2019.01460/full

74. Greenwald RJ, Freeman GJ, Sharpe AH. THE B7 FAMILY REVISITED. Annu Rev Immunol [Internet]. 2005 Apr;23(1):515–48. Disponível em: http://www.annualreviews.org/doi/10.1146/annurev.immunol.23.021704.115611

75. Colaprico A, Silva TC, Olsen C, Garofano L, Cava C, Garolini D, et al. TCGAbiolinks: An R/Bioconductor package for integrative analysis of TCGA data. Nucleic Acids Res. 2016;44(8):e71.

76. Pettenati C, Ingersoll MA. Mechanisms of BCG immunotherapy and its outlook for bladder cancer. Nat Rev Urol [Internet]. 2018 Oct 10;15(10):615–25. Disponível em: http://www.nature.com/articles/s41585-018-0055-4

77. Hong H, Wang Q, Li J, Liu H, Meng X, Zhang H. Aging, Cancer and Immunity. J Cancer [Internet]. 2019;10(13):3021–7. Disponível em: http://www.jcancer.org/v10p3021.htm

78. Bindea G, Mlecnik B, Tosolini M, Kirilovsky A, Waldner M, Obenauf AC, et al. Spatiotemporal Dynamics of Intratumoral Immune Cells Reveal the Immune Landscape in Human Cancer. Immunity [Internet]. 2013 Oct;39(4):782–95. Disponível em: https://linkinghub.elsevier.com/retrieve/pii/S1074761313004378

79. Rieder SA, Wang J, White N, Qadri A, Menard C, Stephens G, et al. B7-H7 (HHLA2) inhibits T-cell activation and proliferation in the presence of TCR and CD28 signaling. Cell Mol Immunol [Internet]. 2020 Jan 31;7(December 2019). Disponível em: http://dx.doi.org/10.1038/s41423-020-0361-7

80. Silva TC, Colaprico A, Olsen C, D'Angelo F, Bontempi G, Ceccarelli M, et al. TCGA Workflow: Analyze cancer genomics and epigenomics data using Bioconductor packages. F1000Research [Internet]. 2016 Dec 28;5:1542. Disponível em: https://f1000research.com/articles/5-1542/v2

81. Mounir M, Lucchetta M, Silva TC, Olsen C, Bontempi G, Chen X, et al. New functionalities in the TCGAbiolinks package for the study and integration of cancer data from GDC and GTEx. Wang E, editor. PLOS Comput Biol [Internet]. 2019 Mar 5;15(3):e1006701. Disponível em: https://dx.plos.org/10.1371/journal.pcbi.1006701

82. Aran D, Hu Z, Butte AJ. xCell: digitally portraying the tissue cellular heterogeneity landscape. Genome Biol [Internet]. 2017 Dec 15;18(1):220. Disponível em: https://genomebiology.biomedcentral.com/articles/10.1186/s13059-017-1349-1

83. Sturm G, Finotello F, Petitprez F, Zhang JD, Baumbach J, Fridman WH, et al. Comprehensive evaluation of transcriptome-based cell-type quantification methods for immuno-oncology. Bioinformatics. 2019;35(14):i436–45.

84. Newman AM, Liu CL, Green MR, Gentles AJ, Feng W, Xu Y, et al. Robust enumeration of cell subsets from tissue expression profiles. Nat Methods [Internet]. 2015 May 30;12(5):453–7. Disponível em: http://www.nature.com/articles/nmeth.3337

85. Gu Z, Eils R, Schlesner M. Complex heatmaps reveal patterns and correlations in multidimensional genomic data. Bioinformatics [Internet]. 2016 Sep 15;32(18):2847–9. Disponível em: https://academic.oup.com/bioinformatics/article-lookup/doi/10.1093/bioinformatics/btw313

86. Morgan M, Obenchain V, Hester J, Pagès H. SummarizedExperiment: SummarizedExperiment container. R package version 1.20.0. 2020.

87. Morgan M, Shepherd L. AnnotationHub: Client to access AnnotationHub resources. R package, version 2.22.0. 2020.

88. Love MI, Huber W, Anders S. Moderated estimation of fold change and dispersion for RNA-seq data with DESeq2. Genome Biol [Internet]. 2014 Dec 5;15(12):550. Disponível em: http://genomebiology.biomedcentral.com/articles/10.1186/s13059-014-0550-8

89. Yamaguchi KD, Ruderman DL, Croze E, Wagner TC, Velichko S, Reder AT, et al. IFN-β-regulated genes show abnormal expression in therapy-naïve relapsing–remitting MS mononuclear cells: Gene expression analysis employing all reported protein–protein interactions. J Neuroimmunol [Internet]. 2008 Mar;195(1–2):116–20. Disponível em: https://linkinghub.elsevier.com/retrieve/pii/S0165572807004456

90. Weiner 3rd J, Domaszewska T. tmod: an R package for general and multivariate enrichment analysis. PeerJ. 2016;4:1–9.

91. Therneau TM, Grambsch PM. Modeling Survival Data: Extending the Cox Model [Internet]. Technometrics. New York, NY: Springer New York; 2000. 125–201 p. (Statistics for Biology and Health; vol. 36). Disponível em: http://link.springer.com/10.1007/978-1-4757-3294-8

92. Storey J, Bass A, Dabney A, Robinson D. qvalue: Q-value estimation for false discovery rate control R package version 2.22.0. 2020.

93. Monaco G, Lee B, Xu W, Mustafah S, Hwang YY, Carré C, et al. RNA-Seq Signatures Normalized by mRNA Abundance Allow Absolute Deconvolution of Human Immune Cell Types. Cell Rep [Internet]. 2019 Feb;26(6):1627-1640.e7. Disponível em: https://linkinghub.elsevier.com/retrieve/pii/S2211124719300592

94. Tierney JF, Vogle A, Poirier J, Min IM, Finnerty B, Zarnegar R, et al. Expression of programmed death ligand 1 and 2 in adrenocortical cancer tissues: An exploratory study. Surg (United States) [Internet]. 2019 Jan;165(1):196–201. Disponível em: https://linkinghub.elsevier.com/retrieve/pii/S0039606018306184

95. Liang J, Liu Z, Pei T, Xiao Y, Zhou L, Tang Y, et al. Clinicopathological and Prognostic Characteristics of CD276 (B7-H3) Expression in Adrenocortical

Carcinoma. Dis Markers [Internet]. 2020 Jan 11;2020:1–10. Disponível em: https://www.hindawi.com/journals/dm/2020/5354825/

96. Kontos F, Michelakos T, Kurokawa T, Sadagopan A, Schwab JH, Ferrone CR, et al. B7-H3: An Attractive Target for Antibody-based Immunotherapy. Clin Cancer Res [Internet]. 2021 Mar 1;27(5):1227–35. Disponível em: http://clincancerres.aacrjournals.org/lookup/doi/10.1158/1078-0432.CCR-20-2584

97. Flem-Karlsen K, Fodstad Ø, Tan M, Nunes-Xavier CE. B7-H3 in Cancer – Beyond Immune Regulation. Trends in Cancer [Internet]. 2018 Jun;4(6):401–4. Disponível em: https://linkinghub.elsevier.com/retrieve/pii/S2405803318300888

98. Yonesaka K, Haratani K, Takamura S, Sakai H, Kato R, Takegawa N, et al. B7-H3 Negatively Modulates CTL-Mediated Cancer Immunity. Clin Cancer Res [Internet]. 2018 Jun 1;24(11):2653–64. Disponível em: http://clincancerres.aacrjournals.org/lookup/doi/10.1158/1078-0432.CCR-17-2852

99. Loos M, Hedderich DM, Friess H, Kleeff J. B7-H3 and Its Role in Antitumor Immunity. Clin Dev Immunol [Internet]. 2010;2010:1–7. Disponível em: http://www.hindawi.com/journals/jir/2010/683875/

100. Zyla J, Marczyk M, Domaszewska T, Kaufmann SHEE, Polanska J, Weiner J. Gene set enrichment for reproducible science: Comparison of CERNO and eight other algorithms. Wren J, editor. Bioinformatics [Internet]. 2019 Dec 15;35(24):5146–54. Disponível em: https://academic.oup.com/bioinformatics/article/35/24/5146/5511403

101. Subramanian A, Tamayo P, Mootha VK, Mukherjee S, Ebert BL, Gillette MA, et al. Gene set enrichment analysis: A knowledge-based approach for interpreting genome-wide expression profiles. Proc Natl Acad Sci [Internet]. 2005 Oct 25;102(43):15545–50. Disponível em: http://www.pnas.org/cgi/doi/10.1073/pnas.0506580102

102. Liberzon A, Birger C, Thorvaldsdóttir H, Ghandi M, Mesirov JP, Tamayo P. The Molecular Signatures Database Hallmark Gene Set Collection. Cell Syst [Internet]. 2015 Dec;1(6):417–25. Disponível em: https://linkinghub.elsevier.com/retrieve/pii/S2405471215002185

103. Li S, Rouphael N, Duraisingham S, Romero-Steiner S, Presnell S, Davis C, et al. Molecular signatures of antibody responses derived from a systems biology study of five human vaccines. Nat Immunol [Internet]. 2014 Feb 15;15(2):195–204. Disponível em: http://www.nature.com/articles/ni.2789

104. Wang H, Najibi AJ, Sobral MC, Seo BR, Lee JY, Wu D, et al. Biomaterial-based scaffold for in situ chemo-immunotherapy to treat poorly immunogenic tumors.

Nat Commun [Internet]. 2020 Dec 10;11(1):5696. Disponível em: http://www.nature.com/articles/s41467-020-19540-z

105. Ramilowski JA, Goldberg T, Harshbarger J, Kloppmann E, Lizio M, Satagopam VP, et al. A draft network of ligand–receptor-mediated multicellular signalling in human. Nat Commun [Internet]. 2015 Nov 24;6(1):7866. Disponível em: http://www.nature.com/articles/ncomms8866

106. Castro MAA, Wang X, Fletcher MNC, Meyer KB, Markowetz F. RedeR: R/Bioconductor package for representing modular structures, nested networks and multiple levels of hierarchical associations. Genome Biol [Internet]. 2012;13(4):R29. Disponível em: http://genomebiology.com/2012/13/4/R29

107. Hoadley KA, Yau C, Hinoue T, Wolf DM, Lazar AJ, Drill E, et al. Cell-of-Origin Patterns Dominate the Molecular Classification of 10,000 Tumors from 33 Types of Cancer. Cell [Internet]. 2018 Apr;173(2):291--304.e6. Disponível em: https://linkinghub.elsevier.com/retrieve/pii/S0092867418303027

108. Xu Y, Zhu Y, Shen Z, Sheng J, He H, Ma G, et al. Significance of heparanase-1 and vascular endothelial growth factor in adrenocortical carcinoma angiogenesis: potential for therapy. Endocrine [Internet]. 2011 Dec 25;40(3):445–51. Disponível em: http://link.springer.com/10.1007/s12020-011-9502-1

109. Pereira SS, Costa MM, Guerreiro SG, Monteiro MP, Pignatelli D. Angiogenesis and Lymphangiogenesis in the Adrenocortical Tumors. Pathol Oncol Res [Internet]. 2018 Jul 10;24(3):689–93. Disponível em: http://link.springer.com/10.1007/s12253-017-0259-6

110. Assié G, Letouzé E, Fassnacht M, Jouinot A, Luscap W, Barreau O, et al. Integrated genomic characterization of adrenocortical carcinoma. Nat Genet [Internet]. 2014 Jun 20;46(6):607–12. Disponível em: http://www.nature.com/articles/ng.2953

111. O'Sullivan C, Edgerly M, Velarde M, Wilkerson J, Venkatesan AM, Pittaluga S, et al. The VEGF Inhibitor Axitinib Has Limited Effectiveness as a Therapy for Adrenocortical Cancer. J Clin Endocrinol Metab [Internet]. 2014 Apr 1;99(4):1291–7. Disponível em: https://academic.oup.com/jcem/article/99/4/1291/2537337

112. Berruti A, Sperone P, Ferrero A, Germano A, Ardito A, Priola AM, et al. Phase II study of weekly paclitaxel and sorafenib as second/third-line therapy in patients with adrenocortical carcinoma. Eur J Endocrinol [Internet]. 2012 Mar;166(3):451–8. Disponível em: https://eje.bioscientifica.com/view/journals/eje/166/3/451.xml

113. Chen Y-L, Lin H-W, Chien C-L, Lai Y-L, Sun W-Z, Chen C-A, et al. BTLA blockade enhances Cancer therapy by inhibiting IL-6/IL-10-induced CD19high B lymphocytes. J Immunother Cancer [Internet]. 2019 Dec 21;7(1):313. Disponível em: https://jitc.bmj.com/lookup/doi/10.1186/s40425-019-0744-4

114. Pestka S, Krause CD, Sarkar D, Walter MR, Shi Y, Fisher PB. Interleukin-10 and related cytokines and receptors. Annu Rev Immunol [Internet]. 2004 Apr;22(1):929–79. Disponível em: http://www.annualreviews.org/doi/10.1146/annurev.immunol.22.012703.104622

115. Rojas K, Baliu-Piqué M, Manzano A, Saiz-Ladera C, García-Barberán V, Cimas FJ, et al. In silico transcriptomic mapping of integrins and immune activation in Basal-like and HER2+ breast cancer. Cell Oncol [Internet]. 2021 Jan 19; Disponível em: http://link.springer.com/10.1007/s13402-020-00583-9

116. Vinay DS, Kwon BS. 4-1BB signaling beyond T cells. Cell Mol Immunol [Internet]. 2011 Jul 10;8(4):281–4. Disponível em: http://www.nature.com/articles/cmi201082

117. Chester C, Sanmamed MF, Wang J, Melero I. Immunotherapy targeting 4-1BB: mechanistic rationale, clinical results, and future strategies. Blood [Internet]. 2018 Jan 4;131(1):49–57. Disponível em: https://ashpublications.org/blood/article/131/1/49/107685/Immunotherapy-targeting-41BB-mechanistic-rationale

118. Jasim S, Habra MA. Management of Adrenocortical Carcinoma. Curr Oncol Rep [Internet]. 2019 Mar 23;21(3):20. Disponível em: http://link.springer.com/10.1007/s11912-019-0773-7

119. Figueiredo BC, Stratakis CA, Sandrini R, DeLacerda L, Pianovsky MAD, Giatzakis C, et al. Comparative Genomic Hybridization Analysis of Adrenocortical Tumors of Childhood 1. J Clin Endocrinol Metab [Internet]. 1999 Mar;84(3):1116–21. Disponível em: https://academic.oup.com/jcem/article-lookup/doi/10.1210/jcem.84.3.5526

120. Kjellman, M Kallioniemi, O P Karhu, R Höög, A Farnebo, L O Auer, G Larsson, C Bäckdahl M. Genetic aberrations in adrenocortical tumors detected using comparative genomic hybridization correlate with tumor size and malignancy. Cancer Res. 1996;56:4219–23.

121. Hodi FS, O'Day SJ, McDermott DF, Weber RW, Sosman JA, Haanen JB, et al. Improved Survival with Ipilimumab in Patients with Metastatic Melanoma. N Engl J Med [Internet]. 2010 Aug 19;363(8):711–23. Disponível em: http://www.nejm.org/doi/abs/10.1056/NEJMoa1003466

122. Zancanella P, Pianovski MAD, Oliveira BH, Ferman S, Piovezan GC, Lichtvan LL, et al. Mitotane Associated With Cisplatin, Etoposide, and Doxorubicin in

Advanced Childhood Adrenocortical Carcinoma. J Pediatr Hematol Oncol [Internet]. 2006 Aug;28(8):513–24. Disponível em: https://journals.lww.com/00043426-200608000-00005

123. Muzzi JCD, Magno JM, Souza JS, Alvarenga LM, de Moura JF, Figueiredo BC, et al. Comprehensive Characterization of the Regulatory Landscape of Adrenocortical Carcinoma: Novel Transcription Factors and Targets Associated with Prognosis. Cancers (Basel) [Internet]. 2022;14(21). Disponível em: https://www.mdpi.com/2072-6694/14/21/5279

124. Gajewski TF, Corrales L, Williams J, Horton B, Sivan A, Spranger S. Cancer Immunotherapy Targets Based on Understanding the T Cell-Inflamed Versus Non-T Cell-Inflamed Tumor Microenvironment. In 2017. p. 19–31. Disponível em: http://link.springer.com/10.1007/978-3-319-67577-0_2

125. Else T, Kim AC, Sabolch A, Raymond VM, Kandathil A, Caoili EM, et al. Adrenocortical Carcinoma. Endocr Rev [Internet]. 2014 Apr 1;35(2):282–326. Disponível em: https://doi.org/10.1210/er.2013-1029

126. Baechle JJ, Hanna DN, Sekhar KR, Rathmell JC, Rathmell WK, Baregamian N. Integrative computational immunogenomic profiling of cortisol-secreting adrenocortical carcinoma. J Cell Mol Med. 2021;25(21):10061–72.

127. Wirapati P, Sotiriou C, Kunkel S, Farmer P, Pradervand S, Haibe-Kains B, et al. Meta-analysis of gene expression profiles in breast cancer: toward a unified understanding of breast cancer subtyping and prognosis signatures. Breast Cancer Res [Internet]. 2008 Aug 28;10(4):R65. Disponível em: http://breast-cancer-research.biomedcentral.com/articles/10.1186/bcr2124

128. Galon J, Costes A, Sanchez-Cabo F, Kirilovsky A, Mlecnik B, Lagorce-Pagès C, et al. Type, density, and location of immune cells within human colorectal tumors predict clinical outcome. Science [Internet]. 2006 Sep 29;313(5795):1960–4. Disponível em: http://www.ncbi.nlm.nih.gov/pubmed/17008531

129. Fassnacht M, Dekkers O, Else T, Baudin E, Berruti A, de Krijger R, et al. European Society of Endocrinology Clinical Practice Guidelines on the management of adrenocortical carcinoma in adults, in collaboration with the European Network for the Study of Adrenal Tumors. Eur J Endocrinol [Internet]. 2018;179(4):G1–46. Disponível em: http://www.ncbi.nlm.nih.gov/pubmed/30299884

130. Mete O, Asa SL, Giordano TJ, Papotti M, Sasano H, Volante M. Immunohistochemical Biomarkers of Adrenal Cortical Neoplasms. Endocr Pathol [Internet]. 2018 Jun;29(2):137–49. Disponível em: http://www.ncbi.nlm.nih.gov/pubmed/29542002

131. Castro MAAA, de Santiago I, Campbell TM, Vaughn C, Hickey TE, Ross E, et al. Regulators of genetic risk of breast cancer identified by integrative network analysis. Nat Genet [Internet]. 2016 Jan 30;48(1):12–21. Disponível em: http://www.nature.com/articles/ng.3458

132. Robertson AG, Kim J, Al-Ahmadie H, Bellmunt J, Guo G, Cherniack AD, et al. Comprehensive Molecular Characterization of Muscle-Invasive Bladder Cancer. Cell [Internet]. 2017 Oct;171(3):540-556.e25. Disponível em: https://linkinghub.elsevier.com/retrieve/pii/S0092867417310565

133. Galon J, Bruni D. Approaches to treat immune hot, altered and cold tumours with combination immunotherapies. Nat Rev Drug Discov [Internet]. 2019 Mar 4;18(3):197–218. Disponível em: http://www.nature.com/articles/s41573-018-0007-y

134. Hegde PS, Karanikas V, Evers S. The Where, the When, and the How of Immune Monitoring for Cancer Immunotherapies in the Era of Checkpoint Inhibition. Clin Cancer Res [Internet]. 2016 Apr 15;22(8):1865–74. Disponível em: https://aacrjournals.org/clincancerres/article/22/8/1865/265993/The-Where-the-When-and-the-How-of-Immune

135. Hodgson A, Pakbaz S, Mete O. A Diagnostic Approach to Adrenocortical Tumors. Surg Pathol Clin [Internet]. 2019 Dec;12(4):967–95. Disponível em: http://www.ncbi.nlm.nih.gov/pubmed/31672302

136. Kamoun A, de Reyniès A, Allory Y, Sjödahl G, Robertson AG, Seiler R, et al. A Consensus Molecular Classification of Muscle-invasive Bladder Cancer. Eur Urol [Internet]. 2020 Apr;77(4):420–33. Disponível em: https://linkinghub.elsevier.com/retrieve/pii/S0302283819306955

137. Cangiano M, Grudniewska M, Salji MJ, Nykter M, Jenster G, Urbanucci A, et al. Gene Regulation Network Analysis on Human Prostate Orthografts Highlights a Potential Role for the JMJD6 Regulon in Clinical Prostate Cancer. Cancers (Basel) [Internet]. 2021 Apr 26;13(9):2094. Disponível em: https://www.mdpi.com/2072-6694/13/9/2094

138. Liu J, Lichtenberg TM, Hoadley KA, Poisson LM, Lazar AJ, Cherniack AD, et al. An Integrated TCGA Pan-Cancer Clinical Data Resource to Drive High-Quality Survival Outcome Analytics. Cell. 2018;173(2):400--416.e11.

139. Fletcher MNCC, Castro MAAA, Wang X, De Santiago I, O'Reilly M, Chin SF, et al. Master regulators of FGFR2 signalling and breast cancer risk. Nat Commun. 2013;4(May):1–12.

140. Peto R, Peto J. Asymptotically Efficient Rank Invariant Test Procedures. J R Stat Soc Ser A [Internet]. 1972;135(2):185. Disponível em: https://www.jstor.org/stable/10.2307/2344317?origin=crossref

141. Wilkerson MD, Hayes DN. ConsensusClusterPlus: a class discovery tool with confidence assessments and item tracking. Bioinformatics [Internet]. 2010 Jun 15;26(12):1572–3. Disponível em: http://www.ncbi.nlm.nih.gov/pubmed/20427518

142. Dolgalev I. msigdbr: MSigDB Gene Sets for Multiple Organisms in a Tidy Data Format [Internet]. R package version 7.5.1. 2022. Disponível em: https://igordot.github.io/msigdbr/

143. Chagas VS, Groeneveld CS, Oliveira KG, Trefflich S, de Almeida RC, Ponder BAJ, et al. RTNduals: an R/Bioconductor package for analysis of co-regulation and inference of dual regulons. Bioinformatics. 2019;35(24):5357–8.

144. Davis S, Meltzer PS. GEOquery: a bridge between the Gene Expression Omnibus (GEO) and BioConductor. Bioinformatics [Internet]. 2007 Jul 15;23(14):1846–7. Disponível em: https://academic.oup.com/bioinformatics/article-lookup/doi/10.1093/bioinformatics/btm254

145. R Core Team. R: A language and environment for statistical computing [Internet]. Vienna: R Foundation for Statistical Computing; Disponível em: https://www.r-project.org/

146. Huber W, Carey VJ, Gentleman R, Anders S, Carlson M, Carvalho BS, et al. Orchestrating high-throughput genomic analysis with Bioconductor. Nat Methods [Internet]. 2015 Feb;12(2):115–21. Disponível em: http://www.ncbi.nlm.nih.gov/pubmed/25633503

147. Wilcoxon F. Individual Comparisons by Ranking Methods. Biometrics Bull [Internet]. 1945 Dec;1(6):80. Disponível em: https://www.jstor.org/stable/10.2307/3001968?origin=crossref

148. Lambert SA, Jolma A, Campitelli LF, Das PK, Yin Y, Albu M, et al. The Human Transcription Factors. Cell [Internet]. 2018 Feb;172(4):650–65. Disponível em: https://linkinghub.elsevier.com/retrieve/pii/S0092867418301065

149. Margolin AA, Wang K, Lim WK, Kustagi M, Nemenman I, Califano A. Reverse engineering cellular networks. Nat Protoc [Internet]. 2006 Aug 27;1(2):662–71. Disponível em: http://www.nature.com/articles/nprot.2006.106

150. Cohen J. Statistical Power Analysis for the Behavioral Sciences [Internet]. Routledge; 2013. Disponível em: https://www.taylorfrancis.com/books/9781134742707

151. Benjamini Y, Hochberg Y. Controlling the False Discovery Rate: A Practical and Powerful Approach to Multiple Testing. J R Stat Soc Ser B [Internet]. 1995 Jan 1;57(1):289–300. Disponível em: https://doi.org/10.1111/j.2517-6161.1995.tb02031.x

152. Cox BDR, Cox DR. Regression Models and Life-Tables. J R Stat Soc Ser B [Internet]. 1972 Jan;34(2):187–202. Disponível em: https://onlinelibrary.wiley.com/doi/10.1111/j.2517-6161.1972.tb00899.x

153. Groeneveld CS, Chagas VS, Jones SJMM, Robertson AG, Ponder BAJJ, Meyer KB, et al. RTNsurvival: An R/Bioconductor package for regulatory network survival analysis. Bioinformatics. 2019;35(21):4488–9.

154. Kaplan EL, Meier P. Nonparametric Estimation from Incomplete Observations. J Am Stat Assoc [Internet]. 1958 Jun;53(282):457. Disponível em: https://www.jstor.org/stable/2281868?origin=crossref

155. Mantel N. Evaluation of survival data and two new rank order statistics arising in its consideration. Cancer Chemother reports [Internet]. 1966 Mar;50(3):163–70. Disponível em: http://www.ncbi.nlm.nih.gov/pubmed/5910392

156. Pianovski MADD, Cavalli LR, Figueiredo BC, Santos SCLL, Doghman M, Ribeiro RC, et al. SF-1 overexpression in childhood adrenocortical tumours. Eur J Cancer [Internet]. 2006 May;42(8):1040–3. Disponível em: https://linkinghub.elsevier.com/retrieve/pii/S0959804906001274

157. Doghman M, Karpova T, Rodrigues GA, Arhatte M, De Moura J, Cavalli LR, et al. Increased Steroidogenic Factor-1 Dosage Triggers Adrenocortical Cell Proliferation and Cancer. Mol Endocrinol [Internet]. 2007 Dec 1;21(12):2968–87. Disponível em: https://academic.oup.com/mend/article/21/12/2968/2738393

158. Sbiera S, Schmull S, Assie G, Voelker HU, Kraus L, Beyer M, et al. High diagnostic and prognostic value of steroidogenic factor-1 expression in adrenal tumors. J Clin Endocrinol Metab. 2010;95(10):161–71.

159. Mann HB, Whitney DR. On a Test of Whether one of Two Random Variables is Stochastically Larger than the Other. Ann Math Stat [Internet]. 1947 Mar;18(1):50–60. Disponível em: http://projecteuclid.org/euclid.aoms/1177730491

160. Kruskal WH, Wallis WA. Use of Ranks in One-Criterion Variance Analysis. J Am Stat Assoc [Internet]. 1952 Dec;47(260):583–621. Disponível em: http://www.tandfonline.com/doi/abs/10.1080/01621459.1952.10483441

161. Dunn OJ. Multiple Comparisons Using Rank Sums. Technometrics [Internet]. 1964 Aug;6(3):241. Disponível em: https://www.jstor.org/stable/1266041?origin=crossref

162. Sengupta S, Harris CC. p53: traffic cop at the crossroads of DNA repair and recombination. Nat Rev Mol Cell Biol [Internet]. 2005 Jan;6(1):44–55. Disponível em: http://www.nature.com/articles/nrm1546

163. Jaber S, Toufektchan E, Lejour V, Bardot B, Toledo F. p53 downregulates the Fanconi anaemia DNA repair pathway. Nat Commun [Internet]. 2016 Apr 1;7(1):11091. Disponível em: http://www.nature.com/articles/ncomms11091

164. Kotoula V, Krikelis D, Karavasilis V, Koletsa T, Eleftheraki AG, Televantou D, et al. Expression of DNA repair and replication genes in non-small cell lung cancer (NSCLC): a role for thymidylate synthetase (TYMS). BMC Cancer [Internet]. 2012 Dec 6;12(1):342. Disponível em: http://bmccancer.biomedcentral.com/articles/10.1186/1471-2407-12-342

165. Ge Z, Leighton JS, Wang Y, Peng X, Chen Z, Chen H, et al. Integrated Genomic Analysis of the Ubiquitin Pathway across Cancer Types. Cell Rep. 2018;23(1):213-226.e3.

166. Kronfol Z, Starkman M, Schteingart DE, Singh V, Zhang Q, Hill E. Immune regulation in cushing's syndrome: Relationship to hypothalamic-pituitary-adrenal axis hormones. Psychoneuroendocrinology [Internet]. 1996 Oct;21(7):599–608. Disponível em: https://linkinghub.elsevier.com/retrieve/pii/S0306453096000212

167. Dong W, Liu X, Yang C, Wang D, Xue Y, Ruan X, et al. Glioma glycolipid metabolism: MSI2–SNORD12B–FIP1L1–ZBTB4 feedback loop as a potential treatment target. Clin Transl Med [Internet]. 2021 May 12;11(5). Disponível em: https://onlinelibrary.wiley.com/doi/10.1002/ctm2.411

168. Xiang T, He K, Wang S, Chen W, Li H. Expression of Zinc Finger and BTB Domain-Containing 4 in Colorectal Cancer and Its Clinical Significance. Cancer Manag Res [Internet]. 2020 Oct;Volume 12:9621–6. Disponível em: https://www.dovepress.com/expression-of-zinc-finger-and-btb-domain-containing-4-in-colorectal-ca-peer-reviewed-article-CMAR

169. Kim K, Chadalapaka G, Lee S-O, Yamada D, Sastre-Garau X, Defossez P-A, et al. Identification of oncogenic microRNA-17-92/ZBTB4/specificity protein axis in breast cancer. Oncogene [Internet]. 2012 Feb 23;31(8):1034–44. Disponível em: https://www.nature.com/articles/onc2011296

170. Yu Y, Shang R, Chen Y, Li J, Liang Z, Hu J, et al. Tumor suppressive ZBTB4 inhibits cell growth by regulating cell cycle progression and apoptosis in Ewing sarcoma. Biomed Pharmacother [Internet]. 2018 Apr;100(December 2017):108–15. Disponível em: https://linkinghub.elsevier.com/retrieve/pii/S0753332217366210

171. Jefferies WM. Cortisol and immunity. Med Hypotheses [Internet]. 1991 Mar;34(3):198–208. Disponível em: https://linkinghub.elsevier.com/retrieve/pii/030698779190212H

172. Howman E V., Fowler KJ, Newson AJ, Redward S, MacDonald AC, Kalitsis P, et al. Early disruption of centromeric chromatin organization in centromere protein A (Cenpa) null mice. Proc Natl Acad Sci [Internet]. 2000 Feb;97(3):1148–53. Disponível em: https://pnas.org/doi/full/10.1073/pnas.97.3.1148

173. Han J, Xie R, Yang Y, Chen D, Liu L, Wu J, et al. CENPA is one of the potential key genes associated with the proliferation and prognosis of ovarian cancer based on integrated bioinformatics analysis and regulated by MYBL2. Transl Cancer Res. 2021;10(9):4076–86.

174. Saha AK, Contreras-Galindo R, Niknafs YS, Iyer M, Qin T, Padmanabhan K, et al. The role of the histone H3 variant CENPA in prostate cancer. J Biol Chem [Internet]. 2020 Jun 19;295(25):8537–49. Disponível em: http://dx.doi.org/10.1074/jbc.RA119.010080

175. Liang YC, Su Q, Liu YJ, Xiao H, Yin HZ. Centromere Protein A (CENPA) Regulates Metabolic Reprogramming in the Colon Cancer Cells by Transcriptionally Activating Karyopherin Subunit Alpha 2 (KPNA2). Am J Pathol. 2021;191(12):2117–32.

176. Zhou H, Bian T, Qian L, Zhao C, Zhang W, Zheng M, et al. Prognostic model of lung adenocarcinoma constructed by the CENPA complex genes is closely related to immune infiltration. Pathol Res Pract [Internet]. 2021;228:153680. Disponível em: https://doi.org/10.1016/j.prp.2021.153680

177. Wang Q, Xu J, Xiong Z, Xu T, Liu J, Liu Y, et al. CENPA promotes clear cell renal cell carcinoma progression and metastasis via Wnt/β-catenin signaling pathway. J Transl Med [Internet]. 2021;19(1):1–17. Disponível em: https://doi.org/10.1186/s12967-021-03087-8

178. Kim KH, Chadalapaka G, Pathi SS, Jin U-HH, Lee J-SS, Park Y-YY, et al. Induction of the Transcriptional Repressor ZBTB4 in Prostate Cancer Cells by Drug-Induced Targeting of MicroRNA-17-92/106b-25 Clusters. Mol Cancer Ther [Internet]. 2012 Sep 1;11(9):1852–62. Disponível em: https://aacrjournals.org/mct/article/11/9/1852/91424/Induction-of-the-Transcriptional-Repressor-ZBTB4

179. Su X, Su J, He H, Zhan Y, Liu H. Hsa_circ_0070269 inhibits hepatocellular carcinoma progression through modulating miR-182/NPTX1 axis. Biomed Pharmacother [Internet]. 2019 Dec;120:109497. Disponível em: https://linkinghub.elsevier.com/retrieve/pii/S0753332219339095

180. Ardolino L, Hansen A, Ackland S, Joshua A. Advanced Adrenocortical Carcinoma (ACC): a Review with Focus on Second-Line Therapies. Horm

Cancer [Internet]. 2020 Aug 17;11(3–4):155–69. Disponível em: https://link.springer.com/10.1007/s12672-020-00385-3

181. Wortmann S, Quinkler M, Ritter C, Kroiss M, Johanssen S, Hahner S, et al. Bevacizumab plus capecitabine as a salvage therapy in advanced adrenocortical carcinoma. Eur J Endocrinol [Internet]. 2010 Feb;162(2):349–56. Disponível em: https://eje.bioscientifica.com/view/journals/eje/162/2/349.xml

182. Mathias C, Muzzi JCD, Antunes BB, Gradia DF, Castro MAA, Carvalho de Oliveira J. Unraveling Immune-Related lncRNAs in Breast Cancer Molecular Subtypes. Front Oncol [Internet]. 2021 May 31;11(May):1–16. Disponível em: https://www.frontiersin.org/articles/10.3389/fonc.2021.692170/full

183. Perou CM, Sùrlie T, Eisen MB, Rijn M Van De, Jeffrey SS, Rees CA, et al. Molecular portraits of human breast tumours. letters to nature 748. Nature [Internet]. 2000;533(May):747–52. Disponível em: www.stanford.edu/molecularportraits/

184. Prat A, Guo H, Ganesan P, Parker JS, Gao M, Moulder S, et al. Phenotypic and molecular characterization of the claudin-low intrinsic subtype of breast cancer. Breast Cancer Res [Internet]. 2010;12(5):68–86. Disponível em: http://breast-cancer-research.com/content/12/5/R68%0ARESEARCH

185. Sørlie T, Perou CM, Tibshirani R, Aas T, Geisler S, Johnsen H, et al. Gene expression patterns of breast carcinomas distinguish tumor subclasses with clinical implications. Proc Natl Acad Sci U S A. 2001;98(19):10869–74.

186. Dai X, Li T, Bai Z, Yang Y, Liu X, Zhan J, et al. Breast cancer intrinsic subtype classification, clinical use and future trends. Am J Cancer Res. 2015;5(10):2929–43.

187. Jiang X, Zhang G, Wu J, Lin S, Liu Y, Ma Y, et al. Long Noncoding RNA Serve as a Potential Predictive Biomarker for Breast Cancer: A Meta-Analysis. Biomed Res Int. 2020;2020.

188. Volovat SR, Volovat C, Hordila I, Hordila DA, Mirestean CC, Miron OT, et al. MiRNA and LncRNA as Potential Biomarkers in Triple-Negative Breast Cancer: A Review. Front Oncol. 2020;10(November):1–15.

189. Durinck S, Moreau Y, Kasprzyk A, Davis S, De Moor B, Brazma A, et al. BioMart and Bioconductor: A powerful link between biological databases and microarray data analysis. Bioinformatics. 2005;21(16):3439–40.

190. Best DJ, Roberts DE. Algorithm AS 89: The Upper Tail Probabilities of Spearman's Rho. Appl Stat [Internet]. 1975;24(3):377. Disponível em: https://www.jstor.org/stable/2347111?origin=crossref

191. Bolar K. Stat: Interactive Document for Working With Basic Statistical Analysis [Internet]. 2019. Disponível em: https://cran.r-project.org/package=STAT.

192. Therneau T. A package for survival analysis in R. R package version 3.2-7 [Internet]. 2020. Disponível em: https://cran.r-project.org/package=survival

193. Korotkevich G, Sukhov V, Sergushichev A. Fast gene set enrichment analysis. bioRxiv [Internet]. 2019; Disponível em: https://www.biorxiv.org/content/early/2019/10/22/060012

194. Loi S, Sirtaine N, Piette F, Salgado R, Viale G, Van Eenoo F, et al. Prognostic and Predictive Value of Tumor-Infiltrating Lymphocytes in a Phase III Randomized Adjuvant Breast Cancer Trial in Node-Positive Breast Cancer Comparing the Addition of Docetaxel to Doxorubicin With Doxorubicin-Based Chemotherapy: BIG 02-98. J Clin Oncol [Internet]. 2013 Mar 1;31(7):860–7. Disponível em: https://ascopubs.org/doi/10.1200/JCO.2011.41.0902

195. Ma B, Liao T, Wen D, Dong C, Zhou L, Yang S, et al. Long intergenic non-coding RNA 271 is predictive of a poorer prognosis of papillary thyroid cancer. Sci Rep [Internet]. 2016 Dec 23;6(1):36973. Disponível em: http://www.nature.com/articles/srep36973

196. Buishand FO, Liu-Chittenden Y, Fan Y, Tirosh A, Gara SK, Patel D, et al. Adrenocortical tumors have a distinct, long, non-coding RNA expression profile and LINC00271 is downregulated in malignancy. Surg (United States) [Internet]. 2020;167(1):224–32. Disponível em: http://dx.doi.org/10.1016/j.surg.2019.04.067

197. Fu X, Zhang L, Dan L, Wang K, Xu Y. LncRNA EWSAT1 promotes ovarian cancer progression through targeting miR-330-5p expression. Am J Transl Res [Internet]. 2017;9(9):4094–103. Disponível em: http://www.ncbi.nlm.nih.gov/pubmed/28979684

198. Zhou Q, Xie Y, Wang L, Xu T, Gao Y. LncRNA EWSAT1 upregulates CPEB4 via miR-330-5p to promote cervical cancer development. Mol Cell Biochem [Internet]. 2020 Aug 17;471(1–2):177–88. Disponível em: https://link.springer.com/10.1007/s11010-020-03778-8

199. Liu J, Huang S, Liao X, Chen Z, Li L, Yu L, et al. LncRNA EWSAT1 Promotes Colorectal Cancer Progression Through Sponging miR-326 to Modulate FBXL20 Expression. Onco Targets Ther [Internet]. 2021 Jan;Volume 14:367–78. Disponível em: https://www.dovepress.com/lncrna-ewsat1-promotes-colorectal-cancer-progression-through-sponging--peer-reviewed-article-OTT

200. Xu D, Dong P, Xiong Y, Chen R, Konno Y, Ihira K, et al. PD-L1 Is a Tumor Suppressor in Aggressive Endometrial Cancer Cells and Its Expression Is Regulated by miR-216a and lncRNA MEG3. Front Cell Dev Biol [Internet]. 2020

Dec 9;8. Disponível em: https://www.frontiersin.org/articles/10.3389/fcell.2020.598205/full

201. Ghafouri-Fard S, Taheri M. Maternally expressed gene 3 (MEG3): A tumor suppressor long non coding RNA. Biomed Pharmacother [Internet]. 2019 Oct;118:109129. Disponível em: https://linkinghub.elsevier.com/retrieve/pii/S0753332219321602

202. Al-Rugeebah A, Alanazi M, Parine NR. MEG3: an Oncogenic Long Non-coding RNA in Different Cancers. Pathol Oncol Res [Internet]. 2019 Jul 21;25(3):859–74. Disponível em: http://link.springer.com/10.1007/s12253-019-00614-3

203. Zhang LH, Li LH, Zhang PF, Cai YF, Hua D. LINC00957 Acted as Prognostic Marker Was Associated With Fluorouracil Resistance in Human Colorectal Cancer. Front Oncol [Internet]. 2019 Aug 21;9. Disponível em: https://www.frontiersin.org/article/10.3389/fonc.2019.00776/full

204. Zhang M, Liu Y, Kong D. Identifying biomolecules and constructing a prognostic risk prediction model for recurrence in osteosarcoma. J Bone Oncol [Internet]. 2021 Feb;26:100331. Disponível em: https://linkinghub.elsevier.com/retrieve/pii/S2212137420300865

205. Lv Y, Wei W, Huang Z, Chen Z, Fang Y, Pan L, et al. Long non-coding RNA expression profile can predict early recurrence in hepatocellular carcinoma after curative resection. Hepatol Res [Internet]. 2018 Dec;48(13):1140–8. Disponível em: https://onlinelibrary.wiley.com/doi/10.1111/hepr.13220

206. Zhang Y-P, Cheng Y-B, Li S, Zhao N, Zhu Z-H. An epithelial-mesenchymal transition-related long non-coding RNA signature to predict overall survival and immune microenvironment in kidney renal clear cell carcinoma. Bioengineered [Internet]. 2021 Jan 1;12(1):555–64. Disponível em: https://www.tandfonline.com/doi/full/10.1080/21655979.2021.1880718

207. Shien T, Iwata H. Adjuvant and neoadjuvant therapy for breast cancer. Jpn J Clin Oncol [Internet]. 2020 Mar 9;50(3):225–9. Disponível em: https://academic.oup.com/jjco/article/50/3/225/5707554

208. Li H, Wang M, Zhou H, Lu S, Zhang B. Long Noncoding RNA EBLN3P Promotes the Progression of Liver Cancer via Alteration of microRNA-144-3p/DOCK4 Signal. Cancer Manag Res [Internet]. 2020 Sep;Volume 12:9339–49. Disponível em: https://www.dovepress.com/long-noncoding-rna-ebln3p-promotes-the-progression-of-liver-cancer-via-peer-reviewed-article-CMAR

209. Dai S, Li N, Zhou M, Yuan Y, Yue D, Li T, et al. LncRNA EBLN3P promotes the progression of osteosarcoma through modifying the miR-224-5p/Rab10

signaling axis. Sci Rep [Internet]. 2021 Jan 21;11(1):1992. Disponível em: https://www.nature.com/articles/s41598-021-81641-6

210. Zarzynska JM. Two Faces of TGF-Beta1 in Breast Cancer. Mediators Inflamm [Internet]. 2014;2014:1–16. Disponível em: http://www.hindawi.com/journals/mi/2014/141747/

211. De Angelis C, Fu X, Cataldo ML, Nardone A, Pereira R, Veeraraghavan J, et al. Activation of the IFN Signaling Pathway is Associated with Resistance to CDK4/6 Inhibitors and Immune Checkpoint Activation in ER-Positive Breast Cancer. Clin Cancer Res [Internet]. 2021 Sep 1;27(17):4870–82. Disponível em: https://aacrjournals.org/clincancerres/article/27/17/4870/671633/Activation-of-the-IFN-Signaling-Pathway-is

212. Ju Q, Zhao Y, Ma S, Li X, Zhang H, Zhang S, et al. Genome-wide analysis of prognostic-related lncRNAs, miRNAs and mRNAs forming a competing endogenous RNA network in lung squamous cell carcinoma. J Cancer Res Clin Oncol [Internet]. 2020 Jul 30;146(7):1711–23. Disponível em: https://link.springer.com/10.1007/s00432-020-03224-8

213. Guo X, Zhang M, Li Q, Zhao J, Wang B, Wang J, et al. Evaluation of Genetic Variants in MIR3142HG in Susceptibility to and Prognosis of Glioma. Am J Clin Oncol [Internet]. 2020 Jan;43(1):1–8. Disponível em: https://journals.lww.com/10.1097/COC.0000000000000587

214. Hadjicharalambous MR, Roux BT, Feghali-Bostwick CA, Murray LA, Clarke DL, Lindsay MA. Long Non-coding RNAs Are Central Regulators of the IL-1β-Induced Inflammatory Response in Normal and Idiopathic Pulmonary Lung Fibroblasts. Front Immunol [Internet]. 2018 Dec 11;9. Disponível em: https://www.frontiersin.org/article/10.3389/fimmu.2018.02906/full

215. Ma W, Zhao F, Yu X, Guan S, Suo H, Tao Z, et al. Immune-related lncRNAs as predictors of survival in breast cancer: a prognostic signature. J Transl Med [Internet]. 2020 Dec 23;18(1):442. Disponível em: https://doi.org/10.1186/s12967-020-02522-6

216. Chen Q, Hu L, Huang D, Chen K, Qiu X, Qiu B. Six-lncRNA Immune Prognostic Signature for Cervical Cancer. Front Genet [Internet]. 2020 Oct 14;11. Disponível em: https://www.frontiersin.org/article/10.3389/fgene.2020.533628/full

217. He Y, Wang X. Identification of molecular features correlating with tumor immunity in gastric cancer by multi-omics data analysis. Ann Transl Med [Internet]. 2020 Sep;8(17):1050–1050. Disponível em: http://atm.amegroups.com/article/view/51769/html

218. Tsang JYS, Tse GM. Molecular Classification of Breast Cancer. Adv Anat Pathol [Internet]. 2020 Jan;27(1):27–35. Disponível em: https://journals.lww.com/10.1097/PAP.0000000000000232

219. Baker K, Lachapelle J, Zlobec I, Bismar TA, Terracciano L, Foulkes WD. Prognostic significance of CD8+ T lymphocytes in breast cancer depends upon both oestrogen receptor status and histological grade. Histopathology [Internet]. 2011 Jun;no-no. Disponível em: https://onlinelibrary.wiley.com/doi/10.1111/j.1365-2559.2011.03846.x

220. Oshi M, Asaoka M, Tokumaru Y, Yan L, Matsuyama R, Ishikawa T, et al. CD8 T Cell Score as a Prognostic Biomarker for Triple Negative Breast Cancer. Int J Mol Sci [Internet]. 2020 Sep 22;21(18):6968. Disponível em: https://www.mdpi.com/1422-0067/21/18/6968

221. Li X, Gruosso T, Zuo D, Omeroglu A, Meterissian S, Guiot M-C, et al. Infiltration of CD8 + T cells into tumor cell clusters in triple-negative breast cancer. Proc Natl Acad Sci [Internet]. 2019 Feb 26;116(9):3678–87. Disponível em: https://pnas.org/doi/full/10.1073/pnas.1817652116

222. Heimes A-S, Härtner F, Almstedt K, Krajnak S, Lebrecht A, Battista MJ, et al. Prognostic Significance of Interferon-γ and Its Signaling Pathway in Early Breast Cancer Depends on the Molecular Subtypes. Int J Mol Sci [Internet]. 2020 Sep 29;21(19):7178. Disponível em: https://www.mdpi.com/1422-0067/21/19/7178

223. Schmid P, Adams S, Rugo HS, Schneeweiss A, Barrios CH, Iwata H, et al. Atezolizumab and Nab-Paclitaxel in Advanced Triple-Negative Breast Cancer. N Engl J Med [Internet]. 2018 Nov 29;379(22):2108–21. Disponível em: http://www.nejm.org/doi/10.1056/NEJMoa1809615

224. Yang B, Chou J, Tao Y, Wu D, Wu X, Li X, et al. An assessment of prognostic immunity markers in breast cancer. npj Breast Cancer [Internet]. 2018 Dec 29;4(1):35. Disponível em: http://www.nature.com/articles/s41523-018-0088-0

225. Zhang X, Zhang J, Zhao W, Dong X, Xin P, Liu X, et al. Long non-coding RNA LINC02446 suppresses the proliferation and metastasis of bladder cancer cells by binding with EIF3G and regulating the mTOR signalling pathway. Cancer Gene Ther [Internet]. 2021 Dec 2;28(12):1376–89. Disponível em: http://www.nature.com/articles/s41417-020-00285-2

226. Tong H, Li T, Gao S, Yin H, Cao H, He W. An epithelial–mesenchymal transition-related long noncoding RNA signature correlates with the prognosis and progression in patients with bladder cancer. Biosci Rep [Internet]. 2021 Jan 29;41(1). Disponível em:

https://portlandpress.com/bioscirep/article/41/1/BSR20203944/227198/An-epithelial-mesenchymal-transition-related-long

227. Meng C, Zhou J-Q, Liao Y-S. Autophagy-related long non-coding RNA signature for ovarian cancer. J Int Med Res [Internet]. 2020 Nov 12;48(11):030006052097076. Disponível em: http://journals.sagepub.com/doi/10.1177/0300060520970761

228. Chen P, Gao Y, Ouyang S, Wei L, Zhou M, You H, et al. A Prognostic Model Based on Immune-Related Long Non-Coding RNAs for Patients With Cervical Cancer. Front Pharmacol [Internet]. 2020 Nov 30;11. Disponível em: https://www.frontiersin.org/articles/10.3389/fphar.2020.585255/full

229. Segovia-Mendoza M, Morales-Montor J. Immune tumor microenvironment in breast cancer and the participation of estrogens and its receptors into cancer physiopathology. Front Immunol. 2019;10(MAR):1–16.

230. Gao M, Wang X, Han D, Lu E, Zhang J, Zhang C, et al. A Six-lncRNA Signature for Immunophenotype Prediction of Glioblastoma Multiforme. Front Genet [Internet]. 2021 Jan 13;11. Disponível em: https://www.frontiersin.org/articles/10.3389/fgene.2020.604655/full

231. Zhong Z, Hong M, Chen X, Xi Y, Xu Y, Kong D, et al. Transcriptome analysis reveals the link between lncRNA-mRNA co-expression network and tumor immune microenvironment and overall survival in head and neck squamous cell carcinoma. BMC Med Genomics [Internet]. 2020 Dec 30;13(1):57. Disponível em: https://bmcmedgenomics.biomedcentral.com/articles/10.1186/s12920-020-0707-0

232. Chen G-R, Sun W, Zheng K, Zhu W. LINC01857 promotes the development of gastric cancer by regulating microRNA-200b. Eur Rev Med Pharmacol Sci [Internet]. 2020 Apr;24(7):3648–56. Disponível em: http://www.ncbi.nlm.nih.gov/pubmed/32329840

233. Hombach S, Kretz M. Non-coding RNAs: Classification, Biology and Functioning. In 2016. p. 3–17. Disponível em: http://link.springer.com/10.1007/978-3-319-42059-2_1

234. Clark MB, Mercer TR, Bussotti G, Leonardi T, Haynes KR, Crawford J, et al. Quantitative gene profiling of long noncoding RNAs with targeted RNA sequencing. Nat Methods. 2015;12(4):339–42.

235. Chan JJ, Tay Y. Noncoding RNA: RNA regulatory networks in cancer. Int J Mol Sci. 2018;19(5).

236. Bolha L, Ravnik-Glavač M, Glavač D. Long Noncoding RNAs as Biomarkers in Cancer. Dis Markers. 2017;2017.

237. Hu G, Liu N, Wang H, Wang Y, Guo Z. LncRNA LINC01857 promotes growth, migration, and invasion of glioma by modulating miR-1281/TRIM65 axis. J Cell Physiol [Internet]. 2019 Dec 2;234(12):22009–16. Disponível em: https://onlinelibrary.wiley.com/doi/10.1002/jcp.28763

238. Xiong Y, Gu Y, Wang F, Li L, Zhu M, Wang N, et al. LINC01857 as an oncogene regulates CREB1 activation by interacting with CREBBP in breast cancer. J Cell Physiol [Internet]. 2019 Aug 9;234(8):14031–9. Disponível em: https://onlinelibrary.wiley.com/doi/10.1002/jcp.28090

239. Li Q, Li B, Lu C-L, Wang J-Y, Gao M, Gao W. LncRNA LINC01857 promotes cell growth and diminishes apoptosis via PI3K/mTOR pathway and EMT process by regulating miR-141-3p/MAP4K4 axis in diffuse large B-cell lymphoma. Cancer Gene Ther [Internet]. 2021 Sep 12;28(9):1046–57. Disponível em: https://www.nature.com/articles/s41417-020-00267-4

240. Wang Q, Yang Y, Fu X, Wang Z, Liu Y, Li M, et al. Long noncoding RNA XXYLT1-AS2 regulates proliferation and adhesion by targeting the RNA binding protein FUS in HUVEC. Atherosclerosis [Internet]. 2020 Apr;298:58–69. Disponível em: https://linkinghub.elsevier.com/retrieve/pii/S002191502030109X

APÊNDICE 1 - RESUMO DE ATIVIDADES REALIZADAS

Em paralelo, as análises realizadas originaram um trabalho de conclusão de curso e duas apresentações em eventos. Alguns dos fluxos de trabalhos desenvolvidos ao longo desse projeto para CCA puderam ser aproveitados para outros tumores, originando estudos que estão em andamento para Neuroblastoma, além de um artigo em tumor de mama intitulado "*Unraveling Immune-Related lncRNAs in Breast Cancer Molecular Subtypes*" publicado na revista *Frontiers in Oncology* (Fator de Impacto = 5.738). Essas e outras atividades realizadas serão descritas abaixo.

Artigos publicados

I. *Adrenocortical Carcinoma Steroid Profiles: In Silico Pan-Cancer Analysis of TCGA Data Uncovers Immunotherapy Targets for Potential Improved Outcomes* (*Frontiers in Endocrinology*, 2021) (60)

Nesse artigo, como primeiro autor, participei da idealização do estudo junto ao prof. Dr. Bonald Figueiredo e à profª Drª Juliana de Moura, selecionei as metodologias sob orientação do prof. Dr. Mauro Castro, executei todas as análises, resultados e figuras, finalizando com a escrita do artigo e resposta aos revisores junto ao prof. Dr. Bonald Figueiredo.

II. *Unraveling Immune-Related lncRNAs in Breast Cancer Molecular Subtypes* (*Frontiers in Oncology*, 2021) (66)

Nesse estudo idealizado pela Drª Carolina Mathias, pude dividir a primeira autoria com ela. Aqui fui responsável por executar todas as análises, produzir os gráficos e participei da interpretação dos resultados, com foco imunológico. Fui responsável pela escrita dos métodos e resultados desse artigo e auxiliei nas demais etapas.

III. *Comprehensive characterization of the regulatory landscape of Adrenocortical Carcinoma: novel transcription factors and targets associated with prognosis* (*Cancers*, 2022) (61)

Fui o responsável pela idealização do estudo e participei da seleção dos métodos junto ao prof. Dr. Mauro Castro. Realizei todas as análises, figuras e gráficos. Participei na interpretação e apresentação dos resultados e fiz a escrita do artigo e resposta aos revisores junto aos demais autores.

Outras produções e trabalhos

I. Análise da expressão do Receptor de Melanocortina 2 (*MC2R*) em CCA (concluído, 2021)

Nesse projeto avaliamos a expressão de *MC2R* em pacientes de CCA e demonstramos sua relação com os perfis esteroidais e consequente associação com o aumento de produção de esteroides e supressão imunológica. Os resultados desse projeto foram defendidos pela aluna de medicina Bruna Mayumi Wagatuma Bottolo em seu trabalho de conclusão de curso da UFPR (2021). Fui responsável pela orientação desse trabalho e execução das análises.

II. Análise pan-cancer da expressão de genes relacionados à hipóxia dentro dos subtipos imunológicos (concluído, 2022)

A relação entre a hipóxia e a resposta imunológica em tumores tem sido objeto de estudos recentes. Nesse projeto, buscamos avaliar como os genes que participam de vias curadas em Hipóxia estavam diferencialmente expressos nos subtipos imunológicos nas quase 10.000 amostras de tumores sólidos diversos do TCGA. Os resultados desse trabalho foram defendidos pela aluna Bruna Borba Antunes em sua dissertação de Mestrado em Genética na UFPR (2022) e estão em submissão na revista Journal of Biomedical Science. Fui responsável pela execução das análises, produção dos gráficos e discussão dos métodos, apresentação e interpretação dos resultados.

III. Análise de marcadores de angiogênese em CCA (concluído, 2021)

Nesse estudo, buscamos avaliar como as vias e marcadores associados a angiogênese se relacionavam com o perfil esteroidal em CCA e como se diferenciavam em amostras de carcinoma, adenoma ou normais de córtex adrenal. Fui responsável pelas análises, produção de gráficos e escolha das metodologias. Os resultados apontaram que não havia diferença significativa nas vias de angiogênese entre as amostras tumorais e benignas, por esse motivo não foram publicados. Os resultados foram entregues ao Prof. Dr. Bonald Figueiredo.

IV. Análise regulatória e imunológica de neuroblastoma (em andamento)

Nesse projeto, pretendemos utilizar os pipelines desenvolvidos e apresentados em meu doutorado para o neuroblastoma em busca de compreender os mecanismos associados e regulons relacionados à resposta imunológica e sobrevida. Estou auxiliando na escolha das metodologias e interpretação dos resultados.

V. Avaliação de repertório imunológico adaptativo em carcinoma de córtex adrenal e neuroblastoma (em andamento)

A análise do repertório imunológico tem trazido novas perspectivas na compreensão de como o sistema imunológico reconhece as células tumorais e dos mecanismos de ativação ou supressão da atividade de células efetoras. Nesse projeto, avaliaremos como a diversidade e riqueza de receptores de células B e de células T se associam aos perfis moleculares e resposta imunológica de pacientes de CCA e neuroblastoma. Estou auxiliando na escolha dos métodos e interpretação dos resultados.

VI. Sequenciamento e análise de amostras de tumor pediátrico de CCA e neuroblastoma (em andamento)

50 amostras de CCA e neuroblastoma pediátricos obtidas pelo Instituto de Pesquisa Pelé Pequeno Príncipe serão sequenciadas por terceiros para posterior análise de transcriptoma e de repertório imunológico por parte de nosso grupo. Estou participando no processo de seleção de métodos de sequenciamento para adequação às análises subsequentes.

Trabalhados apresentados em congresso

I. MATHIAS, C. ; MUZZI, J. C. D. ; ANTUNES, B. B. ; GRADIA, D. F. ; CASTRO, M. A. A. ; OLIVEIRA, J. C. Exploring immune related lncRNAs in breast cancer molecular subtypes. (Noncoding RNA World: From Mechanism to Therapy, 2021).

II. MUZZI, J.C.D.; MAGNO, J. M. ; CARDOSO, M. A. ; DE MOURA, J. ; CASTRO, M. A. A. ; FIGUEIREDO, B. C. Steroid profiles distinguish the immune response in adrenocortical carcinoma and unveil a new strategy for the patients

immunotherapy selection criterion. (XLV Annual Meeting of the Brazilian Society of Immunology, 2021)

Orientação de trabalho de conclusão de curso

I. BRUNA MAYUMI WAGATUMA BOTTOLO. ANÁLISE DA EXPRESSÃO DO RECEPTOR DE MELANOCORTINA 2 (MC2R) EM CARCINOMA DE CÓRTEX DA ADRENAL. 2021. Trabalho de Conclusão de Curso. (Graduação em Medicina) - UFPR.

Cursos e aulas ministrados/monitoria

I. Monitor no mini-curso de Introdução à Linguagem R. Evento da Pós-Graduação em Bioinformática – UFPR. 2020 (4h)

II. Ministrante no Curso de Introdução à Programação em R. III Escola Paranaense de Bioinformática. 2022 (16h)

III. Aula ministrada de Imuno-oncologia para Graduação em Odontologia da UFPR. 2022 (2h)

IV. Aula ministrada de Imunologia e Câncer para Graduação em Enfermagem da UFPR. 2022 (2h)

Formação complementar

I. HMX Pro Immunology – Immuno-oncology. Harvard Medical School 2022 (90h)

II. 6.431x: Probability - The Science of Uncertainty and Data. Massachusetts Institute of Technology (MITx) 2022 (90h)

III. Machine Learning with Python. Massachusetts Institute of Technology (MITx) 2022 (90h)

IV. CS50 - Introduction to Computer Science. Harvard University 2021 (90h)

V. Tópicos em Dinâmica e Docking Molecular. Universidade de São Paulo (USP) 2021 (60h)

VI. Curso de curta duração em Genômica: Introdução à montagem e anotação de genomas. UFPR 2021 (3h)

VII. Curso de curta duração em Imunohistoquímica: Princípios Básicos. Nova Analítica Importação e Exportação Ltda 2021 (2h)

VIII. Curso de curta duração em Análise Espacial como Ferramenta para Estudos Ambientais Aplicado na Parasitologia. UFPR 2021 (4h)

IX. Curso de curta duração em Quantifying Live T Cell Action Dynamics Using Holotomography and Computer Vision. Nova Analítica 2021 (1h)

X. Curso de curta duração em Explorando os Reursos do NCBI e Galaxy para o Desenvolvimento de Pesquisas. UFPR 2021 (4h)

XI. Fundamentals of Statistics. Massachusetts Institute of Technology (MITx) 2022 (90h – em andamento).

Participação em Eventos, Congressos, Exposições e Feiras

I. X Fórum de Metodologias Ativas de Ensino-Aprendizagem na Formação em Saúde e I Seminário Brasileiro de Curricularização da Extensão. 2021.

II. XV Symposium of Biosciences and Biotechnology Applied to Pharmacy. 2020.

III. 6th Brazilian Student Council Symposium: Omics and Data Science. 2021

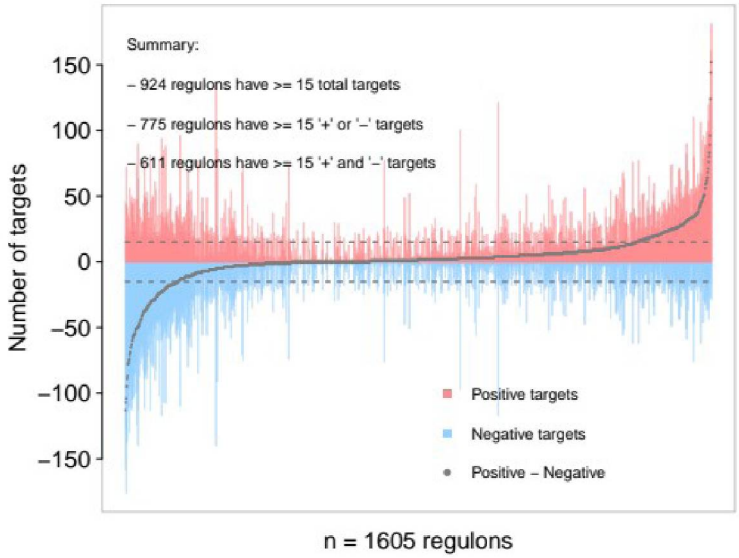
IV. A escrita científica de artigos de alto impacto. RSG Brazil. 2021

V. Liga Brasileira de Bioinformática - 2ª edição. 1ª fase e 2ª fase (17º lugar). 2021

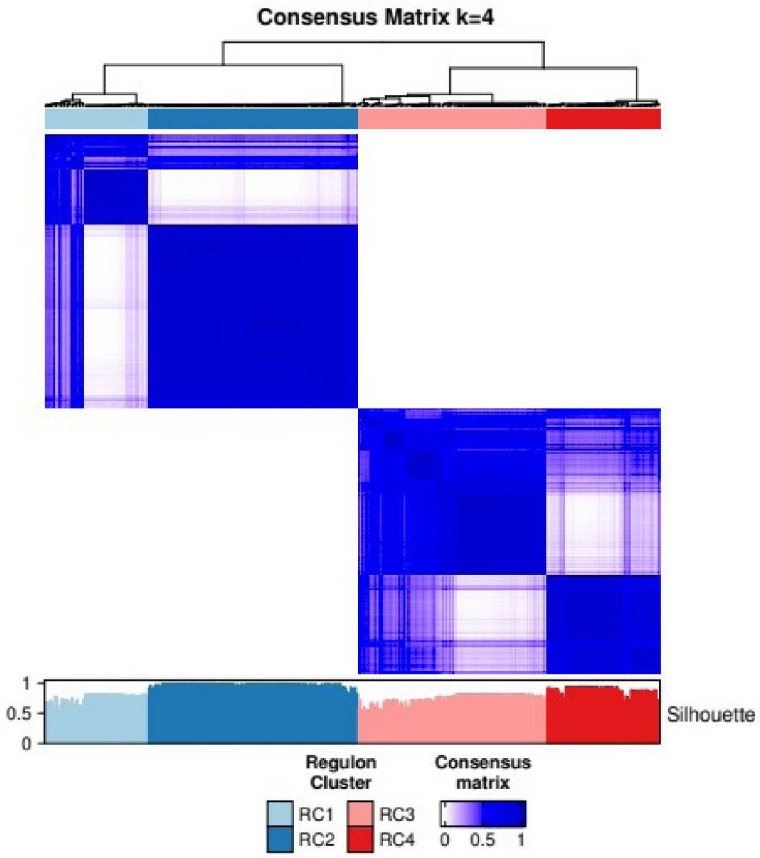
VI. SIG Machine Learning in Bioinformatics. 2021

VII. XLV Annual Meeting of the Brazilian Society of Immunology. 2021

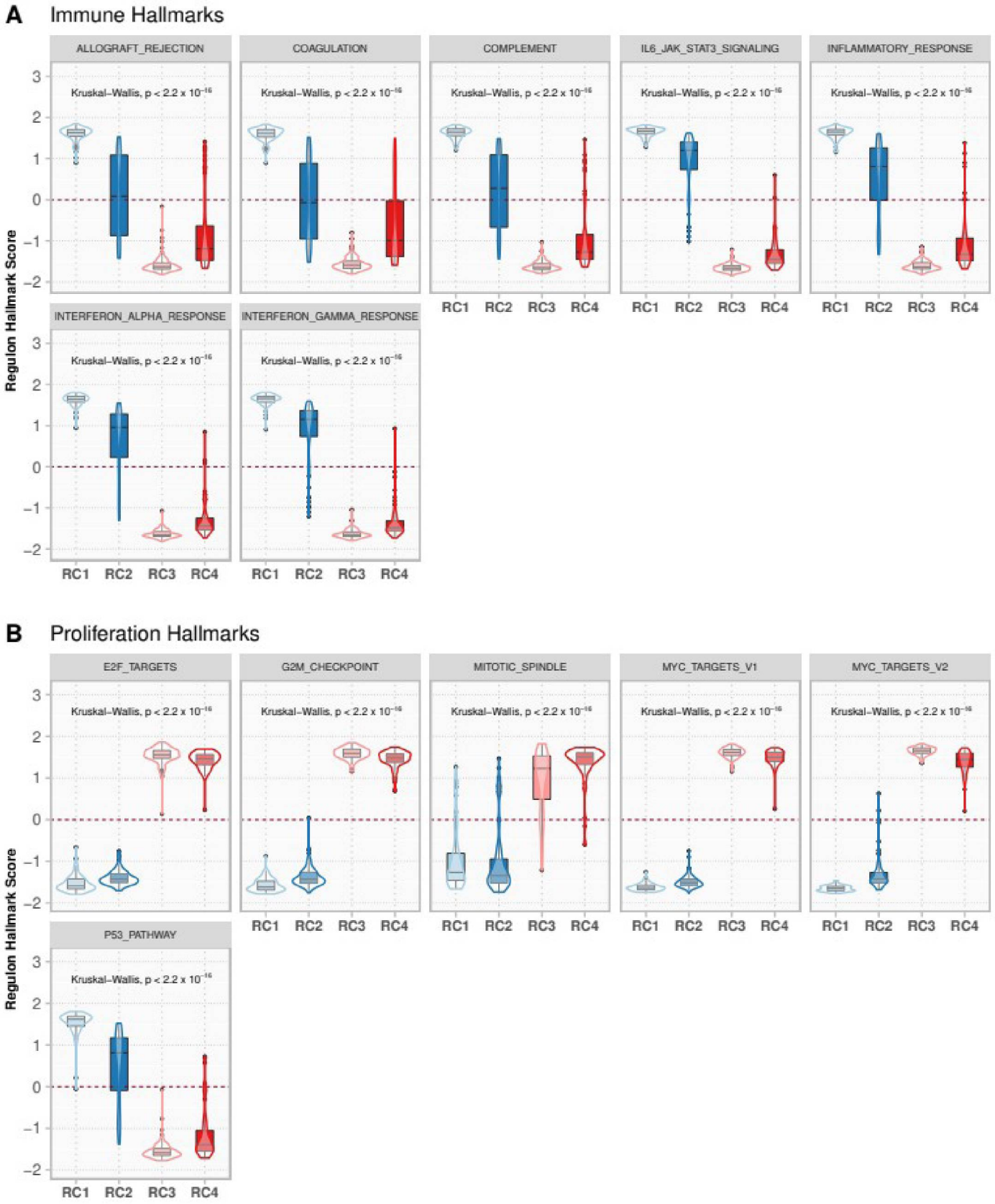
APÊNDICE 2 – MATERIAL SUPLEMENTAR PARA A COMPREHENSIVE CHARACTERIZATION OF THE REGULATORY LANDSCAPE OF ADRENOCORTICAL CARCINOMA: NOVEL TRANSCRIPTION FACTORS AND TARGETS ASSOCIATED WITH PROGNOSIS

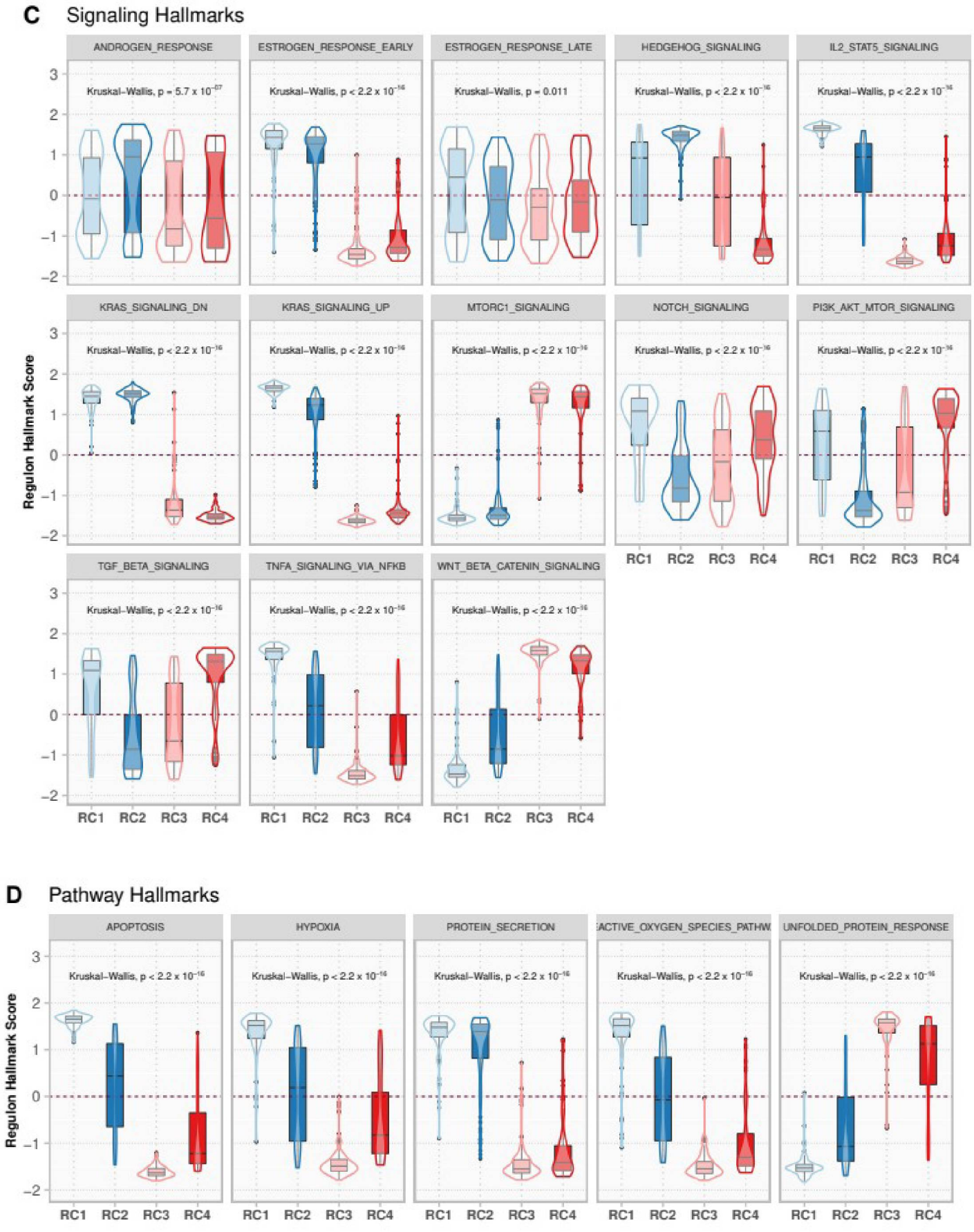


Sup. Figure 1. Distribution of the positive and negative targets of the regulons. The 1,605 regulons ordered by the difference between positive and negative targets are presented on the x-axis. Salmon bars show the number of positive targets and blue bars the number of negative targets for each regulon. The dotted lines represent the threshold of 15 targets, the minimum required for gene set enrichment analysis [30].

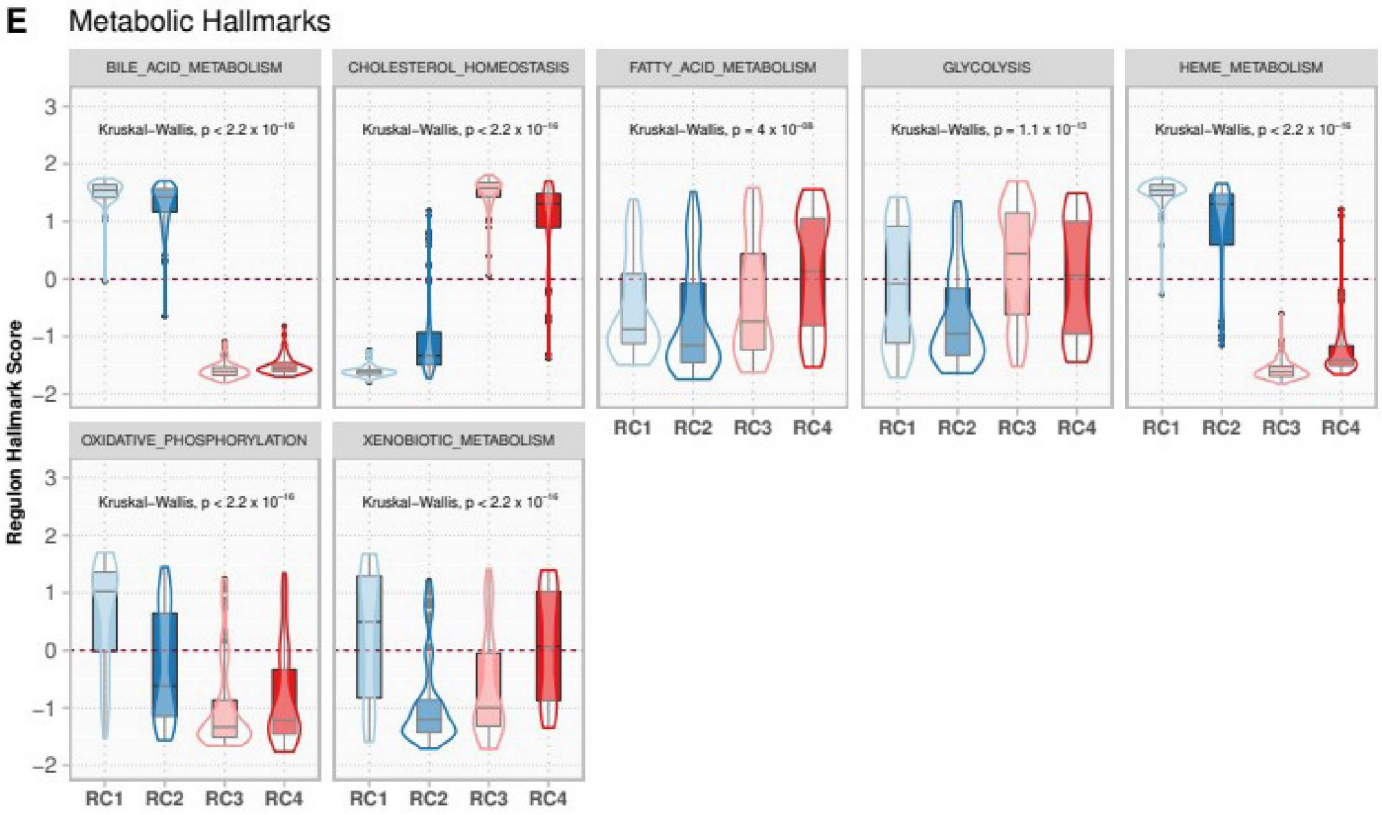


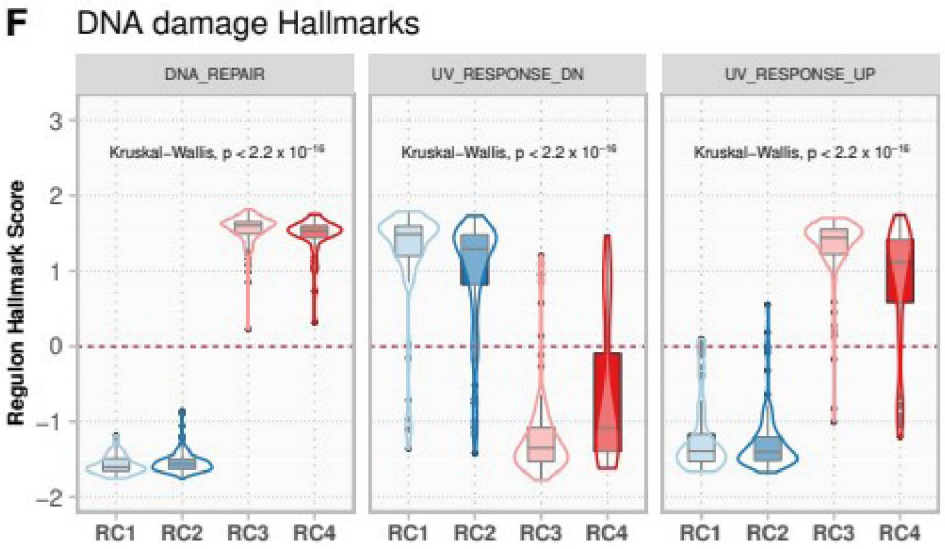
Sup. Figure 2. Consensus matrix and silhouettes of regulon clusters. The regulon activity profile was used for the consensus clustering. The consensus matrix for k = 4 is shown in the main heatmap, and the silhouette for each regulon is presented in the barplot below. Regulons are colored according to their respective cluster.

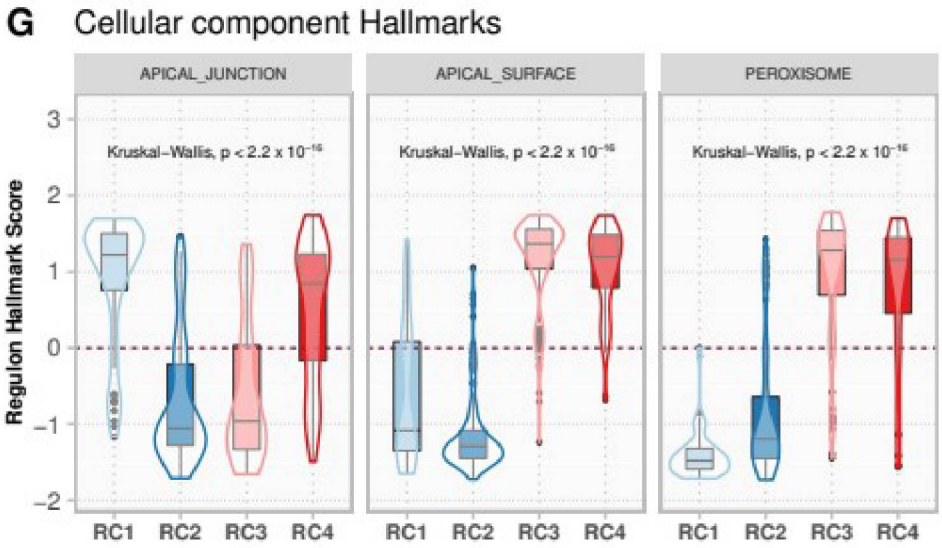

A
Immune Hallmarks
ALLOGRAFT_REJECTION
COAGULATION
COMPLEMENT
IL6_JAK_STAT3_SIGNALING
INFLAMMATORY_RESPONSE
INTERFERON_ALPHA_RESPONSE
INTERFERON_GAMMA_RESPONSE
Kruskal–Wallis, p < 2.2 x 10⁻¹⁶
Regulon Hallmark Score
RC1
RC2
RC3
RC4
B
Proliferation Hallmarks
E2F_TARGETS
G2M_CHECKPOINT
MITOTIC_SPINDLE
MYC_TARGETS_V1
MYC_TARGETS_V2
P53_PATHWAY

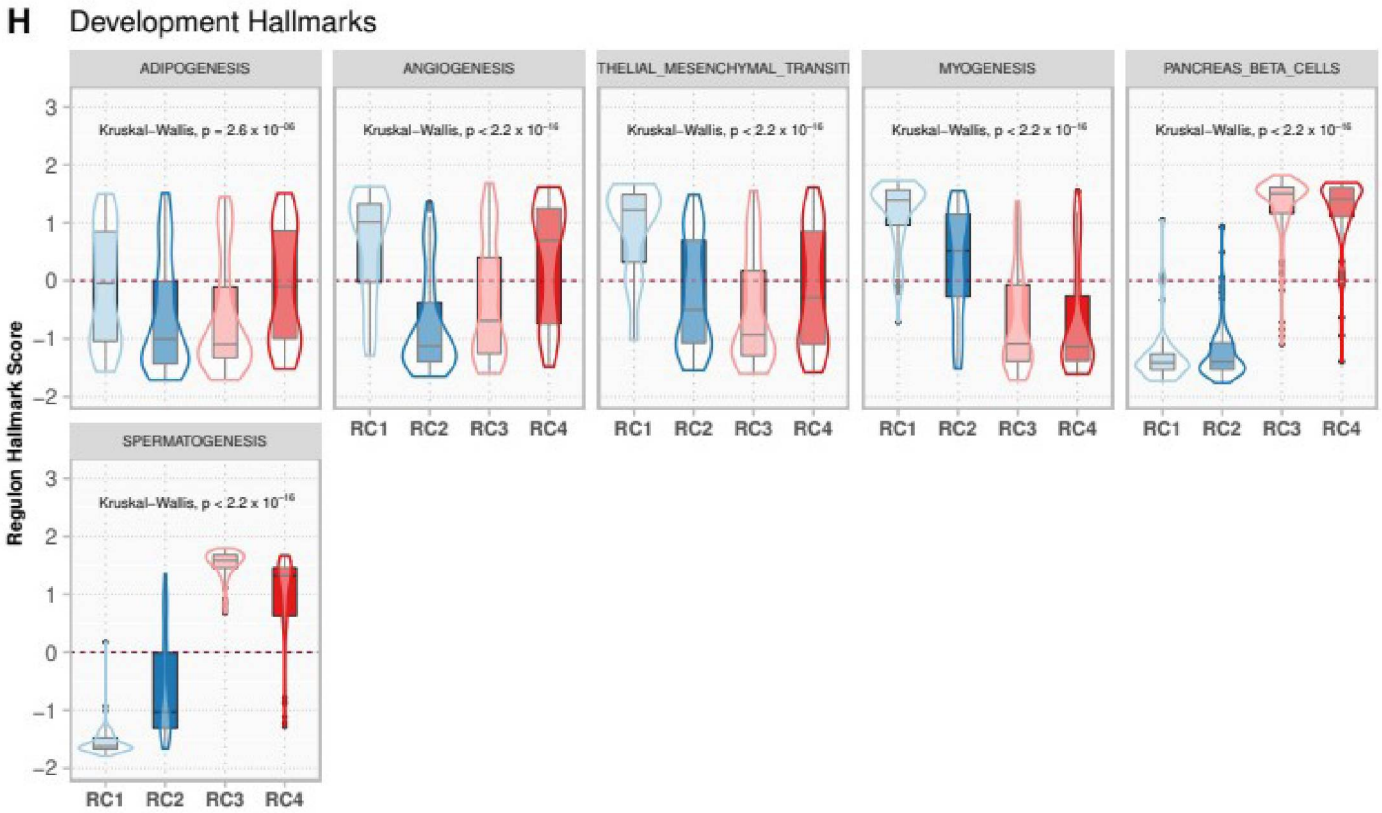

C Signaling Hallmarks
ANDROGEN_RESPONSE
Kruskal–Wallis, p = 5.7 x 10^-07
ESTROGEN_RESPONSE_EARLY
Kruskal–Wallis, p < 2.2 x 10^-16
ESTROGEN_RESPONSE_LATE
Kruskal–Wallis, p = 0.011
HEDGEHOG_SIGNALING
Kruskal–Wallis, p < 2.2 x 10^-16
IL2_STAT5_SIGNALING
Kruskal–Wallis, p < 2.2 x 10^-16
KRAS_SIGNALING_DN
Kruskal–Wallis, p < 2.2 x 10^-16
KRAS_SIGNALING_UP
Kruskal–Wallis, p < 2.2 x 10^-16
MTORC1_SIGNALING
Kruskal–Wallis, p < 2.2 x 10^-16
NOTCH_SIGNALING
Kruskal–Wallis, p < 2.2 x 10^-16
PI3K_AKT_MTOR_SIGNALING
Kruskal–Wallis, p < 2.2 x 10^-16
TGF_BETA_SIGNALING
Kruskal–Wallis, p < 2.2 x 10^-16
TNFA_SIGNALING_VIA_NFKB
Kruskal–Wallis, p < 2.2 x 10^-16
WNT_BETA_CATENIN_SIGNALING
Kruskal–Wallis, p < 2.2 x 10^-16
Regulon Hallmark Score
3
2
1
0
−1
−2
RC1
RC2
RC3
RC4

D Pathway Hallmarks
APOPTOSIS
Kruskal–Wallis, p < 2.2 x 10^-16
HYPOXIA
Kruskal–Wallis, p < 2.2 x 10^-16
PROTEIN_SECRETION
Kruskal–Wallis, p < 2.2 x 10^-16
ACTIVE_OXYGEN_SPECIES_PATHW
Kruskal–Wallis, p < 2.2 x 10^-16
UNFOLDED_PROTEIN_RESPONSE
Kruskal–Wallis, p < 2.2 x 10^-16
Regulon Hallmark Score
3
2
1
0
−1
−2
RC1
RC2
RC3
RC4

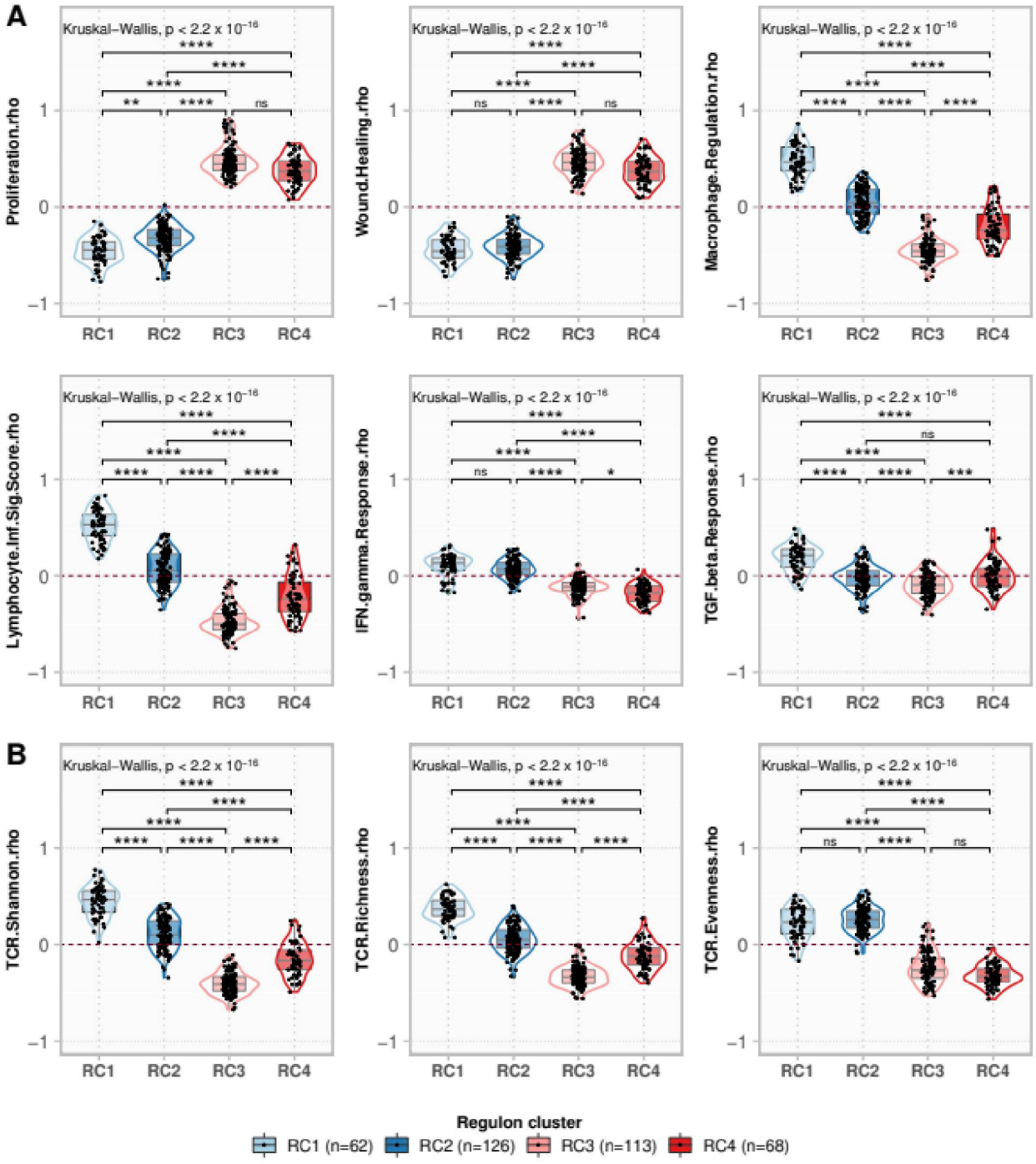

E
Metabolic Hallmarks
BILE_ACID_METABOLISM
CHOLESTEROL_HOMEOSTASIS
FATTY_ACID_METABOLISM
GLYCOLYSIS
HEME_METABOLISM
OXIDATIVE_PHOSPHORYLATION
XENOBIOTIC_METABOLISM
Kruskal–Wallis, p < 2.2 x 10⁻¹⁶
Kruskal–Wallis, p = 4 x 10⁻⁵⁸
Kruskal–Wallis, p = 1.1 x 10⁻¹³
Regulon Hallmark Score
3
2
1
0
−1
−2
RC1
RC2
RC3
RC4


F
DNA damage Hallmarks
DNA_REPAIR
UV_RESPONSE_DN
UV_RESPONSE_UP
Kruskal–Wallis, p < 2.2 x 10⁻¹⁶
Regulon Hallmark Score
3
2
1
0
−1
−2
RC1
RC2
RC3
RC4

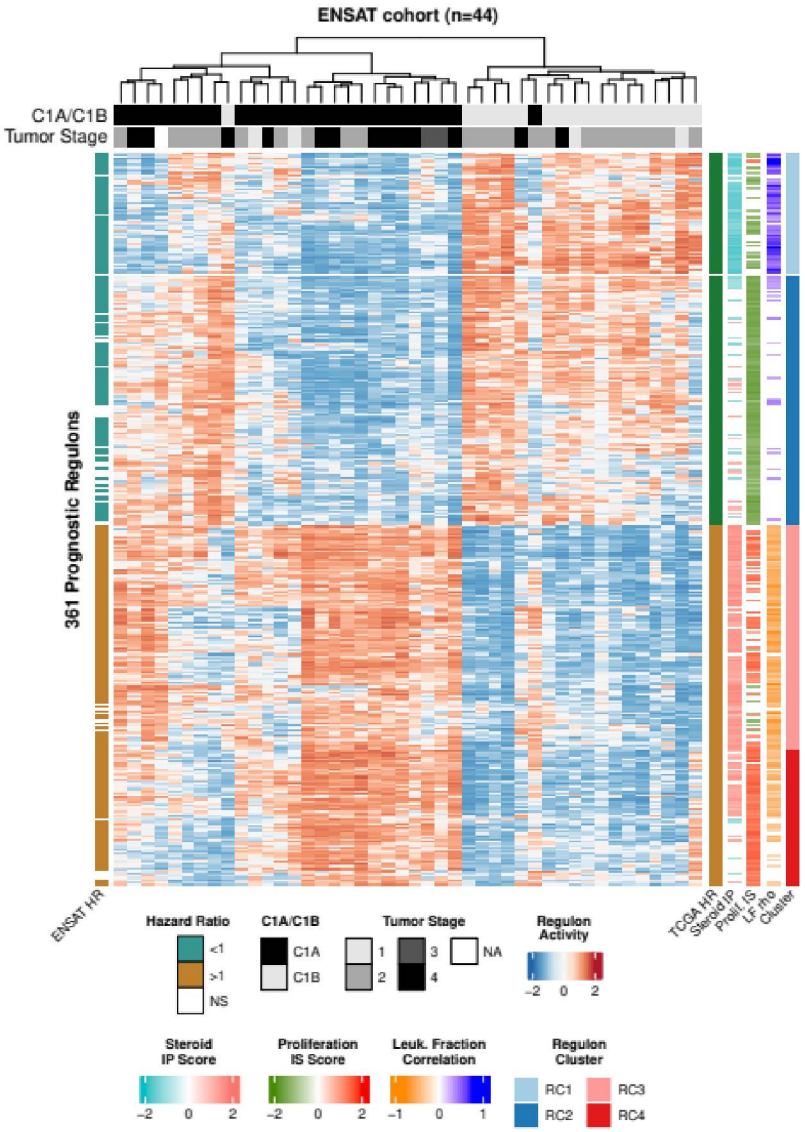

G
Cellular component Hallmarks
APICAL_JUNCTION
APICAL_SURFACE
PEROXISOME
Kruskal–Wallis, p < 2.2 x 10⁻¹⁶
Regulon Hallmark Score
3
2
1
0
−1
−2
RC1
RC2
RC3
RC4


H
Development Hallmarks
ADIPOGENESIS
ANGIOGENESIS
THELIAL_MESENCHYMAL_TRANSITI
MYOGENESIS
PANCREAS_BETA_CELLS
SPERMATOGENESIS
Kruskal–Wallis, p = 2.6 x 10⁻⁰⁶
Kruskal–Wallis, p < 2.2 x 10⁻¹⁶
Regulon Hallmark Score
3
2
1
0
−1
−2
RC1
RC2
RC3
RC4

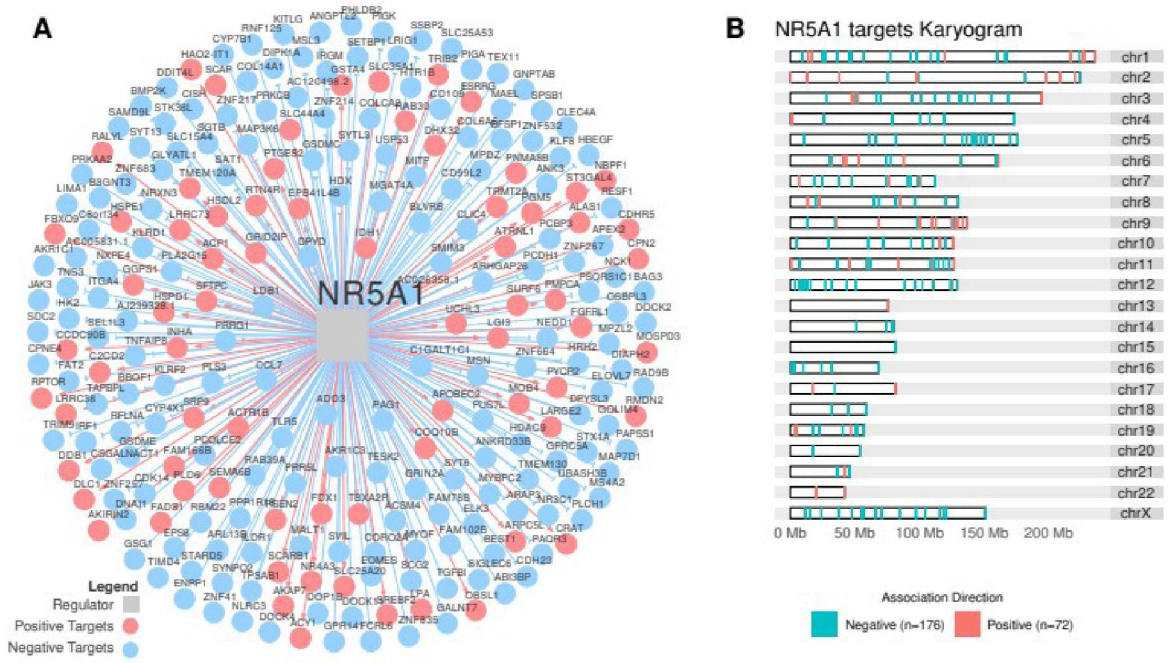
Sup. Figure 3. Boxplots comparing the Hallmark enrichment scores in the regulon clusters. The y-axis shows the enrichment score for the regulon in each Hallmark described, while the x-axis separates the regulons in their clusters. The contour presents the distribution density of the regulons for each cluster. The result for the Kruskal-Wallis test is presented on top. The Hallmarks are divided into the following categories: (**A**) Immune, (**B**) Proliferation, (**C**) Signalling, (**D**) Pathway, (**E**) Metabolic, (**F**) DNA damage, (**G**) Cellular component, and (**H**) Development.



Sup. Figure 4. Boxplots comparing Spearman's correlation between the immune features described by Thorsson et al. (2018) [14] and the regulon activity in the clusters. (**A**) Comparison between the correlation for the regulon activity and the six immune signatures score. (**B**) Comparison of the correlation between the regulon activity with the T cell receptor (TCR) metrics. Each point represents a regulon separated by the regulon cluster in the x-axis and vertically spread according to its Spearman correlation to each immune feature. The contour presents the distribution density of the regulons for each cluster. The results of the Kruskal-Wallis and Dunn's tests for pairwise multiple comparisons of the ranked data are presented on top. Asterisks indicate the significance level as follows: *p ≤ 0.05, **p ≤ 0.01, ***p ≤ 0.001, and ****p ≤ 0.0001. Non-significant p-values (p > 0.05) are represented by "ns".



Sup Figure 5. A heatmap showing regulon activity in the ENSAT cohort (n = 44 ACC samples). Each column represents a sample, while the rows represent the 361 prognostic regulons present in the gene expression matrix. The upper track shows the tumor stage and C1A/C1B classification for each sample as described by Assié et al. (2014) [31]. The right track shows the regulon characteristics inferred in the TCGA-ACC cohort, as presented in Figure 3A, while the left track shows the overall survival (OS) hazard ratio (HR) calculated for the ENSAT cohort.



Sup Figure 6. Targets of the *NR5A1* regulon and the related karyogram. (**A**) The transcription factor *NR5A1* (grey square at the center) and its targets inferred by the regulatory network analysis. Blue circles indicate targets with a negative association, while red circles indicate targets with a positive association. (**B**) The karyogram presents the distribution of *NR5A1* targets in the chromosomes.

References

14. Thorsson, V.; Gibbs, D.L.; Brown, S.D.; Wolf, D.; Bortone, D.S.; Ou Yang, T.-H.; Porta-Pardo, E.; Gao, G.F.; Plaisier, C.L.; Eddy, J.A.; et al. The Immune Landscape of Cancer. *Immunity* **2018**, *48*, 812-830.e14, doi:10.1016/j.immuni.2018.03.023.
30. Liberzon, A.; Birger, C.; Thorvaldsdóttir, H.; Ghandi, M.; Mesirov, J.P.; Tamayo, P. The Molecular Signatures Database Hallmark Gene Set Collection. *Cell Syst.* **2015**, *1*, 417–425, doi:10.1016/j.cels.2015.12.004.
31. Assié, G.; Letouzé, E.; Fassnacht, M.; Jouinot, A.; Luscap, W.; Barreau, O.; Omeiri, H.; Rodriguez, S.; Perlemoine, K.; René-Corail, F.; et al. Integrated Genomic Characterization of Adrenocortical Carcinoma. *Nat. Genet.* **2014**, *46*, 607–612, doi:10.1038/ng.2953.

APÊNDICE 3 - UNRAVELING IMMUNE-RELATED LNCRNAS IN BREAST CANCER MOLECULAR SUBTYPES

Carolina Mathias[1†], João Carlos Degraf Muzzi[2,3,4†], Bruna Borba Antunes[1,2], Daniela F. Gradia[1], Mauro A. A. Castro[2‡] and Jaqueline Carvalho de Oliveira[1*‡]

https://www.frontiersin.org/articles/10.3389/fonc.2021.692170/full

- [1]Department of Genetics, Federal University of Parana, Post-graduation Program in Genetics, Curitiba, Brazil
- [2]Bioinformatics and Systems Biology Lab, Federal University of Parana (UFPR), Polytechnic Center, Curitiba, Brazil
- [3]Immunochemistry Laboratory (LIMQ), Federal University of Parana, Post-graduation Program in Microbiology, Parasitology and Pathology, Curitiba, Brazil
- [4]Instituto de Pesquisa Pelé Pequeno Príncipe, Oncology Division, Curitiba, Brazil

ABSTRACT

Breast cancer (BRCA) is the most leading cause of cancer worldwide. It is a heterogeneous disease with at least five molecular subtypes including luminal A, luminal B, basal-like, HER2-enriched, and normal-like. These five molecular subtypes are usually stratified according to their mRNA profile patterns; however, ncRNAs are increasingly being used for this purpose. Among the ncRNAs class, the long non-coding RNAs (lncRNAs) are molecules with more than 200 nucleotides with versatile regulatory roles; and high tissue-specific expression profiles. The heterogeneity of BRCA can also be reflected regarding tumor microenvironment immune cells composition, which can directly impact a patient's prognosis and therapy response. Using BRCA immunogenomics data from a previous study, we propose here a bioinformatics approach to include lncRNAs complexity in BRCA molecular and immune subtype. RNA-seq data from The Cancer Genome Atlas (TCGA) BRCA cohort was analyzed, and signal-to-noise ratio metrics were applied to create these subtype-specific signatures. Five immune-related signatures were generated with approximately ten specific lncRNAs, which were then functionally analyzed using GSEA enrichment and survival analysis. We highlighted here some lncRNAs in each subtype. LINC01871 is related to immune response activation and favorable overall survival in basal-like samples; EBLN3P is related to immune response suppression and progression in luminal B, MEG3, XXYLT1-AS2, and LINC02613 were related with immune response activation in luminal A, HER2-enriched and normal-like subtypes, respectively. In this way, we emphasize the need to know better the role of

lncRNAs as regulators of immune response to provide new perspectives regarding diagnosis, prognosis and therapeutical targets in BRCA molecular subtypes.

Introduction

Breast cancer (BRCA) is a molecular and histological heterogeneous disease with at least five intrinsic molecular subtypes (1, 2). Based on gene expression, BRCA can be mainly classified into luminal A (LumA), luminal B (LumB), HER2-enriched (Her2), basal-like (Basal), and normal-like (Normal) (3, 4). These subtypes have a distinct prognosis and also differ according to therapeutic response. LumA and LumB tumors respond well to hormonal interventions, while HER2+ tumors respond effectively when anti-HER2 therapy is used (5). Basal tumors are very aggressive and associated with the shortest survival times, with no current molecular-based targeted therapies available (6).

Immunotherapy brought a new line of action in cancer care; however its response varies across cancer types and patients. The immune system response in the tumor microenvironment may help to guide immunotherapy drug discovery and clinical decisions (7). In general, tumors more responsive to immune checkpoint inhibitors are related to high levels of leukocyte fraction in the tumor microenvironment (8). Besides gene expression differences in BRCA molecular subtypes, they differ significantly concerning the composition of cells that form the tumor microenvironment, especially the immune system's cells. A substantial proportion of natural killer cells and neutrophils have been found in luminal tumors. In contrast, in these tumors, cytotoxic T cells (T CD8+) and naïve and memory T cells are found less frequently. In BRCA Basal tumors, T regs, associated macrophages 2, and activated mast cells form a significant portion of the immune infiltrate cells. The immune infiltrate composition is not widely described in the Her2 subtype. It is known that it is mainly formed by dendritic cells, mast cells, γδ T lymphocytes, T regs and neutrophils (9).

A landscape of tumors' immune microenvironment was characterized from immunogenomics data by Thorsson and colleagues (8). In this study, using an integrated analysis, they could classify solid tumors (from The Cancer Genome Atlas) into six major immune subtypes, which they called C1-C6. These subtypes have distinct immune signature sets, which could also be related to prognosis. C1 (wound

healing) exhibited elevated expression of angiogenic genes, a high proliferation rate, and a Th2 cell bias to the adaptive immune infiltrate. C2 (IFN-γ dominant) had a strong T CD8+ signal, the greatest TCR diversity, and a high proliferation rate. C3 (inflammatory) was the subtype that presented high Th17 and Th1 genes and low to moderate tumor cell proliferation. C4 (lymphocyte depleted) displayed a more prominent macrophage signature with Th1 suppressed and high M2 response. C5 (immunologically quiet) was enriched by brain tumors and exhibited the lowest lymphocyte and most increased macrophage responses. Finally, C6 (TGF-β dominant) displayed the highest TGF-β signature and a high lymphocytic infiltrate with an even distribution of type I and type II T cells (8).

According to this approach, BRCA could be classified into five subtypes (C1, C2, C3, C4 and C6), being C2 (n=345) the most representative subtype, followed by C1 (n=320). Immune subtypes were also described according to BRCA molecular subtypes, and as expected, the subtypes varied significantly according to these immune groups. For example, LumA was more representative of the C1 subtype, while Basal samples of C2 (8).

Gene expression sets based on mRNAs were used for the classification and determination of molecular and immune subtypes. However, it is already known that the most abundant part of the human genome is not translated into proteins. These transcripts are organized in a class called “non-coding RNAs.” Non-coding RNAs can be classified into two major categories based on their size: small non-coding RNAs (<200 nucleotides) and long non-coding RNAs (>200 nucleotides) (10). LncRNAs are usually transcribed by RNA polymerase II, polyadenylated, and capped. They exhibit high tissue specificity and great regulatory versatility, acting at different gene expression regulation levels (11, 12).

Due to its high tissue specificity, lncRNAs can be evaluated as potential disease biomarkers, including BRCA (13–15). Based on this, we looked for molecular subtype specific lncRNAs signatures that could help differentiate the immune profiles described in Thorsson (8). These lncRNAs were also analyzed if impact the patient’s overall survival and progression free interval and were also investigated in differential expression and enrichment analysis to explore other possible biological roles of these lncRNAs in BRCA molecular and immune subtypes.

Material and Methods

Breast Cancer Immune Data

BRCA molecular and immune subtypes, leukocyte fraction, and survival information were downloaded from Thorsson et al. (8) Supplementary Material. According to samples' barcode expression and immune type, data were integrated to perform the analysis. In Supplementary Table 1, we organized data according to breast cancer molecular and immune subtypes.

Breast Cancer RNA-Seq Data

Log2 normalized FPKM RNA-Seq data from The Cancer Genome Atlas (TCGA) breast cancer cohort was downloaded from XenaBrowser (https://xenabrowser.net/datapages/), and primary tumor samples were selected and merged with Thorsson et al. (8) master table using patients' barcode. The lncRNAs and protein-coding gene expression profiles were filtered from the RNA-Seq data using the R package biomaRt v 2.46.3 (16). For lncRNAs, when available, HGNC Symbol was used; otherwise, Ensembl gene name was used. All Ensembl and HGNC Symbols from lncRNAs used in this study are available in Supplementary Table 2. The non-tumoral samples were selected based on TCGA barcodes ending with 11A or 11B. The molecular BRCA subtypes were defined as described in Thorsson et al. (8) Supplementary Material, based on PAM50.

The expression profiles of immunomodulatory genes listed (8) (https://www.cell.com/cms/10.1016/j.immuni.2018.03.023/attachment/8d3ffc74-4db4-4531-a4ad-389dfc8bb7ec/mmc7.xlsx) previously were obtained from the gene expression matrix. Of the 75 immune modulators, only one (C10orf54) was not found in the expression matrix. For heatmap construction using *ComplexHeatmap* package (17), samples were displayed in columns and genes in the rows. Column-wise z-score was calculated for gene expression values, and maximum and minimum values were limited to +2 and −2 standard deviations, respectively. Samples were clustered within each BRCA subtype.

The BRCA lncRNAs expressions were further filtered above the first quartile for lncRNA expression sum, which means lncRNAs with expression sum above 8.04

log2 FPKM in the whole BRCA cohort (1,060 samples). Signal-to-noise ratio (SNR) was calculated for each molecular subgroup individually as follow:

$$SNR = \mu 1 - \mu 2 \sigma 1 + \sigma 2$$

being μ_1 the mean of lncRNA expression in the group analyzed and μ_2 the mean of lncRNA expression in the patients out of the group analyzed. σ refers to the standard deviation from the respective groups mentioned. We selected the lncRNAs above the SNR 0.95 quantile for each BRCA molecular subtype, that means the lncRNAs with higher expression in the subtype analyzed compared with the rest of the cohort. Venn diagram was constructed using *InteractiVenn* (http://www.interactivenn.net/) demonstrating the intersection of lncRNA between groups. Then, we calculated the SNR within each molecular subgroup based on the immune subtypes described previously (8). We considered for the analysis the immune groups with more than five patients in each molecular subtype. In this way, Basal and Her2 samples were divided into C1 and C2 subtypes; LumA and Normal into C1, C2, C3, C4, and C6 subtypes and LumB into C1, C2, C3, and C4 subtypes. After absolute SNR sum calculation, we selected lncRNAs considered in 0.98 quantile, which means the lncRNAs with the most significant variation within the immune subtypes for each molecular subgroup. For histogram construction, the absolute SNR sum was scaled using z-score. The 53 lncRNAs selected from this analysis are presented in Supplementary Table 3.

Leucocyte Fraction Correlation

The lncRNAs expression was used to calculate Spearman correlation with the leucocyte fraction observed in each BRCA subtype, and the p-value was calculated with AS 89 algorithm (18) using cor. test function from stats R package v.4.0.4 (19) and adjusted by False Discovery Rate (FDR) method.

Survival Analysis

Survival analysis was firstly performed using the *coxph* function available in the survival R package v3.2-10 (20) based on lncRNA expression for both Overall Survival (OS) and Progression-Free Interval (PFI) for each lncRNA individually in its respective BRCA molecular subgroup. The univariate Cox p-value for each lncRNA was calculated and adjusted by the FDR method; values below 10% FDR level were considered significant.

One lncRNA was selected on each BRCA subtype based on Cox results or Leukocyte Fraction correlation for further analysis. Kaplan-Meier was calculated, and patients were divided by the median lncRNA expression value in High Expression and Low Expression; p-value was calculated by log-rank test.

Enrichment Analysis

The protein-coding genes expression profile was filtered for each molecular subgroup by patients' barcode, and genes with zero sum expression were removed. Patients were divided by the median lncRNA expression value, and High versus Low Expression groups were used for SNR calculus. Genes were ordered by SNR value, and gene set enrichment analysis (GSEA) was inferred using fgsea R package v1.16.0 (21) with MSigDb v7.2 Hallmarks gene sets (22, 23) for 10,000 permutations.

Results

Immune Modulator Genes Expression Demonstrates Distinct Patterns Within BRCA Molecular Subtypes

Based on the gene expression profile related to immune response, Throsson et al. (8) analyzed over 10,000 TCGA samples, from which 1,087 were from BRCA samples and clustered them in six immune subtypes. We merged the barcodes with the gene expression matrix downloaded from XenaBrowser, remaining 1,060 BRCA primary tumor samples. The molecular classification as presented in Thorsson et al. (8) master table as TCGA Subtype was used, dividing the samples into five groups, LumA (n=499), LumB (n = 184), Basal (n=169), Normal (n=136) and Her2 (n=72). In Supplementary Table 1, we represented the number of samples according to each molecular subgroup's immune subtype.

Supplementary Figure 1 shows a distinct pattern of immune modulators gene expression in all molecular subtypes. In general, most genes seem to be upregulated in the same samples (columns of the heatmap) independent of its classification as an inhibitor or stimulator of the immune system. Overall, the immune activation seen in the gene expression follows the rising in Leukocyte Fraction and tends to group the C2 immune subtype. Simultaneously, the inverse is observed for a low expression pattern associated with low Leukocyte Fraction and C1 immune subtype. Basal and Her2 demonstrate a more apparent separation of C1 and C2. These two immune subtypes are the major representatives in these molecular groups; for instance, C1

and C2 represent 95.9% and 93.1% of all Basal and Her2 samples, respectively (Supplementary Table 1).

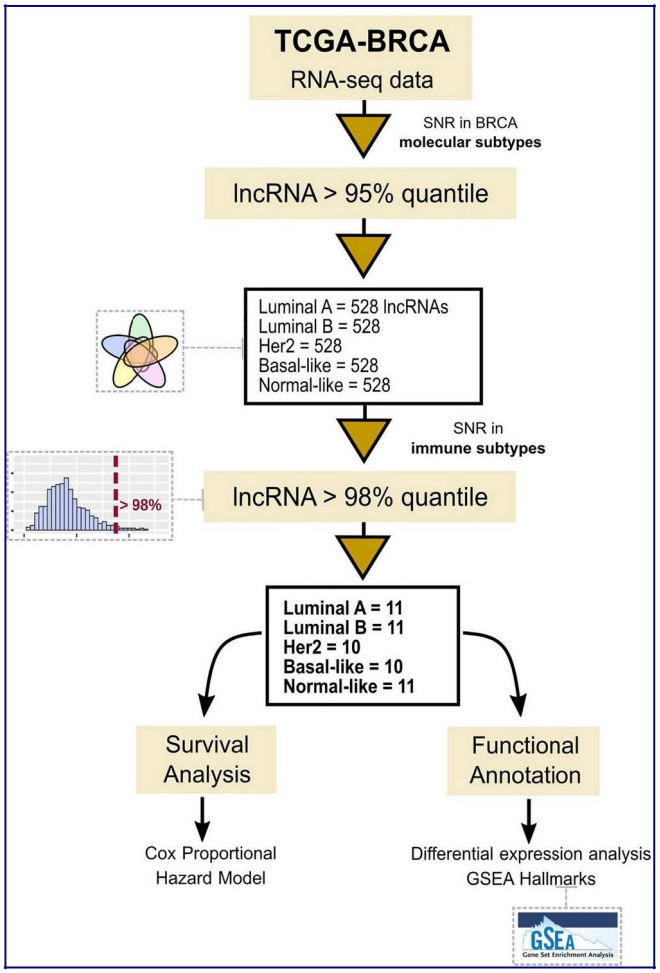


Figure 1 Workflow representation of the used methodology to study immune-related lncRNAs.

SNR Highlights Specific lncRNAs for Each BRCA Molecular Subgroups Related to Immune Subtypes Distinction

The first step of our strategy is to search for lncRNAs that could be associated with immune subtypes in BRCA patients. For this, lncRNAs with greater distinct expression patterns among the five molecular subgroups were selected (Figure 1). After selecting the 0.95 quantile in SNR values and including the only 5% more differentially expressed in each subtype, we obtained 528 lncRNAs for each BRCA molecular subtype. Figure 2A shows how these lncRNAs were intersected between the five subgroups. None lncRNA was shared between all subgroups, and most of them (over 80%) were specific for each molecular subtype. The most significant intersections were seen between LumA and LumB (44 lncRNAs), LumB and Her2 (33 lncRNAs), Basal and Normal (30 lncRNAs) and Basal and Her2 (26

lncRNAs), which represents less than 10% of the 528 lncRNAs defined for each subgroup. Even when selecting the 0.90 quantile in SNR values, none lncRNA was shared between all molecular subtypes (Supplementary Figure 2) which shows that the SNR was able to distinguish specific lncRNAs for each molecular subtype.

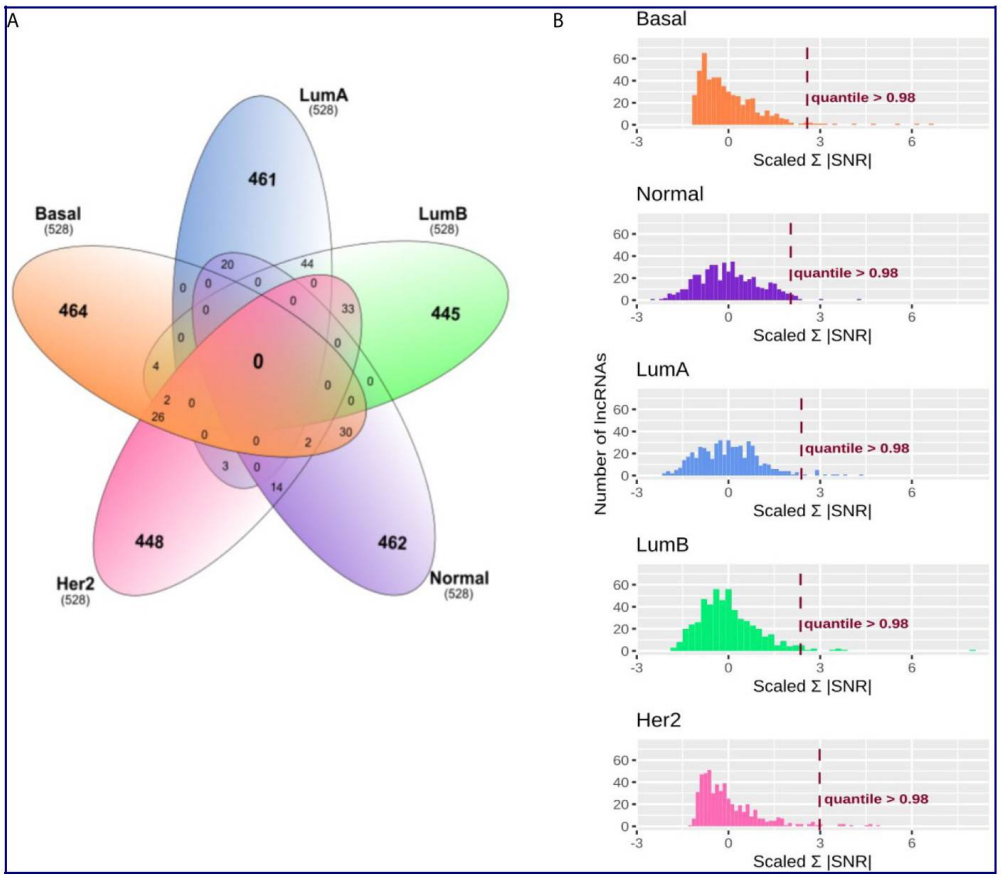


Figure 2 Immune related lncRNAs filter and selection in breast cancer (BRCA) molecular subtypes. **(A)** Venn diagram representing specific and shared immune related lncRNAs in breast cancer molecular subtypes. After filtering for 0.95 quantile in signal to noise ratio (SNR) for the BRCA molecular subtypes, 528 lncRNAs were selected for the next analysis. **(B)** Absolute SNR sum filter selection. SNR was calculated within each BRCA molecular subtype for the immune subtypes. Only groups with more than five patients were used. The histograms represent the amount of lncRNAs in each range of absolute SNR sum for the BRCA molecular subtypes. X-axis was scaled for z-score to allow comparison. The lncRNAs were filtered according to the 0.98 quantile as represented as the dashed line on the histograms.

Secondly, we calculated the absolute SNR sum for the immune subtypes for these 528 lncRNAs selected for each BRCA molecular subgroup. Figure 2B shows the distribution of absolute SNR sum for the lncRNAs. Z-score was calculated to allow comparison between groups. The five groups demonstrated different distributions, being Basal and Her2, characterized for most lncRNAs with slight variation between the immune subtypes, while LumA and Normal presented higher

variation. After selecting the 0.98 quantile (Figure 2B and Supplementary Table 3), 11 lncRNAs remained, of which only one was shared between Her2 and Basal, the lncRNA KLHDC7B-DT (ENSG00000272666). This lncRNA was removed for further analysis as we looked for a specific lncRNA signature related to each BRCA molecular subgroup. Eleven specific lncRNAs were selected for LumA, LumB and Normal and ten for Her2 and Basal. All results for the first and the second SNR calculation as well as the quantile for each lncRNA is presented in Supplementary Table 3.

Specific lncRNAs in BRCA Molecular Subgroups Are Associated With Immune Subtypes Differentiation

The remaining specific lncRNAs related to immune subtypes are presented in Figure 3; only immune subtypes with more than five patients are shown. These were the groups used for SNR analysis. For LumA, the lncRNAs clearly distinguished the C4 and C6 subtypes while demonstrating a mixed pattern in C1, C2 and C3. Nevertheless, EWSAT1, LINC00271 and AC105285.1 show higher activation in C3 than in C2, for example. No significant correlation with OS or PFI was observed for lncRNAs expression in Cox univariate analysis in LumA patients (Figure 3A and Supplementary Table 4).

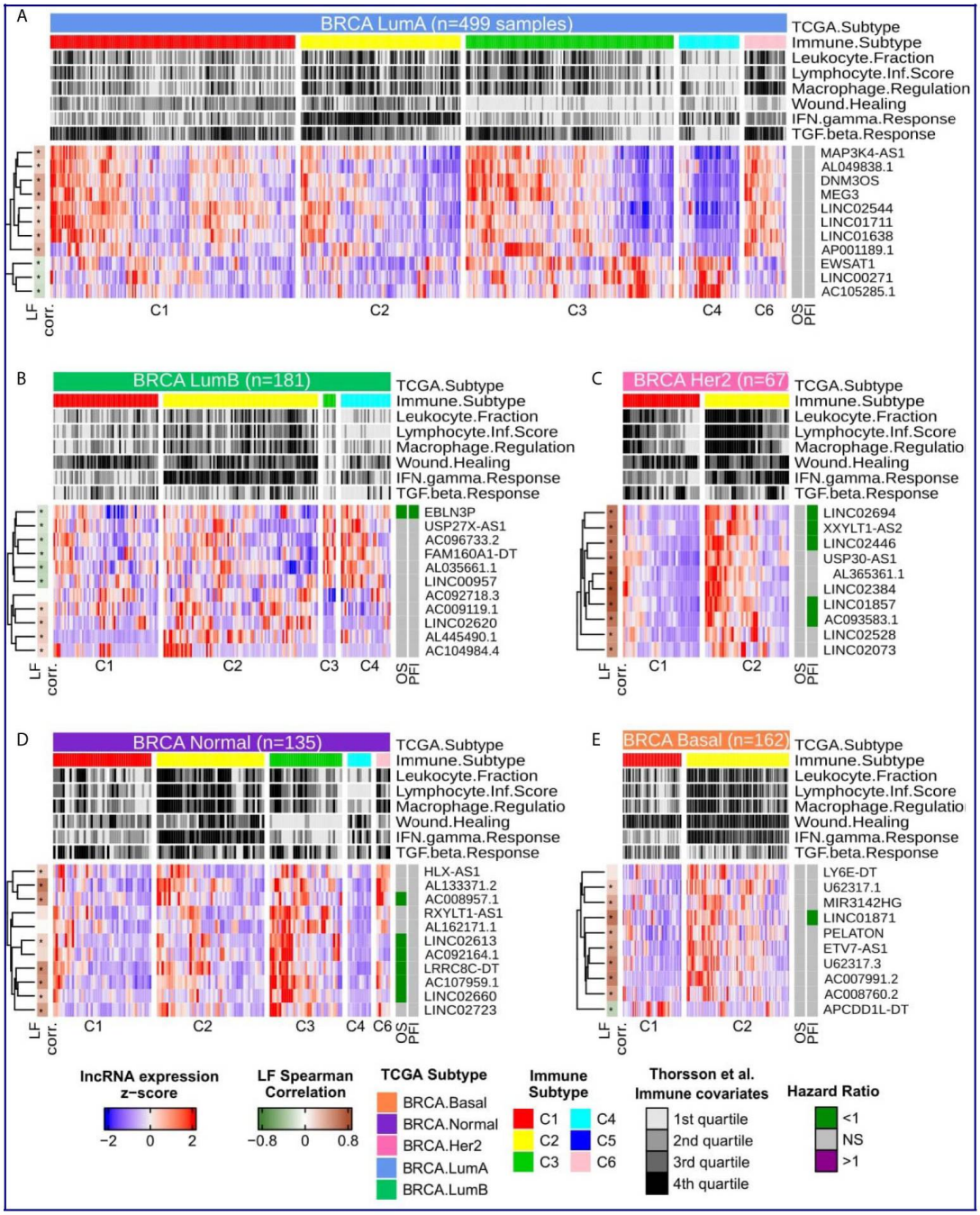


Figure 3 Heatmap with column-wise z-scores for immune related lncRNAs for each BRCA molecular subtype. For color gradient, maximum and minimum z-scores were set to +2 and −2 respectively. Each column represents a sample and were semi-supervised clustered within the immune subtypes. Immune subtypes groups with less than 5 patients are not represented as they were not used in SNR calculation. The top annotations present the molecular subtype with the number of samples, the immune subtype and the immune covariates as described by Thorsson et al. (8). The immune covariates are presented as quartiles in all TCGA-BRCA primary tumor samples. The left annotation shows the Spearman's correlation for each lncRNAs with Leukocyte Fraction, being dark green for negative and brown for positive ρ values, asterisks represent Spearman's correlation adjusted p-values values below 0.05. The right annotation represents the Hazard Ratio (HR) inferred by Cox Univariate analysis for Overall Survival (OS) and Progression Free Interval (PFI). Cox results with

adjusted p-values greater than 0.1 are considered non significant and are colored in grey, otherwise, HR values above 1 are colored purple while HR values below 1 are colored in green. **(A)** LumA samples. **(B)** LumB samples. **(C)** HER2-enriched samples. **(D)** Normal-Like samples. **(E)** Basal-Like samples.

For LumB (Figure 3B), a clear distinction can be seen between C3 and C4 in the gene expression pattern, while LINC02620 and mainly AL445490.1 showed a higher expression pattern in C3. Only EBLN3P correlated with a good prognosis in both OS and PFI for Cox univariate analysis (Figure 3B and Supplementary Table 4). In the Her2 samples (Figure 3C), all ten specific lncRNAs selected demonstrated a higher expression pattern in C2 and a strong positive correlation with Leukocyte Fraction. From the Cox univariate analysis, after p-values adjustment, half of the ten lncRNAs were associated with good prognosis in PFI, but none related to OS (Figure 3C and Supplementary Table 4).

In Normal (Figure 3D), all 11 lncRNAs were suppressed in the C4 subtype and, in general, showed a higher activation pattern in C3 and less evidently in C2. Despite C6 being represented by only six patients, HLX-AS1 and AL133371.2 appeared highly expressed in the C6 group. In Cox analysis, after p-adjustment, six from the 11 lncRNAs had a hazard ratio (HR) < 1 for OS, although none presented significant values for PFI. Finally, in the Basal group (Figure 3E), nine lncRNAs presented a higher expression in C2 and a lower expression in C1, while APCDD1L-DT presented an inverse pattern. Only LINC01871 showed a significant correlation with PFI, but not for OS (Figure 3E and Supplementary Table 4).

lncRNAs Functional Annotations and Survival Analysis

We used MSigDb Hallmarks gene sets for GSEA analysis to infer possible biological roles associated with the specific lncRNAs expression (Figure 3); the results for all 53 lncRNAs are presented in Supplementary Tables 5–9 and Supplementary Figure 3. We selected one lncRNA from each BRCA molecular subgroup to focus. For LumB, Her2, Basal and Normal, we chose the smallest p-value in Cox univariate analysis. As LumA did not present any significant p-values in Cox univariate analysis, we selected MEG3 as it showed a higher correlation with Leukocyte Fraction (Spearman's ρ=0.4, p-adjusted < 2.2×10^{-16}).

BRCA Basal-Specific lncRNAs Are Associated With Interferon Gamma Response and Allograft Rejection Gene Sets. LINC01871 Is More Expressed in Basal and Relates to Better OS and PFI

The GSEA analysis for the selected lncRNAs from BRCA Basal group revealed immune related gene sets, like Interferon Gamma Response, Allograft Rejection and Interferon Alpha Response, enriched in all ten lncRNAs, being negatively associated only with APCDD1L-DT (Supplementary Table 5 and Supplementary Figure 3A), which was also the only one from the ten lncRNAs negatively related to Leukocyte Fraction (Supplementary Table 4).

Focusing on LINC01871, this lncRNA presented a higher expression in Basal than all other BRCA molecular subtypes (Figure 4A) and was mainly associated with immune activation, for instance, enriched in Interferon Gamma Response, Allograft Rejection, Interferon Alpha Response and Inflammatory Response gene sets (Figure 4D). Within Basal samples, it appears significantly suppressed in C1 (Figure 4B), while in Kaplan-Meier analysis, it was associated with better OS and PFI (Figure 4C and Supplementary Figure 4A).

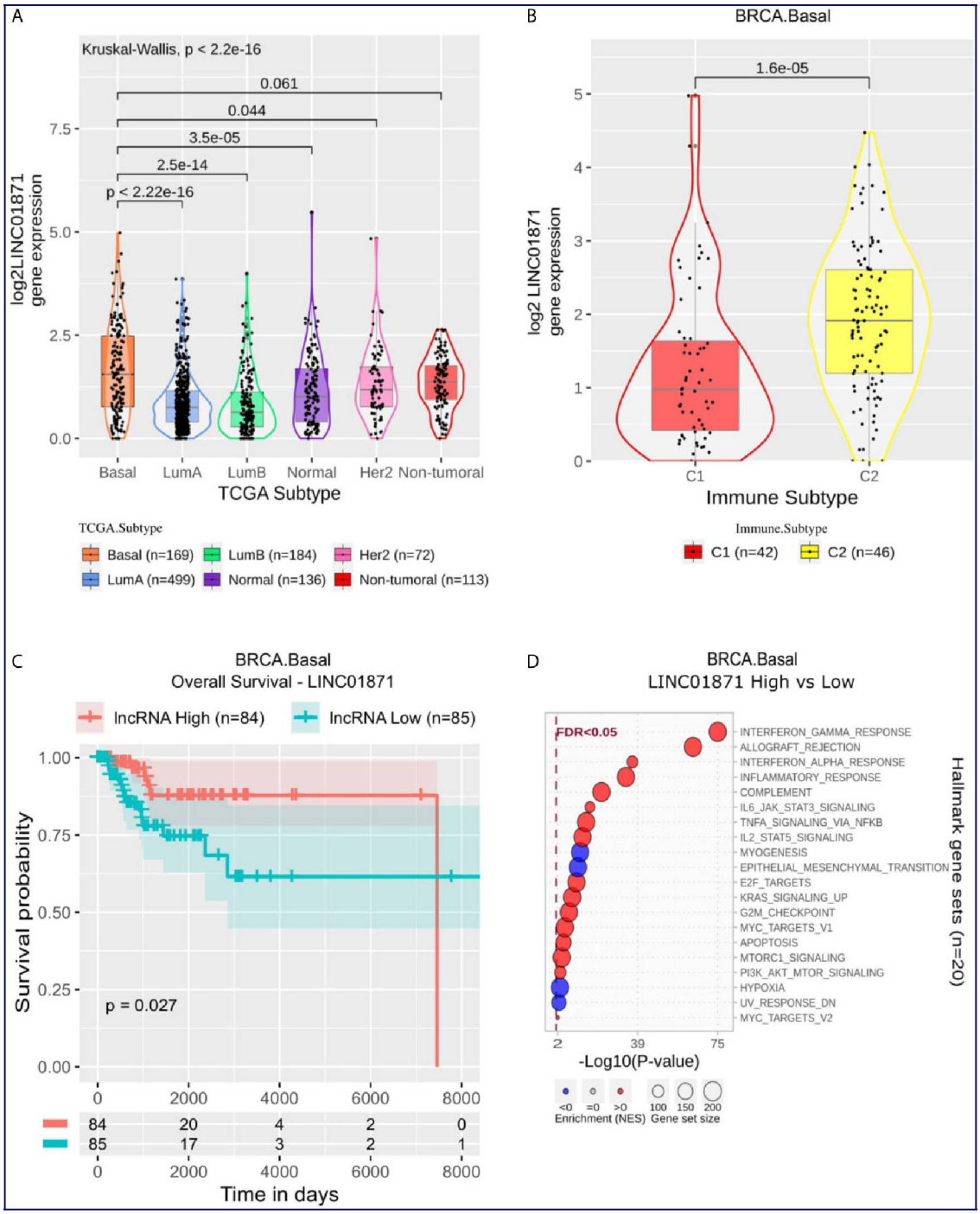


Figure 4 LINC01871 panel representation in basal-like subtype. **(A)** Box-plots representing LINC01871 expression among all breast cancer molecular subtypes. The Kruskal-Wallis test (p-value represented in the panel left top position) was used to differentiate expression between groups, followed by the Wilcoxon test (p-values represented emphasizing comparisons between subtypes). **(B)** Box-plot representing LINC01871 in C1 and C2 immune subtypes in basal-like patients. **(C)** LINC01871 overall survival curves. To define the two groups, LINC01871's median expression classified the patients into "high" and "low" groups. Logrank p-value represented as 0.027. **(D)** Enrichment analysis using Hallmarks gene sets. Red circles refers to activation while blue circles to

inactivation. In the X axis, a p-value scale is represented. The circle size varies according to the number of genes in the identified gene set.

BRCA Normal Specific lncRNAs Are Associated With Suppression of Proliferation Gene Sets. LINC02613 Is Suppressed in C4 and Relates to OS

The 11 BRCA Normal specific lncRNAs were related to the suppression of gene sets like G2M checkpoint, E2F and MYC targets associated with proliferation (Supplementary Table 6 and Supplementary Figure 3B). Mainly AL133371.2, AC008957.1, LRRC8C−DT, AC107959.1, LINC02660 and LINC02723 presented immune-related gene sets positively enriched (Allograft Rejection, Coagulation, Complement, IL6 JAK STAT3 Signaling, Inflammatory, Interferon Alpha and Interferon Gamma Response). LINC02613 follows this enrichment pattern (Figure 5D). It is worth noting that Estrogen Response Early and Late gene sets appear suppressed only for this lncRNA and AC092164.1. Although its expression significantly differs from BRCA Normal to all other molecular subtypes (Figure 5A), it is more expressed in non-tumoral samples followed by BRCA Basal and Normal. At the same time, it seems suppressed in LumA, LumB and Her2. Within Normal samples, it is more expressed in C3 and significantly suppressed in C4 (Figure 5B) and correlates with a better OS (Figure 5C) but not in PFI (Supplementary Figure 4B).

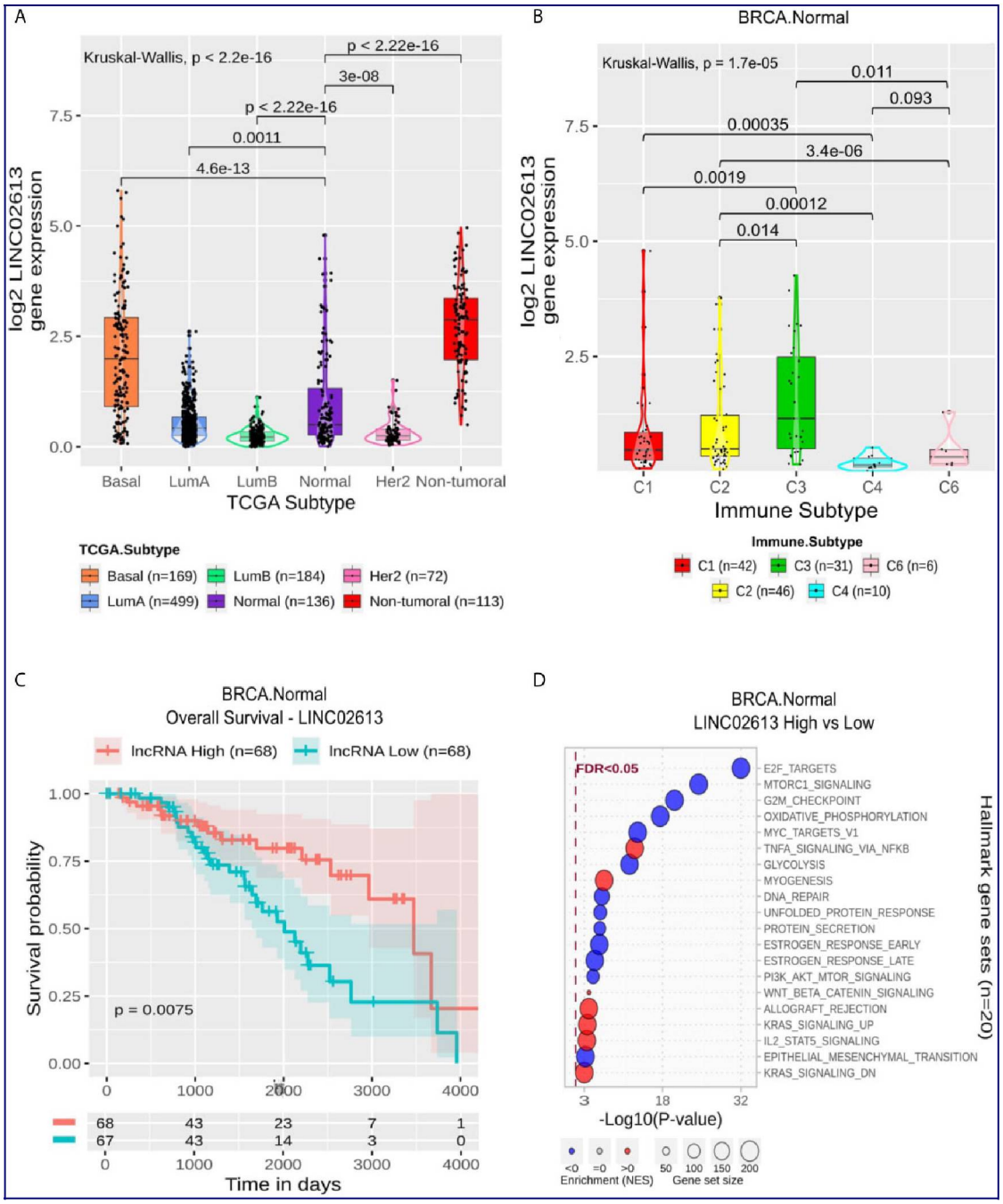


Figure 5 LINC02613 panel representation in normal-like subtype. **(A)** Box-plots representing LINC02613 expression among all breast cancer molecular subtypes. The Kruskal-Wallis test (p-value represented in the panel left top position) was used to differentiate expression between groups, followed by the Wilcoxon test (p-values represented emphasizing comparisons between subtypes). **(B)** Box-plot representing LINC02613 in C1,C2, C3, C4 and C6 immune subtypes in normal-like patients. **(C)** LINC02613 overall survival curves. To define the two groups, LINC02613's median expression classified the patients into "high" and "low" groups. Logrank p-value represented as 0.0075. **(D)** Enrichment analysis using Hallmarks gene sets. Red circles refers to activation while blue circles to inactivation. In the X axis, a p-value scale is represented. The circle size varies according to the number genes in of the identified gene set.

LumA-Specific lncRNAs Relate to Epithelial-Mesenchymal Transition, Immune and Proliferation Gene Sets. MEG3 Is Suppressed in BRCA Compared With Non-Tumoral Samples

For LumA (Supplementary Table 7 and Supplementary Figure 3C), the Epithelial-Mesenchymal Transition (EMT) module was enriched in all 11 lncRNAs, being EWSAT1, LINC00271, and AC105285.1 associated negatively with this module and the other eight lncRNAs positively. In general, this pattern was followed for the immune-related gene sets and the correlation with Leukocyte Fraction (Figure 3 and Supplementary Table 4), that is to say, EWSAT1, LINC00271, and AC105285.1 with the negative association and the other lncRNAs with a positive one. Gene sets associated with proliferation (E2F targets, Myc targets V1 and V2) were overall suppressed in all lncRNAs. Oxidative phosphorylation appeared suppressed in the lncRNAs positively associated with immune gene sets (MAP3K4-AS1, AL049838.1, DNM3OS, MEG3, LINC02544, LINC01711, LINC01638, and AP001189.1).

MEG3 presented a lower expression on BRCA compared with non-tumoral samples and a significant difference when comparing its expression in LumA with other BRCA molecular subtypes except Normal (Figure 6A). Within LumA samples, the immune subtypes comparisons resulted in a p-value of 3.2×10^{-14} in the Kruskal-Wallis test with a higher expression pattern in C3 and C6. At the same time, C4 stands out with a significantly lower pattern compared with all other immune subtypes (Figure 6B). In general, the GSEA analysis resulted in modules associated with immune response enriched with MEG3 overexpression and modules related to proliferation enriched with MEG3 suppression (Figure 6D). As expected by the Cox analysis, the Kaplan-Meier did not significantly impact MEG3 expression on OS or PFI (Figure 6C and Supplementary Figure 4C).

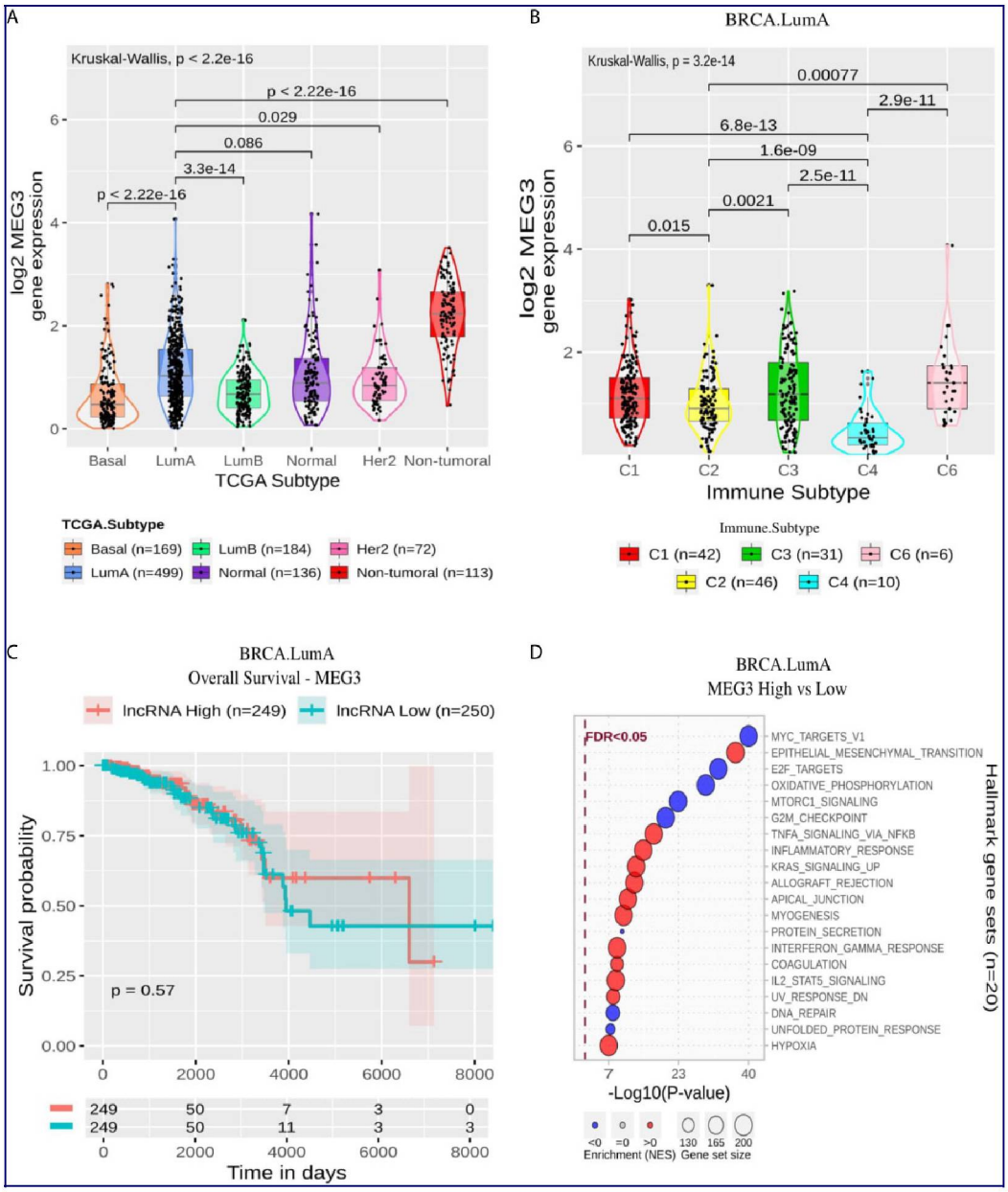


Figure 6 MEG3 panel representation in LumA subtype. **(A)** Box-plots representing MEG3 expression among all breast cancer molecular subtypes. The Kruskal-Wallis test (p-value represented in the panel left top position) was used to differentiate expression between groups, followed by the Wilcoxon test (p-values represented emphasizing comparisons between subtypes). **(B)** Box-plot representing MEG3 in C1,C2, C3, C4, and C6 immune subtypes in LumA patients. **(C)** MEG3 overall survival curves. To define the two groups, MEG3's median expression classified the patients into "high" and "low" groups. Logrank p-value represented as 0.57. **(D)** Enrichment analysis using Hallmarks gene sets. Red circles refers to activation while blue circles to inactivation. In X axis, a p-value scale is represented. The circle size varies according to the number of genes in the identified gene set.

Most Specific lncRNAs in LumB Are Associated With Immune Pathways. EBLN3P Is Associated With a Good Prognosis in OS and PFI

LumB specific lncRNAs demonstrated a higher variation in the enriched modules (Supplementary Table 8 and Supplementary Figure 3D). AC009119.1, LINC02620, AL445490.1, and AC104984.4 high expressions were positively related with immune gene sets, while with exception of LINC02620, no clear relation was observed for the proliferation ones. These four lncRNAs were also positively correlated with Leukocyte Fraction (Supplementary Table 4). AC092718.3, which did not present a significant correlation with Leukocyte Fraction, was also not related to the enrichment of immune gene sets; otherwise, its enrichment revealed proliferation modules upregulated. USP27X-AS1, AC096733.2, FAM160A1-DT, AL035661.1 and LINC00957 were associated with suppressing gene sets like Allograft Rejection, Interferon Gamma Response and Inflammatory Response; they also related negatively with Leukocyte Fraction (Supplementary Table 4).

EBLN3P is also related negatively to Leukocyte Fraction and with some immune modules. Still, its enrichment revealed a mixed pattern of modules suppressed like Epithelial-Mesenchymal Transition, Oxidative Phosphorylation, Myogenes and Myc Targets (Figure 7D). In LumB, its expression was higher in C3 and C4 than C1 and C2 (Figure 7B). In comparison, it presented a significantly higher expression in LumB samples than in the other BRCA molecular subtypes except for LumA (Figure 7A). In LumB samples, the higher expression of EBLN3P was related to a better outcome in OS but not with PFI in Kaplan-Meier analysis (Figure 7C and Supplementary Figure 4D).

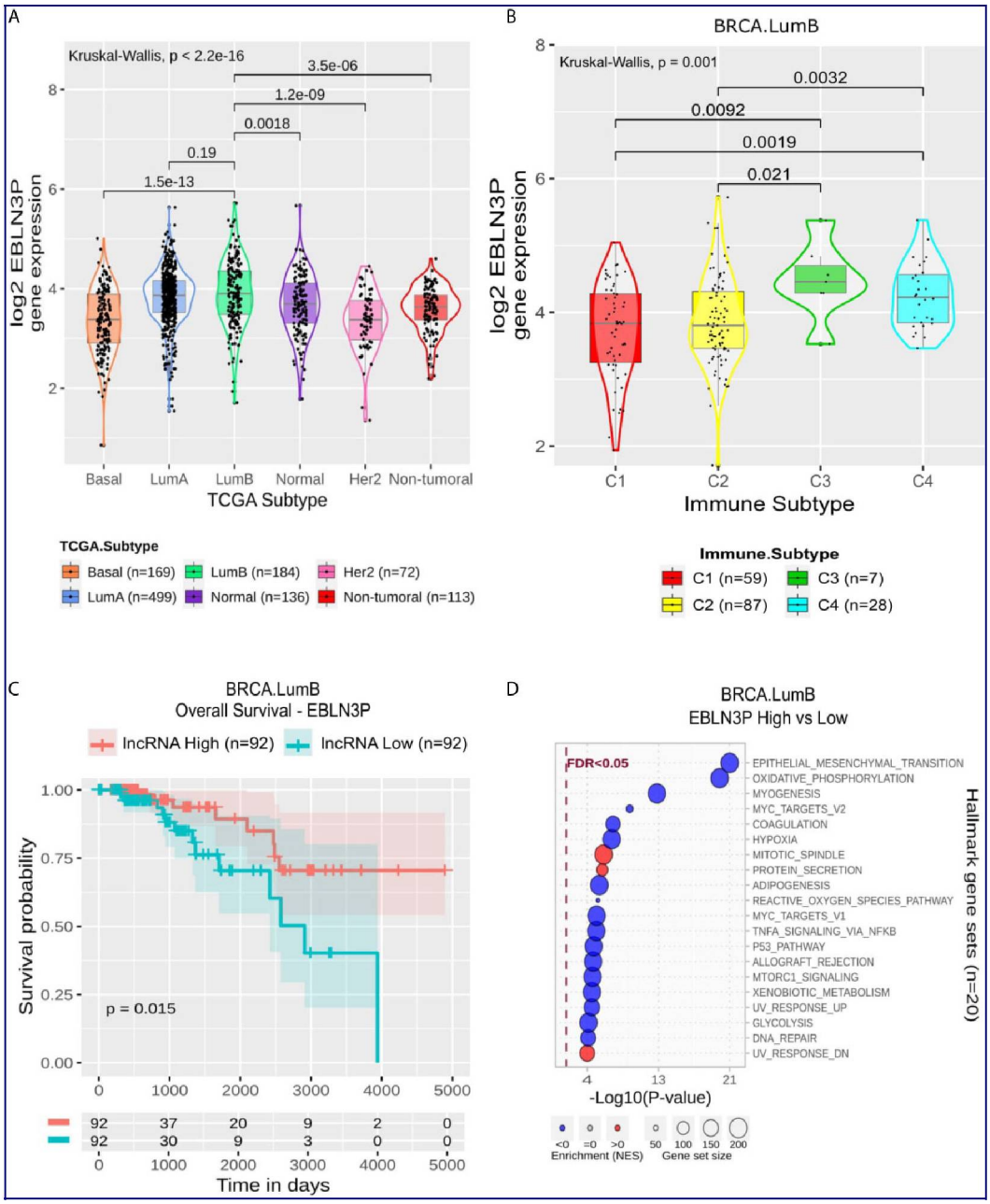


Figure 7 EBLN3P panel representation in LumB subtype. **(A)** Box-plots representing EBLN3P expression among all breast cancer molecular subtypes. The Kruskal-Wallis test (p-value represented in the panel left top position) was used to differentiate expression between groups, followed by the Wilcoxon test (p-values represented emphasizing comparisons between subtypes). **(B)** Box-plot representing EBLN3P in C1,C2, C3, and C4 immune subtypes in LumB patients. **(C)** EBLN3P overall survival curves. To define the two groups, EBLN3P's median expression classified the patients into "high" and "low" groups. Logrank p-value represented as 0.015. **(D)** Enrichment analysis using Hallmarks gene sets. Red circles refers to activation while blue circles to inactivation. In X axis, a p-value scale is represented. The circle size varies according to the number of genes in the identified gene set.

Her2-Specific lncRNAs Are Associated With Immune Activation and XXYLT1-AS2 Associated With Higher PFI

All 10 Her2 specific lncRNAs were related with immune activation as can be seen in their enrichment pattern of Allograft Rejection, Interferon Gamma and Alpha Response, Inflammatory Response, IL6 JAK STAT3 signaling and Complement (Supplementary Table 9 and Supplementary Figure 3E) and in the strong positive correlation with Leukocyte Fraction (ρ range from 0.49 to 0.82 in Spearman's Correlation, p-adjusted from 1.5×10^{-5} to $<2.2 \times 10^{-16}$). LINC02384 and LINC02073 are also related to the suppression of proliferation pathways (E2F Targets, G2M checkpoint and MYC Targets).

XXYLT1-AS2 showed a significantly higher expression in Her2 than in LumA, LumB and Normal (Figure 8A). Within Her2 samples, it was significantly more expressed in the C2 immune subtype (Figure 8B) and associated with better prognosis in PFI (Figure 8C) but not with OS (Supplementary Figure 4E). Its enrichment revealed high positive correlation with Allograft Rejection, Interferon Gamma Response, Inflammatory Response and IL6 and IL2 signaling and negative relation mainly with EMT, Hypoxia and Myogenesis (Figure 8D).

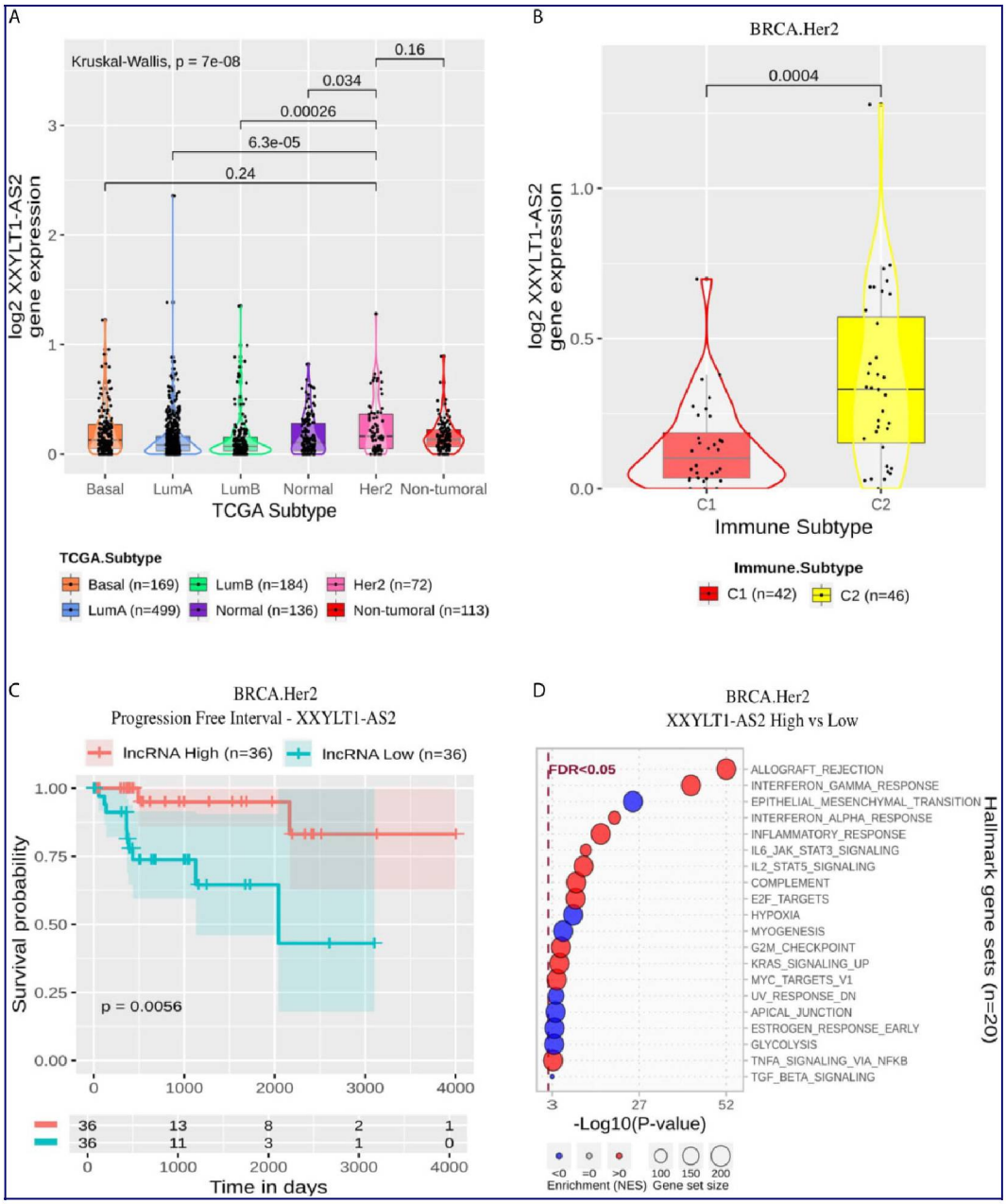


Figure 8 XXYLT1-AS2 panel representation in Her2 subtype. **(A)** Box-plots representing XXYLT1-AS2 expression among all breast cancer molecular subtypes. The Kruskal-Wallis test (p-value represented in the panel left top position) was used to differentiate expression between groups, followed by the Wilcoxon test (p-values represented emphasizing comparisons between subtypes). **(B)** Box-plot representing XXYLT1-AS2 in C1, C2, C3, and C4 immune subtypes in Her2 patients. **(C)** XXYLT1-AS2 progression free interval curves. To define the two groups, XXYLT1-AS2's median expression classified the patients into "high" and "low" groups. Logrank p-value represented as 0.0056. **(D)** Enrichment analysis using Hallmarks gene sets. Red circles refer to activation while blue circles to inactivation. In X axis, a p-value scale is represented. The circle size varies according to the number of genes in the identified gene set.

Discussion

Using breast cancer immunogenomics data already published (8), we propose here five distinct immune-related lncRNAs signature according to BRCA molecular subtypes using a two steps SNR selection. Each molecular subtype presented a specific immune-related lncRNAs signature and in GSEA, in general, these lncRNAs functions varied between proliferation and immune activation or suppression, which demonstrates that our selection methodology was able to filter lncRNAs related to the immune response. The survival impact of the selected lncRNAs diverged across the molecular subtypes, in agreement with the fact that the immune activation also differs in terms of prognosis importance between the molecular subtypes (24). For instance, the tumor-infiltrating lymphocytes (TIL) was not related to prognosis in Estrogen Positive BRCA tumors, which may explain the lack of immune-related lncRNAs associated with OS or PFI in LumA/B (24). Nevertheless, most lncRNAs selected for Her2 and Normal were associated with PFI and OS, respectively, reinforcing BRCA molecular subtypes' well-known heterogeneity. In the article used as a reference (8), the authors elaborated a list of 75 immunomodulatory genes. With this in mind, in Supplementary Figure 1, we represented the expression variation (as log2 gene expression z-score) among the molecular subtypes, also considering the immune-related subtype. It is possible to observe a distinct expression pattern in all molecular groups, as expected, regarding breast cancer as a heterogeneous disease. This result reflects the high heterogeneity observed in BRCA molecular subtypes, emphasizing the relevance of characterizing them better molecularly, and we included lncRNA analysis in this complexity.

A specific immune-related signature was proposed to LumA subtype using 11 lncRNAs. Among them, three were suggested related to immune response repression (AC105285.1, LINC00271 and EWSAT1), and none of these were previously investigated under BRCA or immune response aspects (Supplementary Table 7 and Supplementary Figure 3C). However, LINC00271 and EWSAT1 had already been associated with other cancer types. LINC00271 low expression was associated with poor prognosis in papillary thyroid cancer (25) and in adrenocortical tumors (26). EWSAT1 was associated with progression in several cancer types, such as ovarian (27), cervical (28) and colorectal (29).

The lncRNA maternally expressed gene 3 (MEG3) is highlighted here in LumA immune response context. MEG3 is up-regulated in C3 and C6 subtypes and is related to neither overall nor progression aspects (Figure 6). The immune subtypes C3 and C6 demonstrate high scores of lymphocyte infiltrate, macrophage regulation and TGF-β response (Figure 3). Thus, the increased expression of this lncRNA can be related to immune response activation. Indeed, our functional characterization revealed that MEG3 high expression is associated with several immune hallmarks, such as: “TNFA Signaling Via NFKB,” “Inflammatory Response,” and “Interferon Gamma Response” (Figure 6D). MEG3’s role in BRCA immune response is to the best of our knowledge the first time cited here. This lncRNA has only been described in endometrial cancer cells down-regulating *PD-L1* (30). MEG3 is found downregulated in several cancer types, such as BRCA, liver, colorectal and cervical cancer and was experimentally evidenced as *TP53*’*s* regulator (31). In BRCA, MEG3’s downregulation is associated with poor overall survival and tumor staging (32).

In LumB subtype, 11 specific lncRNA were selected, and five of them (LINC00957, AL035661.1, FAM160A1-DT, AC096733.2 and EBLN3P) have their expression related to immune response hallmarks repression (Supplementary Table 8 and Supplementary Figure 3D). These lncRNAs were detected up-regulated in immune subtypes with lower lymphocyte fraction, such as C4. Among these lncRNAs only LINC00957, AL035661.1, and EBLN3P had already been studied in cancer context. LINC00957 high expression was associated with bad prognosis in colorectal cancer (33) and osteosarcoma (34). The lncRNA AL035661.1 was found in a lncRNA profile that managed to efficiently predict early recurrence in hepatocellular carcinoma after curative resection (35) and was associated with EMT in Kidney renal clear cell carcinoma (36).

The lncRNA endogenous Bornavirus-like nucleoprotein 3 (EBLN3P) was highlighted in the LumB subtype. EBLN3P is still not well characterized in the literature since few published studies have focused on its mechanisms and effects on human diseases (37). Dai and colleagues (38) noted that EBLN3P is expressed in osteosarcoma tissues and cell lines. They pointed out that its overexpression promotes proliferation, migration and invasion. Li et al. (37) have already reported EBLN3P as a novel oncogene for liver cancer for similar aspects (37, 38).

EBLN3P's expression is higher in C3 (Inflammatory) and C4 (Lymphocyte depleted) immune subtypes in LumB samples (Figure 7B). In fact, in LumB samples, these immune subtypes exhibit a low TGF-β response score. The role of TGF-β response is still controversial in cancer, depending on the tumor stage. Indeed, TGF-β promotes EMT (39), thus being related to cell proliferation. According to the immune subtypes described by Thorsson et al. (8), the C3 subtype exhibits a low proliferation rate and C4 a moderate one. Using this data with our analysis, we observed a concordance of the data since EBLN3P negatively correlates with TGF-β (Supplementary Table 8). In this way, while this lncRNA is highly expressed in these subtypes, TGF-β has a lower expression. The lncRNA EBLN3P's expression was associated with better survival and disease progression outcomes (Figure 7C). Regarding its enrichment analysis in LumB samples, the most significant result was achieved considering "Epithelial Mesenchymal Transition" gene sets. In this scenario, EBLN3P's low expression is related to EMT activation.

Interestingly, most LumA and LumB lncRNAs were related positively or negatively to the Interferon Gamma Response module. Recently, a study demonstrated that the activation of the interferon signaling pathway in ER+ BRCA relates to resistance to CDK4/6 inhibitors and immune checkpoint activation (40). Understanding the role of lncRNAs in this context may be the subject of future studies.

A total of 10 Basal lncRNAs were selected after SNR analysis. According to functional annotation analysis of these lncRNAs. (Supplementary Table 5 and Supplementary Figure 3A), only the lncRNA APCDD1L-DT's high expression was related to immune response inhibition. This lncRNA was only evaluated in a competing endogenous RNA network in lung cancer (41), so its immune response regulation role needs to be better understood. The remaining nine lnRNAs were associated with immune response activation (Supplementary Figure 3A), and only MIR3142HG was previously studied in cancer context. MIR3142HG polymorphisms were associated with glioma susceptibility and/or prognosis (42). An interesting fact is that MIR3142HG was evidenced as a regulator of IL-1β induced inflammatory response in lung fibroblasts (43). In our analysis, inflammatory response appears to be induced by MIR3142HG (Supplementary Figure 3A).

In the Basal, we highlight the lncRNA LINC01871. According to immune subtypes classification, LINC01871 is up-regulated in C2 samples, which is called IFN-γ dominant, and its high expression is associated with a better prognosis (Figure 4). Our enrichment analysis (Figure 4D) showed a strong relation to immune processes. Considering only Basal samples, LINC01871 was associated with "Allograft rejection," "Interferon Gamma," "Interferon Alpha," and "Inflammatory," for example. In these processes, high expression LINC01871 was associated with the activation of these immune responses. We observe a strong relationship with the leucocyte fraction, which might be related to this observed immune response activation. These results emphasize the relevance of LINC01871 in immune response activation in breast tumor samples, especially in Basal samples, which might be related to better prognosis response.

This lncRNA has already been related to immunity in breast, cervical and gastric cancer. LINC01871 was detected in an immune-related prognosis signature in BRCA and exhibited a strong positive correlation with genes associated with immune response such as *GZMB*, *CTLA4* and *PDCD1*. The authors suggested that this lncRNA may play an important role, mainly related to the above immune processes and immune genes (44). In cervical cancer, LINC01871 was also found in an immune-related prognostic signature being related to immune response and TGF-β signaling pathway (45); additionally, in gastric cancer, LINC01871 expression was positively correlated with CD8+ T cell enrichment levels, cytolytic immune activity, and *CD274* (*PD-L1*) expression levels in TCGA gastric cancer cohort (46).

Taking together our results and background literature is possible to correlate LINC01871 with a cytotoxic immune response. Our enrichment analysis showed an association with Interferon alpha and gamma, which are strongly related to cytotoxic response, going in line with what was observed in other studies (44, 46). In BRCA, CD8+ T cells are reported as prognostic significance in estrogen receptor (ER)-negative BRCA, but not in ER-positive cases, being associated with better clinical outcomes survival and response to treatment (47). Also, CD8+ responses have significantly elevated expression of multiple immune checkpoint molecules, such as programmed cell death 1 (PD-1), programmed death-ligand 1 (PD-L1) and 2 (PD-L2) and cytotoxic T-lymphocyte-associated protein 4 (CTLA4) (48). In this way, a stronger

infiltration of CD8+ T cells can predict patient response to standard of care chemotherapy and immune checkpoint blockade therapy, such as anti-PD-1 (49).

According to Figure 3, it is possible to observe a distinct pattern of expression of LINC01871, both considering immune subtype and Interferon Gamma response. Recently, Interferon Gamma low expression level was associated with worse prognosis in Basal patients (50). In our analysis, LINC01871 high expression was associated with better prognosis and Interferon Gamma response activation (Figure 4D), reinforcing the fact that LINC01871 can be used as a good prognosis marker for Basal patients. This can also be evaluated focusing on therapy response, mainly on immunotherapy. Recently, a combination of an immunotherapy drug with chemotherapy was approved for metastatic triple-negative BRCA (51); however, due to this group's high heterogeneity, only a fraction of patients respond well to this treatment. Yang and colleagues (52) defend that an immunity score may be used together with PD-L1 expression to a better design for trials testing immune-checkpoint inhibitors. In this context, lncRNAs like LINC01871 may be used to enhance this selection criterion. However, to be fully applicable as a biomarker, the molecular aspects by which LINC01871 is involved in the immune system activation process need to be better understood.

In the Her2 subtype, ten lncRNAs were evidenced using our selection methodology. All of these lncRNAs were related to immune response activation, as represented in Supplementary Table 9 and Supplementary Figure 3E. Among the ten lncRNAs, four of them had already been related to cancer. LINC02446 is associated with prognosis (53) and EMT activation (54) in bladder cancer. Similarly, USP30-AS1 is associated with prognosis in bladder cancer (54). This lncRNA was also associated with autophagy in ovarian cancer (55), and was related to immune response in cervical cancer (56) and glioblastoma (57). AL365361.1 was associated with good prognosis and immune response in head and neck squamous cell carcinoma (58) and with early recurrence in hepatocellular carcinoma (35). The lncRNA LINC01857 was related to progression in gastric cancer (59), glioma (60), BRCA (61) and B-cell Lymphoma (62). Thus, this lncRNA can be suggested to act as an oncogene. We highlight the lncRNA XXYLT1-AS2, which was associated with progression-free survival in Cox proportional hazard ratio analysis (HR = 0.0011; p-adjusted = 4×10^{-2}). XXYLT1-AS2 is up-regulated in C2 subtype (Figure 8B), and its high

expression is related to better progression-free interval (p-logrank = 5.6 × 10^{-3}). According to our functional annotation analysis, XXYLT1-AS2 is associated with immune response activation and EMT repression (Figure 8D). This result converges with what we observed concerning the progression-free interval since EMT is one of the main pathways activated during the disease progression process. XXYLT1-AS2 is, to the best of our knowledge, the first time described associated with cancer. This lncRNA was only evaluated in Human umbilical vein endothelial cells (HUVECs), and its up-regulation was related to the inhibition of these cell's proliferation and migration (63).

Finally, for the Normal subtype, a signature composed of 11 lncRNAs was predicted. Most of them are associated with immune response activation and overall survival, and we discuss here LINC02613. This lncRNA is up-regulated in the C3 subtype (Figure 5B) and is significantly related to the patient's overall survival. LINC02613's high expression is associated with a better prognosis (p-logrank = 7.5 × 10^{-3}). The enrichment analysis evidenced that LINC02613 is related to immune response activation and mainly involves cell cycle repression (Figure 5D). Indeed, the C3 subtype was described as one with the lowest proliferation rates (8). LINC02613 has not been described in any biological context yet. So we emphasize here the relevance to better characterize this lncRNA.

Considering all the generated and discussed data in this work, we highlight the applied methodology's significance to look for immune-related lncRNAs. The filtering steps followed by functional annotation efficiently got lncRNAs that might be related to immune response. The role of lncRNAs in regulating immune response is increasingly being explored. Our study is limited to *in silico* analysis; however it brings up new lncRNAs candidates as it is a hypothesis generator article.

Another aspect that is important to discuss here is that we found distinct lncRNAs signature for each molecular subtype that may help find important lncRNAs in the immune response process that may be used to guide therapy candidates or as biomarkers; also our results point out that different lncRNAs may be implicated in immune response depending on BRCA molecular subtypes. Our findings are in agreement with what has been discussed about the heterogeneity of BRCA. We identified that different lncRNAs in each molecular subtype are related to the immune system activation. For example, MEG3 and LINC01871 were associated with

activation of Interferon Gamma, in LumA and Basal, respectively. This finding highlights the importance of molecularly characterizing each subtype in order to enable increasingly personalized therapeutic approaches.

Nonetheless, the lncRNAs presented here certainly do not cover all important immune-related lncRNAs in BRCA. Our focus was to find lncRNAs that, in some order, could play a significant role in the immune distinction for each molecular subgroup.

Conclusion

In conclusion, we present a BRCA specific molecular subtype immune-related lncRNAs signature that may guide future studies aiming to look for important biomarkers in BRCA and highlight the relevance of lncRNAs in the immune subtype's classification.

Data Availability Statement

All scripts, datasets, software and algorithms used to generate results, figures, and tables for this study are available on the GitHub repository (https://github.com/sysbiolab/Sup_Material_Mathias2021) and Supplementary Table 10.

DATA SETS.

RESOURCE	SOURCE	IDENTIFIER
Normalizad transcriptome data for TCGA BRCA cohort	XenaBrowser	https://xenabrowser.net/datapages/
Leukocyte fraction, immune characteristics, and classification for TCGA samples	Thorsson et al., 2018 (8)	https://www.cell.com/cms/10.1016/j.immuni.2018.03.023/attachment/1b63d4bc-af31-4a23-99bb-7ca23c7b4e0a/mmc2
List of immune modulators (used for Supplementary Figure 1)	Thorsson et al., 2018 (8)	https://www.cell.com/cms/10.1016/j.immuni.2018. 03.023/attachment/8d3ffc74-4db4-4531-a4ad-389dfc8bb7ec/mmc7.xlsx
Hallmark gene sets	GSEA-MSigDb v7.2, Liberzon et al. (2015) (22, 23)	https://data.broadinstitute.org/gsea-msigdb/msigdb/release/7.2/msigdb_v7.2.xml

SOFTWARE AND ALGORITHMS

RESOURCE	SOURCE	IDENTIFIER
biomaRt v 2.46.3	Durinck et al., 2005 (16)	https://bioconductor.org/packages/release/bioc/html/biomaRt.html
Bioconductor	n/a	http://www.bioconductor.org/
ComplexHeatmap v2.6.2	Gu et al., 2016 (17)	http://www.bioconductor.org/packages/devel/bioc/html/ComplexHeatmap.html
fgsea v1.16.0	Korotkevich et al., 2019 (21)	https://bioconductor.org/packages/release/bioc/html/fgsea.html
survival v3.2-10	Therneau, 2020 (20)	https://cran.r-project.org/web/packages/survival/index.html
survminer v0.4.8		http://www.sthda.com/english/rpkgs/survminer/

Author Contributions

CM, JM, and BA conceived the presented idea. CM, JM, and BA developed the theory and performed the computations. DG, MC, and JO verified the analytical methods. DG, MC, and JO supervised the findings of this work. All authors contributed to the article and approved the submitted version.

Funding

This work was supported by the Public Research Agencies CAPES (001-Coordenação de Aperfeiçoamento de Pessoal de Nível Superior) and CNPq (Conselho Nacional de Desenvolvimento Científico e Tecnológico) processo 153771/2018-6. JM received scholarship from the BIG DATA innovation program from the Associação Hospitalar de Proteção à Infância Raul Carneiro-AHPIRAC (2020).

Conflict of Interest

The authors declare that the research was conducted in the absence of any commercial or financial relationships that could be construed as a potential conflict of interest.

Acknowledgments

Data used in this manuscript were obtained from The Cancer Genome Atlas (TCGA) BRCA database.

Supplementary Material

The Supplementary Material for this article can be found online at: https://www.frontiersin.org/articles/10.3389/fonc.2021.692170/full#supplementary-material

Supplementary Figure 1 | Heatmap of Immune modulators gene set (n=74) proposed by the reference article Thorsson et al. (8) in breast cancer molecular subtypes. For color gradient, maximum and minimum column-wise z-scores were set to +2 and −2 respectively. Each column represents a sample and were semi-supervised clustered within the molecular subtypes.

Supplementary Figure 2 | Venn diagram representing specific and shared immune related lncRNAs in breast cancer (BRCA) molecular subtypes after filtering for 0.90 quantile in signal to noise ratio (SNR) for the BRCA molecular subtypes. 593 lncRNAs were filtered by this criterion for each molecular subtype.

Supplementary Figure 3 | Enrichment map for immune-related lncRNA signature for each molecular subtype: **(A)** Basal, **(B)** LumA, **(C)** LumB, **(D)** Normal, and **(E)** Her2. The lncRNAs are organized in the X axis and Hallmarks gene sets in the Y axis. Red circles refer to positive enrichment scores while blue circles to negative. The circle size varies according to -log10 (adjusted p-value), bigger circles mean greater significance.

Supplementary Figure 4 | Kaplan-Meier analysis for overall survival for LINC01871 in Basal **(A)** and XXYLT1-AS2 in Her2 **(E)** and for Progression Free Interval for MEG3 in LumA **(B)**, EBLN3P in LumB **(C)** and LINC02613 in Normal **(D)**. The groups of High and Low expressions are based on the median value of its respective lncRNA expression. Confidence interval and logrank p-value are shown and values below 0.05 are considered significant.

Supplementary Table 1 | Breast cancer cohort stratification into the immune subtypes.

Supplementary Table 2 | Ensembl and HGNC Symbol from lncRNAs used in this study.

Supplementary Table 3 | First and second SNR calculated for lncRNAs for each molecular subtype.

Supplementary Table 4 | Cox Proportional Hazard models for the specific immune-related lncRNAs and Leukocyte correlation.

Supplementary Tables 5–9 | GSEA Hallmarks analysis for the specific immune-related lncRNAs organized by the molecular subtype.

Supplementary Table 10 | Data sets, software and algorithms used in this study.

References

1. Perou CM, Sørlie T, Eisen MB, van de Rijn M, Jeffrey SS, Rees CA, et al. Molecular Portraits of Human Breast Tumours. *Nature* (2000) 406:747–52. doi: 10.1038/35021093
PubMed Abstract | CrossRef Full Text | Google Scholar
2. Prat A, Parker JS, Karginova O, Fan C, Livasy C, Herschkowitz J, et al. Phenotypic and Molecular Characterization of the Claudin-Low Intrinsic Subtype of Breast Cancer. *Breast Cancer Res* (2010) 12(5):R68. doi: 10.1186/BRCAr2635
PubMed Abstract | CrossRef Full Text | Google Scholar
3. Sørlie T, Perou CM, Tibshirani R, Aas T, Geisler S, Johnsen H, et al. Gene Expression Patterns of Breast Carcinomas Distinguish Tumor suBRCAlasses With Clinical Implications. *Proc Natl Acad Sci USA* (2001) 98(19):10869–74. doi: 10.1073/pnas.191367098
PubMed Abstract | CrossRef Full Text | Google Scholar
4. Dai X, Li T, Bai Z, Yang Y, Liu X, Zhan J, et al. Breast Cancer Intrinsic Subtype Classification, Clinical Use and Future Trends. *Am J Cancer Res* (2015) 5(10):2929–43. doi: 10.1371/journal.pone.0124964
PubMed Abstract | CrossRef Full Text | Google Scholar
5. Shien T, Iwata H. Adjuvant and Neoadjuvant Therapy for Breast Cancer. *Jpn J Clin Oncol* (2020) 50(3):225–9. doi: 10.1093/jjco/hyz213
PubMed Abstract | CrossRef Full Text | Google Scholar

6. Tsang JYS, Tse GM. Molecular Classification of Breast Cancer. *Adv Anat Pathol* (2020) 27(1):27–35. doi: 10.1097/PAP.0000000000000232
PubMed Abstract | CrossRef Full Text | Google Scholar
7. Sturm G, Finotello F, Petitprez F, Zhang JD, Baumbach J, Fridman WH, et al. Comprehensive Evaluation of Transcriptome-Based Cell-Type Quantification Methods for Immuno-Oncology. *Bioinformatics* (2019) 35:i436–45. doi: 10.1093/bioinformatics/btz363
PubMed Abstract | CrossRef Full Text | Google Scholar
8. Thorsson V, Gibbs DL, Brown SD, Wolf D, Bortone DS, Ou Yang TH, et al. The Immune Landscape of Cancer. *Immunity* (2018) 48(4):812–30.e14. doi: 10.1016/j.immuni.2018.03.023
PubMed Abstract | CrossRef Full Text | Google Scholar
9. Segovia-Mendoza M, Morales-Montor J. Immune Tumor Microenvironment in Breast Cancer and the Participation of Estrogen and Its Receptors in Cancer Physiopathology. *Front Immunol* (2019) 10:348. doi: 10.3389/fimmu.2019.00348
PubMed Abstract | CrossRef Full Text | Google Scholar
10. Hombach S, Kretz M. Non-Coding RNAs: Classification, Biology and Functioning. *Adv Exp Med Biol* (2016) 937:3–17. doi: 10.1007/978-3-319-42059-2_1
PubMed Abstract | CrossRef Full Text | Google Scholar
11. Clark MB, Mercer TR, Bussotti G, Leonardi T, Haynes KR, Crawford J, et al. Quantitative Gene Profiling of Long Noncoding RNAs With Targeted RNA Sequencing. *Nat Methods* (2015) 12(4):339. doi: 10.1038/nmeth.3321
PubMed Abstract | CrossRef Full Text | Google Scholar
12. Chan JJ, Tay Y. Noncoding RNA:RNA Regulatory Networks in Cancer. *Int J Mol Sci* (2018) 19(5):1310. doi: 10.3390/ijms19051310
CrossRef Full Text | Google Scholar
13. Bolha L, Ravnik-Glavač M, Glavač D. Long Noncoding RNAs as Biomarkers in Cancer. *Dis Markers* (2017) 2017:7243968. doi: 10.1155/2017/7243968
PubMed Abstract | CrossRef Full Text | Google Scholar
14. Jiang X, Zhang G, Wu J, Lin S, Liu Y, Ma Y, et al. Long Noncoding RNA Serve as a Potential Predictive Biomarker for Breast Cancer: A Meta-Analysis. *BioMed Res Int* (2020) 2020:9045786. doi: 10.1155/2020/9045786
PubMed Abstract | CrossRef Full Text | Google Scholar
15. Volovat SR, Volovat C, Hordila I, Hordila DA, Mirestean CC, Miron OT, et al. MiRNA and LncRNA as Potential Biomarkers in Triple-Negative Breast Cancer: A Review. *Front Oncol* (2020) 10:526850. doi: 10.3389/fonc.2020.526850
PubMed Abstract | CrossRef Full Text | Google Scholar
16. Durinck S, Moreau Y, Kasprzyk A, Davis S, De Moor B, Brazma A, et al. BioMart and Bioconductor: A Powerful Link Between Biological Databases and Microarray Data Analysis. *Bioinformatics* (2005) 21(16):3439–40. doi: 10.1093/bioinformatics/bti525
PubMed Abstract | CrossRef Full Text | Google Scholar
17. Gu Z, Eils R, Schlesner M. Complex Heatmaps Reveal Patterns and Correlations in Multidimensional Genomic Data. *Bioinformatics* (2016) 32(18):2847–9. doi: 10.1093/bioinformatics/btw313
PubMed Abstract | CrossRef Full Text | Google Scholar
18. Best DJ, Roberts DE. Algorithm AS 89: The Upper Tail Probabilities of Spearman's Rho. *Appl Stat* (1975) 24(3):377. doi: 10.2307/2347111
CrossRef Full Text | Google Scholar

19. Bolar K. *Stat: Interactive Document for Working With Basic Statistical Analysis. R Package Version 0.1.0* (2019). Available at: https://CRAN.R-project.org/package=STAT.
Google Scholar
20. Therneau T. *A Package for Survival Analysis in R_. R Package Version 3.2-10* (2021). Available at: https://CRAN.R-project.org/package=survival.
Google Scholar
21. Korotkevich G, Sukhov V, Sergushichev A. Fast Gene Set Enrichment Analysis. *bioRxiv* (2019) 060012. doi: 10.1101/060012
CrossRef Full Text | Google Scholar
22. Subramanian A, Tamayo P, Mootha VK, Mukherjee S, Ebert BL, Gillette MA, et al. Gene Set Enrichment Analysis: A Knowledge-Based Approach for Interpreting Genome-Wide Expression Profiles. *Proc Natl Acad Sci USA* (2005) 102(43):15545–50. doi: 10.1073/pnas.0506580102
PubMed Abstract | CrossRef Full Text | Google Scholar
23. Liberzon A, Birger C, Thorvaldsdóttir H, Ghandi M, Mesirov Jill P, Tamayo P. The Molecular Signatures Database Hallmark Gene Set Collection. *Cell Syst* (2015) 1:417–25. doi: 10.1016/j.cels.2015.12.004
PubMed Abstract | CrossRef Full Text | Google Scholar
24. Loi S, Sirtaine N, Piette F, Salgado R, Viale G, Van Eenoo F, et al. Prognostic and Predictive Value of Tumor-Infiltrating Lymphocytes in a Phase III Randomized Adjuvant Breast Cancer Trial in Node-Positive Breast Cancer Comparing the Addition of Docetaxel to Doxorubicin With Doxorubicin-Based Chemotherapy: BIG 02-98. *J Clin Oncol* (2013) 31(7):860–7. doi: 10.1200/JCO.2011.41.0902
PubMed Abstract | CrossRef Full Text | Google Scholar
25. Ma B, Liao T, Wen D, Dong C, Zhou L, Yang S, et al. Long Intergenic non-Coding RNA 271 is Predictive of a Poorer Prognosis of Papillary Thyroid Cancer. *Sci Rep* (2016) 6:36973. doi: 10.1038/srep36973
PubMed Abstract | CrossRef Full Text | Google Scholar
26. Buishand FO, Liu-Chittenden Y, Fan Y, Tirosh A, Gara SK, Patel D, et al. Adrenocortical Tumors Have a Distinct, Long, non-Coding RNA Expression Profile and LINC00271 is Downregulated in Malignancy. *Surgery* (2020) 167(1):224–32. doi: 10.1016/j.surg.2019.04.067
PubMed Abstract | CrossRef Full Text | Google Scholar
27. Fu X, Zhang L, Dan L, Wang K, Xu Y. LncRNA EWSAT1 Promotes Ovarian Cancer Progression Through Targeting miR-330-5p Expression. *Am J Transl Res* (2017) 9(9):4094–103.
PubMed Abstract | Google Scholar
28. Zhou Q, Xie Y, Wang L, Xu T, Gao Y. LncRNA EWSAT1 Upregulates CPEB4 Via miR-330-5p to Promote Cervical Cancer Development. *Mol Cell Biochem* (2020) 471(1-2):177–88. doi: 10.1007/s11010-020-03778-8
PubMed Abstract | CrossRef Full Text | Google Scholar
29. Liu J, Huang S, Liao X, Chen Z, Li L, Yu L, et al. LncRNA EWSAT1 Promotes Colorectal Cancer Progression Through Sponging miR-326 to Modulate FBXL20 Expression. *Onco Targets Ther* (2021) 14:367–78. doi: 10.2147/OTT.S272895
PubMed Abstract | CrossRef Full Text | Google Scholar
30. Xu D, Dong P, Xiong Y, Chen R, Konno Y, Ihira K, et al. PD-L1 Is a Tumor Suppressor in Aggressive Endometrial Cancer Cells and Its Expression Is Regulated by miR-216a and lncRNA Meg3. *Front Cell Dev Biol* (2020) 8:598205. doi: 10.3389/fcell.2020.598205

PubMed Abstract | CrossRef Full Text | Google Scholar
31. Ghafouri-Fard S, Taheri M. Maternally Expressed Gene 3 (MEG3): A Tumor Suppressor Long non Coding RNA. *BioMed Pharmacother* (2019) 118:109129. doi: 10.1016/j.biopha.2019.10912
PubMed Abstract | CrossRef Full Text | Google Scholar
32. Al-Rugeebah A, Alanazi M, Parine NR. MEG3: An Oncogenic Long Non-Coding RNA in Different Cancers. *Pathol Oncol Res* (2019) 25(3):859–74. doi: 10.1007/s12253-019-00614-3
PubMed Abstract | CrossRef Full Text | Google Scholar
33. Zhang LH, Li LH, Zhang PF, Cai YF, Hua D. LINC00957 Acted as Prognostic Marker Was Associated With Fluorouracil Resistance in Human Colorectal Cancer. *Front Oncol* (2019) 9:776. doi: 10.3389/fonc.2019.00776
PubMed Abstract | CrossRef Full Text | Google Scholar
34. Zhang M, Liu Y, Kong D. Identifying Biomolecules and Constructing a Prognostic Risk Prediction Model for Recurrence in Osteosarcoma. *J Bone Oncol* (2020) 26:100331. doi: 10.1016/j.jbo.2020.100331
PubMed Abstract | CrossRef Full Text | Google Scholar
35. Lv Y, Wei W, Huang Z, Chen Z, Fang Y, Pan L, et al. Long Non-Coding RNA Expression Profile can Predict Early Recurrence in Hepatocellular Carcinoma After Curative Resection. *Hepatol Res* (2018) 48(13):1140–8. doi: 10.1111/hepr.13220
PubMed Abstract | CrossRef Full Text | Google Scholar
36. Zhang YP, Cheng YB, Li S, Zhao N, Zhu ZH. An Epithelial-Mesenchymal Transition-Related Long non-Coding RNA Signature to Predict Overall Survival and Immune Microenvironment in Kidney Renal Clear Cell Carcinoma. *Bioengineered* (2021) 12(1):555–64. doi: 10.1080/21655979.2021.1880718
PubMed Abstract | CrossRef Full Text | Google Scholar
37. Li H, Wang M, Zhou H, Lu S, Zhang B. Long Noncoding RNA EBLN3P Promotes the Progression of Liver Cancer Via Alteration of microRNA-144-3p/DOCK4 Signal. *Cancer Manag Res* (2020) 12:9339–49. doi: 10.2147/cmar.s261976
PubMed Abstract | CrossRef Full Text | Google Scholar
38. Dai S, Li N, Zhou M, Yuan Y, Yue D, Li T, et al. LncRNA EBLN3P Promotes the Progression of Osteosarcoma Through Modifying the miR-224-5p/Rab10 Signaling Axis. *Sci Rep* (2021) 11(1):1992. doi: 10.1038/s41598-021-81641-6
PubMed Abstract | CrossRef Full Text | Google Scholar
39. Zarzynska JM. Two Faces of TGF-beta1 in Breast Cancer. *Mediators Inflammation* (2014) 2014:141747. doi: 10.1155/2014/141747
CrossRef Full Text | Google Scholar
40. De Angelis C, Fu X, Cataldo ML, Nardone A, Pereira R, Veeraraghavan J, et al. Activation of the IFN Signaling Pathway is Associated With Resistance to CDK4/6 Inhibitors and Immune Checkpoint Activation in ER-Positive Breast Cancer. *Clin Cancer Res* (2021). doi: 10.1158/1078-0432.CCR-19-4191
CrossRef Full Text | Google Scholar
41. Ju Q, Zhao YJ, Ma S, Li XM, Zhang H, Zhang SQ, et al. Genome-Wide Analysis of Prognostic-Related lncRNAs, miRNAs and mRNAs Forming a Competing Endogenous RNA Network in Lung Squamous Cell Carcinoma. *J Cancer Res Clin Oncol* (2020) 146(7):1711–23. doi: 10.1007/s00432-020-03224-8
PubMed Abstract | CrossRef Full Text | Google Scholar
42. Guo X, Zhang M, Li Q, Zhao J, Wang B, Wang J, et al. Evaluation of Genetic Variants in MIR3142HG in Susceptibility to and Prognosis of Glioma. *Am J Clin Oncol* (2020) 43(1):1–8. doi: 10.1097/COC.0000000000000587

PubMed Abstract | CrossRef Full Text | Google Scholar
43. Hadjicharalambous MR, Roux BT, Feghali-Bostwick CA, Murray LA, Clarke DL, Lindsay MA. Long Non-Coding RNAs Are Central Regulators of the IL-1β-Induced Inflammatory Response in Normal and Idiopathic Pulmonary Lung Fibroblasts. *Front Immunol* (2018) 9:2906. doi: 10.3389/fimmu.2018.02906
PubMed Abstract | CrossRef Full Text | Google Scholar
44. Ma W, Zhao F, Yu X, Guan S, Suo H, Tao Z, et al. Immune-Related lncRNAs as Predictors of Survival in Breast Cancer: A Prognostic Signature. *J Transl Med* (2020) 18(1):442. doi: 10.1186/s12967-020-02522-6
PubMed Abstract | CrossRef Full Text | Google Scholar
45. Chen Q, Hu L, Huang D, Chen K, Qiu X, Qiu B. Six-LncRNA Immune Prognostic Signature for Cervical Cancer. *Front Genet* (2020) 11:533628. doi: 10.3389/fgene.2020.533628
PubMed Abstract | CrossRef Full Text | Google Scholar
46. He Y, Wang X. Identification of Molecular Features Correlating With Tumor Immunity in Gastric Cancer by Multi-Omics Data Analysis. *Ann Transl Med* (2020) 8(17):1050. doi: 10.21037/atm-20-922
PubMed Abstract | CrossRef Full Text | Google Scholar
47. Baker K, Lachapelle J, Zlobec I, Bismar TA, Terracciano L, Foulkes WD. Prognostic Significance of CD8+ T Lymphocytes in Breast Cancer Depends Upon Both Oestrogen Receptor Status and Histological Grade. *Histopathology* (2011) 58(7):1107–16. doi: 10.1111/j.1365-2559.2011.03846.x
PubMed Abstract | CrossRef Full Text | Google Scholar
48. Oshi M, Asaoka M, Tokumaru Y, Yan L, Matsuyama R, Ishikawa T, et al. CD8 T Cell Score as a Prognostic Biomarker for Triple Negative Breast Cancer. *Int J Mol Sci* (2020) 21(18):6968. doi: 10.3390/ijms21186968
CrossRef Full Text | Google Scholar
49. Li X, Gruosso T, Zuo D, Omeroglu A, Meterissian S, Guiot MC, et al. Infiltration of CD8+ T Cells Into Tumor Cell Clusters in Triple-Negative Breast Cancer. *Proc Natl Acad Sci USA* (2019) 116(9):3678–87. doi: 10.1073/pnas.1817652116
PubMed Abstract | CrossRef Full Text | Google Scholar
50. Heimes AS, Härtner F, Almstedt K, Krajnak S, Lebrecht A, Battista MJ, et al. Prognostic Significance of Interferon-γ and Its Signaling Pathway in Early Breast Cancer Depends on the Molecular Subtypes. *Int J Mol Sci* (2020) 21(19):7178. doi: 10.3390/ijms21197178
CrossRef Full Text | Google Scholar
51. Schmid P, Adams S, Rugo HS, Schneeweiss A, Barrios CH, Iwata H, et al. Atezolizumab and Nab-Paclitaxel in Advanced Triple-Negative Breast Cancer. *N Engl J Med* (2018) 379(22):2108–21. doi: 10.1056/NEJMoa1809615
PubMed Abstract | CrossRef Full Text | Google Scholar
52. Yang B, Chou J, Tao Y, Wu D, Wu X, Li X, et al. An Assessment of Prognostic Immunity Markers in Breast Cancer. *NPJ Breast Cancer* (2018) 4:35. doi: 10.1038/s41523-018-0088-0
PubMed Abstract | CrossRef Full Text | Google Scholar
53. Zhang X, Zhang J, Zhao W, Dong X, Xin P, Liu X, et al. Long non-Coding RNA LINC02446 Suppresses the Proliferation and Metastasis of Bladder Cancer Cells by Binding With EIF3G and Regulating the mTOR Signalling Pathway. *Cancer Gene Ther* (2021). doi: 10.1038/s41417-020-00285-2
CrossRef Full Text | Google Scholar

54. Tong H, Li T, Gao S, Yin H, Cao H, He W. An Epithelial-Mesenchymal Transition-Related Long Noncoding RNA Signature Correlates With the Prognosis and Progression in Patients With Bladder Cancer. *Biosci Rep* (2021) 41(1):BSR20203944. doi: 10.1042/BSR20203944
PubMed Abstract | CrossRef Full Text | Google Scholar
55. Meng C, Zhou JQ, Liao YS. Autophagy-Related Long Non-Coding RNA Signature for Ovarian Câncer. *J Int Med Res* (2020) 48(11):300060520970761. doi: 10.1177/0300060520970761
PubMed Abstract | CrossRef Full Text | Google Scholar
56. Chen P, Gao Y, Ouyang S, Wei L, Zhou M, You H, et al. A Prognostic Model Based on Immune-Related Long Non-Coding RNAs for Patients With Cervical Cancer. *Front Pharmacol* (2020) 11:585255. doi: 10.3389/fphar.2020.585255
PubMed Abstract | CrossRef Full Text | Google Scholar
57. Gao M, Wang X, Han D, Lu E, Zhang J, Zhang C, et al. A Six-lncRNA Signature for Immunophenotype Prediction of Glioblastoma Multiforme. *Front Genet* (2021) 11:604655. doi: 10.3389/fgene.2020.604655
PubMed Abstract | CrossRef Full Text | Google Scholar
58. Zhong Z, Hong M, Chen X, Xi Y, Xu Y, Kong D, et al. Transcriptome Analysis Reveals the Link Between lncRNA-mRNA Co-Expression Network and Tumor Immune Microenvironment and Overall Survival in Head and Neck Squamous Cell Carcinoma. *BMC Med Genomics* (2020) 13(1):57. doi: 10.1186/s12920-020-0707-0
PubMed Abstract | CrossRef Full Text | Google Scholar
59. Chen GR, Sun W, Zheng K, Zhu W. LINC01857 Promotes the Development of Gastric Cancer by Regulating MicroRNA-200b. *Eur Rev Med Pharmacol Sci* (2020) 24(7):3648–56. doi: 10.26355/eurrev_202004_20827
PubMed Abstract | CrossRef Full Text | Google Scholar
60. Hu G, Liu N, Wang H, Wang Y, Guo Z. LncRNA LINC01857 Promotes Growth, Migration, and Invasion of Glioma by Modulating miR-1281/TRIM65 Axis. *J Cell Physiol* (2019) 234(12):22009–16. doi: 10.1002/jcp.28763
PubMed Abstract | CrossRef Full Text | Google Scholar
61. Xiong Y, Gu Y, Wang F, Li L, Zhu M, Wang N, et al. LINC01857 as an Oncogene Regulates CREB1 Activation by Interacting With CREBBP in Breast Cancer. *J Cell Physiol* (2019) 234(8):14031–9. doi: 10.1002/jcp.28090
PubMed Abstract | CrossRef Full Text | Google Scholar
62. Li Q, Li B, Lu CL, Wang JY, Gao M, Gao W. LncRNA LINC01857 Promotes Cell Growth and Diminishes Apoptosis Via PI3K/mTOR Pathway and EMT Process by Regulating miR-141-3p/MAP4K4 Axis in Diffuse Large B-cell Lymphoma. *Cancer Gene Ther* (2020). doi: 10.1038/s41417-020-00267-4
CrossRef Full Text | Google Scholar
63. Wang Q, Yang Y, Fu X, Wang Z, Liu Y, Li M, et al. Long Noncoding RNA Xxylt1-AS2 Regulates Proliferation and Adhesion by Targeting the RNA Binding Protein FUS in HUVEC. *Atherosclerosis* (2020) 298:58–69. doi: 10.1016/j.atherosclerosis.2020.02.018
PubMed Abstract | CrossRef Full Text | Google Scholar